PKA phosphorylation and compartmentalisation of cAMP-phosphodiesterases

A thesis submitted to the

FACULTY OF BIOMEDICAL AND LIFE SCIENCES

for the degree of

DOCTOR OF PHILOSOPHY

by

Theresa McSorley

Division of Biochemistry & Molecular Biology

Institute of Biomedical and Life Sciences

University of Glasgow

September 2004

ProQuest LLC.
789 East Eisenhower Parkway
P.O. Box 1346
Ann Arbor, MI 48106 – 1346

Declaration

I declare that the work described in this thesis has been carried out by myself unless otherwise cited or acknowledged. It is entirely of my own composition and has not, in whole or in part, been submitted for any other degree.

Theresa McSorley

September 2004.

Abstract

cAMP is a ubiquitous second messenger which conveys its cellular effects mainly through the activation of protein kinase A (PKA). Within a cell, activated PKA serves to phosphorylate, and alter the conformational change of a wide variety of proteins. Cyclic-phosphodiesterases (PDEs) play a pivotal role in the regulation of cAMP signalling by determining the breakdown of cAMP to 5'-AMP. It is now well-accepted that cAMP signalling is a compartmentalised response, with PKA being tethered to distinct subcellular regions by A-kinase anchoring proteins (AKAPs). The PDE4 family exclusively hydrolyse cAMP.

I studied the PKA phosphorylation of the two sites within PDE4D3 and found that the phosphorylation of Ser54 (responsible for activation) precedes that of Ser 13. I showed, for the first time, that long form PDE4s from each subfamily can be phosphorylated and consequentially activated by PKA in intact cells. I used a novel approach to appreciate the functional consequences of the compartmentalisation of PDE4 cAMP-phosphodiesterases. To do this, I overexpressed different catalytically inactive long form PDE4s which, I hypothesised, would alter distinct cAMP 'pools' by displacing the cognate endogenous active PDE4s from their anchor sites. By detecting the phosphorylation of the inactive PDE4 by PKA, the catalytically inactive PDE4 itself acted as readout of localised PKA activity. Through this approach, I found that different PDE4 isoforms are capable of controlling distinct pools of cAMP generated by different Gs-coupled receptors. Specifically I showed that the PDE4D3 and PDE4C2 may be held in close proximity to, and play a role in the regulation of discrete sub-populations of PKA under basal levels of cAMP generation.

Through microarray analysis, I studied the effect of altering compartmentalised cAMP signalling on gene expression. This was again done by overexpressing catalytically inactive PDE4s in HEK293 cells. My experiments suggest that specific PDE4 isoforms can selectively influence gene regulation in these cells.

Additionally, I analysed the function of distinct PDEs within cardiac myocytes. I showed that manipulation of cAMP levels with PDE inhibitors alone, or with PDE inhibitors and selected GPCR activation, selectively altered ability of phospholamban (PLB) and ERK1/2 to be regulated by PKA, suggesting that PLB and ERK1/2 can be differentially controlled by specific PDE families.

Acknowledgements

I would like thank my supervisor Prof. M. Houslay for allowing me to carry out this project in his laboratory, for guidance and support. A big thank you to Dr. George Baillie firstly for his guidance, and secondly for being a constant source of amusement and banter.

A thank you to Dr.Elaine Hill, Dr. Angela McCahill, Dr. Elaine Huston, Carolynn MacKenzie, Dr. Martin Lynch and Irene Gall for all their advice and putting up with my constant questions! Thank you to the rest of the Gardiner for all their help.

I would also like to mention and thank my supervisor at Novartis, Dr.Gino van Heeke for his support and providing me the opportunity to carry out this project. Also, thanks to Rachael Barber at Novartis for all her help.

Of course, I would also like to give very special thanks my fellow PhD student and good friend Jenni Millen. You helped me more than you know. Without you it would not have been as fun?!.....I miss our evening tea and Double Decker/ Boost ritual! Finally, I would like to thank my mum, dad and Heather for providing me with their support and encouragement. I couldn't have managed without!

Table of contents

List of figures

Chapter 1

Chapter 3

Chapter 4

Chapter 5

Chapter 6

List of tables

Chapter 1

Chapter 5

Abbreviations

AC	adenylyl cyclase
AKAP	A kinase anchoring protein
ATP	adenosine trisphosphate
Ca^{2+}/CaM	calcium/calmodulin
cAMP	cyclic 3'5' adenosine monophosphate
CRE	cAMP response element
CREB	cAMP response element binding protein
cDNA	complementary DNA
cGMP	cyclic guanosine monophosphate
DEAE	diethyl aminoethyl
DMEM	Dulbecco's modified Eagle's Medium
DMSO	dimethylsulphoxide
DNA	deoxyribonucleic acid
dNTP	deoxynucleotide trisphosphate
DTT	dithiothreitol
ECL	Enhanced chemiluminescence
EDTA	Diaminoethanetetra-acetic acid
EGF	epidermal growth factor
EGTA	Ethylene glycol-bis(β-aminoethyl ether)-N,N,N',N-tetraacetic acid
Epac	Exchange protein directly activated by cAMP
ERK	Extracellular signal-regulated kinase
FCS	foetal calf serum
GEF	Guanine nucleotide exchange factor
GIRK1	G-protein coupled inwardly rectifying potassium channel
GPCR	G-protein coupled receptor
G-protein	guanine nucleotide binding regulatory protein

GRK	G-protein receptor specific kinase
GST	Glutathione S-transferase
GTP	guanosine triphosphate
h	hour
HEK	Human embryo kidney
HEPES	N-2-Hydroxyethylpiperazine-N'-2-ethanesulfonic acid
IBMX	isobutylmethylxanthine
IC_{50}	Concentration of inhibitor required to inhibit half the specific activity
K_m	Michealis-Menton constant
kb	kilobase
kDa	kiloDaulton
l	litre
LB	Luria-Bertoni
LR	linker region
M	molar
mg	milligram
MAP kinase	mitogen-activated protein kinase
MEK	MAPK kinase
min	minute
mRNA	messenger RNA
PA	phosphatidic acid
PAGE	Polyacrylamide gel electrophoresis
PBS	phosphate buffered saline
PCR	polymerase chain reaction
PDE	phosphodiesterase
PGE2	prostaglandin E2
PKA	protein kinase A
PKC	protein kinase C
PLB	phospholamban
RACK	receptor for activated C kinase

RNA	ribonucleic acid
rpm	revolutions per minute
RT	reverse transcription
SDS	sodium dodecyl sulphate
sec	second
SH2 domain	Src homology 2 domain
SH3 domain	Src homology 3 domain
TAE	tris/acetate/EDTA
TBS	tris buffered saline
TE	tris/EDTA
TEMED	N,N,N',N'-Tetramethyl-ethylenediamine
TLC	Thin-layer cellulose
Ub	Ubiquitin
UCR	upstream conserved region
VSV	vesicular stomatitis virus
VSMC	vascular smooth muscle cell

General introduction

Cells respond to extracellular stimulatory molecules, such as hormones and neurotransmitters, through the activation of signal transduction cascades. Such stimulatory molecules, also known as first messengers, usually initiate the signal cascade at the level of the plasma membrane via a transmembrane receptor protein. Signal transduction involves the extracellular signal being propagated to its target effector via a defined signal transduction pathway. However, studies over the last few decades have revealed that no one signal transduction pathway acts in isolation, in fact a great deal of complexity exists through the integration of different signalling pathways. The range of possible networks of 'cross-talk', and the orchestration of compartmentalised signalling events within specialised cells, is only now becoming apparent. I will give a general overview of the cyclic AMP signalling system, focusing on the cyclic AMP-specific phosphodiesterases and finally discuss the importance of cAMP within the cardiovascular system.

1.1 cAMP signalling

The nucleotide cyclic adenosine 3', 5'-monophosphate (cAMP) was discovered in 1958 (Sutherland & Rall, 1958) and is regarded as the classical second messenger molecule. Cyclic AMP has been implicated in the mediation of many cellular processes such as certain metabolic events, muscle contraction, cytokine-inflammatory events, differentiation and growth (Houslay and Milligan, 1997). Various components are involved in its synthesis, detection and degradation (Houslay and Milligan, 1997). Over the decades, studies have defined some of the molecular machinery involved in the basic cAMP signalling system; many transmembrane receptors, heterotrimeric G-proteins, over nine different adenylyl cyclase (AC) species, multiple protein kinases/phosphatases and, to date, eight phosphodiesterase (PDE) families. All of the above enzymes are involved in the relay of the signal from the plasma membrane, conversion of the signal to the second messenger cAMP and the tailoring of the cellular response and also in signal termination through degradation of cAMP to 5' AMP (Houslay and Milligan 1997;

Houslay, 1998; Antoni, 2000). A cell can exploit this choice of multiple forms of cAMP signalling machinery to achieve a specific response to a variety of different ligands, or achieve different responses to the same ligand.

1.1.1 G-proteins and G-protein coupled receptors

G-protein coupled receptors (GPCRs) consist of a family of over 1000 receptors which mediate biological responses of a wide array of different stimuli. These receptors are often referred to as heptahelical or serpentine receptors, as the best-known family of GPCRs contains a conserved structure of seven transmembrane helices. Activation of GPCRs causes a change in the transmembrane α helices, which unmasks G protein binding sites (Bourne, *et al.*, 1997). The interaction of the GPCR-G-protein promotes the release of guanosine diphosphate (GDP) bound to the G protein α sub-unit and exchange for guanosine triphosphate (GTP). Gα and Gβγ sub-units of the G-proteins then dissociate and thus serve to initiate intracellular signalling responses by acting on a variety of different effector molecules (Bourne, *et al.*, 1997).

To date, 20 different Gα sub-units have been identified, and, according to sequence similarity, can be divided into four families: G_s, G_i, G_q and G_{12}. The Gα sub-units can regulate the generation of several different second messengers (Bourne, *et al.*, 1997; Wilkie, *et al.*, 1992). Members of the G_q family, for example, can control the regulation of phospholipase C-β (PLC-β) which hydrolyses phosphatidylinositol 4,5-bisphosphate to two second messengers, namely inositol 1,4,5-triphosphate (IP_3) and diacylglycerol (DAG) (Rhee & Bae, 1997). The generation of IP_3 and DAG can lead to an increase in free intracellular Ca^{2+}, and activation of a number of protein kinases including protein kinase C (PKC).

Members of the G_s and G_i family can regulate the adenylyl cyclases (AC) family of enzymes, and thereby control cAMP levels. Members of the G_s activate ACs (figure 1.1), while members of the G_i inhibit ACs. So far, nine different ACs have been cloned and each seems to be distinctly regulated by G_s, G_i, βγ–sub-units, $[Ca^{2+}]$ and PKCs (Sunahara

et al., 1996). Thus, the impact of cAMP levels on the cell following stimulation of GPCRs will depend on which forms of AC are expressed in the cell.

However, cAMP signalling specificity may also be achieved at the level of the GPCR itself as it has been shown by various researcher groups that compartmentalisation exists at the level of the plasma membrane and GPCR. For example, in the cardiac myocytes, a different distribution patterns have been seen for the prostanoid receptor EP3, as well as the β1–Ad and β2-Ad receptors within the plasma membrane. This research shows that β2–Ad receptors are enriched in caveolae (defined as membrane invaginations and classed as a subset of lipid rafts) yet β1–Ad and EP3 receptors are excluded (Lasley & Smart, 2001; Xiang *et al.*, 2002).

Additionally, 12 different Gγ sub-units and 6 Gβ sub-units have been cloned. When Gβγ dimers are released upon Gα–activation, they can also regulate the activity of a variety of signalling molecules such as phosphatidylinositol kinases, ACs, phospholipases and receptor kinases (Bourne, *et al.*, 1997).

1.1.2 Adenylyl cyclase

1.1.2.1 Regulation of adenylyl cyclases

Over nine different mammalian isoforms of the cAMP producing enzymes, named ACs, have been cloned and identified (Sunahara *et al.*, 1996). The ACs can be broadly sub-divided based on their relatedness and their responsiveness to Ca^{2+}. The first AC to be cloned was termed AC1 and was found to be stimulated by Ca^{2+}/calmodulin, with the similarly regulated AC3 and AC8 being cloned quite soon afterwards (Cali *et al.*, 1994). However, the regulation of AC3 by Ca^{2+}/calmodulin remains uncertain, as reports have provided ambiguous results (Cooper, 2003). Certain adenylyl cyclases are inhibited by Ca^{2+} without the requirement of calmodulin, namely AC5 and AC6 (Cooper, *et al.*, 1995). AC2, AC4 and AC7 are insensitive to Ca^{2+}, however they can be stimulated as a result of

the activation of the phosphoinositide signalling pathway and through PKC activation (Cooper, 2003). PKC has also been reported to inhibit the activity of AC6 by phosphorylation of its N-terminus (Lai *et al.*, 1999).

Desensitisation of the AC system can occur at the level AC itself, as it has been shown that PKA can directly phosphorylate and reduce the activity of AC5 (Iwami *et al.*, 1995). Nitric Oxide (NO) has also been reported to be a regulator of AC activity as NO donors inhibit the forskolin simulated activation of AC5/AC6 (Cooper, 2003).

1.1.2.2 Localisation of adenylyl cyclase in caveolae and rafts

The plasma membrane is comprised of 'microdomains' of different lipid and protein composition. The microdomains are often termed lipid rafts, with distinct G-protein coupled receptors (GPCRs) and transmembrane proteins including ACs being found enriched in such rafts. Caveolae are described as membrane invaginations and are regarded as a subset of lipid rafts. In cardiac myocytes, AC5/AC6 and β_2-adrenergic are enriched in caveolae, and thereby provide the production of distinct pools of cAMP (Rybin *et al.*, 2000; Ostrom *et al.*, 2000).

1.1.3 Effectors of cAMP

1.1.3.1 Protein kinase (PKA)

Protein kinases are a family of enzymes, which can phosphorylate and alter the activation state of a plethora of protein targets (Krebs & Beavo, 1979). Protein phosphorylation is a fundamental mechanism through which cells can respond to, and transduce intracellularly, the effect of extracellular stimuli. One of the most studied and best-understood protein kinases is the cAMP-dependent protein kinase (PKA). First characterised in 1968 (Walsh *et al.*, 1968) it is activated through the cooperative binding of cAMP (figure 1.2). The inactive holoenzyme consists of two regulatory (R) sub-units and two catalytic (C) sub-units. The cooperative binding of two cAMP molecules to each of the R sub-units exerts a conformational change which results in the release of the C

sub-units to phosphorylate their target proteins (figure 1.2) (Johnson *et al.*, 2001). More and more proteins that can be phosphorylated and activated by PKA are still being identified; in fact, the list of PKA substrates has increased dramatically over the last two decades (Shabb, 2001). The consensus sites for PKA phosphorylation have been identified as: Arg-Arg-ϕ-Ser/Thr (ϕ: hyrophobic), Arg/Lys-ϕ -ϕ-Ser/Thr (ϕ: hydrophobic) and Arg/Lys-ϕ-Ser/Thr (ϕ: hydrophobic) (Kennelly & Krebs, 1991; Shabb, 2001).

It is now known that three different genes encode the catalytic sub-units of PKA: Cα, Cβ and Cγ, and four genes express the regulatory sub-units: RIα, RIβ, RIIα and RIIβ (Jahnsen *et al.*, 1986; Scott *et al.*, 1987; Chrivia *et al.*, 1988). Two types of heterotetramers have been reported to exist *in vivo*: PKA holoenzyme type I (RIα and RIβ) and type II (RIIα and RIIβ). The type I PKA is predominantly cytosolic, while over 80% of type II PKA associates with cellular structures and organelles (Taylor *et al.*, 1990; Michel & Scott, 2002). PKA, along with other signalling proteins, can be targeted to distinct subcellular regions through the interaction with A-kinase anchoring protein (AKAPs) (figure 1.2).

1.1.3.2 ERK and cAMP signalling cross-talk

It is now widely accepted that cross-talk between the cAMP and ERK mitogen-activated protein kinase pathways occurs at a number of distinct points (Houslay & Baillie, 2003). The effects of such cross-talk can be mediated in a cell-type specific manner by the selective expression of specific isoforms of enzymes positioned at specific control points (Houslay & Kolch, 2000).

The identification ERK/cAMP signalling cross-talk originated from studies based on the protein kinase Raf. The cell-type specific expression of the Raf isoforms, Raf-1 or B-Raf, allow either the inactivation or activation of ERK (Houslay & Kolch, 2000; Houslay & Baillie, 2003). Inhibition of Raf-1 and hence inhibition of ERK can be achieved by elevated cAMP and activation of PKA. On the other hand, elevation of cAMP can lead

the activation of B-Raf and hence activation of ERK. Although the precise mechanism for activation has still to be elucidated, it is suggested that activation of B-Raf in response to elevation of cAMP occurs via the activation of the monomeric G-protein Rap-1 (Houslay & Baillie, 2003). It was originally suggested that Rap-1 activation is achieved upon binding of cAMP to Epac (exchange proteins activated by cAMP), however, the recent emergence of an Epac-specific inhibitor indicates that this unlikely (Bos, 2003). Thus many questions regarding cAMP activation of the ERK pathway remain unanswered.

1.1.3.3 Epac

A general consensus exists that cAMP exerts its intracellular effects mainly by activating cAMP. However, cAMP can also act in a PKA-independent manner via the direct activation of ion channels (Shabb, 2001) or by cyclic nucleotide-regulated guanine nucleotide exchange factors (cAMP-GEFS), also referred to as Epacs (exchange protein activated by cAMP) (Kawasaki *et al.*, 1998; de Rooi *et al.*, 1998).

Two Epac isoforms, Epac1 and Epac2, upon direct binding of cAMP activate the small G-proteins Rap-1 and Rap-2 (figure 1.3) (Kawasaki *et al.*, 1998; de Rooi *et al.*, 1998). Several studies have indicated that Rap-1 is a mediator in the cAMP-induced inhibition of Raf-1 (Schmitt & Stork, 2002; Bos, 2003). It was initially believed that Rap-1 antagonises Ras signalling towards ERK by trapping the Ras effector, Raf-1 in an inhibitory complex (Schmitt & Stork, 2002). However, it appears that Epac mediates the cAMP induced-activation of Rap-1, whilst the inhibition of Raf-1 is mediated by PKA (Bos, 2003). Additionally, studies using the Epac-specific activator 8-pCPT-2'-*O*-Me-cAMP did not result in an inactivation of the Ras-Raf1-ERK pathway (Enserink *et al.*, 2002).

Rap-1 has also been implicated in the cAMP-induced activation of ERK (Vossler *et al.*, 1997). It is proposed that Epac mediates the binding of Rap-1 to, and activation of, B-Raf. However, that this effect also requires PKA and the use of 8-pCPT-2'-*O*-Me-cAMP activator casts doubt on the involvement of Epac (Bos, 2003).

Epac is known to be involved in the control of cAMP-regulated integrin-mediated cell adhesion (Rangarajan *et al.*, 2003). There is also increasing evidence that Epac is involved in the cAMP-mediated modulation of insulin secretion (Ozaki *et al.*, 2002; Bos, 2003). Since the development of the Epac-specific activator (8-pCPT-2'-*O*-Me-cAMP), it is anticipated that the recognised list of functions of Epac will grow rapidly.

1.1.3.4 Cyclic nucleotide-gated channels

Cyclic nucleotide-gated (CNG) cation channels on the cell membrane are biological effectors of cyclic nucleotide action. To date, over 20 genes encoding different subtypes of CNGs have been cloned from invertebrates and vertebrates (Wei *et al.*, 1997). Functionally, CNG channels belong to the class of ligand-gated cation channels and are activated by the binding of cAMP or cGMP. The best-studied cAMP gated channel is the olfactory cyclic nucleotide channel, which is activated equally by both cAMP and cGMP (Shabb, 2001). This nonselective ion channel is activated in response to odorant binding to G protein-coupled olfactory receptors which, in turn, results in the activation of adenylyl cyclase (Shabb, 2001).

1.2 The phosphodiesterase superfamily

Cyclic nucleotide phosphodiesterases (PDEs) are represented by a large super family of enzymes which hydrolyze both cAMP and cGMP. To date, the PDE superfamily includes 21 different genes encoding over 30 different PDEs, which are sub-grouped into 11 different PDE families (Houslay & Milligan, 1997; Conti & Jin, 1999; Soderling & Beavo, 2000; Houslay & Adams, 2003). The nomenclature of the PDE superfamily is indicated as follows; the family is indicated as an Arabic numeral, a capital letter indicating a gene within the family and a second Arabic numeral indicating a splice variant e.g. PDE4D3: family 4, gene D and 3rd splicing variant. Each sub-family of PDE is distinguished by different enzymatic characteristics, different regulatory properties (table 1.1) and differential inhibitory pharmacological profiles (see table 1.2 for list of

available PDE inhibitors) (Houslay-review, 1998; Houslay and Kolch, 2000; Soderling and Beavo, 2000).

1.2.1 The PDE1 family

Variants of the PDE1 family are activated upon binding of Ca^{2+}/CaM. Three PDE1 genes encode PDE1A, PDE1B and PDE1C sub-families. The variants of PDE1C hydrolyse both cAMP and cGMP with high affinity, while variants of the PDE1A and PDE1B genes selectively hydrolyse cGMP. The PDE1A and PDE1B encode two splice variants each, PDE1A1 and PDE1A2, and PDE1B1 and PDE1B2 respectively. The PDE1C gene provides five products, PDE1C1-5.

Antagonists of CaM inhibit PDE1 activity but are not only selective for PDE1. Catalytic site inhibitors such as vinpocetine (table 1.2) inhibit all PDE1, but PDE1C with less potency, and are not specific for any individual variant (Kakkar *et al.*, 1989; Zhao *et al.*, 1997).

PDE1C variants have been implicated in VSMC proliferation (Rybalkin *et al.*, 1997), insulin secretion (Han *et al.*, 1999), and in cardiac tissue (Maurice *et al.*, 2003). PDE1A variants have also been identified the cardiovascular system (Rybalkin *et al.*, 1997; Zhao *et al.*, 1997), while PDE1B2 has also been identified in VSMC (Rybalkin *et al.*, 1997).

1.2.2 The PDE2 family

The splice variants of PDE2 are encoded by a single gene and these enzymes can hydrolyse both cAMP and cGMP (Yang *et al.*, 1994; Rosman *et al.*, 1997). The activation of PDE2 enzyme occurs following the binding of cGMP to the N-terminally located GAF domains (table 1.1) (Martinez *et al.*, 2002). A few selective inhibitors exist, of which EHNA is the best recognised (Mery *et al.*, 1995), although it does also serve as an inhibitor of adenosine deaminase (table 1.2). A role for PDE2 within the cardiovascular system has been proposed, and PDE2 has been shown to be expressed in cardiac myocytes, VSMC and vascular endothelial cells (Sandhu *et al.*, 1999). One

PDE2A variant, PDE2A2, is expressed in cardiac myocytes (Sandhu *et al.*, 1999). In cardiac myocytes, direct inhibition of PDE2 by EHNA increases L-type Ca^{2+} currents (Vandcasteele *et al.*, 2001). cGMP-activation of PDE2, in conjunction with PDE3, has been implicated in the regulation of Ca^{2+} currents and contractility (Vandcasteele *et al.*, 2001).

1.2.3 The PDE3 family

Two genes encode the PDE3 family, PDE3A and PDE3B. Through alternative start codons, three PDE3A isoforms exist (PDE3A1-3), while only one isoform of the PDE3B gene exists (Movsesian *et al.*, 2002; Wechsler *et al.*, 2002). The analysis of mRNA expression to determine tissue distribution has shown differential expression. PDE3A enzymes have been reported to be expressed in blood vessels, cardiovascular system and oocytes (Reinhardt *et al.*, 1995; Maurice *et al.*, 2002; Movsesian *et al.*, 2002). The highest level of PDE3B has been reported in brain, renal collecting duct epithelium, hepatocytes, adipocytes and developing spermatocytes (Reinhardt *et al.*, 1995; Maurice *et al.*, 2002; Movsesian *et al.*, 2002).

1.2.3.1 Regulation and targeting of the PDE3 family

Full length PDE3A and PDE3B possess two N-terminal hydrophobic membrane association domains, named NH1 and NH2. These regions allow the different PDE3A variants which possess NH1 and NH2, or only NH2, or neither, the ability to localise to different cellular regions. PDE3A1 possesses both NH1 and NH2 regions is found mainly in the particulate fraction, PDE3A2 possesses only NH2 is found both in the cytosol and the particulate fraction, and PDE3A3 which lacks both domains is cytosolic (Maurice *et al.*, 2002; Movsesian *et al.*, 2002; Wechsler *et al.*, 2002). PDE3A and PDE3B enzymes can be phosphorylated and activated by PKA and PKB (Manganiello & Degerman, 1999).The hydrolysis of cAMP by PDE3 enzymes is directly inhibited by the binding of cGMP to the catalytic unit (Manganiello & Degerman, 1999). A number of PDE3 inhibitors exist, such as cilostamide, milirone and amrinone (table 1.2). Inhibitors that

distinguish between PDE3A and PDE3B are not available, and given their similarity, are unlikely to be achievable.

The use of PDE3 inhibitors has been discussed in the treatment of type 2 diabetes and cardiac myopathies. Insulin-induced activation of PDE3B in 3T3-L1 adipocytes has been shown to occur via the phosphorylation of PDE3B by Akt/protein kinase B (PKB) (Kitamura *et al.*, 1999). It has also been reported the selective inhibition of PDE3 activity in pancreatic β–cells stimulates insulin secretion (Harndahl *et al.*, 2002). In this study, PDE3B has been implicated in the cAMP-dependent insulin secretion from the β-cells of pancreatic islets (Harndahl *et al.*, 2002). Enzymes of the PDE3 family also play an important role in the regulation the cyclic nucleotide-mediated responses in cardiac and vascular smooth muscle myocytes (Movsesian, 2003). In the case of dilated cardiomyopathy, PDE3 inhibitors have both inotropic and vasodilatory properties, and were shown in early studies to have beneficial effects on myocardial contraction and vascular relaxation in clinical trials (Jaski *et al.*, 1985; Movsesian, 2003). However, subsequently it was shown that chronic clinical application of these inhibitors, such as milrinone, resulted in an increase in mortality (Movsesian, 2003). From these trials, it has been suggested that increases in cAMP within cardiac myocytes have beneficial effects in the short term and adverse effects in the long term. It is now thought that milrinone exerts an effect on PDE4 as well as PDE3 (Shakur *et al.*, 2002).

1.2.4 The PDE4 family

The PDE4 phosphodiesterase family exclusively hydrolyses cAMP. To date over 16 different isoforms of the PDE4 family have been identified (table 1.3) (Houslay *et al.*, 1998; Conti *et al.*, 2003). Four PDE4 genes (A, B, C, D) encode the PDE4 isoforms and can produce a number of different isoforms through alternative mRNA splicing and the use of alternative promoters. Within each PDE4 family, each isoform possesses unique N-terminal., common catalytic region, and a common C-terminal region. PDE4 isoforms can be classed as short or long forms depending on the absence of presence of upstream

conserved regions (UCRs). Long form PDE4s possess both UCR1 and UCR2, short forms lack UCR1 (figure 1.4).

1.2.5 The PDE5 family

The cGMP-specific PDE5 family plays a pivotal role in the control of smooth muscle relaxation (Corbin & Francis, 1999). PDE5 is highly specific for cGMP both in its catalytic site and within two allosteric binding sites within the N-terminal GAF domains of the protein (McAllister-Lucas *et al.*, 1995). PDE5 is a multi-domain protein that is regulated by phosphorylation as well as by the allosteric binding of cGMP to the GAF domains. cGMP-binding to the GAF domains has been shown to be required for the phosphorylation of PDE5 by PKA or PKG (Thomas *et al.*, 1995). The important physiological role of PDE5 in the regulation of smooth muscle tone has been shown by the clinical use of sildenafil (Viagra®) to treat erectile dysfunction (Ballard *et al.*, 1998). Recently other drugs, such as tadafil (Cialis™) and vardenafil (Levitra™), which target PDE5 in vascular smooth muscle have been reported (de Tejada, *et al.*, 2001; Eardley & Cartledge, 2002). It has also been reported that PDE5 plays a role in the development and maintenance of pulmonary hypertension. Murray *et al* show that, following chronic hypoxic treatment of rats, PDE5A1/A2 and PDE3A mRNA transcript and protein levels are increased in the main intrapulmonary and resistance pulmonary arteries (Murray *et al.*, 2002).

1.2.6 The PDE6 family

The cGMP-specific PDE6 family is also known as the photoreceptor cGMP phosphodiesterases. This family of PDEs are exclusively expressed in the rod and cone photoreceptors of the retina and play a pivotal role as an effector protein in vertebrate signal transduction, which is mediated by the rhodopsin-coupled G protein, transducin (Yarfitz & Hurley, 1994; Beavo, 1995). Retinal rod PDE6 is composed of two catalytic sub-units, α and β, each is tightly associated with the inhibitory γ sub-unit (Deterre *et al.*, 1988). Cone PDE6 consists of two α sub-units associated with two of the cone-specific

γ sub-units (Hamilton & Hurley, 1990). The γ sub-units inhibit cGMP hydrolysis in the dark, and upon light stimulation of photoreceptors PDE6 is activated by GTP-bound transducin, which displaces γ from the catalytic domain (Beavo, 1995). PDE5 and PDE6 display a homology of 45-48% identity between catalytic domains and are similarly inhibited by competitive inhibitors, zaprinast, dipyridamole, and sildenafil (table 1.2) (Ballard *et al.,* 1998; Turko *et al.,* 1999).

1.2.7 The PDE7 family

The PDE7 family encodes a cAMP-specific PDE that is insensitive to cGMP, have an amino acid sequence that is distinct from the other cAMP phosphodiesterases, and are insensitive to PDE3 and PDE4 inhibitors (Michaeli, *et al.,* 1993). Two genes, PDE7A and PDE7B encode, through alternative mRNA splicing, different PDE7 isoforms. Three isoenzymes, PDE7A1, PDE7A2 and PDE7A3 have been identified (Bloom & Beavo, 1996). PDE7A1 is expressed in multiple tissues, and PDE7A2 is expressed mainly in skeletal muscle and cardiac myocytes (Wang *et al.,* 2000).

1.2.8 The PDE8 family

PDE8A has been shown to be expressed in testis, eye, liver, kidney, skeletal muscle and brain in mice and humans (Soderling *et al.,* 1998; Fisher *et al.,* 1998).The non-selective PDE inhibitor IBMX does not inhibit this cAMP-specific PDE (Soderling & Beavo, 2000). PDE8 has been shown to contain a PAS (Period, Arnt, Sim) domain, but the function of this domain has yet to be discovered.

1.2.9 The PDE9 family

PDE9 is specific for hydrolysis of cGMP and is not inhibited by the general PDE inhibitor, IBMX (Soderling *et al.,* 1998). To date, four variants of the PDE9 family has been identified (Guipponi *et al.,* 1998). PDE9 is expressed in the small intestine, kidney, liver, lung, brain, skeletal muscle, heart, thymus and spleen (Soderling & Beavo, 2000).

1.2.10 The PDE10 family

Studies have shown that the PDE10 family can hydrolyse both cGMP and cAMP, but may function as a cAMP-inhibited cGMP-hydrolysing phosphodiesterase (Loughney *et al.*, 1999; Soderling *et al.*, 1999). Like PDE2, PDE5, PDE6 and PDE11A, PDE10A contains two GAF domains. PDE10A transcripts have been found in the testis, caudate nucleus and putamen (Matsumoto *et al.*, 2003).

1.2.11 The PDE11 family

The PDE11 family is represented by PDE11A and hydrolyses both cGMP and cAMP (Fawcett *et al.*, 2000). It has unique splice variants, PDE11A1 possesses an incomplete GAF domain, PDE11A3 has one complete GAF domain and one incomplete GAF domain, and PDE11A4 contains two complete GAF domains (Yuasa *et al.*, 2000; Fawcett *et al.*, 2000). PDE11A3 transcripts are specifically expressed in the testis, and PDE11A4 transcripts are most abundant in the prostrate (Yuasa *et al.*, 2000).

1.3 PDE4 cAMP-specific phosphodiesterases

To date, eleven PDE families have been identified, of which PDE4, PDE7 and PDE8 specifically hydrolyse cAMP. However, it is the PDE4 family that accounts for the most cAMP hydrolysing activity of many cell types (Conti *et al.*, 2002). The *Drosophila dunce* gene was the first PDE gene to be characterised, and soon thereafter four PDE4 paralogues were identified on different mammalian chromosomes (Houslay & Adams, 2003).

1.3.1 PDE4 isoforms

The four PDE4 genes encode four different sub-families, PDE4A, PDE4B, PDE4C and PDE4D. Over 16 different isoforms are generated through the use of different promoters and alternative mRNA splicing and each isoform is characterised by a unique N-terminal region (figure 1.4) (Houslay & Adams, 2003).

PDE4 isoforms also possess a C-terminal region, which is unique to each sub-family. The highly conserved catalytic region is flanked at its N-terminal side by regulatory domains termed Upstream Conserved Region 1 (UCR1) and Upstream Conserved Region 2 (UCR2) (Conti *et al.*, 2003; Houslay & Adams 2003). The PDE4 isoforms can be divided into sub-groups; long forms, short forms or super short forms, depending on the presence or absence of UCR1 and the size of UCR2. Long forms possess both UCR1 and UCR2, short forms lack UCR1, whilst 'super' short forms possess only a truncated UCR2 (figure 1.4). In the case of long forms, the UCR1 is joined to the UCR2 by linker region 1 (LR1), and the UCR2 module is joined to the catalytic unit by linker region 2LR2 (figure 1.4).

UCR1 and UCR2 appear to function as a regulatory module that controls the functioning of the catalytic region. Indeed, yeast two-hybrid analysis and pull-down studies have shown that UCR1 can interact with UCR2 (Lim *et al.*, 1999; Beard *et al.*, 2000), and UCR2 is thought to interact with the catalytic domain (Lim *et al.*, 1999). The UCR1/UCR2 module is also considered to influence the quaternary structure of PDE4 whereby isoforms possessing both modules behave as dimers, yet isoforms lacking UCR1 behave as monomers (Richter & Conti, 2002).

1.3.2 Catalytic domain

A key insight into the structure of the catalytic site was provided following the determination of the crystal structure of the PDE4B2 isoform [Brookhaven Protein Data Bank (PDB) accession number 1FOJ] (Xu *et al.*, 2000). The crystal structure of residues 152-528 of the active PDE4B2, which is conserved throughout the PDE4 family, revealed that the compact PDE4 catalytic unit is comprised of 17 αhelices folded into three subdomains. Helices 6-13 contain residues critical for substrate binding, bind tightly a Zn^{2+} ion, and loosely bind an Mg^{2+} ion (Xu *et al.*, 2000; Houslay & Adams, 2003). Since the publication of the crystal structure of the catalytic site of PDE4B2, a number of other crystal structures of PDE4 isoforms have been published which provide further

understanding of the catalytic mechanism (Lee *et al.*, 2002; Huai *et al.*, 2003; Xu *et al.*, 2004).

With regards to PDE4 activity, the physiological relevant state is thought to be an enzyme having both a tightly bound Zn^{2+} and exchangeable Mg^{2+} at sites within the catalytic site itself (Houslay & Adams, 2003). Thus, the Mg^{2+} ion binds to the metal ion binding site 2 (Mc2) and is believed to be the subject to rapid exchange, which is attributable to the number of reported different conformational states of the catalytic domain (Lui *et al.*, 2001;Conti *et al.*, 2002). PDE4 inhibitors bind to the enzyme with kinetics suggesting the presence of multiple conformational states, and it is now accepted that prototype PDE4 inhibitor rolipram binds to two or more conformers of the catalytic domain (Conti *et al.*, 2002). It has been suggested that the high affinity rolipram binding state requires the presence of Mg^{2+}, whereas the low affinity rolipram binding state was seen in the apoenzyme , although this will be inactive (Laliberte *et al.*, 2000; Conti *et al.*, 2002). It is now well recognised that PDE4 enzymes can switch their conformational states through interacting with other proteins, such as PDE4A enzyme with SRC family tyrosyl kinases and the immunophilin, XAP2 and that PDE4D3 can alter its conformation and sensitivity to rolipram upon phosphorylation by PKA (McPhee *et al.*, 1999; Hoffman *et al.*, 1998).

1.3.3 Regulation of PDE4 activity by PKA

PKA phosphorylation of PDE4 long forms results in activation, altered rolipram sensitivity, altered Mg^{2+} sensitivity and the re-programming of the functional output of ERK phosphorylation (Houslay & Adams, 2003).

As discussed above, the UCR1/UCR2 of PDE4 functions as a regulatory module. It is now known that PDE4s from all four sub-families can be phosphorylated at a single serine residue within the UCR1 and activated (Sette *et al.*, 1994; Sette & Conti, 1996; Hoffman *et al.*, 1998; MacKenzie *et al.*, 2002). UCR1 possesses the PKA consensus

sequence RRESF, and PKA activation of PDE4 can be mimicked by replacing the target serine with either aspartate or glutamate residues (Hoffman *et al.*, 1998). In mammalian cells, PKA phosphorylation of PDE4 enzymes has been shown to increase their activity by some 60% (Hoffman *et al.*, 1998). However, such PKA phosphorylation of PDE4D3 produces a much larger increase in activity (2-3 fold) than is seen in PDE4A4 (50%), which may suggest a regulatory role for their N-terminal regions, or they undergo an additional modification which enhances the ability of PKA phosphorylation to increase PDE4D3 activity (Houslay & Adams, 2003).

It has been postulated that the glutamate residue, adjacent to the target serine of PKA, is involved in an ion-pair interaction that holds the enzyme in a low affinity state (Hoffman *et al.*, 1998). As a mutation of the glutamate residue to a neutral amino acid mimics activation, the phosphorylation of the serine residue is believed to disrupt the ion-pair interaction, resulting in activation (Hoffman *et al.*, 1998). PKA phosphorylation of the UCR1 is also believed to cause a conformational change that disrupts the UCR1/UCR2 interaction (Beard *et al.*, 2000) and, in the case of PDE4D3, this results in increase in its sensitivity to inhibition by rolipram (Sette *et al.*, 1994; Hoffman *et al.*, 1998; MacKenzie *et al.*, 2002;).

UCR2 has been suggested to exert a tonic inhibitory function upon the PDE4 enzyme, and phosphorylation of the UCR1 by PKA has been suggested to disrupt the interaction of UCR2 and the catalytic domain (Lim *et al.*, 1999). A similar activation of PDE4D3, as observed with PKA phosphorylation, was shown following the use of an antiserum generated to a C-terminal portion of the UCR2 (Lim *et al.*, 1999). This antiserum is thought, like PKA phosphorylation, to disrupt the interaction of UCR2 and the catalytic domain (Lim *et al.*, 1999).

PKA phosphorylation of PDE4D3 enhances the sensitivity of the enzyme to Mg^{2+} ions. The Mg^{2+} ion binds to the metal ion binding site 2 (Me2) within the catalytic domain and is essential for catalysis (Xu *et al.*, 2000).

1.3.4 Regulation of PDE4 by ERK

The third subdomain of the catalytic unit of all PDE4 sub-families, with the exception of PDE4A, contains an ERK consensus motif (Pro-Xaa-Ser-Pro). It has been shown both *in vitro* and *in vivo*, that the serine residue within this sequence can be phosphorylated by ERK (MacKenzie *et al.*, 2000; Hoffman *et al.*, 1999). Further, the ERK consensus site within the catalytic domain has been shown to be flanked by a kinase docking site, namely KIM, and a FXF motif which allows ERK specificity (MacKenzie *et al.*, 2000) (figure 1.5).

The phosphorylation of long form PDE4s by ERK leads to inhibition of the PDE4, where the serine target within the ERK consensus sequence is the only phosphorylated residue (Hoffman *et al.*, 1999; MacKenzie *et al.*, 2000). Such inhibition of long form PDE4s can cause a localised increase in cAMP (Houslay & Adams, 2003). However, the ERK-mediated inhibition of PDE4 long forms is transient, as the localised increase in cAMP allows PKA phosphorylation and activation of the long PDE4 isoform (figure 1.6) (Hoffman *et al.*, 1999; Houslay & Kolch, 2000). In contrast, PDE4 short forms, which lack UCR1, are activated by ERK (MacKenzie *et al.*, 2000). It was shown that ERK phosphorylation of short form PDE4D1 caused a small increase in cAMP levels (MacKenzie *et al.*, 2000). Interestingly, ERK has been shown exert either no effect or inhibits the 'super' short from PDE4D2, which lacks UCR1 and possesses a truncated UCR2, and on a catalytic unit construct that is free of both UCR1 and UCR2 (MacKenzie *et al.*, 2000).

1.3.5 Activation of PDE4s by negatively charged phospholipids

Various studies have shown that negatively charged phospholipids such as phosphatidic acid (PA) or phospholipids phosphatidyl-serine (PS) can increase PDE4 activity (DiSanto *et al.*, 1995; Nemoz *et al.*, 1997). An increase in activation of some 0.7-3 fold was observed for various PDE4 long forms, but activation of PDE4 short forms or 'super' short forms was not observed (DiSanto *et al.*, 1995; Nemoz *et al.*, 1997). The UCR1

region of long forms is ideally suited to interact with PA or PS as it is an amphipatic structure with a polar N-terminal half (positive net charge) and an apolar C-terminal half (Houslay & Adams, 2003). Thus, it is the placing of a negative charge by PKA (phosphorylation of RRESF), or by the binding of an acidic phospholipids that causes a similar conformational change and leads to the activation of the PDE4 (Houslay & Adams, 2003)

1.3.6 Signalling complexes and PDE4s

PDE4s can be targeted to specific subcellular regions and can interact with other signalling proteins to form distinct signalling modules (Houslay & Adams, 2003). The formation of such spatially confined signalling modules allows the generation and monitoring of 'pools' of cAMP (figure 1.7)

1.3.6.1 PDE4 and AKAPs

PKA can be held in discrete subcellular locations by interaction of the R sub-units with A-kinase anchoring proteins (AKAPs). AKAPs provide a means of compartmentalised signalling complexes which allow the close association of upstream signalling proteins with downstream targets. They were first discovered as contaminants of PKA type II holoenzyme preparations (Michel & Scott, 2002), and since this initial discovery, over fifty different members of the AKAP family have been identified (Michel & Scott, 2002).

The discrete localisation of type II PKA has mainly been attributed to association of the R sub-unit with an AKAP. Each AKAP contains an amphipathic helix that binds to the N-terminus of the RII sub-units and each contains a unique subcellular targeting domain, which allows localisation to discrete cellular regions (Carr *et al.*, 1991; Colledge & Scott, 1999). Although the association of RII-AKAP occurs at 100-fold greater affinity than RI-AKAP interaction (Burton *et al.*, 1997), AKAP interaction is not exclusive to the RII sub-unit. A number of "dual" specificity AKAPs which bind both RI and RII sub-units have

been identified, such MAP2d expressed in rat ovarian granulosa cells (Salvador *et al.*,2004) and AKAP7γ in oocytes (Brown *et al.*, 2003).

The ability of PDE4s to interact with AKAPs, and thus the overall signalling module, provides a control for the PKA activity. To date, the long form PDE4D3 has been shown to bind to several different AKAPS (Dodge *et al.*, 2001; Tasken *et al.*, 2001; Kapiloff *et al.*, 2001). In cardiac myocytes, PDE4D3, through its unique N-terminal binds to muscle selective AKAP (mAKAP) (Dodge *et al.*, 2001). The PDE4D3-mAKAP-PKA complex provides a self-regulatory module whereby cAMP levels rise, PKA bound to mAKAP is activated and will phosphorylate and activate PDE4D3. As the activity of PDE4D3 increases rapidly following PKA phosphorylation of UCR1, PDE4D3 amplifies the de-activation of the mAKAP-bound PKA and then PDE4D3 itself becomes de-phosphorylated (Houslay & Adams, 2003). Under hypertrophic conditions a redistribution of the PDE4D3-mAKAP-PKA complex from the cytosol to the perinuclear compartment is observed (Dodge *et al.*, 2001). Such 'reprogramming' of PDE4D3 may contribute to altered cellular functioning in the hypertrophic process (Dodge *et al.*, 2001; Houslay & Adams, 2003). It has also been suggested that PDE4D3 is part of the mAKAP complex associated with the Ca^{2+} channel RyR (ryanodine receptor) within cardiac myocytes (Mark *et al.*, 1999; Kapiloff *et al.*, 2001). A publication, which appeared while writing my thesis, indicates that the PKA phosphorylation of Ser13 within the N-terminal of PDE4D3 facilitates its binding to mAKAP (Michel *et al.*, 2004).

In Sertoli cell primary complex, PDE4D3 has been found to co-immunoprecipitate with AKAP450 and RIIα sub-units (Tasken *et al.*, 2001).The PDE4D3-AKAP450-RIIα signal complex is localised to the centrosomal area and implies a tight regulation of the phosphorylation state of centrosomal proteins.

1.3.6.2 Arrestin

Arrestins are scaffolding proteins, which play an important role in desensitisation of GPCR signalling. To date, four members of the arrestin family have been identified, β-arrestin1, β-arrestin2 and two visual arrestins (Luttrell *et al.*, 2001). Following agonist occupancy of the β_2-adrenergic receptor, desensitisation of the process of AC activation

has been shown by the means of the decoupling the Gs protein from the GPCR (Luttrell *et al.*, 2001). In this process the rapid desensitisation occurs when G-protein-receptor kinases (GRK) phosphorylates the β-AR, allowing the recruitment of cytosolic β–arrestin to the β–AR and thus uncoupling the receptor from Gs (Luttrell *et al.*, 2001).

Challenge of cells with a β–agonist shows a recruitment of a PDE4-arrestin complex to the β_2–AR (Perry *et al.*, 2002). This formation of a complex including β–arrestin1/2 and a PDE4 thus provides a means of cAMP degradation directly to the active site of cAMP synthesis (Perry *et al.*, 2002). In cardiac myocytes the recruitment of PDE4D3 and PDE4D5 to the plasma membrane is shown following β-adrenergic stimulation (Baillie *et al.*, 2003). Further, the recruitment of PDE4D to the β_2–AR in cardiac myocytes regulates the switching of the receptor coupling from Gs to Gi (Baillie *et al.*, 2003). In this report, it is suggested that the PDE4 controls the PKA-mediated switching of the β_2–AR coupling to the Gs, thus activation of AC, to coupling to Gi and thus activation of ERK (figure 1.8).

1.3.6.3 RACK1

The scaffold protein RACK1 (receptor for activated C kinase 1) was originally shown to bind protein kinase C (Ron *et al.*, 1994). However, RACK1 has now been shown to interact with a variety of proteins (McCahill *et al.*, 2002) including PDE4D5, to which it binds through a helical domain named RAID1 (RACK1 interaction domain) in the unique N-terminal PDE4D5 (Yarwood *et al.*, 1999; Bolger *et al.*, 2002). The functional consequence of the interaction of PDE4D5 with RACK1 has yet to be determined. Although, it has been proposed that most probable role of the recruitment of PDE4D5 to the RACKI complex, is to control cAMP levels in the vicinity of the complex and thereby the activity of any putative associated Epac/PKA (Houslay & Adams, 2003).

1.3.6.4 Src, Lyn and Fyn

Src, Lyn and Fyn are protein-tyrosine kinases, which play important roles in controlling a wide variety of cellular processes, and they contain SH3 domains. SH3 domains are globular units of ~60 residues which allow protein-protein interaction by binding proline-

containing motifs that have PXXP at their core (Pawson, 1995). The PDE4 isoforms, PDE4A4, PDE4A5 and PDE4D4 have been to interact with these tyrosine kinases via PXXP motifs (O'Connell *et al.*, 1996; Beard *et al.*, 1999; McPhee *et al.*, 1999). A role of this interaction is intracellular targeting, such as the localisation of PDE4A5 to peripheral membrane ruffles, and also localisation to the perinuclear region (Beard *et al.*, 2002).

It is believed that PDE4 enzymes exist in distinct conformational states that can be detected by alterations in sensitivity to rolipram (Houslay, 2003). Binding of Src family tyrosyl kinases through their SH3 domains to the LR2 region of PDE4A4 increases its sensitivity to rolipram (Beard *et al.*, 1999; McPhee *et al.*, 1999).

1.3.6.5 XAP2

XAP2, also known as ARA9 or AIP, is an immunophilin which has been shown to interact with Hsp90 as part of a complex containing the aryl hydrocarbon (dioxin) receptor (Carver & Bradfield, 1997). Recently, a novel function of XAP2 was identified, whereby it binds to PDE4A5 via its immunophilin domain. This interaction inhibits the activity of PDE4A5 and attenuates the ability of PDE4A5 to be phosphorylated by PKA (Bolger *et al.*, 2003). The functional significance of such interaction has yet to be determined. However, as other immunophilin domains have been shown to interact with different signalling components, it is thought that the PDE4A5-XAP2 interaction may act as a means of recruitment to distinct cellular regions (Bolger *et al.*, 2003).

The interaction of XAP2 with PDE4A5 may provide an additional mechanism of changing the conformation of this enzyme to alter its rolipram sensitivity (Bolger *et al.*, 2003).

1.3.6.6 TAPAS-1

The unique N-terminal region of PDE4A1 contains a novel microdomain called TAPAS-1 which allows this PDE4 to be exclusively membrane-associated (Baillie *et al.*, 2002). TAPAS1 selectivity interacts with phosphatidic acid (PA), which has been shown to be Ca^{2+} dependent, and allows the anchoring of PDE4A1 to lipid bilayers (Baillie *et al.*, 2002). This unique means of targeting may serve to shape gradients of cAMP. Also, the

unique structural feature of TAPAS-1 may also, in the future, play an important role in the identification and interpretation of other putative phospholipid binding domains (Baillie *et al.*, 2002).

1.3.6.7 Myomegalin

Myomegalin is a scaffold protein which is localised to the Golgi/centrosomal region. It has a domain similar to that dynactin/centractin, which can bind to activator protein-1, a SH3-like domain, a leucine-zipper region and a helix-loop-helix domain (Houslay and Adams, 2003). Yeast two-hybrid analysis done on PDE4D3 identified myomegalin as a potential binding partner (Verde *et al.*, 2001). Truncation analyses have shown that the extreme C-terminal of myomegalin interacts with N-terminal portion of UCR2 and confers targeting to perinuclear Golgi/centrosomal region (Verde *et al.*, 2001). It has yet to be reported if other PDE4 isoforms can interact with myomegalin.

1.4 cAMP signalling and PKA phosphorylation of proteins regulating cardiac function.

The function of the heart is regulated by the sympathetic nervous system. During sympathetic stimulation, activation of β–adrenergic receptors by adrenaline and other β–agonists initiate the production of cAMP and hence activation of PKA.

1.4.1 Interaction of cAMP and Ca^{2+} signalling within the myocardium

Cardiac myocytes comprise the majority of the cellular mass of the heart, they also account for over 60% of the number of cells of the heart. In cardiac myocytes, PKA plays a central role in many cellular processes, including contraction and relaxation, ion fluxes and gene expression (Walsh & Van Patten, 1994; Kapiloff *et al.*, 2002). PKA can phosphorylate and alter the function of several cardiac proteins, which in turn alters the overall function of the heart. PKA substrates in cardiac myocytes include the ryanodine

receptor (RyR), the cAMP-responsive element binding protein (CREB), troponin I (TnI), L-type Ca^{2+} channel or the dihydropyridine receptors (DHPR), and phospholamban to name but a few. In the case of relaxation and contraction, the cAMP signalling pathway can interact with and control some facets of the Ca^{2+} signalling pathway (figure 1.9).

Phospholamban (PLB) is an important protein, which is regulated by PKA and is involved in the regulation of cardiac contraction. This protein is found located in the cardiac sarcoplasmic reticulum (SR) and, depending on its phosphorylation state it regulates the Ca^{2+} pump SERCA2A; sarcoplasmic reticulum Ca^{2+} ATPase (MacLennan & Kranias, 2003). SERCA2A determines the rate of removal of Ca^{2+} from the cytosol into the SR, which is the intracellular Ca^{2+} 'store' (figure 1.9). This ATP-facilitated uptake of Ca^{2+}into the SR by SERCA2A accounts for over 70% of cytosolic Ca^{2+} removal, and determines the rate of relaxation of the heart (MacLennan & Kranias, 2003). SERCA2A can also influence cardiac contractility by determining the actual size of the Ca^{2+} store that is available for release for the next beat. Phospholamban (PLB), which means "phosphate receptor", in its dephosphorylated state binds to and inhibits SERCA2A at resting Ca^{2+} concentrations. Phosphorylation of PLB by either PKA (Ser 16) or by CaM kinase (Thr 17) results in a disruption of the interaction between PLB and SERCA2A, thus relieving the inhibition of SERCA2A and enhancing the relaxation rate of the heart (Simmerman & Jones 1998; MacLennan & Kranias, 2003).

The trigger for cardiac contraction is the elevation of Ca^{2+} concentration in the cytosol. A number of different receptors and channels are involved in the elevation of cytosolic Ca^{2+}, namely the ryanodine receptors (RyRs), the L-type Ca^{2+} channels (dihydropyridine receptors; DHPRs), plasma membrane Ca^{2+}-ATPases (PMCAs) and Na^{+}/Ca^{2+} exchangers (NCXs). It is known that both the RyRs and the L-type Ca^{2+} channels are phosphorylated and their function altered by PKA. The L-type Ca^{2+} is a voltage channel which allows the influx of Ca^{2+} into the cytoplasm in response to membrane depolarisation (Bers, 2002). The ryanodine receptor opening is stimulated primarily by Ca^{2+} influx through the L-type Ca^{2+} channel (Bers, 2002). Both the conductance of the L-type Ca^{2+} channels and RyRs can be potentiated by PKA phosphorylation (Kapiloff, 2002).

1.4.2 Compartmentalisation of cAMP signalling within cardiac myocytes

With respect to cAMP signalling, cardiac myocytes appear to be highly compartmentalised. Zaccolo and colleagues have shown by use of a fluorescence-resonance-transfer (FRET) reporter, the presence of distinct pools of cAMP and the spatial confinement of PDEs (Zaccolo & Pozzan, 2002; Mongillo *et al.*, 2004). To date, 13 different AKAPs, which play an important role in compartmentalisation, have been identified in cardiac myocytes. These include ezrin, AKAP-Lbc, AKAP15/18, mAKAP, AKAP79, gravin, yotiao, BIG2, AKAP220, AKAP95, AKAP149, AKAP121 and D-AKAP-1 (Ruehr *et al.*, 2004). Figure 1.10 depicts the intracellular targeting of some of these AKAPs within cardiac myocytes. The PDE4 isoform, PDE4D3 is believed to interact with the mAKAP complex, which is targeted to the RyR (Kapiloff *et al.*, 1999; Kapiloff *et al.*, 2001). The conductance of Ca^{2+} from the SR into the cytosol is increased by the PKA phosphorylation of the RyR (Ruehr *et al.*, 2003). The specific targeting of PDE4D3, via its interaction with mAKAP, provides a localised source of cAMP degradation and thus implicates PDE4D3 in the control of the phosphorylation status of RyR.

1.5 Assessment of intracellular cAMP gradients

The recent development of fluorescence resonance energy transfer (FRET) reporters provides a method studying the compartmentalisation of cAMP signalling in live cells. A sensor monitoring changes in cAMP has been generated and has played an important role in studying the compartmentalisation of cAMP signalling (Zaccolo & Pozzan, 2002; Mongillo *et al.*, 2004). This sensor is based on FRET between a donor fluorophore (CFP) and an acceptor fluorophore (YFP) fused to the regulatory (R) and catalytic (C) sub-units of PKA (figure 1.11). Zaccolo *et al* have been able to show, following β-adrenergic stimulation, the generation of microdomains of cAMP in neonatal cardiac myocytes (Zaccolo & Pozzan, 2002). Furthermore, by the use of such a reporter, they revealed the prominent role of PDE4s in the regulation of increases in cAMP within cardiac myocytes (Mongillo *et al.*, 2004).

A FRET reporter of PKA activity, named A-kinase activity reporter (AKAR), has also been developed (Zhang *et al.*, 2001). This reporter consists of a cyan fluorescence protein, a phosphoamino acid binding domain (14-3-3τ), a consensus substrate for PKA, and a yellow fluorescence protein. FRET changes are observed upon activation of PKA, and the phosphorylation of the substrate peptide within AKAR.

More recently, an Epac based FRET reporter, named Epac-camps has been used to gain further insight into the spatio-temporal organisation of cAMP signalling in live cells (Nikolaev *et al.*, 2004). Unlike the PKA FRET-reporter developed by Zaccolo *et al*, which is restricted by the binding to AKAPs, Epac-camps is distributed throughout the cellular cytosol and provides a novel method to image free cAMP concentrations. By use of Epac-camps, it was shown that following isoprenaline stimulation of hippocampal neurons, cAMP propagates from the site of the β_2-adrenergic receptor throughout the whole cell in a matter of milliseconds. Overall, FRET-reporters provide an important tool in the study of compartmentalisation of cAMP signalling.

1.6 Aims and objectives

For the first part of my study, I aimed to analyse the time-dependent PKA phosphorylation of Ser54 and Ser13 sites within PDE4D3. In addition, I studied the ability of other PDE4 long forms to be phosphorylated by PKA. Overall, the aim of my research was study the compartmentalisation of PDE4s by means of a dominant negative strategy, and finally, to gain functional insight into the compartmentalisation of PDEs within cardiac myocytes.

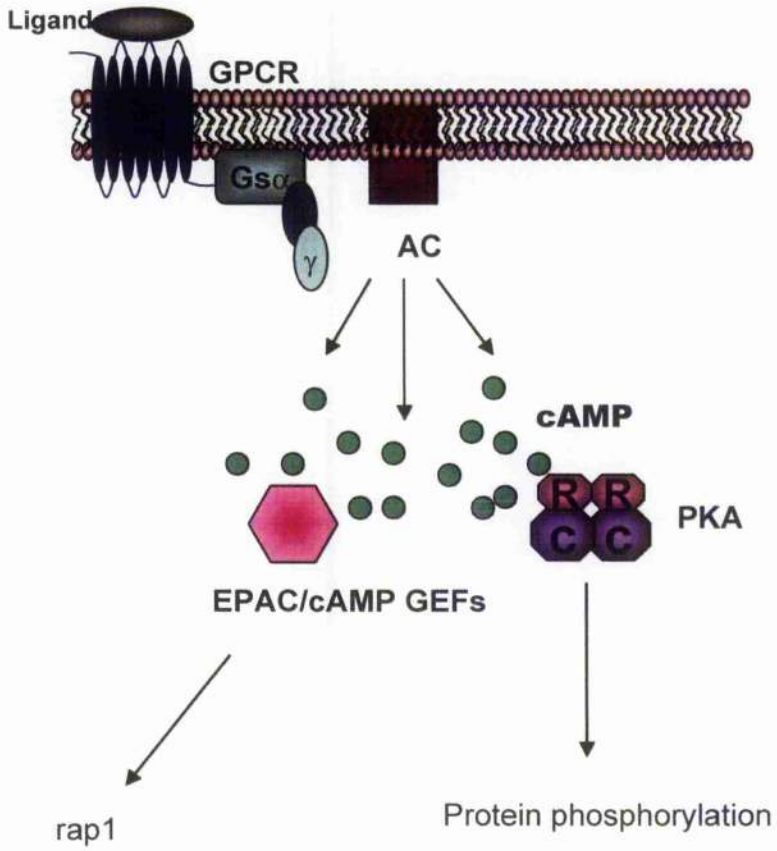

Figure 1.1. General schematic of initiation of cAMP signalling by G-protein coupled receptor activation. A ligand binds to the G-protein coupled receptor (GPCR) and leads the dissociation of the Gsα subunit. The Gsα subunit can stimulate adenylyl cyclase (AC) to produce cyclic AMP(cAMP). cAMP can exert its celluar effects via the activation of protein kinase A (PKA), Epac, or cyclic nucleotide gated ion channels.

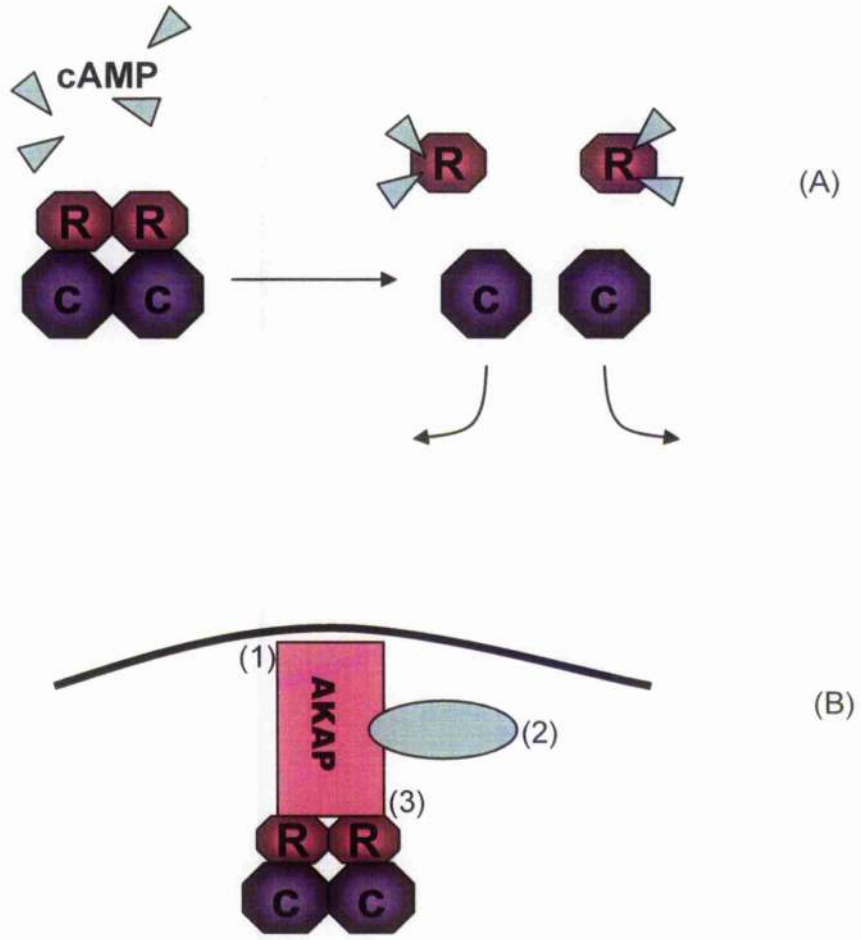

Figure 1.2. General schematics of PKA activation and AKAP interaction and function. (A) Binding of two molecules of cAMP to the regulatory (R) subunits of PKA induces the dissociation of the catalytic (C) subunits which are free to phosphorylate their target proteins. (B) (1) Represents the targeting domain which directs the AKAP to distinct subcellular regions (2) Represents other signalling complexes, of which include various PKA substrates (3) indicates the conserved amphipatic helix of AKAP which binds to the N-termini of the regulatory subunits of PKA.

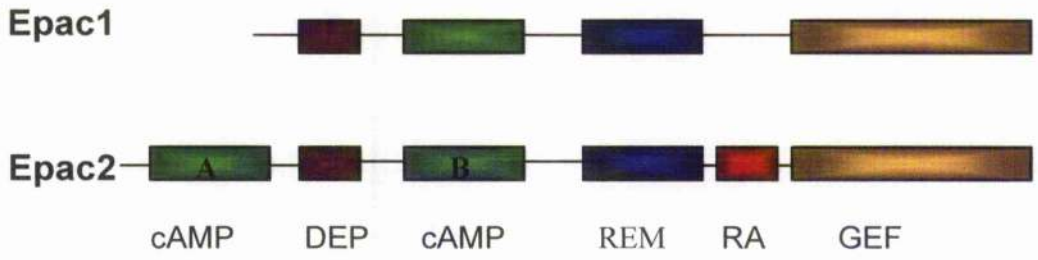

Figure 1.3. The domains of Epac1 and Epac2. The REM (Ras-exchanger motif) and GEF (guanine nucleotide exchange factor) form the catalytic region of Epac. The other indicated domains are : cAMP, cyclic AMP-binding domain; DEP, dishevelled Egl-10 Pleckstrin domain; RA , Ras association domain (adapted from Bos, 2003).

PDE family	Regulatory domains	Nucleotide Specificity
PDE1	Ca/CaM	cAMP/cGMP
PDE2	GAF	cAMP/cGMP
PDE3		cAMP
PDE4	UCR1/UCR2	cAMP
PDE5	GAF	cGMP
PDE6	GAF	cGMP
PDE7		cAMP
PDE8	PAS/PAC	cAMP
PDE9		cGMP
PDE10	GAF	cAMP/cGMP
PDE11	GAF	cAMP/cGMP

Table 1.1. PDE families and their regulatory domains. The PDE1-PDE11 families are listed including their regulatory domains and their nucleotide specificity (adapted from Houslay review, 2002).

Family	Inhibitor
PDE1	Vinpocetine, 8-MeoM-IBMX
PDE2	EHNA
PDE3	Milirone, cilostamide, amrinone, enoximone (and many others)
PDE4	Rolipram, Ro 20-1724, denbufyline zadaverine, RP73401, CDP840, SB207499, RS25344, LAS31025
PDE5	Sildenafil, zaprinast, DMPPO, dipyramidole, E4021, GF248
PDE6	zaprinast, dipyridamole
PDE7	none known
PDE8	Dipyridamole
PDE9	Zaprinast, SCH 51866
PDE10	IBMX, ?
PDE11	Dipyridamole

Table 1.2. Second-generation PDE isozyme inhibitors. The "second-generation" PDE inhibitors listed exhibit about 100-fold selectivity of PDE isozymes of a particular family (Dousa, 1999). However, at higher concentrations, the selective inhibitors are not absolutely specific. (Please see Dousa review for potencies and selectivity of the PDE inhibitors listed). The general PDE inhibitor IBMX, effectively inhibits isoforms from all families (K_i ~1-10μM), with the exception of the PDE8 and PDE9 families (adapted from Francis review, 2001).

PDE4 isoforms

Human	Clone	Rat	Clone	Type
4A1 (hRD1)	U97584	4A1 (RD1)	L27062	Supershort
4A4 (pde46)	L20965	4A4 (rpde6)	L27057	Long
4A7 (2el)	U18088	4A7		Catalytically inactive
4A8		4A8 (rpde39)	L36467	Long
PDE4A11	L20967	PDE4A11		Long
4A10	AF073745	4A10	AF110461	Long
4B1	L20966	4B1	J04563	Long
4B2	L20971	4B2	L27058	Short
4B3	U85048	4B3	U95748	Long
4B4		4B4	AF202733	Long
4C1	Z46632	4C1	L27061	Long
4C2	U88712	4C2		Long
4C3	U88713	4C3		Long
4D1	U50157	4D1	M25349	Short
4D2	U50158	4D2	U09456	Super-short
4D3	U50159	4D3	U09457	Long
4D4	L20969	4D4	AF031373	Long
4D5	AF012073	4D5		Long
4D6	AF536975	4D6		Super-short
4D7	AF536976	4D7		Long
4D8	AF536977	4D8		Long
4D9	AY245867			Long

Table 1.3. PDE4 isoforms. All human and Rat PDE4 isoforms identified to date are listed (adapted from Houslay review, 2002).

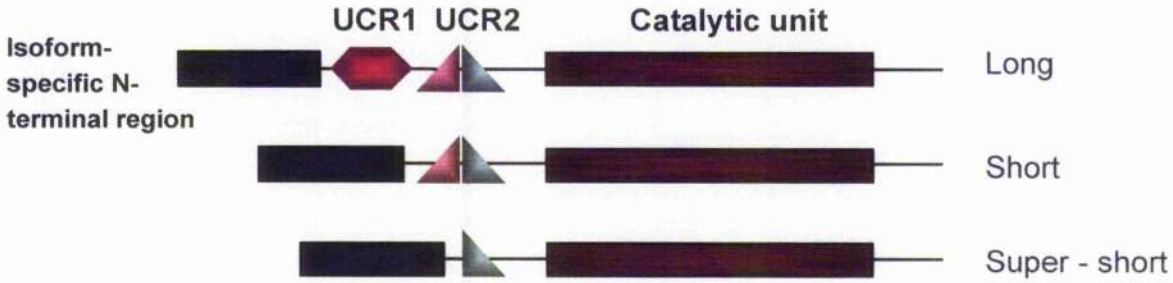

Figure 1.4. Schematic of the PDE4 enzyme family. PDE4 isoforms can be divided into categories of long, short or super-short isoforms depending the upstream conserved regions (UCR) regions. Long isoforms possess both UCR1 and UCR2, short isoforms lack UCR1 and super-short isoforms possess only a truncated UCR2.

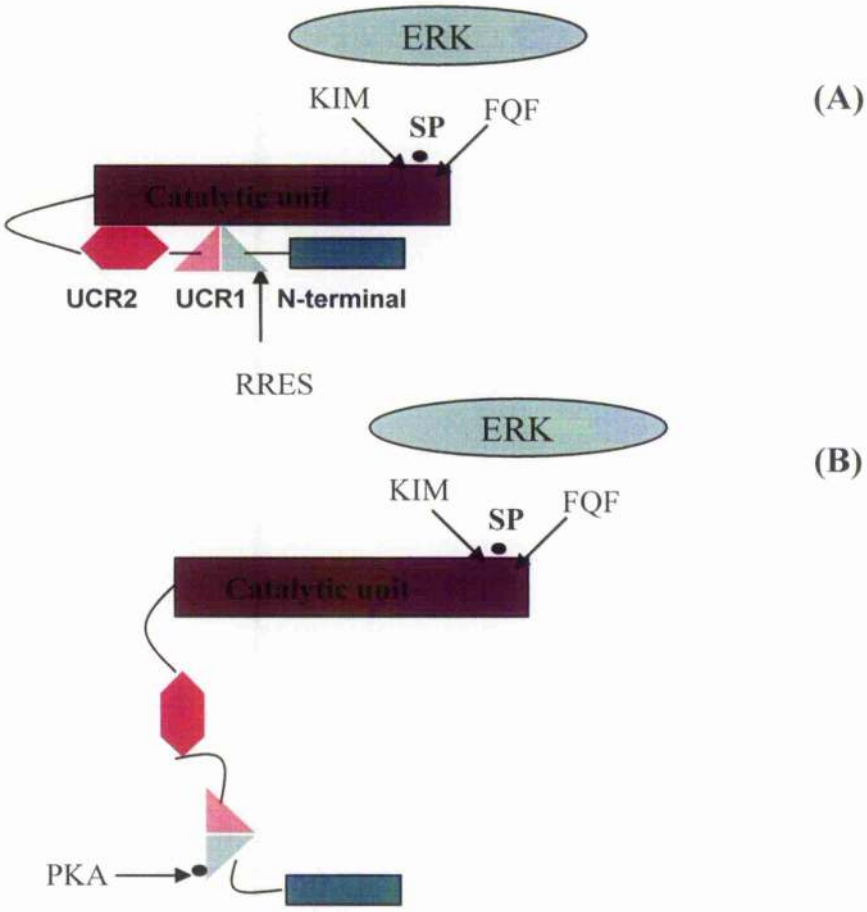

Figure 1.5. The regulation of PDE4 long forms by ERK2. (A) Inhibitory regulation by ERK2 phosphorylation. (B) PKA phosphorylation uncouples the inhibitory regulation by ERK2.

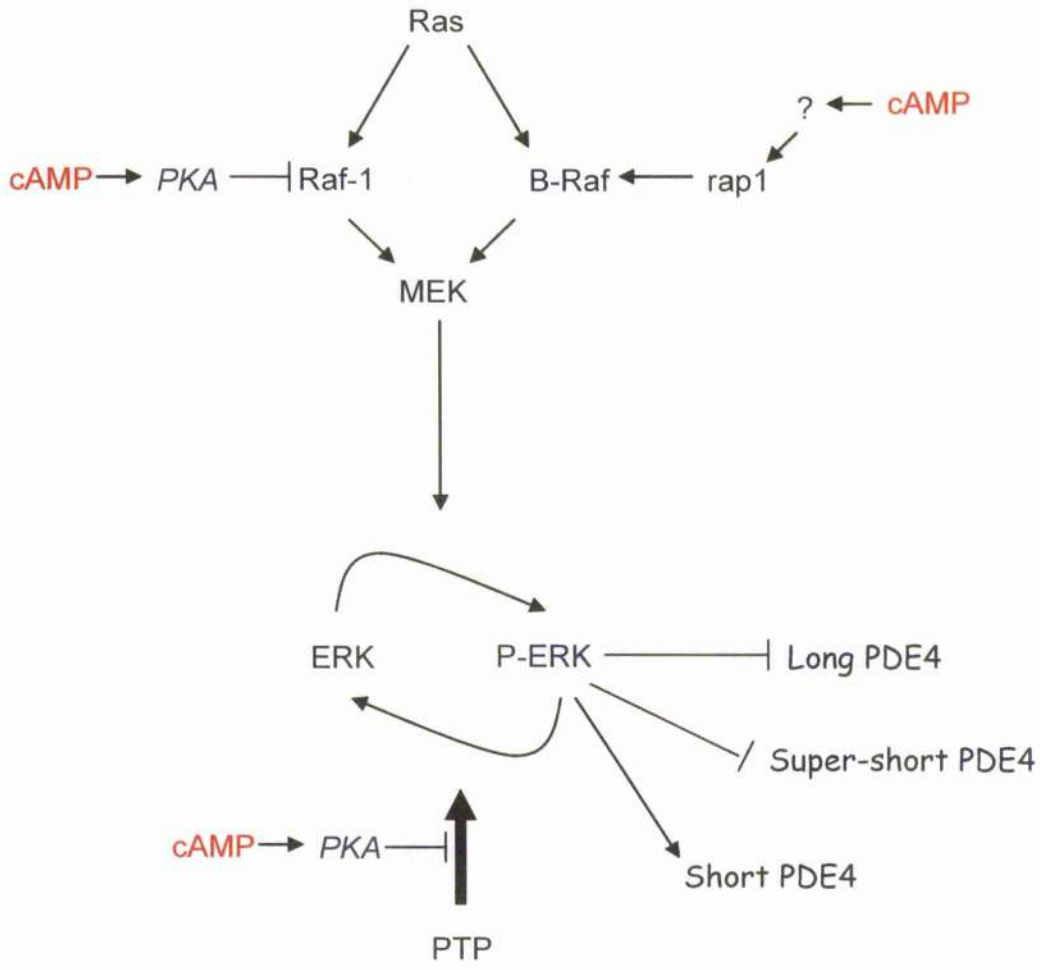

Figure 1.6. Crosstalk between cAMP and ERK signalling pathways. This basic schematic shows the points at which cAMP can influence control of the ERK signalling pathway. Arrows indicated positive coupling; blunt ended lines indicate inhibitory coupling; p-ERK indicates phosphorylated ERK. (Adapted from Houslay & Baillie, 2003)

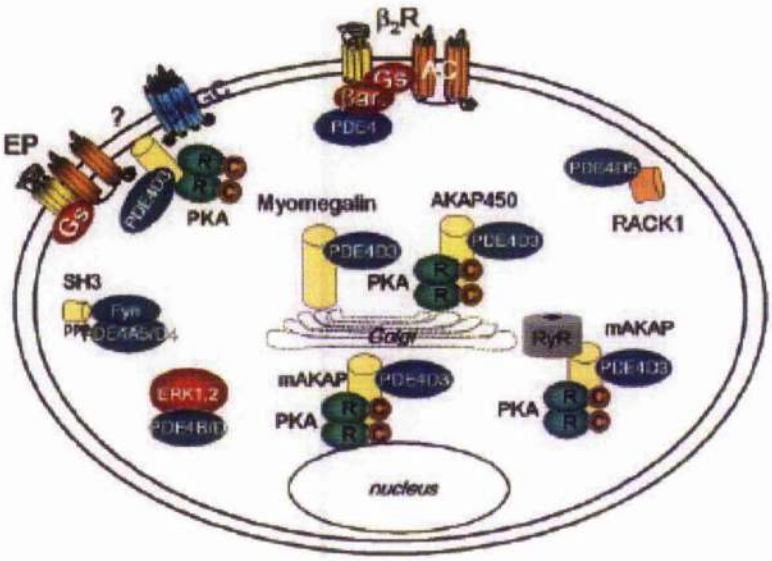

Figure 1.7. Compartmentalisation of PDE4s. A hypothetical cell to show the subcellular localisation of known PDE4 complexes. The yellow coloured 'barrels' represent anchoring proteins. (Taken from Conti *et al.*, 2003).

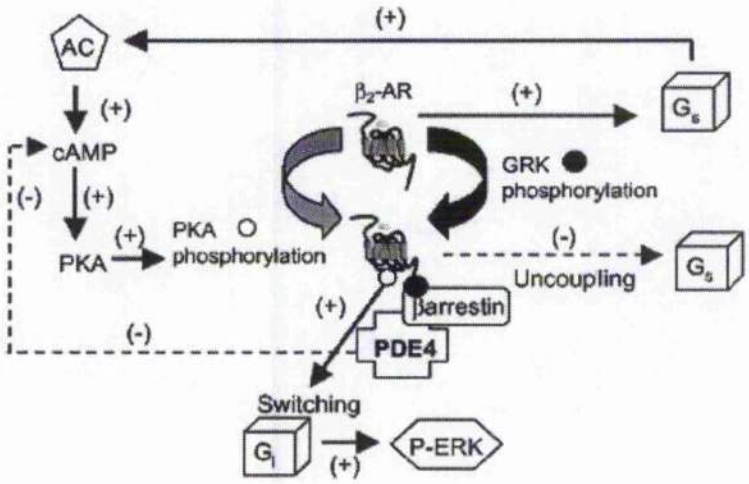

Figure 1.8. The role of recruitment of PDE4 by β–Arrestin in the regulation of the switching of Gs-Gi. Binding of ligand to the β_2 receptor results in the coupling to Gs, activation of AC, elevation of cAMP and activation of PKA. The PKA phosphorylation of the β_2 receptor facilitates switching from Gs to Gi and results in the activation of ERK1/2. The β–arrestin recruitment of PDE4 to the β_2 receptor attenuates the ability of PKA to phosphorylate the receptor and thus is involved in the control of the 'switching' (Taken from Baillie *et al.*, 2003).

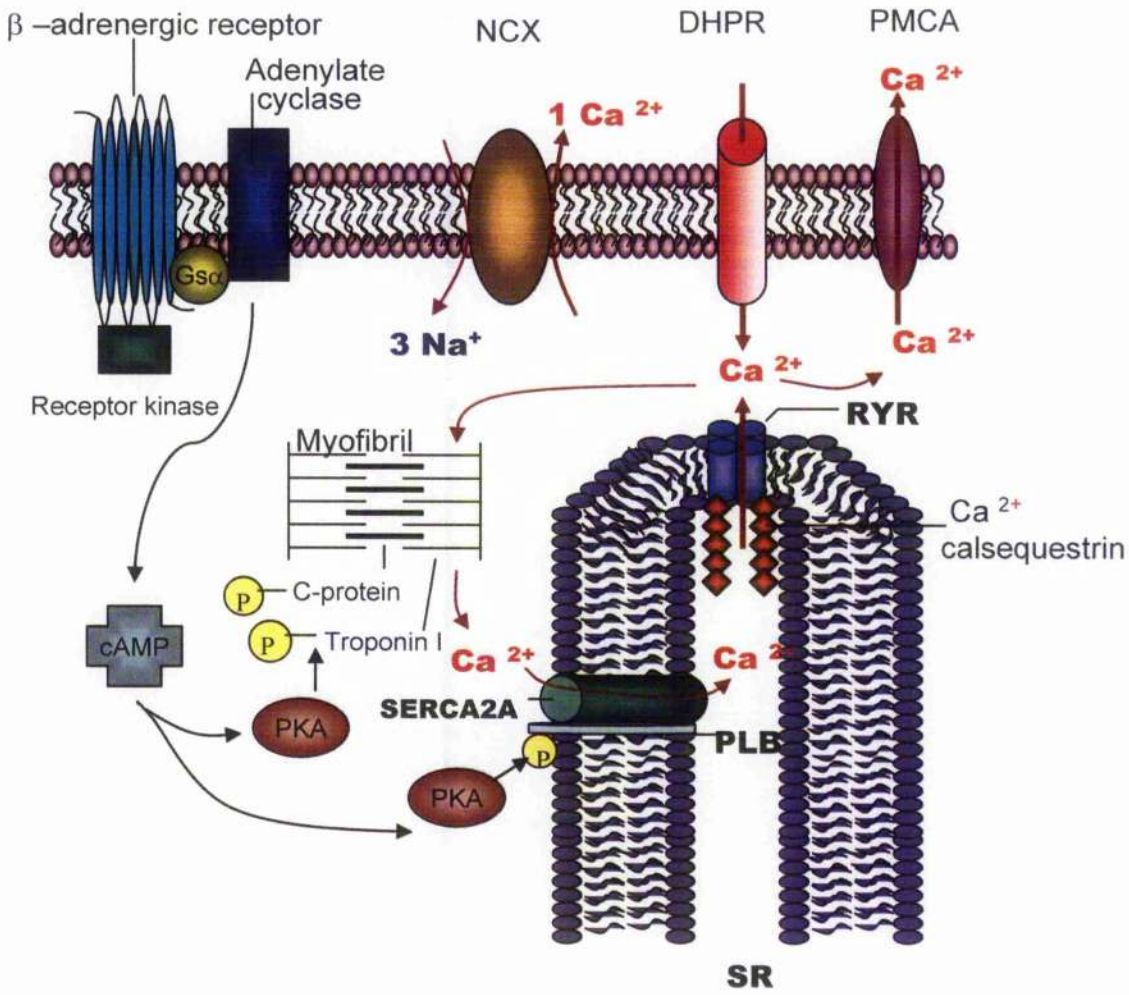

Figure 1.9. The interaction of the cAMP and Ca^{2+} pathways in cardiac myocytes following β-agonist stimulation. SR: sarcoplasmic reticulum, Ca^{2+} store, **RYR**; ryanodine receptor, releases Ca^{2+} from SR to the cytosol, **SERCA2A**; ATP dependent transport of Ca^{2+} from cytosol to SR, **PLB ;** phospholamban, -ve regulator of SERCA2A, **DHPR**; L-type, voltage dependent Ca^{2+}-entry channel (adapted from MacLennan & Kranias, 2003)

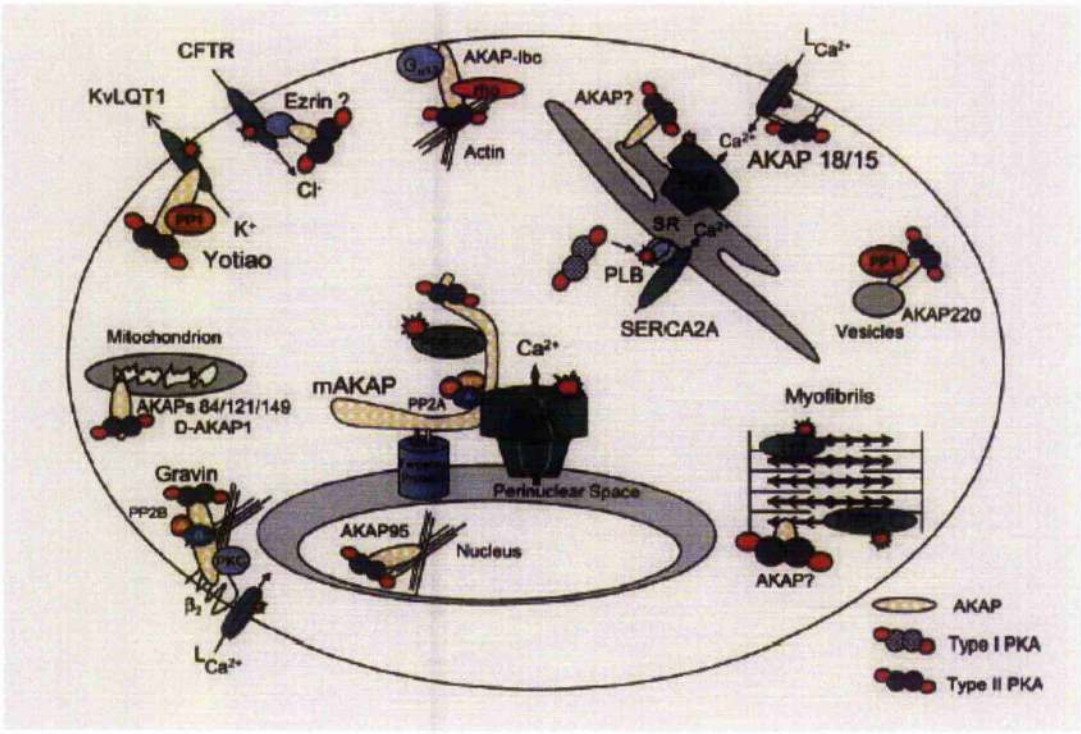

Figure 1.10. An illustration of the location of AKAPs identified in cardiac myocytes. AKAPs are associated with ion channels including the L-type Ca^{2+} channel ($L_{Ca}{}^{2+}$), the KCNQ1 delayed rectifier potassium channel (KvLQT1), ryanodine receptors (RyR), the cystic fibrosis transmembrane conductance regulator (CFTR), with the β_2 adrenergic receptor, sarcomeric proteins such as Troponin I and myosin binding protein- C (MBC) (taken from Kapiloff, 2003).

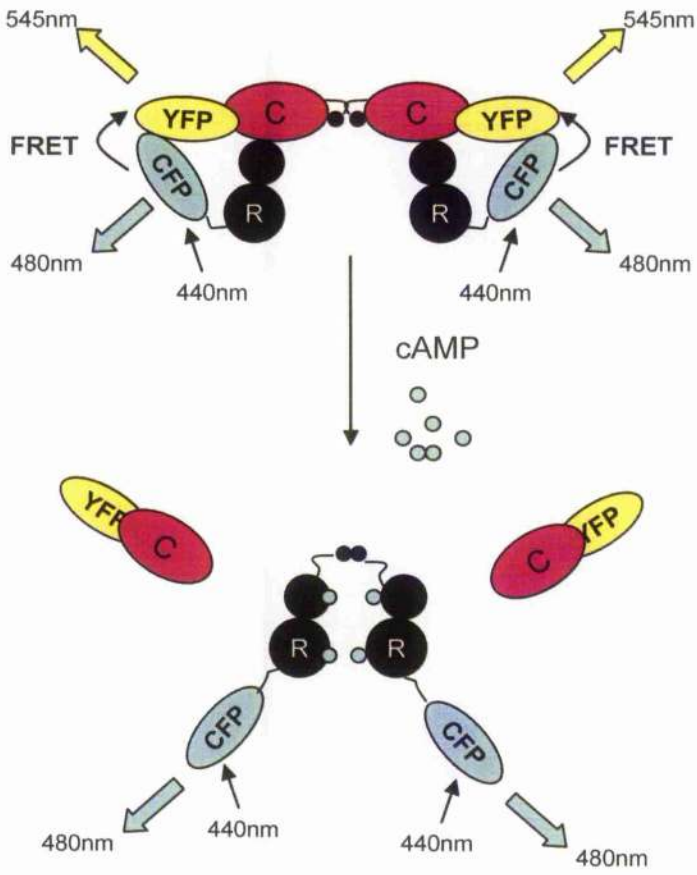

Figure 1.11. Schematic of a cAMP probe. In low cAMP concentrations the GFP tagged PKA is in its inactive tetrameric form and the FRET signal is maximal. When cAMP rises, active PKA catalytic subunits (C) are released; CFP and YFP diffuse apart and FRET is abolished (taken from Zaccolo & Pozzan, 2002).

Chapter 2

Materials and methods

2.1 Mammalian cell culture

2.1.1 HEK-293 cell line

HEK-293 cell line (ATCC CRL 1573) is a human embryonic cell with epithelial cell morphology. Cells were maintained in Dulbecco's Modified Eagles Medium (DMEM) supplemented with 2mM glutamine, 10% foetal bovine serum (FBS), 100 units/ml penicillin and 100 µg/ml streptomycin in an atmosphere of 5% CO_2 and 37 °C. Cells were passaged at 80-90% confluency, they were split 1:5. To passage the cells, they were rinsed with pre-warmed PBS and 1-2mls of pre-warmed 0.25% tripsin/0.03% EDTA solution was added. Flasks were incubated at 37 °C until cells detached. Cells were collected by adding 10 mls of culture media and centrifugation at 1000 g for 3 min. The cells were then resuspended in fresh culture media and transferred into new culture flasks at approximately 10^5 cells/ml final volume.

2.1.2 COS-1/ COS-7 cell lines

The COS-1/COS-7 cell lines (ATCC CRL 1650) are an African green-monkey derived cell line, with fibroblast morphology and are transformed with the SV40 virus. These cell lines were maintained and passaged as with HEK-293 cell line.

2.1.3 Neonatal rat ventricular myocytes

The ventricles were isolated fom 2-3 day old Spague-Dawley rat hearts enymatically digested at 37 °C using 0.48 mg/ml collagenase type II (Worthington) and 0.6 mg/ml pancreatin (Sigma) and suspended in a mix of 4 :1 DMEM :M199 supplemented with 10% horse serum and 5% fetal calf serum (all Sigma or Life Technologies) and were plated for 1 h on plastic culture plates to deplete fibroblasts. The non-adherent myocytes were the plated out at concentration of 1 million cells/well in 1% (w/v) gelatin pre-coated 6-well plates. After 24 hs the medium was changed to low serum medium (DMEM:M199) containing 4% horse serum and no calf serum.

2.2 Transfection of cells

2.2.1 DEAE-Dextran transfection of COS-1 cell line

The cells were passaged the day prior to transfection and allowed to grow to 50-70% confluency. The plasmid DNA (10 μg) was diluted to 250 μl with sterile TE buffer (1 mM Ethylenediaminetetra-acetic acid (EDTA), 10 mM Tris/HCL, pH 7.5) in sterile 15 ml centrifuge tube. To this tube, 200 μl sterile DEAE Dextran (10 mg/ml in PBS) was added, mixed and incubated at room temperature for 15 min. 10 ml of media supplemented with 10 % FCS, 2 mM glutamine and 100 units/ml penicillin and 100 μg/ml streptomycin. 1 mM filter sterilised chloroquine was added to the DNA. This solution was mixed an added to the cells which were then incubated at an atmosphere of 5% CO_2 and 37 °C for 3-4 h. After incubation, the media was removed and replaced with 10 ml sterile PBS supplemented with 10 % DMSO. Cells were incubated for 2 min, washed with PBS and fresh culture media was added. The transfected cells were incubated at an atmosphere of 5% CO_2 and 37 °C for 24-48 h.

2.2.2 PolyFect® transfection of HEK-293 cells

Transfection of HEK-293 cells was carried using PolyFect® reagent (Qiagen). The cells were passaged into 100mm dishes the day prior to transfection and grown to 50%-80% confluency. DNA, 8μg was diluted to a total of 300μl in basal medium (DMEM) in a sterile 15ml centrifuged and mixed. 80 μl of PolyFect® was added to the DNA solution, and it was mixed by vortexing for 10 sec. The DNA solution was incubated at room temperature for 10-15 min. Growth medium, 1 ml was added to the DNA solution and mixed by gentle pipetting. The growth medium from the cells was aspirated and replaced with 7 ml of fresh growth medium. The total DNA mixture was then added to the cells and mixed by gentle swirling. The cells were harvested 24-48 h post transfection.

2.3 Protein analysis

2.3.1 Whole cell lysate

Cell culture dishes were maintained on ice and all buffers used were ice-cold to minimise protein degradation and denaturing of enzymes. The cell growth media was aspirated and the cells washed with PBS. The PBS was drained and approx 100µl/100 mm dish 3T3-lysis buffer (20 mM N-2-Hydroxyethylpiperazine-N'-2-ethanesulfonic acid (HEPES), pH7.4, 50 mM NaCl, 50 mM NaF, 10 % glycerol, 1 % triton X-100, 10 mM Ethyleneglycol-bis(P-aminoethylether)-N,N,N',N'-Tetra-acetic acid (EGTA), 30 mM sodium pyrophosphate, proteases inhibitor cocktail) was added. The cells were scraped, transferred to a 1.5 ml eppendorf tube and snap-frozen. The cell samples were then thawed at 4 °C and subjected to mechanical disruption using a micropestle (Eppendorf). The cell debris was removed by centrifugation for 3 min at 10000g (4 °C). The cell lysates were stored at –80 °C until required for use.

2.3.1.1 Protein quantification (Bradford assay)

All protein assays were carried on 96 well titre plates. A standard curve of protein concentration was generated using 0.5 mg bovine serum albumin (BSA) diluted to 1 ml in distilled water. A protein concentration range of 1 µg/µl - 5 µg/µl was used for the assay. The protein quantification was carried out by taking 2 µl of lysate and placing (each sample in triplicate) in the microtitre plate. Bio-Rad Assay reagent was diluted 1/5 with distilled water, 200 µl was added to each well of BSA and lysate sample. The 96 well plate was then analysed using the Revelation program and an MRX microtitre plate reader (absorbance read at 590 nm). Protein concentrations were obtained by plotting the standard curve and using the least squared regression analysis to obtain the line of best fit. The equation of the line was used to determine the protein concentration of samples.

2.3.2 Gel electrophoresis and Western blotting.

2.3.2.1 Sample preparation

Lysate obtained from cells were assayed for protein concentration and 25 –100 µg protein diluted 1/5 with 5 x laemmli sample buffer (260 mM Tris/HCl pH 6.7), 55.5 % Glycerol, 8.8 % SDS, 0.007 % Bromophenol blue, 11.1 % 2-mercaptopethanol (Laemmli, Beguin *et al.*, 1970). The sample was boiled for 3-5 min to allow denaturation and reduction of the protein

2.3.3.2 SDS PAGE gels

Gels were run on a Bio-Rad Protean II xi cell. A resolving gel containing the appropriate percentage of acrylamide (determined by the molecular weight of the protein of interest), usually 8 % unless otherwise stated, was cast between the two plates of the gel apparatus (8 % 29 :1 acrylamide:N,N'-methylenebisacrylamide mix, 375 mM Tris/HCl (pH8.8), 0.1 % SDS, 0.1 % Ammonium persulphate, 0.06 % N,N,N',N',-tetramethylethylenediamine (TEMED)). This was overlaid with 1ml water and allowed to polymerise at room temperature, the water was then removed, the resolving gel overlaid with stacking gel (5 % 29 :1 acrylamide:N,N'-methylenebisacrylamide mix, 125 mM Tris/HCl (pH6.8), 0.1 % SDS, 0.1 % Ammonium persulphate, 0.1 % TEMED). A comb was then placed into the stacking gel and it was left for 30 mins to polymerise. The comb was removed and the wells were washed out with tris-glycine running buffer (192 mM Glycine, 25 mM Tris, 0.15 % SDS) to remove un-polymerised acrylamide. The gels were then assembled onto the central running stand according to the manufacturer's instructions and placed into the running tank containing tris-glycine running buffer. The pre-boiled samples were loaded into each well and a standard lane was loaded with 10 µl Bio-Rad prestained broad range precision protein markers to determined protein migration weight by gel electrophoresis. The top reservoir of the gel running tank was filled with running buffer and run for approximately 5 h at 35 mA per plate or 16 h at 8 mA per plate, until the dye front reached the bottom of the gel.

2.3.2.3 Nu- Page™ gel system

Pre-cast 4-12% Bis-Tris 1.0mm gels (Invitrogen) were used unless otherwise stated. The gels were assembled in Xcell *SureLock™* tanks according to the manufacturer's instructions. Depending on the molecular weight of protein of interest, either Nu- Page ™ MOPS buffer or Nu- Page ™ MES buffer was used to fill the tank. The pre-boiled samples were loaded into each well and a standard lane was loaded with 5 µl Bio-Rad prestained broad range precision protein markers to determined protein migration weight. The gels were run at 190 V constant for 1 h.

2.3.2.4 Protein transfer

A piece of Whatmann 3 MM paper was soaked in transfer buffer (192 mM Glycine, 25 mM Tris, 20 % Methanol). The SDS gel was placed on this and overlaid with a piece of nitrocellulose paper (Schleicher & Schuell) soaked in transfer buffer, ensuring that all air bubbles were excluded from between all layers. The nitrocellulose was in turn covered by another piece of Whatmann 3MM paper and the resulting sandwich was placed in a cassette between two pieces of foam soaked in transfer buffer. The cassette was placed with the nitrocellulose to the positive electrode in the Hoefer TE series transphor electrophoresis unit, filled with transfer buffer. The proteins were transferred with an applied current of 0.7 amps for 90-120 mins or 0.05 amps overnight.

2.3.2.5 Immunoblotting

Once transferred onto the nitrocellulose, ponceau S stain (0.1% Ponceau S, 3 % Trichloroaceatic Acid) was used to visualise the proteins. The ponceau S was added to the nitrocellulose for a few mins until the proteins became stained, the nitrocellulose membrane was then washed with distilled water. The unoccupied protein binding sites on the nitrocellulose were blocked with 5 % skimmed milk powder in TBS-tween20 (137 mM NaCl, 20 mM Tris/HCl (pH7.6), 0.1% tween20) for 1 h at room temperature with agitation. After blocking the membrane was washed several times in TBS-tween20 and the appropriate primary antibody added to the membrane diluted 1:10000, unless

otherwise stated, in 1 % skimmed milk powder in TBS-tween20. This incubation was carried out for 2 hs with vigorous shaking. The nitrocellulose was washed several times in TBS-tween20 before adding the secondary antibody, diluted as with the primary, to the membrane. The secondary antibody was anti-immunoglobulin (IgG) antibody conjugated to horse-radish peroxidase (HRP) and directed against the primary antibody. This was incubated with the nitrocellulose membrane for 1 h with vigorous shaking, after which the nitrocellulose was washed several times in TBS-tween20.The membrane was then incubated with ECL reagents (Amersham), according to the manufacturer's instructions. A piece of x-ray film (Kodak) was exposed to the membrane in a darkroom and then developed using a Kodak X-omat.

2.3.3 Immunopreciptation

Depending on which antibody is used to immunoprecipitate the target protein, either protein G sepharose or protein A sepharose was used. If a monoclonal antibody or a polyclonal antibody raised in a sheep was required for the immunoprecipitation, protein G beads were used. Protein A beads were used when the target protein was being immunoprecipitated with any other polyclonal antibodies.

2.3.3.1 Pre-clearing

30 µl of the appropriate beads were washed in 200 µl of lysis buffer and recovered by centrifugation at 13,000 g for 2 min at 4 °C (Heraeus refrigerated bench-top centrifuge). This was carried out three times. The beads were then added to the cell lysate diluted to a total of 500 µl with lysis buffer (approx 300 µg of protein) and incubated with end-over-end rotation at 4 °C, for 30 mins. The samples were then centrifuged at 13,000 g for 2 min at 4 °C to recover beads

2.3.3.2 Pre-Immune

If a pre-immune antibody was available, it was incubated with the cell lysate with end-over-end rotation at 4 °C for 30 mins. 30 µl of beads were then added to the lysate and again it was incubated with end-over-end rotation at 4 °C for 30 mins. The beads were recovered by centrifugation.

2.3.3.3 Binding of antibody and target protein complex to beads

After pre-clearing/incubation with pre-immune antibody the beads were collected by centrifugation at 13,000 g at 4 °C for 2 min, the supernatant was removed and placed into a fresh eppendorf tube. To this fresh tube 1-5 µl of the antibody was added and the tube rotated end-over-end at 4 °C for at least 2 hs, to enable the protein and antibody to bind. Then, 60 µl pre-washed protein beads was added to the sample and rotated end-over-end for at least 1 h at 4 °C. The beads were isolated from solution by centrifugation at 13,000 g at 4 °C for 2 min and washed to remove any non-specifically bound protein. The beads were washed at least five times in lysis buffer. A final wash of the beads was carried out with PBS if the isolated protein was to be used in SDS-PAGE or final wash was carried out in 20 mM Tris (pH 7.4), when the protein was used in a PDE assay.

2.4 Assays

2.4.1 Phosphodiesterase activity assay

A cAMP hydrolysis assay was used to measure phosphodiesterase activity. This used a modification of the two step procedure of Thompson and Appleman (Thompson and Appleman, 1971) as described previously by Marchmont and Houslay (Marchmont and Houslay, 1980). The assay worked on the basis that a ^{3}H-cyclic nucleotide (8 position of the adenine or guanine ring) was hydrolysed to form labelled nucleotide mono-phosphate. The nucleotide mono-phosphate ring was converted to the corresponding labelled

nucleoside by incubation with snake venom which has 5'-nucleotidase activity. The conditions were such that complete conversion takes place within the incubation time. Unhydrolysed cyclic nucleotide was separated from the nucleoside by batch binding of the mixture to Dowex-1-chloride. This removes the charged nucleotides but not the uncharged nucleosides.

2.4.1.1 Activation of dowex

To activate, 4 l of 1 M NaOH was added to 400 g of the Dowex 1 X8 -400 resin, and the mixture was incubated for 15 mins at room temperature with gentle mixing. The resin was allowed to settle by gravity and the 1M NaOH removed. The resin was then extensively washed with 4 l distilled water (30 washes). After its last wash the resin was resuspended in 4 l 1 M HCl and incubated for 15 mins at room temperature with gentle mixing before being allowed to settle by gravity. The HCl was removed and the activated resin resuspended 1:1 in distilled water and stored at 4°C until required.

2.4.1.2 Assay preparation

Samples of cell lysate (0.1 -50 µg depending on activity) were placed into 1.5 ml eppendorf tubes and made up to a volume of 25µl with 20 mM Tris/HCl, pH7.4. Each sample was assayed in triplicate. All tubes were set up on ice, and remained on ice until all components for the assay had been added. To every tube 50 µl 2 µM cAMP containing 3 µCi [^{3}H]cAMP in 20 mM Tris/HCl and 10 mM $MgCl_2$ pH7.4 was added, the tubes vortexed and incubated at 30 °C for 10 mins. After this time, the tubes were boiled for 2 mins to inactivate any PDE present and then cooled on ice. 25 µg snake venom (either *Ophiophagus Hannah* or *Crotalus atrox* venom) in 25 µl 20 mM Tris/HCl, pH 7.4 was added to each tube, mixed by vortexing and incubated at 30 °C for 10 mins. The tubes were cooled on ice and 400 µl Dowex/ethanol/water, in a 1 :1 :1 ratio was added and mixed. The tubes were then further incubated on ice for at least 20 mins. The tubes were vortexed and the dowex separated from supernatant by centrifugation at

13000 g for 2 min (Heraeus bench top centrifuge). Finally, 150 µl of the clear supernatant was added to 1 ml Opti-scint scintillation fluid and counted on a Wallac 1409 liquid scintillation counter.

2.4.1.3 Determination of PDE4 and PDE3 activity

The PDE3 family is specifically inhibited by the drug cilostamide and the PDE4 family by rolipram. PDE inhibitors were dissolved in DMSO as 10 mM stocks and the inhibitors were diluted in PDE assay dilution buffer for use in assay. DMSO itself does not affect PDE activity at the concentrations used (Rena *et al.*, 1995). Measurement of PDE activity with and without cilostamide (10 µM) and rolipram (10 µM) present gave the contribution of PDE3 and PDE4, respectively.

2.4.2 cAMP assay

Briefly, cells were stimulated and lysed, releasing the cyclic nucleotides. Following the release of the cyclic nucleotides, cAMP concentrations were determined using bovine crude PKA and 5' 8'-^{3}H cAMP.

2.4.2.1 Extraction of cAMP and neutralisation

Cells, plated in 6-well culture dishes, were incubated in growth medium containing 100 µM IBMX for 10 min. The cells were then stimulated with the named agonist for the indicated time, the growth medium removed and 100 µl of chilled 2% perchloric acid (PA) added. The cells were incubated on ice for 15 min, scraped and transferred to 1.5 ml eppendorf tubes. The precipitated protein was pelleted by centrifugation at 13000 g at room temperature.

2.4.2.2 Neutralisation of sample

The supernatants were transferred to eppendorf tubes containing 5 µl of Universal Indicator (pH 4.0 – 11.0, BDH) and a pink colour was observed- indicating pH 4.0. Initially, 5 µl of a neutralisation solution (2 M KOH, 0.5 M Triethanolamine) was added and the samples vortexed. The neutralisation was then achieved by the gradual addition of the neutralisation solution and observation of a colour change of the sample to green, indicating pH 7.5. Samples were then stored at 4 °C for up to 1 week before continuation of next steps of the assay.

2.4.2.3 Reagent preparation

The following reagents were prepared on day of assay:

cAMP assay buffer: 50 mM Tris+ 4mM EDTA pH 7.4

Binding protein: (10 mg bovine crude fraction PKA (Sigma) + 125 mg BSA)/ 25 ml cAMP assay buffer. Dilute 5-fold in cAMP assay buffer on day of use.

[^{3}H] 5', 3' cAMP: 8.7 µl of [^{3}H] 5', 3' cAMP/ 10 ml of cAMP assay buffer

Charcoal solution: In assay buffer, 2% (w/v) activated charcoal and 1% BSA and was stirred on ice for at least 20 min before it was required.

cAMP standards: A starting concentration of 16 pmol of cAMP was required. To obtain this, 16 µl of 10 µM cAMP was diluted to 500 µl in assay buffer. A series of 2-fold dilutions were then made.

2.4.2.4 Assay procedure

A standard curve was obtained using a range of cAMP concentrations between 0.0625 pmo l and 16 pmol. These tubes, along with the samples, were set up as follows:

Tube no.	cAMP (pmol/50 µl)	Buffer (µl)	[^{3}H] cAMP (µl)	Binding protein (µl)
1, 2	-	200	100	-
3, 4	-	100	50	100
5, 6	0.0625	100	50	100
7, 8	0.125	100	50	100
9, 10	0.250	100	50	100
11, 12	0.500	100	50	100
13, 14	1.00	100	50	100
15, 16	2.00	100	50	100
17, 18	4.00	100	50	100
19, 20	8.00	100	50	100
21, 22	16.0	100	50	100
23 -	samples	100	50	100

The tubes were set up as described on ice, adding the binding protein to the tubes last. Each tube was vortexed, incubated on ice for 2 h. Following incubation, 250 µl of charcoal solution was added and vortexed. The tubes where then centrifuged at 13000 g for 3 min, 300 µl of supernatant was decanted and added to 1 ml of scintillant. The [^{3}H] cAMP was counted on a Wallac 1409 liquid scintillation counter. Curve-fitting software was used to calculate pmol unlabelled cAMP per sample.

2.4.3 In vitro PKA phosphorylation assay

The PKA phosphorylation assay was set up in eppendorf tubes on ice as follows; the required concentration of purified recombinant PDE4, 1 unit of active PKA catalytic subunit (Promega), phosphorylation buffer (100 mM Tris, 10 mM $MgCl_2$ pH 7.4) to a final volume of 45 µl. To each assay tube, 5 µl of radiolabelled substrate (10 µCi [γ ^{32}P-ATP], 2 mM ATP) was added and the tubes were incubated at 30 °C for 15 min. The samples were prepared for gel electrophoresis as described previously, and phosphorylation was detected using a Biorad Personal Fx phosphoimager. All densitometry was performed using Quantity One software.

2.5 Laser Scanning Confocal Microscopy (LSCM)

2.5.1 Preparation of slides

COS1 cells were transfected as described previously. 48 h post-transfection, the cells were plated onto coverslips (22 mm x 22 mm) in 6-well tissue culture plates. 72 h post-transfection, the cells were stimulated as stated and fixed for 10 min using 4 % paraformaldehyde (dissolved in Tris buffered saline (TBS) (150 mM NaCl, 20 mM Tris, pH 7.4). The coverslips were then washed three times, for 5 min each time, in TBS. The cells were then permeabilised by incubating each slide for 15 min in 0.2 % Triton dissolved in TBS. Cells were then blocked for 1 h using a blocking solution (10 % goat serum, 4 % BSA dissolved in TBS). The primary antibody was diluted to the required concentration in diluant (Blocking buffer diluted 2-fold in TBS), 200 µl the antibody solution was added to each slide and incubated at room temperature for 1 h. The coverslips were washed three times with 5 min incubations in blocking solution and then incubated for 1 h with the relevant fluorescent probes at 1:200 dilution (Alexa 594-conjugated anti-mouse igG, Alexa 594-conjugated anti-rabbit or Alexa 488-conjugated

anti-rabbit (Molecular Probes). The cells were then washed five times in blocking solution before mounting the coverslips on slides with Immunomount (Sandon).

2.5.1.1 Visualisation of cells

The cells were visualised using a Plan-Apo 40 x 1.4 NA oil immersion objective and the Zeiss Axiovert 100 laser scanning confocal microseppe (Zeiss, Oberkochken, Germany). The Alexa 594-conjugated antibody was excited at 543 nm and detected at 590 nm. The Alexa 488-conjugated antibody was excited at 495 nm and detected at 518 nm.

2.6 Molecular biology techniques

All molecular biology techniques were carried out with sterilised equipment and buffers, to prevent contamination.

2.6.1 Large scale production of plasmid DNA

The antibiotic Ampicillin or Kanamycin (100 mg/ml), depending on the antibiotic resistance of the plasmid, was added to sterilised 500 ml LB growth media (170 mM NaCl, 0.5 % (w/v) BactoYeast Extract, 1 % (w/v) Bacto-Tryptone, pH7.5). A sample of DNA of interest was taken from a glycerol stock of transformed cells and transferred to to the 2 l flask of culture medium by means of a sterile pipette. The culture was incubated at 37 °C overnight with agitation. The cells were harvested the next day by centrifugation at 6000 g for 15 min using the JA-14 rotor in the Beckman refrigerated centrifuge. The DNA was extracted from the cell pellet using the Wizard Maxi-prep kit (Promega) according to the manufacturer's instructions.

DNA was precipitated from the eluted solution by the addition of 0.7 volumes room temperature isopropanol. The solutions were mixed and centrifuged at 15000 g for 30

min at 4 °C. The DNA pellet was washed with 5 ml room temperature 70 % ethanol and air-dried for 5-10 min before being resuspended in 500 µl dH_2O.

2.6.2 RNA isolation

Mammalian cells were grown to 70 – 90% confluency in $75cm^3$ tissue culture flasks. The cells were removed with Trypsin, transferred to 15 ml falcon tube and centrifuged at 1000 g. The supernatant was removed, the pelleted cells snap frozen and stored at – 80 °C until required. Total RNA was isolated from the cell pellet using a RNeasy Kit (Qiagen) and QIAshredders (Qiagen) in accordance to the manufacturer's instructions.

2.6.3 Quantification of DNA and RNA

Both DNA and RNA concentrations were measured using a WPA lightwave spectrophotometer blanked with distilled water. 5 µl DNA or RNA was diluted to 1ml with distilled water and absorbance measurements were taken at 260 nM and 280 nM.

The concentration of nucleic acid was then calculated using the following approximations:

An absorbance of 1 at 260 nM corresponds to	50 µg/ml double stranded DNA
	37 µg/ml single stranded DNA
	40 µg/ml of single stranded RNA

The ratio between the absorbance measurements at 260 nM and 280 nM provided an indication of the purity of the nucleic acid. In solution, DNA or RNA have A_{260} :A_{280} ratios of 1.8 or 2.0, respectively. If the absorbance ratio is significantly less than this it indicates that the nucleic acid may be impure.

2.6.4 Analysis of plasmid DNA

2.6.4.1 DNA restriction digest

The restriction enzyme and the optimum restriction buffer used in the reaction depended on the site of digestion of the DNA for subsequent manipulations. If two restriction enzymes were used and the optimum restriction buffers were not compatible ethanol, precipitation of the DNA between restriction digests was carried out. Each digest was carried out on 300 ng DNA in a total volume of 10 µl per restriction enzyme used in the reaction. 1 unit of restriction enzyme was used and the appropriate volume of 10 x restriction added to the mix. The digests were carried out for 1-2 hs at the optimal temperature for the enzyme, usually 37 °C.

2.6.4.2 Agarose gel analysis of DNA

DNA was visualised using agarose gel electrophoresis, the percentage of agarose used in the gel was dependent on the size of DNA fragment to be identified. Generally 1 % agarose was dissolved in 1 x TBE (9 M Tris base, 20 mM EDTA, 0.9 M Boric acid acid) by heating until the agarose dissolved. To this 0.01 % ethidium bromide was added, which enables visualisation of the DNA under a UV light source. The molten agar was poured into the gel apparatus, set up according to the manufacturer's instructions and allowed to set completely. The comb and end stoppers were removed, the gel tank filled with 1x TBE and the samples loaded into the lanes. All DNA samples were diluted 6:1 in Blue/Orange 6X loading dye (Promega). 5 µl standard 1Kb DNA ladder markers (Roche) were added to one of the lanes, which enabled prediction of the size of DNA fragments run on the gel. The gel was run at 50 V until the dye front had migrated along the gel and the fragments of DNA were separated. The gel was removed from the tank and the DNA observed under UV light.

2.6.5 Reverse transcription PCR

Total RNA was isolated as described previously. Frozen samples of total RNA were sent to Rachael Barber (Novartis) and she carried out the RT-PCR as follows:

Briefly, RNA samples were treated with Dnase (Qiagen) for 30 min at 37 °C and then tested by RT-PCR with and without reverse transcriptase. When this showed no contaminating DNA remained, samples were used to synthesise cDNA. 5µg of RNA was synthesised into first strand cDNA, and this was used for PCR profiling. Each PCR reaction mix used was tested with nuclease-free water as a negative control and brain cDNA as a positive control. All completed PCRs were run on 2 % agarose gels.

2.6.5.1 Dnase treatment

Each sample of RNA was made up to 75 µl with nuclease free water:

75 µl RNA

5 µl 20X DNase Buffer (0.6 mM Tris HCl, 72 mM $MgCl_2$, 120 mM NaCl)

20 µl RQ1 DNase

Reaction mix incubated for 30 min at 37 °C. Each sample was then re-purified up using Qiagen's RNeasy Mini Kit (Clean-Up protocol). The RNA was measured for concentration.

2.6.5.2 RT-PCR Test

The clean samples were then tested by RT-PCR with and without reverse transcriptase to ensure no contaminating DNA remained. Promega's Access RT-PCR Kit was used. Only when a sample had passed this test was it used to synthesise cDNA. A small volume of each RNA sample was diluted to 20 ng/ µl, and the following reaction set up in duplicate, one with AMV-RT and one with the same volume of nuclease-free water in replacement:

5 µl Reaction Buffer (kit)

0.5 µl dNTPs (kit)

1 µl 25mM Mg SO_4 (kit)

0.5 µl Tfl DNA Polymerase (kit)

2.5 µl β-actin Forward primer at 10 pmol/ µl

2.5 µl β-actin Reverse primer at 10 pmol/ µl

5 µl Nuclease-free water

5 µl RNA 20 ng/ ml

3 µl AMV-RT or Nuclease-free water

These were run on the following PCR program (RT-PCR60):

Step 1 48 °C for 45 min	Step 5 68 °C for 2 min
Step 2 94 °C for 2 min	Cycle back to Step 3, 39 times
Step 3 94 °C for 30 sec	Step 6 68 °C for 7 min
Step 4 60 °C for 1 min	Step 7 4 °C pause

Completed reactions were run on a 2% agarose gel and visualised using EtBr and UV light.

2.6.5.2 cDNA Synthesis

RNA was synthesised into first strand cDNA using Amersham Pharmacia Biotech's First Strand cDNA Synthesis kit. 5 µl of each RNA was diluted to 20 or 40 µl with nuclease-free water, and then heated to 65 °C for 10 min to denature any RNA secondary structure. Then 14 or 28 µl of cDNA reaction mix was added, and incubated for 1 h at 37 °C. The

completed reactions were made up to 100 µl with nuclease-free water so they would represent 50 ng of RNA per µl.

2.7 Microarray

Total RNA was isolated as described previously. Frozen samples of total RNA were sent to Novartis (Basle, Switzerland) and microarray analysis using the U133A chip was carried out as follows:

There were a total of 27 chips, grouped into 9 groups, as follows :

- PDE4A4 (3 chips)
- PDE4D3 (3 chips)
- PDE4D5 (3 chips)
- PDE4B2 (3 chips)
- PDE4A_2EL (3 chips)
- Ariflo (3 chips)
- Rolipram (3 chips)
- pCDNA control (3 chips)
- HEK control (3 chips)

Each group was compared with each other. Regulated genes were identified based upon fold-change and p-value.

Data Upload :

The data was downloaded from the DEMON database and then uploaded into GeneSpring for analysis.

Data Evaluation :

The data was plotted on box-plots to visualise the normality. The raw data displayed considerable variation. The following normalisation techniques were implemented :

- Measurments below 0 were set to 0.
- Each chip was normalised to the 50^{th} percentile.

The normalised data, when viewed on a box-plot showed much less variation. In order to reduce the number of false positive results, the normalised data was used for the analysis procedure.

Data Cleaning :

Probes showing no expression in more than 50% of the experiments were excluded from the analysis.

The U133A chip contains probes for a total of 22283 genes. After filtering out the absent calls there were 14022 genes remaining. The analysis procedure is based upon these genes.

Data Analysis :

Fold-Change : Mean expression values for each group were used to calculate the fold change between any two groups.

P-Value : A T-test was used to compare the mean values of each single gene between to groups. A heteroscedastic students t-test was used as this assumed unequal variances.

Chapter 3

PKA phosphorylation and activation of PDE4 cAMP phosphodiesterases

3.1 Introduction

3.1.1 Protein kinase A (PKA)

In eukaryotic cells, protein phosphorylation namely the introduction of one or more negatively charged phosphate groups, invariably produces a conformational change which can affect protein functioning. Within the cAMP signalling system, PKA serves to activate a plethora of specific target proteins which ultimately lead to altered cellular functions. Protein kinase A (PKA) is regarded as the main target and detector of cAMP, and through binding of cAMP is activated and can phosphorylate its target protein(s), which usually have a consensus motif of R-R-ϕ-S (ϕ: hydrophobic).

In the absence of cAMP, PKA is an inactive enzyme consisting of two catalytic subunits (C) bound to a dimerised regulatory subunit (R). Upon the cooperative binding of two cAMP molecules to each of the R subunits, the active C subunits dissociate and are free to phosphorylate serine and threonine residues on target proteins (Tasken and Skalhegg, 2000). Multiple isoenzymes of PKA exist and are suggested to be targeted within the cell through association with different A kinase anchoring proteins (AKAPS). The R-I subunits are found mainly in the cell cytosol whilst the R-II subunits are mostly found associated with the cellular membranes and cytoskeleton. This association of R-II subunits with the cell membranes is generally considered to be mediated by interaction with AKAPs. Thus an anchored isoform of PKA R-II is able to sample gradients of cAMP created by localised adenylyl cyclase isoforms, and anchored and/or cytosolic PDEs (Houslay, 1998).

3.1.2 PKA phosphorylation of PDE4D3

The PDE4 family is encoded by four different genes (PDE4A, PDE4B, PDE4C and PDE4D) and can produce a number of different isoforms through alternative mRNA splicing and the use of different promoters. Within a specific PDE4 subfamily, each isoform possesses a common catalytic region and C-terminal region but each possesses a

unique N-terminal region. Each isoform of the PDE4 family can be classed as short or long form depending of the presence or absence of UCR1; long form PDE4s possess both UCR1 and UCR2, short form PDE4s lack UCR1. Truncation studies have shown that the UCR1 and UCR2 can influence catalytic activity (Bolger *et al.*, 2000). It is thought that these regions of PDE4s can interact directly with each other via electrostatic interactions forming a regulatory module (Bolger *et al.*, 2000) and this regulatory effect can be altered by ERK MAP kinase and PKA (MacKenzie *et al.*, 2000). Extensive studies have shown that the PDE4D3 long isoform is rapidly activated and uniquely phosphorylated by PKA. Such phosphorylation occurs at two sites, namely Ser 13 in its unique N-terminal region and Ser 54 in the UCR1 (figure 3.1) (Conti and Sette, 1996; Hoffman *et al.*, 1999; Lim *et al.*, 1999; Liu and Maurice, 1999; Liu *et al.*, 2000; MacKenzie *et al.*, 2000; Baillie *et al.*, 2000). Mutational studies have shown that only PKA phosphorylation of Ser 54 is however required for activation (Sette and Conti, 1996), with the role of Ser 13 unknown. Interestingly, several investigators have suggested that a decrease in mobility of PDE4D3 is observed upon PKA phosphorylation and that mobility shift is related to enzyme activation.

This chapter follows the time-dependent phosphorylation by PKA, of both Ser 13 and Ser 54 within PDE4D3. For the first time, a phopho-specific antiserum has been generated to assess the individual PKA phosphorylation state of each of these sites.

Sequence alignments (figure 3.2) have shown that the PKA consensus sequence (RRESF) found in the UCR1 of PDE4D3 is also found in the UCR region of all PDE4 longforms from all PDE4 subfamilies. An antiserum was generated to the phosphopeptide sequence: SQRRES*FLYSDSDYDLSP (which reflects the amino acid sequence 49-67 of PDE4D3). This antiserum was shown to be specific for Ser 54(P) and employed to assess the capability of long PDE4 isoforms from each of the subfamilies to be phosphorylated by PKA. The over-expression of the selected PDE4 isoforms in the COS1 cell line was chosen for all experiments.

Results

3.2 Analysis of PKA phosphorylation of PDE4D3 and selected various other PDE4 long isoforms.

In this study, phospho-specific antibodies were used to assess the PKA phosphorylation state of PDE4D3 and other selected PDE4 long isoforms. Concerning the PKA phosphorylation of PDE4D3, I showed that the phosphorylation of both the Ser 13 and Ser 54 sites are required to obtain the low mobility species of PDE4D3 commonly observed upon SDS-PAGE analysis (Sette and Conti, 1996). The PDE4D3 PKA phosphorylation data also suggests that the phosphorylation of the Ser 54 may even precede that of Ser 13. In this chapter, I show that long isoforms from each of the four sub-families can be phosphorylated by PKA.

3.2.1 The detection of PKA phosphorylated at Ser 54 and Ser 13 sites by novel polyclonal antisera.

The phospho-specific antibodies were generated to the phospho-peptide sequences SQRRES*FLYSDSDYDLSP (reflects amino acids 49-67 of PDE4D3; within UCR1) and FRRHS*WISFDVDNGTSAGR (reflects amino acids 9-27 of PDE4D3; within unique N-terminal region). The antibodies were named PS54-UCR1 and PS13-4D3, respectively.

To test the novel antibodies for specificity, COS1 cells were first transfected to express PDE4D3. In order to raise cAMP levels and thereby activate PKA, the cells were treated for 10 min with the general PDE inhibitor IBMX (100 μM) together with the general adenylyl cyclase activator forskolin (100 μM) prior to harvesting. Lysates from untreated cells (basal) and IBMX/forskolin (IBMX/fsk) treated cells were subjected to SDS-PAGE electrophoresis. The immunoblots were then used to test the PS54-UCR1 and PS13-4D3 antibodies (figure 3.3). Neither antibody detects any immunoreactive species of PDE4D3

under basal conditions. However, both antibodies clearly detect an immunoreactive species at the PKA at raised cAMP levels (IBMX/fsk treated cells), consistent with PDE4D3 being PKA phosphorylated. Indeed, the detection of this species is blocked by treating the cells with the PKA inhibitor, H89 (1μM) and also by pre-incubating the antibodies with the peptide to which they were raised prior to blotting (MacKenzie *et al.*, 2002).

3.2.2 PKA phosphorylation and activation of PDE4D3

As the antibodies appeared specific for both PKA consensus sites in PDE4D3, they were used to study further the PKA phosphorylation and regulation of this PDE. To follow the phosphorylation rates of both Ser 13 and Ser 54 sites, COS1 cell were transfected with VSV-tagged PDE4D3 and subjected to an IBMX/forskolin time course (0-20 min) (figure 3.4).

In the absence of IBMX/ forskolin, PDE4D3 migrated as a single 'high-mobility' species (panel A). At 1-2 min IBMX/forskolin challenge both a 'high-mobility' and 'low-mobility' (doublet) was evident. The blots were stripped and reprobed with the PS54-UCR1 and a very similar pattern was observed (panel B). At 0 min a phosphorylated species was not detected, at 1-2min a doublet was observed and PDE4D3 migrated identically to the 'high-mobility' and 'low-mobility' identified with the VSV antibody. However, at 0 min the PS13-UCR1-4D3 antibody did not detect a phosphorylated species. Each film exposure from the PS54-UCR1, VSV and PS13-UCR1-4D3 blots were overlayed. According to the overlay, and the direct comparison of the VSV and PS13-UCR1-4D3 blots, only a single reduced mobility species of Ser 13 was evident (MacKenzie *et al.*, 2002).

The cAMP hydrolysing activity of PDE4D3 for the IBMX/Fsk time course described in the previous figure was assessed. COS1 cell were transfected with VSV-tagged PDE4D3 and subjected to an IBMX/forskolin time course (0-20 min). Cells were harvested at the indicated time points and the specific PDE activity was measured by PDE assay from

developed by Marchmont and Houslay (Marchmont and Houslay, 1980). This shows that the activity of PDE4D3 increased 2-3 fold in response to IBMX/forskolin treatment.

3.2.3 Analysis of the putative PKA phosphorylation of PDE4 long isoforms

It has been pointed out that an identical PKA consensus sequence to that found in the UCR1 of PDE4D3 is also found in the UCR1 of all long isoforms from each PDE4 subfamily (Sette & Conti, 1996; Souness & Rao, 1997) (figure 3.2). However, it had not been shown whether PKA could either phosphorylate or activate these various long isoforms from other PDE4 sub-families and it could not be simply be presumed that they are either able to be phosphorylated by PKA, and if so, activated. Indeed, the linker regions which connect the UCR1, UCR2 and catalytic regions have different primary amino acid sequences which may affect the accessibility of PKA to these enzymes and generation of an active state. I set out to assess whether PKA can phosphorylate long isoforms from each subfamily and if they were then activated.

3.2.3.1 PKA can phosphorylate long isoforms from PDE4A, B, C and D sub-families.

I wished to study if PKA did indeed phosphorylate the target serine within the UCR1 of long PDE4 isoforms from each sub-family in response to an IBMX/forskolin-induced increase in cAMP. COS1 cells were transfected with selected PDE4 long isoforms or mutants of these long isoforms where the putative target serine was mutated to alanine. The transiently transfected cells were pretreated with H89 or not and challenged for 10 min with IBMX/forskolin. The lysates analysed by western blot using PS54-UCR1 antibody to detect PKA phosphorylated species (figure 3.6a). In this experiment, after the challenge of the cells with IBMX/forskolin a PKA phosphorylated species was detected with the PS54-UCR1 antiserum for PDE4A8 (96 kDa), PDE4B1 (104 kDa), PDE4C2 (80 kDa) and PDE4D3 (105 kDa). Phosphorylation was not detected at basal cAMP levels, following pretreatment with H89 or in mutant isoforms.

In a separate experiment (performed by Simon MacKenzie, Houslay laboratory), the *in vitro* PKA phosphorylation of the long isoforms used in the previous experiment was shown (MacKenzie *et al.*, 2002). Here, COS1 cells were transfected with either wild type or mutant PDE4 long isoforms as in the previous experiment. Lysates were treated with activated PKA catalytic sub-unit and [^{32}P] ATP and analysed by SDS-PAGE and a phosphorimager (figure 3.6b). Phosphorylation was detected in the presence of the active catalytic PKA sub-unit, however, phosphorylation was not detected in the presence of the PKA inhibitor H89, in the PKA target serine mutants and in the absence of the PKA catalytic subunit.

3.2.3.2 PKA phosphorylation of the novel rat PDE4 long isoform PDE4B4.

During the study of the PKA phosphorylation of long PDE4 isoforms, a new cDNA termed pRPDE90 was cloned. This encoded a novel PDE4B isoform which we called PDE4B4. This PDE4B isoform is a long isoform, which possesses UCR1 and UCR2, and differs from the other PDE4B isoforms by a unique 17 amino acid N-terminal region (figure 3.7a). As it also possesses a PKA consensus sequence at the beginning of the UCR1, I set out to see if PKA phosphorylates PDE4B4 over-expressed in COS7 in response to treatment of the cells with either a cAMP analogue or to elevate cAMP levels with IBMX/fsk.

In this set of experiments, the PS54-UCR1 antibody was used to detect the PKA phosphorylated species of PDE4B4. COS7 cells were transfected with Flag-tagged PDE4B4 (C-terminal epitope tag), and were treated with the cAMP analogue dibutryl cAMP (dbcAMP; 100μM) in the absence and presence of H89 (0.5 μM). Lysates were analysed by western blotting with PS54-UCR1 and anti-Flag antibodies (figure 3.7b&3.7c). A PKA phosphorylated species was observed in the presence of dbcAMP, and the phosphorylation was reduced upon pretreatment with H89. A phosphorylated species was not observed in resting cell (basal) or in the mock control.

To analyse the PKA phosphorylation and activation of PDE4B4 in response to an elevation in cAMP generated by adenylyl cyclase, COS7 cells were transfected with

Flag-tagged PDE4B4, subjected to 10 min with IBMX (100 μM)/forskolin (100 μM) challenge either with or without H89 (0.5 μM) pretreatment. The PDE4B4 isoform was immunoprecipitated with anti-Flag agarose beads, analysed for PDE activity and immunoblotted with PS54-UCR1 and anti-Flag antibodies (figure 3.7b). A phosphorylated species was observed in the presence of IBMX/forskolin and was ablated with H89. The PDE activity of PDEB4 increased by approximately 50% in response to IBMX/forskolin challenge, and this activation was blocked with H89.

3.2.4 Analysis of endogenous PDE4D3 and PDE4D5 in COS1 cells.

It is now recognised that cAMP signaling is compartmentalized and many studies suggest that PDE4s can be distributed in distinct subcellular locations (Houslay and Adams, 2003) (See chapter 1). As compartmentalisation of PDE4s would allow the control of distinct pools of PKA, the PS54-UCR1 antibody may be useful in analysing the activation of different PDE4 long-forms phosphorylated and activated in response to the generation of distinct cAMP pools and gradients.

In this experiment, I set out to assess the possibility of using the PS54-UCR1 antibody to detect the phosphorylation status of endogenous PDE4D3 and PDE4D5 endogenously expressed in COS1 cells. To achieve near maximum cAMP levels and PKA activity, COS1 cells were subjected to an IBMX (100μM) /forskolin (100μM) challenge with analysis over the indicated time course (figure 3.8). As a control, cells were pretreated with H89 (0.5 μM) before being challenged for 10 min with IBMX/forskolin. Cells were lysed at the indicated time points, lysates analysed by SDS-PAGE and immunoblotting with PS54-UCR1 (panel A) and pan PDE4D antibodies (panel B). The PS54-UCR1 antibody appeared to detect many other 'non-specific' bands, however using the pan-PDE4 immunoblot as an overlay, phosphorylated PDE4D3 and PDE4D5 is indicated with arrows. A time-dependent increase in phosphorylation was observed, and phosphorylation of the 10 min time point was ablated by H89. Panel B shows a time-

dependent mobility shift of PDE4D3, which was blocked by H89. However, from 0 to 8 min of the time course (indicated by blue arrows), a non-specific phosphorylated band which migrated at the same weight of PDE4D3 was also observed.

3.3 Discussion

It had been previously established the long isoform PDE4D3 is a target for phosphorylation and activation by PKA (Sette and Conti, 1996; Hoffman *et al.*, 1998). This isoform is ubiquitously expressed in a variety of different tissues and cells. The PKA phosphorylation of PDE4D3 has been shown to result in a rapid 2-3 fold activation of this enzyme (Sette *et* al., 1994; Alvarez *et* al., 1995; Sette and Conti, 1996; Hoffman *et al.*, 1998) and this rapid activation has been suggested to act as means of desensitization to the cellular cAMP response (Sette and Conti, 1996; Houslay review, 1998). Biochemical analysis has shown that Ser 13 within the unique N-terminal and Ser 54 within the UCR1 are phosphorylated by PKA (Hoffman *et al.*, 1998; Sette and Conti, 1996). For the first time antiserum had been developed to two specific PKA sites in PDE4D3, namely, Ser 54 in the UCR1 and Ser 13 in the unique N-terminus. The development of these antisera provided me with the means to study the PKA phosphorylation of PDE4D3.

PKA phosphorylation of PDE4D3 results in an altered electrophoretic mobility on SDS-PAGE. The reason for this mobility 'shift', which has been suggested to indicate the activation of this enzyme, has yet to be explained (Sette and Conti, 1996; Oki *et al.*, 1998). I show, through activation of adenylyl cyclase, a time-dependent decrease in the mobility of PDE4D3. At 1 min of IBMX and forskolin challenge both a low mobility and high mobility species existed and for the remainder of the time points, the majority of PDE4D3 shifts to a low mobility species. Within the same time course and, this 'band shift' was paralleled using the antisera specific for PKA phosphorylated Ser 54 (PS54-UCR1) within the UCR1. At the 1 min time point, PS54-UCR1 detected a 'band-shift' which, following the overlay of the film exposures of VSV and PS54-UCR1 blots, is akin to both de-phosphorylated and phosphorylated PDE4D3. However, the antiserum specific for PKA phosphorylated Ser 13 (PS13-4D3) within the unique N-terminal,

following the overlay of the film exposures of PS13-4D3 and VSV blots, only detected a single low mobility species at all time points. A time-dependent increase in phosphorylation was also observed with PS13-UCR1. This suggests that in COS1 cells the PKA phosphorylation of both sites are required for the mobility shift and that the phosphorylation of Ser 54 may even precede that of Ser 13. The notion that the phosphorylation of both sites is required for the 'band-shift' is further suggested by mutation of either these sites to alanine preventing the PKA mediated change in mobility of long-form PD4D3 (MacKenzie *et al.*, 2002).

Other than the generation of PDE4D3 by the PDE4D gene, three other PDE4 gene families (A, B and C) also generate a range of long-form PDE4s. All long-forms contain a PKA consensus sequence Arg-Arg-Glu-Ser-Phe. I show, using selected long isoforms, that PKA can phosphorylate the cognate target serine within the UCR1 of long-form PDE4s from each sub-family. In intact cells the PS54-UCR1 antibody detected the PKA phosphorylation of transiently transfected PDE4A8, PDE4B1, PDE4C2 and PDE4D5 following the activation of adenylyl cyclase. For each long-form, this phosphorylation was ablated using the PKA inhibitor H89 and by mutating the putative target serine to alanine. The PKA phosphorylation of these isoforms has been demonstrated *in vitro* (figure 3.6b). In this experiment, recombinant active catalytic unit of PKA is shown to phosphorylate the wild type but not the mutated alanine forms. Further experiments from our research group have shown that these isoforms are activated by PKA. Thus, it has been shown by two approaches that PKA phosphorylates a cognate serine residue in UCR1, and that this phosphorylation results in an activation of the PDE4. This analysis may serve as a model of the phosphorylation and activation of endogenous PDE4s where PKA is activated in response to localised increases in cAMP.

During my PKA studies, as discussed above, a new PDE4B long form (pRPDE90) was cloned from cDNA isolated from rat brain and characterized (Shepherd *et al.*, 2003). This novel PDE4B long form was named PDE4B4 and differed from the other previously isolated PDE4B long forms due to its 17 amino acid N-terminus. It had been found to be more active than PDE4B1 and exclusively found in the cytosol. As with all the other

previously characterized PDE4 long forms, PDE4B4 possesses a PKA consensus sequence within the UCR1, however, its unique N-terminal region might have conferred a conformational alteration which could prevent the access of PKA. I set out to ascertain if PDE4B4 was phosphorylated and activated by PKA in response to elevated levels of cAMP. Using the PS54-UCR1 antiserum I found in COS7 cells transiently transfected with PDE4B4, that this novel PDE4 long form was indeed phosphorylated by PKA in response to elevation of cAMP (via activation of adenylyl cyclase). This phosphorylation was ablated by pre-incubation with the general PKA inhibitor H89. An elevation in cAMP through the activation of adenylyl cyclase also resulted in a 1.5-2 fold increase in the activity of PDE4B4. Additionally, I show by treating cells with a cAMP analogue (dibutryl cAMP), PDE4B4 becomes phosphorylated by PKA and that H89 ablated this phosphorylation.

There is growing evidence that PDE4s are anchored to specific subcellular locations (Houslay & Miligan, 1997; Houslay *et al.*, 1998; Houslay, 2001) and anchored, localised PKA can sample and respond to cAMP gradients (Colledge and Scott, 1999). Therefore, the PS54-UCR1 antiserum may provide an interesting tool to analyse the PKA phosphorylation status of endogenous long form PDE4s in response to generation of localized cAMP pools by different Gs-coupled agonists. As a prelude to examining the putative differential PKA phosphorylation of PDE4 longforms in response to localized cAMP gradients, I devised a basic experiment to test the PS54-UCR1. I chose the COS1 cell line which is known to endogenously express a range of PDE4 long forms including PDE4D3 and PDE4D5. In order to obtain a time-dependent near maximal increase in cAMP levels within these cells, I subjected them to IBMX/forskolin time course. The lysates were then analysed with the PS54-UCR1 antiserum in order to compare the phosphorylation PDE4D3 and PDE4D5. After many changes in experimental conditions, the PS54-UCR1 antibody was decided to be inappropriate to use for the detection of PKA phosphorylated PDE4s as it detected too many 'non-specific' bands upon western blotting.

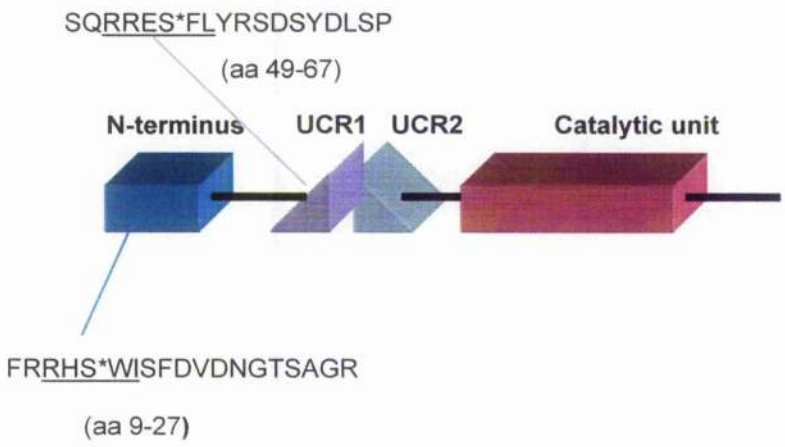

Figure 3.1 A schematic of long form PDE4D3. The novel antiserum PS13-4D3 and PS54-UCR1 were generated to the peptide sequences which represent amino acids 9-27 (unique N-terminus) and 49-67 (UCR1) of 4D3, respectively. Underlined are the PKA consensus sequences, and the phosphorylated serine is indicated as (S*).

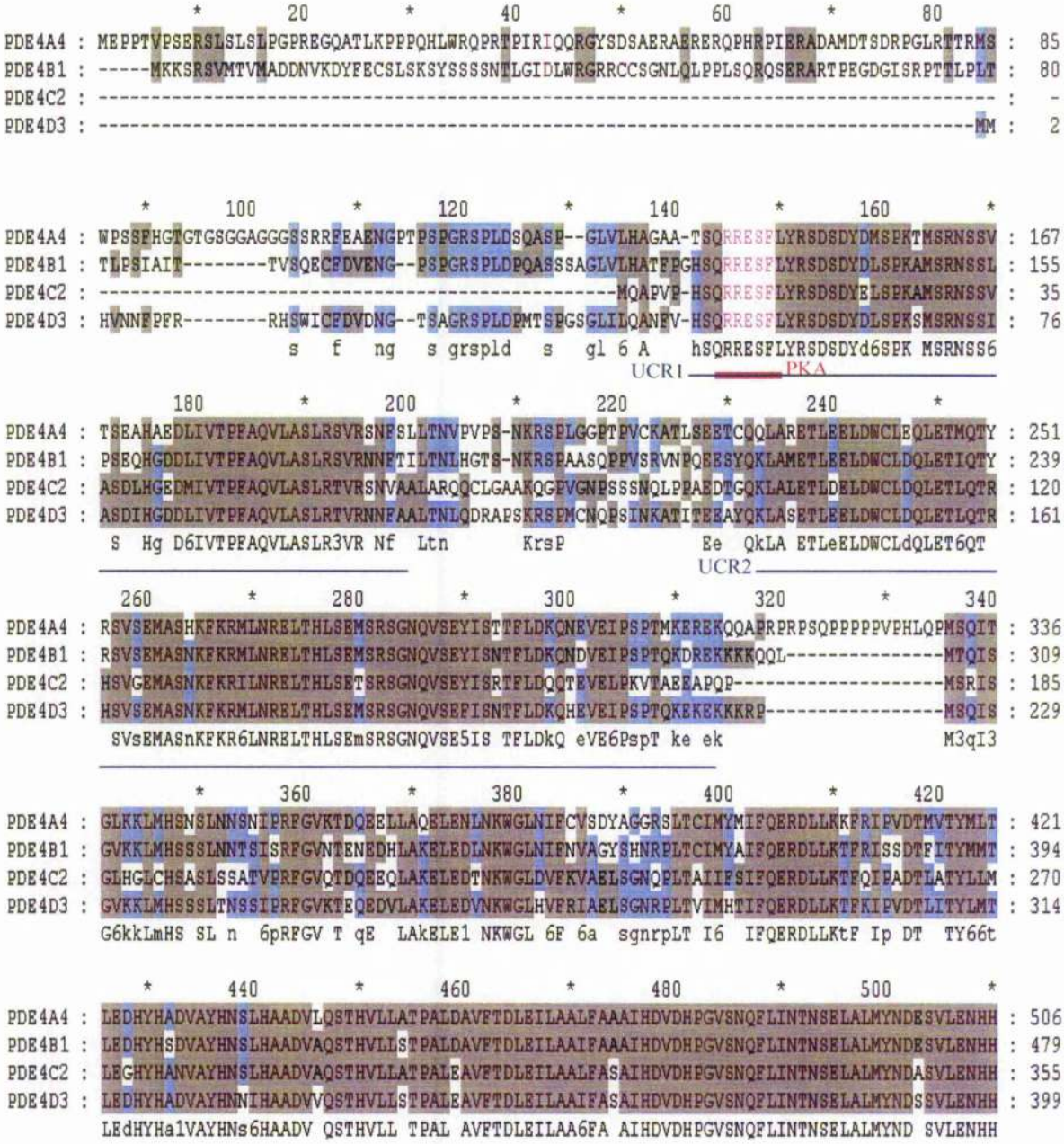
UCR1
PKA
UCR2

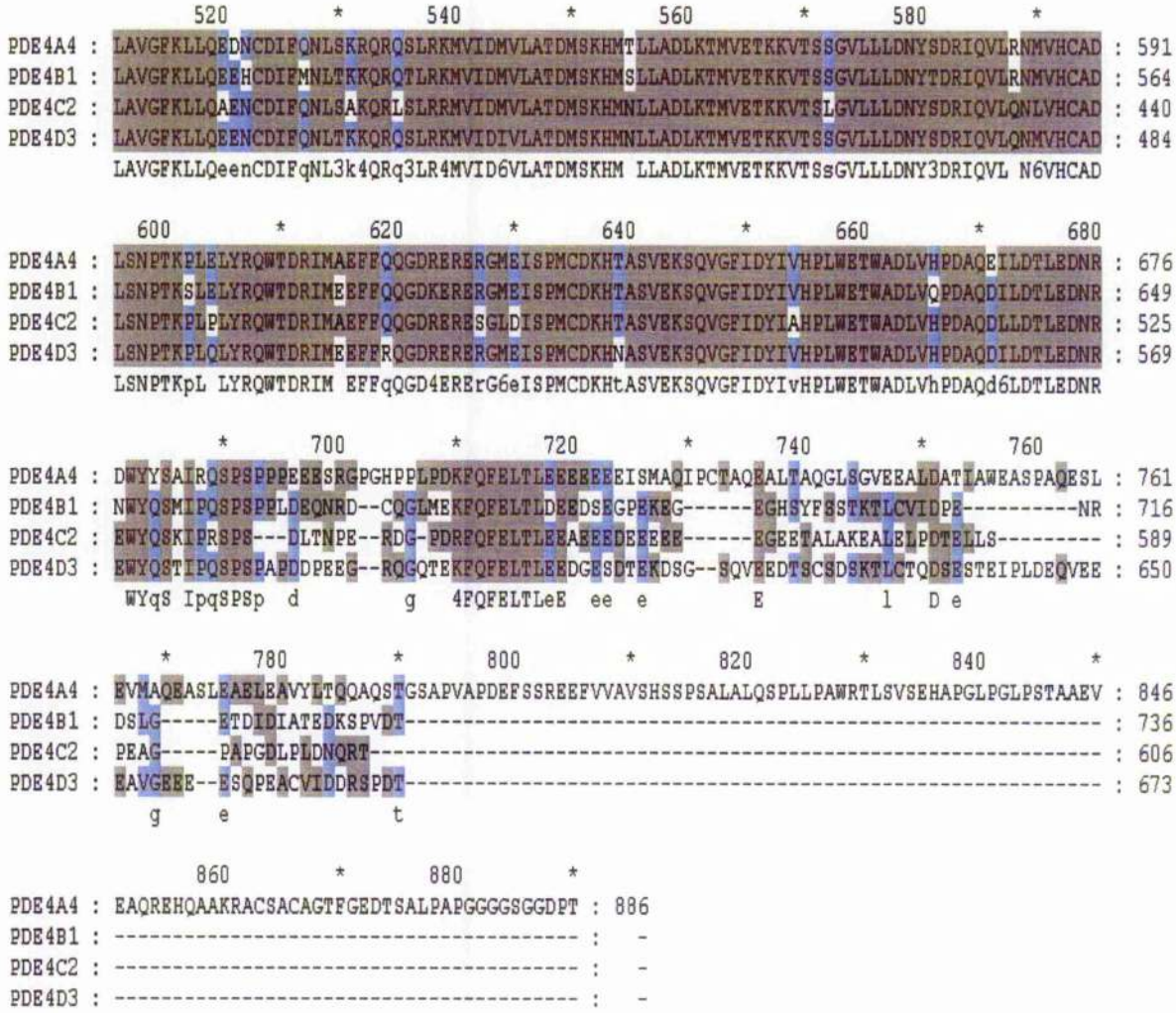

Figure 3.2 Sequence alignment of selected long PDE4 isoforms from each PDE4 subfamily. The amino acid sequences of PDE4A4, PDE4B1, PDE4C2 and PDE4D3 are aligned, The PKA consensus sequence (RRSEF) is found in the upstream conserved region (UCR1) is highlighted in purple, the UCR1 and UCR2 regions are underlined. Sequences were obtained from Genbank and aligned using Clustal Program.

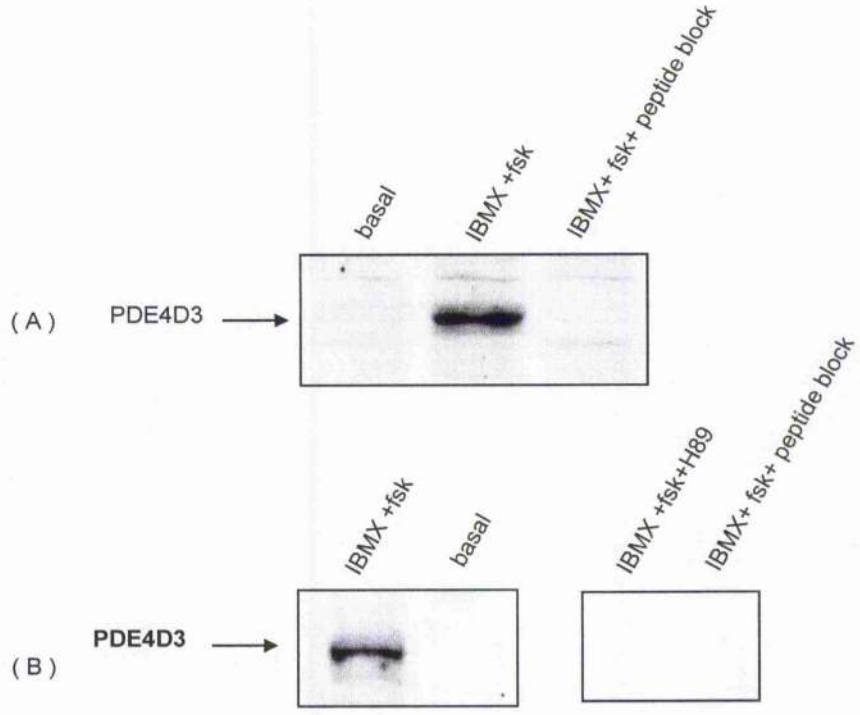

Figure 3.3 Detection of PKA phosphorylated PDE4D3. COS1 cells were transfected with wildtype PDE4D3 and were treated with IBMX (100μM) and forskolin (100 μM) to increase cAMP levels. Cells were there then harvested and analysed by western blot. Blots were probed with PS54-UCR1 antiserum (panel A) and PD13-4D3 (panel B). The antiserum was also treated with the phosphopeptide used to generate it (in 10 fold excess) .

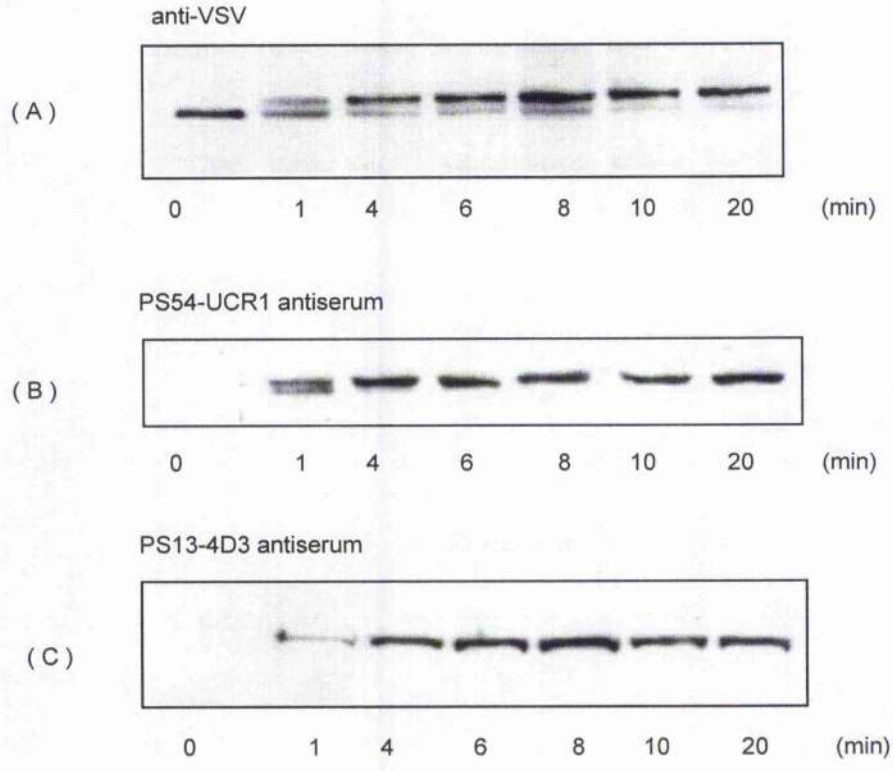

Figure 3.4 Determination of the tim- dependent mobility shift of PDE4D3 using the PS13-4D3 and PS54-UCR1 antisera. COS1 cells were transfected with VSV-tagged PDE4D3 and treated with IBMX (100μM) and forskolin (100 μM) over a time course of 0-20 min. Cells were harvested and analysed by western blot. Blots were probed with anti-VSV (panel A), PS54-UCR1 (panel B) and PD13-4D3 antisera (panel C). This data represents at three separate experiments using separate transfections.

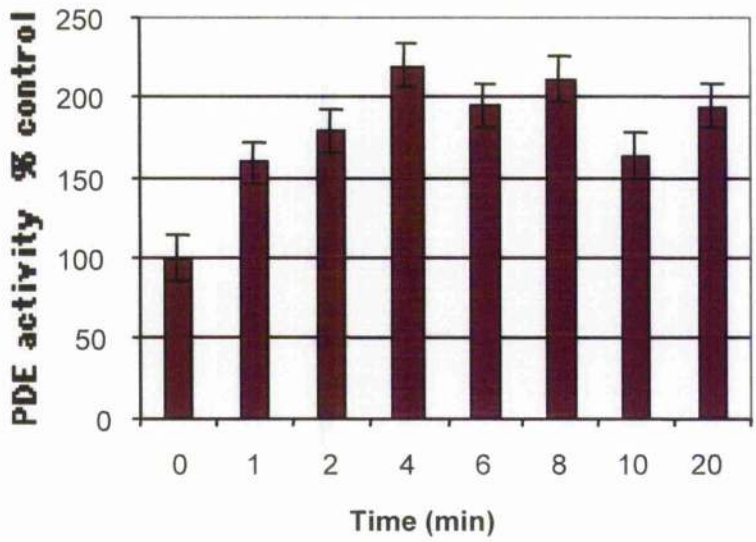

Figure 3.5 PDE4D3 activity in response to IBMX/forskolin challenge. COS1 cells were transfected with VSV-tagged PDE4D3 and treated with IBMX (100μM) and forskolin (100 μM) over a time course of 0-20 min. Cells were harvested at the indicated time points for the analysis of PDE4 activity (pmol/min/mg). Data shown as the percentage of represents three experiments +/- S.E.

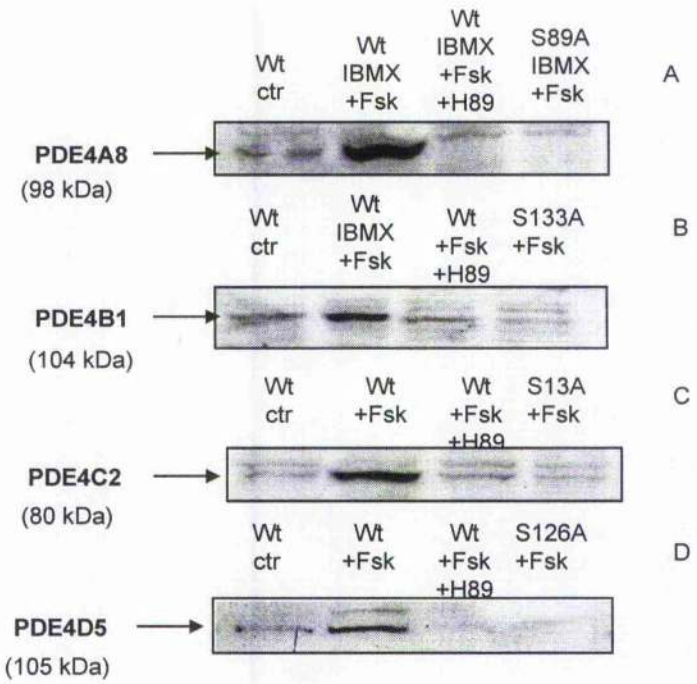

Figure 3.6a PKA phosphorylation of longform PDE4s. COS1 cells were transfected with the indicated PDE4 isoform. The cells were treated with IBMX (100 μM) and forskolin (100 μM) (indicated as fsk). Also, Cells were pre-treated with H89 (0.5 μM) prior to fsk treatment. Wildtype (Wt) isoforms and isoforms were the putative serine target for PKA phosphorylation was mutated to alanine where used in this experiment. These mutants were (A) Ser 89 Ala- PDE4A8, (B) Ser 133 Ala- PDE4B1, (C) Ser 13 Ala- PDE4C2 and (D) Ser 126 Ala- PDE4D5. Data represents three experiments. Blots were stripped ad re-probed for the appropriate isoform (data not shown)

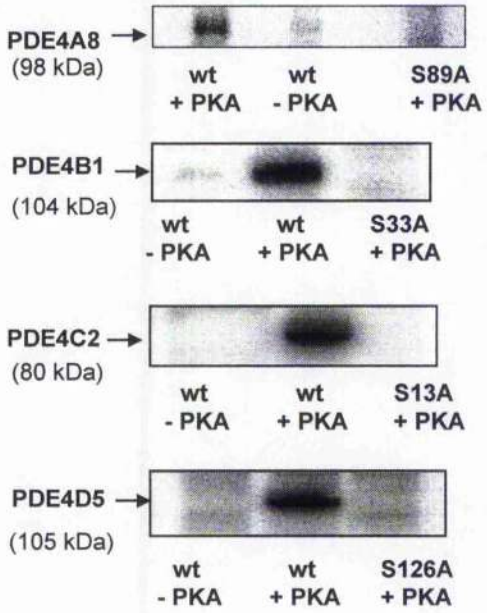

Figure 3.6b PKA phosphorylation of long form PDE4s. COS1 cells were transfected with the indicated PDE4 isoform. The lysates were treated with a phosphorylation mixture including [^{32}P] ATP in the presence of absence of active PKA catalytic subunit. Lysates were analysed by SDS-PAGE gel and phosphoimager. Isoforms where the putative serine target for PKA phosphorylation was mutated to alanine were used in this experiment. These mutants were as in previous figure (figure 3.6). Data represents three experiments performed by S.J. MacKenzie (S.J. MacKenzie *et al*, 2002).

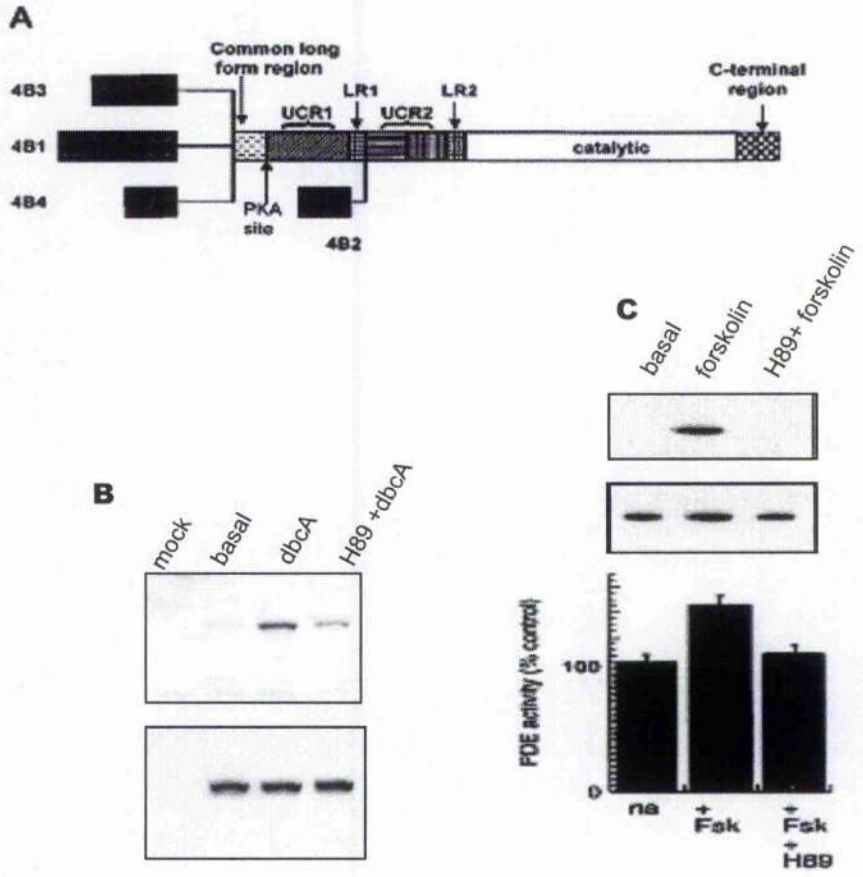

Figure 3.7 PKA phosphorylation of the rat longform PDE4B4. (A) A schematic of rat PDE4 transcripts and their encoded proteins. The four dark boxes represent the unique N-terminal regions of each isoform (taken from Shepherd *et al,* 2003*)*. (B) COS1 cells were transfected with Flag-tagged PBE4B4. The cells were treated with 100 μM dibutyrl cAMP (dbcA) for 10 min with and without 0.5 μM H89 , analysed by SDS-PAGE and immunoblotted with PS54-UCR1 (upper panel) and anti-flag antiserum (lower panel). (C) Also, transfected cells were treated with for 15 min with IBMX (100 μM) and forskolin (100 μM) with and without H89 (0.5 μM), PDE4B4 was immunoprecipitated from the lysates using using anti-Flag agarose beads, and analysed by immunoblotting with PS54-UCR1 (upper panel) and anti-Flag antiserum (lower panel). Data represents n=3.

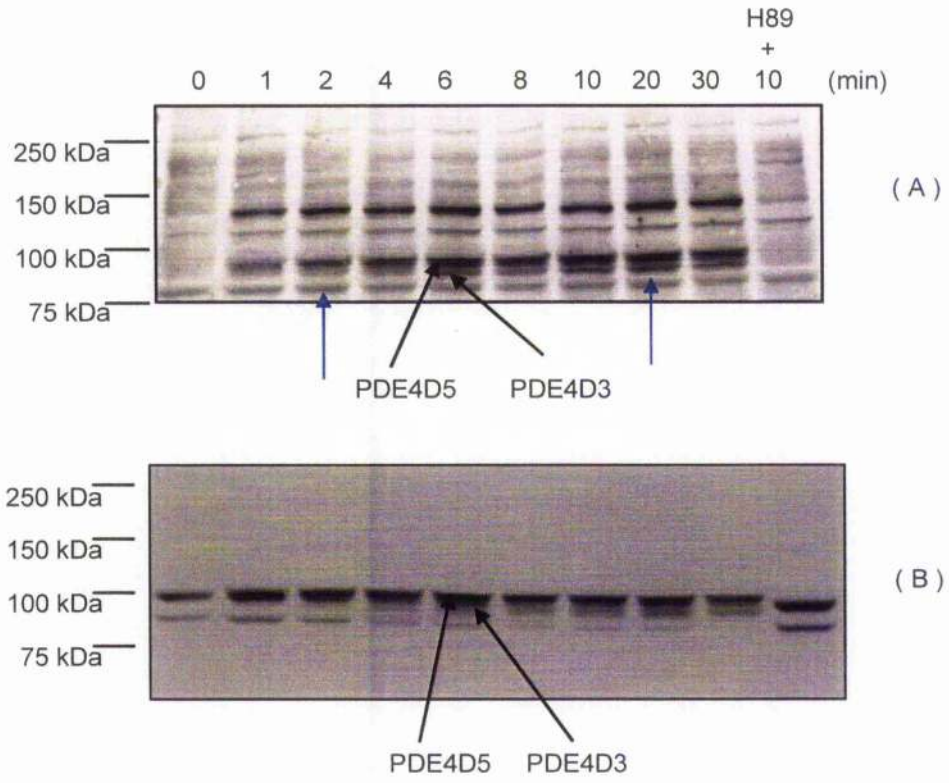

Figure 3.8 Analysis of the PKA phosphorylation of endogenously expressed PDE4D3 and PDE4D5 . COS1 cells were treated with IBMX (100 μM) and forskolin (100 μM) for the indicated time points. Cell lysates were analysed by Western blot. Panel A was probed with PS54-UCR1 antiserum. The blot was stripped and re-probed with pan-PDE4D antiserum. In panel B, The arrows indicate endogenous PDE4D3 and PDE4D5 . In panel A, the arrows indicate bands which may represent PKA phosphorylated PDE4D3 and PDE4D5. The blue arrow indiactes a non-specific band which migrated at the same weight as PDE4D3 from 0 to 8 min of the time course.

Chapter 4

The differential susceptibility of dominant negative/catalytically inactive PDE4 isoforms to PKA phosphorylation in COS1 cells

4.1 Introduction

The idea of signalling molecules being tethered to distinct subcellular compartments has long been discussed in the field of second messenger signalling, in particular cAMP signalling where the first notion of compartmentalisation of a signalling system was formulated (Brunton *et al.*, 1981).

Protein kinase A (PKA) is the main effector of cAMP. However, depending on the cellular response required, it has a large array of possible targets which are expressed in a cell-type specific fashion. Over the last decade, researchers have elegantly shown that a specific cellular response to cAMP can be achieved through the compartmentalisation of signalling proteins (Brunton *et al.*, 1981; Zaccolo and Pozzan., 2002; Mongillo *et al.*, 2004; Ruehr, 2004; Brunton). This requires that gradients of cAMP are formed and shaped within cells. Degradation of cAMP through PDE activity provides a clear route to achieve this, especially so as both soluble and membrane-bound PDE forms have been noted. It has been shown that various members of the PDE4 cAMP specific phosphodiesterase family are targeted to distinct intracellular locations (Houslay & Adams, 2003). As such they are poised to tailor pools and gradients of cAMP in cells and, thereby, 'control' the activation of localised PKA. The family of AKAPs (A kinase anchoring proteins) has been shown to act as signalling scaffolds, able to organise PKA, protein phosphatases, protein kinase C, various PKA substrates and even PDE4s. Thus AKAPS may serve to recruit and organise signalling proteins including PKA and PDE4 together in discrete regions of cells (Dodge *et al.*, 2001; Tasken *et al.*, 2001).

A large family isoforms provide adenylyl cyclase (AC) activity. Remarkably little detailed understanding is available concerning this important family. However, one key feature is their very different basal activity and different degrees of activation by Gs. That AC has a basal activity leads to the possibility that cells will slowly accumulate cAMP, thereby leading to the activation of PKA. Indeed, basal PKA activity is evident in many cells and investigators invariably assess the degree (fold) to which this is increased by the

action of G-protein coupled receptor (GPCR) agonist that activate AC through Gs. Of course the steady state level of cAMP that is reached in resting cells will depend not only on AC activity but also on the prevailing PDE activity in cells. Given that AC is localised to the cell plasma membrane, and even sub-domains within it, then anchored PDEs will have the role of creating and shaping cAMP gradients within resting cells. However, little is known about how PDEs may influence gradients of cAMP in unstimulated cells. This is despite the fact that PDE inhibitors are being developed for use therapeutically in, presumably attempting to regulate cell functioning under such conditions. The identification then of particular PDEs that may be specifically involved in regulating PKA activity in unstimulated cells may be of particular importance.

We hypothesised that in resting cells, PDE4s anchored either directly or indirectly to AKAPs may be particularly poised to regulate anchored PKA activity. For such anchored PDEs may be expected to exert spatial effects on signalling by controlling cAMP levels in the immediate vicinity of AKAP-anchored PKA, in this instance through the regulation of cAMP levels generated by basally active adenylyl cyclase. In order to investigate this possibility we need to have a specific readout for PDE action and for PKA activity. Fortunately, PDE4 long isoforms provide such a means for assessment. Firstly, they can be phosphorylated by PKA in their conserved UCR1, hence providing an immediate read-out for PKA action on a specific PDE. Secondly, we have developed an approach whereby a single minimal point mutation in the catalytic of PDE4 isoforms which can render them inactive. This has allowed us to develop a dominant negative strategy whereby catalytically inactive long PDE4 isoforms from each of the four sub-families can be chronically overexpressed in cells where they dominate native PDE4s by some 100-fold. Under such conditions we surmise that according to the law of Mass Action these inactive species will replace the cognate, active endogenous PDE4 isoforms from any signalling complexes they are involved in forming in the transfected cells. We surmised that if such signalsomes involved anchored PKA where cAMP is channeled in resting cells, PKA would now be active as there is no active anchored PDE4 to constrain its activity by lowering cAMP levels. Consequently, the catalytically inactive PDE4 would become phosphorylated by PKA. This approach may thus identify specifc PDE4

isoform as being specifically involved in constraining the activity of a distinct pool of PKA from activating by basal AC activity in resting cells.

Results

4.2 A study of the differential susceptibility of catalytically/dominant negative PDE4 isoforms to phosphorylation by PKA.

Using the dominant negative strategy, I show that in the COS1 cell model system, certain, but not all, dominant negative/catalytically inactive PDE4 isoforms detect active PKA under basal/resting conditions.

4. 2.1 The mRNA PDE4 profile of the COS1 cell model

Previously, western blot analysis has shown the endogenous expression of long form PDE4A4, PDE4C2, PDE4D3 and PDED5. Also short forms PDE4B2, PDE4D1 and PDE4D2 have been identified. I confirm the presence of these isoforms by mRNA transcript analysis (figure 4.1). Total RNA was isolated from COS1 cells and sent to Rachael Barber at Novartis (Horsham, UK) for analysis. PDE4 generic primers and primers designed to detect specific PDE4 isoforms (see Appendix for details) were used to build a PDE4 profile of this cell line. cDNA from brain tissue was used as a positive control and water as a negative control. Amplicons for generic PDE4A, PDE4B, PDE4C, PDE4D, PDE3B and PDE7A were observed. The isoform specific primers identified the following PDE4 isoforms: PDE4A4, PDE4A10, 2EL, PDE4B1, PDE4B2, PDE4B3, PDE4D1, PDE4D1/D2, PDE4D3 and PDE4D5 (figure 4.1).

4.2.2 The generation of catalytically inactive/dominant negative PDE4s

A range of catalytically inactive/dominant negative PDE4s were generated by the Houslay laboratory. The laboratory took advantage of the publication of the X-ray crystal structure of the active catalytic unit PDE4B2 (Xu *et al.,* 2000). As the catalytic domain is highly conserved throughout the PDE4 family, the crystal structure [Brookhaven Protein

Data Bank (PDB) accession number 1FOJ] provides an insight into the structure of the catalytic site of the PDE4 enzyme. Using the information from 1FOJ, it was determined that the catalytic centre comprises a binuclear motif with a tightly held Zn^{2+} ion coupled to a more loosely held Mg^{2+} (figure 4.2) (Houslay and Adams, 2003). A single point mutation of D392 to A392 disrupts the Zn^{2+} ion binding and renders the enzyme inactive. This point mutation results in a very conservative change which prevents the hydrolysis of cAMP but does not alter the interaction of cAMP. It can be assumed that if the dominant negative species acts as a sink, cAMP-dependent processes would be inhibited and one would expect to observe a null effect. It has already been demonstrated by Baillie *et al,* that dominant negative PDE4D5 can enhance the PKA phosphorylation status of the β_2-adrenoceptor (Baillie *et al.,* 2003). To generate the dominant negative PDE4 isoforms used within this chapter, a point mutation was made in the cognate Zn^{2+} ion binding aspartate residue for each isoform.

I selected a range of long form dominant negative PDE4s from each sub family to study in COS1 cell model system. Firstly, I tested the constructs for PDE activity, noting that wild type enzymes and their dominant negative counterparts are cloned into the same vectors (pcDNA3). COS1 cells were transiently transfected with dominant negative and wild type PDE4A4, PDE4B1, PDE4C2 and PDE4D3 isoforms. PDE activity of the cell lysates was determined by phosphodiesterase assay (Marchmont and Houslay, 1980) and is given here as pmol of cAMP hydrolysed per min per mg of PDE (pmol/min/mg). This PDE assay clearly shows that the overexpressed dominant negative PDE4s have minimal activity compared to the wild type enzymes. Indeed, the dominant negative species have an activity that is comparable to that of the mock control (empty vector transfection). In order to establish whether the over expression of the dominant negative themselves altered basal cAMP levels within the COS1 cells, cAMP assays were performed following the transfection of each dominant negative construct (figure 4.4). Total cAMP levels were measured for each population of cells over expressing each dominant negative and compared to a mock transfection. It was concluded from these assays, that the global, averaged cAMP levels did not significantly change following the expression

of any of the dominant negatives. A total cAMP level of approximately 10 pmol per 10^6 cells was observed.

4.2.3 Phosphorylation status of catalytically inactive/dominant negative PDE4 isoforms

In a COS1 cell model, I studied the ability of the dominant negative long PDE4 isoforms to provide targets for PKA action using the phospho-specific PS54-UCR1 antibody (as in previous chapter). This specifically detects the phosphorylation of a single serine in a conserved PKA consensus motif (RRESF), located in the UCR1 found in all long PDE4 isoforms. For this study, cells were transfected with the dominant negative and wild type long PDE4 isoforms. It was surmised that the dominant negative PDE4s, compared to their respective wild-types, would be more accessible to PKA as they displace the cognate active PDE4 and they lack cAMP-hydrolysing activity. As a consequence of this, the dominant negative PDE4s, unlike their wild type counterparts, would allow an increase in the compartmentalised cAMP pool, an activation of PKA would ensue and subsequently PKA phosphorylation of the dominant negative PDE4 would be observed.

Under resting conditions, cells transfected with either inactive PDE4A4 or PDE4A10, or wild type PDE4A4 or PDE4A10 show that none of the these species are phosphorylated by PKA (figure 4.5a). However, they clearly have the potential to be phosphorylated by PKA as such PKA phosphorylation of both wild type and inactive forms of PDE4A4 and PDE4A10 is clearly evident following the addition, to cells, of the general PDE inhibitor IBMX and direct activator of AC, forskolin (figures 4.5b&4.5c). In contrast, analysis of the phosphorylation status of catalytically inactive PDE4C2 and PDE4D3 showed that both of these species became highly phosphorylated under resting conditions (figure 4.5a). Treatment of cells with forskolin, in either the absence or presence of IBMX, led only to a small further increase in phosphorylation (figures 4.5b&4.5c). This suggests that in resting cells PDE4C2 and PDE4D3 come into contact with active PKA whereas PDE4A4 and PDE4A10 do not.

4.2.3.1 Phosphorylation status of inactive PDE4D3 and PDE4C2 following endogenous PDE4 and PDE3 inhibition

The other major PDE activity in COS1 cells is provided by PDE3. In order to address possibility that PDE3 activity could influence the phosphorylation state of inactive PDE4D3 and PDE4C2, transfected cells were treated with the PDE3 inhibitor cilostamide. Additional studies were also done with the PDE4 inhibitor rolipram. It was observed that upon inhibition of the entire PDE3 family, with cilostamide, the PKA phosphorylation status of the catalytically inactive PDE4C2 is increased, however, using rolipram to selectively inhibit the entire pool of active PDE4 enzymes causes little or no further increases in phosphorylation of catalytically inactive PDE4C2 (figure 4.6). In contrast to this, inhibition of the entire pool of active PDE4 enzymes markedly increases the phosphorylation state of catalytically inactive PDE4D3 and whilst inhibition of the entire pool of PDE3 has little effect. These data strongly suggest that different pools of active PKA are able to phosphorylate PDE4C2 and PDE4D3 in theses cells and thus, presumably, are being separately controlled by these particular enzymes. In the case of PDE4C2 other endogenous PDE4 enzymes in COS1 cells do not feed into this, whilst PDE3 can. Whilst in the case of PDE4D3 other endogenous PDE4 enzymes in COS1 cells can feed into this, whilst PDE3 cannot.

4.2.3.2 Action of GPCR stimulation by isoproterenol and PGE2 on the phosphorylation status of catalytically inactive/dominant negative PDE4 isoforms

I wished to determine whether differential phosphorylation states of the inactive long PDE4 isoforms was evident following stimulation of different Gs-coupled receptors. I chose to evaluate one particular example of a catalytically inactive PDE4 from each sub family and determined their phosphorylation status following stimulation of either β–adrenergic receptors with isoproterenol or prostacyclin receptors with PGE2. As a control, transfected cells were also treated with forskolin which can be expected to activate the entire pool of AC in cells. The phosphorylation status of catalytically inactive PDE4A4, PDE4B1, PDE4C2 and PDE4D3 is shown here in basal, forskolin,

isoproterenol and PGE2 stimulated cells (figure 4.7a). The western blots of the PS54-UCR1 were quantified using densitometry software, and the phosphorylation states of each isoform shown as percentage control of the maximum value observed upon stimulation with forskolin stimulation (figure 4.7b). It is clear that the agonist stimulation of these two different receptors both increase the phosphorylation of catalytically inactive PDEC2 and PDE4D3, where isoproterenol is as twice as effective as PGE2 in increasing the phosphorylation of both these enzymes . In contrast, isoproterenol causes a 5-fold increase in phosphorylation of inactive PDE4B1 compared to the PGE2 agonist. Both PGE2 and isoproterenol have a similar minimal effect on the phosphorylation of PDE4A4.

4.2.3.3 cAMP levels following Isoproterenol or PGE treatment in cells over expressing the inactive PDE4s

I wished to establish if the differences in phosphorylation states of the inactive PDE4s observed upon isoproterenol stimulation and PGE2 stimulation are due differences in the abilities of these ligands to increase global cAMP levels. Cells were transfected with the catalytically inactive PDE4 species, and then stimulated with either isoproterenol or PGE2 and subsequently cAMP levels measured (figure 4.7c). The data is shown here as fold change compared to basal cAMP levels. It is clear that the cells overall cAMP response to PGE2 stimulation is similar in cells that over express any of the catalytically inactive PDE4s. Cells over expressing PDE4A4, PDE4C2 and PDE4D3 also respond similarly with respect to global cAMP levels in response to isoproterenol challenge (5-fold greater than response to PGE2), whereas a slightly higher cAMP level was observed in cells transfected with inactive PDE4B1 and stimulated with isoproterenol. The upper graph shows the fold changes of cAMP levels observed in native COS1 cells following PGE2 or isoproterenol treatment (figure 4.7c). On comparing the cAMP levels observed following PGE2 or isoproterenol stimulation of COS1 cells and COS1 cells overexpressing each of the dominant negatives, it appears that the dominant negatives may reduce cAMP levels.

4.2.4 Quantification of expression levels of catalytically inactive/dominant negative PDE4A4 and PDE4D3

As western blot analysis of the expression levels of the transfected inactive PDE4s relied on the use of PDE4 pan sub-family antibodies, the expression levels of the inactive PDE4s could not be directly compared to each other. I, therefore, wished to establish if the observed differences in phosphorylation states between PDE4A4 and PDE4D3 may be simply due to different expression levels of these various catalytically inactive species expressed in cells. To quantify and compare the actual expression levels between these two isoforms I selected lysates used in the previous Gs-coupled agonist experiments. The lysates with the same protein concentration were subjected to electrophoretic separation alongside a range of protein concentrations of the pure recombinant form of the isoforms (figure 4.8a). From the range of purified recombinant PDE4, a standard curve was generated by densitometry analysis of the bands. The equation of the line and the densitometry analysis of the cell lysates were used to calculate the number of pmol of the catalytically inactive PDE4 species present in 5μg of lysates (figure 4.8b). The mean expression levels of 0.026 +/- 0.002 pmol for PDE4A4 and 0.024 +/- 0.014 pmol for PDE4D3 were calculated. These data showed that the expression level of these various catalytically inactive PDE4 species was at very similar levels. Thus the differences in phosphorylation seen in these studies are very unlikely to be due to any major differences in total concentration making one species rather than the other more likely to be phosphorylated by PKA.

4.2.5 Pharmacological analysis to determine whether it is RI or RII PKA isoform that phosphorylates catalytically inactive PDE4C2 and to assess AKAP involvement

From previous experiments, it was observed that inactive PDE4C2 and PDE4D3 were both phosphorylated by PKA at basal cAMP levels. The interaction of PDE4D3 with an AKAP, namely mAKAP, has already been reported in cardiac myocytes (Dodge *et al.*, 2001). Also PDE4D3 has been shown to interact with AKAP 450 in Sertoli cells (Tasken

et al., 2001). The basal phosphorylation of PDE4D3 may be an indication of the association of this isoform with an AKAP as this would provide an ideal platform for the anchoring of both the PDE4 and PKA in close proximity to each other. As inactive PDE4C2 is also phosphorylated at basal cAMP levels, I wished to examine the possibility of the involvement of an AKAP-bound PKA and to identify which type, RI or RII PKA phosphorylates this enzyme.

The type of PKA isoforms endogenously expressed in COS1 cell model was determined by western blot analysis with the isoform specific antibodies (Signal Transduction Laboratories) (figure 4.9). Whole cell lysate was probed for the presence of RIα, RIIα and RIIβ forms of the PKA regulatory sub-units (RIβ specific antibody was commercially unavailable). Immunoreactive species corresponding to weights of RIα (48kD), RIIα (51kD) and RIIβ (53kD) forms were observed following western blotting.

The preferential phosphorylation of inactive PDE4C2 by the RI agonist compared to the RI agonist was further examined. In this experiment, antagonists of the RI and RII forms were used, and the phosphorylation state of inactive PDE4C2 was analysed as with the previous agonist experiments. Cells were transfected with the inactive PDE4C2 and treated for 18-24 hr with the RI antagonist, R-Cl cAMPs or the RII antagonist R-Cpt cAMPs. Lysates were analysed by western blotting with the PS54-UCR1 antiserum and the phosphorylation state of the inactive PDE4s quantified by densitometry (figures 4.10a &4.10b). This data shows that the RI antagonist reduces the basal phosphorylation level of PDE4C2 but the RII antagonist appears to have no effect on the phosphorylation level. In the same experiment, the possibility of an AKAP-PKA complex regulating the phosphorylation of this PDE4 was examined. A widely used AKAP-PKA complex 'disrupter' was chosen to assess the involvement of any AKAP. If the PKA form responsible for the basal phosphorylation of inactive PDE4C2 was held in an AKAP complex, Ht31 would be expected to reduce this basal phosphorylation as PKA would no longer be 'held' in close proximity to the PDE. Inactive PDE4C2 was co-transfected with a plasmid which expressed a GFP-tagged Ht31 fragment. It was shown via western

blotting with anti-GFP and pan PDE4C antibodies (figure 4.10a), and immunofluorescence (figure 4.10c) that PDE4C2 and Ht31 were both expressed in the same cell. Following densitometry analysis and correction for expression levels of PDE4C2 (figure 4.10b), Ht31 appeared to reduce the phosphorylation. RI- and RII-specific agonists (Biolog, Germany) were then employed in order to establish which isoforms of PKA phosphorylated inactive PDE4C2 and inactive PDE4D3 at basal adenylyl cyclase activity. Cells over expressing the inactive PDE4s were treated with the RI synergistic agonists (8-PIP-cAMP and 6-MBC-cAMP; Biolog, Germany) or RII synergistic agonists (8-HA-cAMP and 6-MBC-cAMP; Biolog, Germany) for 10 min. The phosphorylation status of the PDE4 isoforms were then assessed by western blotting with the PS54-UCR1 antiserum and densitometry analysis (figure 4.11). The data is shown as fold change basal and indicates that a RI form, rather than a RII form of PKA preferentially phophosphorylated inactive PDE4C2. In contrast, it appears that neither form of PKA preferentially phosphorylated PDE4B1 as both the RI and RII agonists caused similar, but minimal, increases in phosphorylation.

4.3 Discussion

In this chapter I show, by utilising catalytically inactive PDE4 isoform, that of the selected PDE4 long-forms studied, only PDE4C2 and PDE4D3 are able to be phosphorylated by PKA under basal adenylyl cyclase activity in COS1 cells. This selectivity suggests that PDE4C2 and PDE4D3 may be held in close proximity to discrete PKA sub-populations whereby they regulate such activities at basal cAMP levels.

For this study, COS1 cells were chosen as the model cell line. COS1 cells endogenously express PDE4s from each sub family (A, B, C and D) as shown by mRNA expression profile (figure 4.1) and by western blot analysis (unpublished data, Houslay laboratory). Dominant negative/ catalytically inactive long-form PDE4s from each sub family were chosen, tested for activity and shown to be inactive compared to their wild-types (figure 4.3). As a control, to ensure that the catalytically inactive enzymes themselves do not alter basal adenylyl cyclase activity, global cAMP levels were measured following the

over-expression of the catalytically inactive species (figure 4.4). Here it was shown that the over-expression and transfection process itself do not significantly alter global cAMP level within COS1 cells.

Firstly, the PKA phosphorylation status of catalytically inactive PDE4A4, PD4A10, PDE4C2 and PDE4D3 were compared to the respective wild types at basal cAMP levels (figure 4.5a). In this experiment, PKA phosphorylation of the UCR1 PDE4s were detected with the phospho-specific PS54-UCR1 antiserum, the blots stripped and probed with the pan PDE4 subfamily antibodies to show loading between catalytically inactive PDE4 long isoforms and the respective wild type species. The pan PDE4 antibodies are sub-family specific (generated to the C-terminal region) thus the level of over-expression between the PDE4A, PDE4C and PDE4D isoforms described in this experiment cannot be directly compared. This is addressed later in this chapter as is the possibility that the different PDE4 isoforms may have varying sensitivity to PKA. As shown in figure 4.5a, only the PKA phosphorylation of the catalytically inactive PDE4C2 and PDE4D3 isoforms was observed. A non-specific band was detected for the PDE4A4 standard and phosphorylation of the wild type isoforms was not detected. In the next set of experiments, global cAMP levels were raised by the activation of the entire pool adenylyl cyclase using forskolin, and also by the inhibition of the entire pool of PDEs together with activation of adenylyl cyclase (IBMX & forskolin treatment). Following the addition of forskolin, phosphorylation of catalytically inactive PDE4A4 was observed (figure 4.5b), and a small increase in phosphorylation of catalytically inactive PDE4C2 and PDE4D3 was evident compared to basal conditions (figures 4.5a and 4.5b). Finally, following IBMX and forskolin treatment, phosphorylation of all catalytically inactive and all wild type isoforms was observed (figure 4.5c), and increases in phosphorylation of the catalytically inactive PDE4C2 and PDE4D3 was observed. Although phosphorylation of dominant negative PDE4A4 and PDE4A10 was not observed at basal cAMP levels, phosphorylation was observed following the combination of forskolin and IBMX treatment. This suggests that PDE4A4 and PDE4A10 are accessible to PKA, but with reduced sensitivity. Overall, this 'selective' phosphorylation of PDE4C2 and PDE4D3

suggests that these isoforms may be sampling different pools of cAMP than PDE4A4 and PDE4A10, and may also be in close proximity to PKA.

As described in the previous experiment, catalytically inactive PDE4C2 and PDE4D3 were phosphorylated by PKA at basal adenylyl cyclase activity and this phosphorylation only increased slightly by forskolin treatment. As a larger increase in phosphorylation of these isoforms was evident following general PDE inhibition, with IBMX together with forskolin, I decided to investigate if the selective inhibition of entire pools of PDE3 and PDE4 activities affected the phosphorylation of PDE4C2 or PDE4D3. The mRNA profile (figure 4.1) showed that generic PDE3B and an array of PDE4s other than PDE4C2 and PDE4D3 were expressed endogenously in COS1 cells. If PDE3 isoforms or other PDE4 isoforms were also targeted to the same region as the catalytically inactive species, one would expect either the selective PDE3 inhibitor cilostamide or the selective PDE4 inhibitor rolipram to increase the phosphorylation of the catalytically inactive species. A simple experiment was performed where catalytically inactive PDE4C2 and PDE4D3 were overexpressed in the COS1 cell model, and the level phosphorylation analysed with the PS54-UCR1 (figure 4.6). It is clear from this data that inhibition of PDE3s resulted in an increase in phosphorylation of catalytically inactive PDE4C2 compared to basal. On the other hand, the inhibition of PDE4 resulted only in an increase in the phosphorylation of PDE4D3. This suggests that PDE4C2 may be targeted to a region of higher PDE3 expression or activity, whereas PDE4D3 may be targeted to a region of higher PDE4 expression or activity. As this data represents only two experiments, further experiments should be performed to provide fold changes in phosphorylation of statistical significance.

The differential effects of PDE3 and PDE4 inhibition on the phosphorylation of the catalytically inactive PDE4C2 and PDE4D3 suggest that these PDE4s may be sampling different pools of cAMP. To investigate this further by means of the catalytically inactive PDE4 strategy, the effect of activating different Gs-coupled receptors on the phosphorylation of selected catalytically inactive PDE4 species was studied. A catalytically inactive PDE4 long-form was selected from each sub-family and their

phosphorylation in response to the activation of the β-adrenergic receptor with isoproterenol or activation of the EP receptors with PGE2, was studied. It has been previously reported that these agonists can generate different cellular responses via the elevation on cAMP (Brunton, 2003), thus they provide an ideal way to investigate if the dominant negatives are indeed sampling distinct pools of cAMP. In this experiment, the effects of forskolin, PGE2 and isoproterenol stimulation on catalytically inactive PDE4A4, PDE4B1, PDE4C2 and PDE4D3 was studied (figures 4.7a & figure 4.7b). The western blot data was analysed by densitometry. As different basal phosphorylation levels were observed between isoforms, the response of each isoform to the agonists was compared to the forskolin induced phosphorylation state and this allowed each isoform to be compared to one another. It is clear that following agonist stimulation, the phosphorylation pattern of catalytically inactive PDE4D3 and PDE4C2 was almost identical. However, the phosphorylation pattern of catalytically inactive PDE4A4 and PDE4B1 appeared to be quite different; PGE2 and isoproterenol had similar effect on PDE4A4, yet only isoproterenol stimulation resulted in phosphorylation of PDE4B1. The differential effects of the Gs coupled agonists may indicate that these PDE4s are being targeted to different sub-cellular regions.

I also set out to investigate if the actual over-expression of the different isoforms impaired the generation of cAMP by agonist treatment. The cells over-expressing each of the isoforms were subjected to agonist stimulation and global cAMP level measured (figure 4.7c). The data is represented as fold change over basal cAMP levels, and it is evident that the over-expression of any of catalytically inactive PDE4s did not alter total cAMP levels significantly. However, it appears that following overexpression of inactive PDE4B1, a larger response to isoproterenol was observed. Thus, it appears that the differences in phosphorylation of catalytically inactive PDE4A4 and PDE4B1 compared to catalytically inactive PDE4C2 and PDE4D3 observed is not due to the catalytically inactive species either impairing or enhancing the receptor activation and subsequent generation of cAMP.

For the next control experiment I investigated the expression levels of the catalytically inactive species in COS1 cells. As a pan PDE4 antibody was not available, I could not compare expression levels of each the catalytically inactive constructs by using the pan PDE4 sub-family antibody (used for normalisation of data). To address this problem, I chose to calculate the number of pmol of the catalytically inactive PDE4A4 and PDE4D3 forms in whole cell lysates from the experiments involving GPCR challenge (isoproterenol stimulated lysates). Known concentrations of the lysates (calculated by Bradford assay) were subjected to SDS-PAGE analysis alongside a range of concentrations of recombinant *E.coli* expressed PDE4A4 and PDE4D3 (figure 4.8a). The purified *E.coli* expressed PDE4s were used to generate a standard curve and following densitometry analysis, the approximate number of pmol of the catalytically inactive enzyme present in the cell lysates were calculated. From the previous agonist experiments it was clear that isoproterenol stimulation caused quite different levels of phosphorylation of the catalytically inactive PDE4A4 and PDE4D3, however, it is evident that the expression levels of catalytically inactive PDE4A4 and PDE4D3 did not vary significantly (figure 4.8b).

In summary, the PDE4C2 and PDE4D3 data suggests that the over-expression of the dominant negatives did not alter the cAMP generation in response to agonist treatment, the expression levels of each did not vary markedly. Therefore, the differential phosphorylation of the catalytically inactive PDE4s observed at basal adenylyl cyclase activity and agonist stimulated adenylyl cyclase activity may be due to targeting and sampling of spatially distinct 'pools' or gradients of PKA that sample distinct gradients of cAMP.

It is now well established that PKA can be anchored to discrete sub-cellular locations by AKAPs, and can sample gradients of cAMP within the cell (Klauk & Scott, 1995; Colledge & Scott, 1999). The PDE4D3 isoform has also been shown to be anchored to AKAPs where it can regulate the activity of PKA by a feedback control mechanism involving the PKA phosphorylation of the PDE itself (Dodge *et al.*, 2001; Tasken *et al.*, 2001). At basal adenylyl cyclase activity in COS1 cells, I observed PKA phosphorylation of both catalytically inactive PDED3 and PDE4C2, and hypothesised that this may be due

to the close proximity of PKA. As mentioned above, PDE4D3 has already been reported to be anchored alongside PKA to an AKAP (Dodge *et al.*, 2001; Tasken *et al.*, 2001), yet no such anchoring has been reported for PDE4C2. I decided to investigate the possibility of an AKAP involvement in the PKA phosphorylation and control of activity of PDE4C2, and also to identify which PKA isoform phosphorylated this PDE4 isoform at basal cAMP levels. Firstly, I identified which isoforms of PKA were endogenously expressed in the COS1 cell model (figure 4.9). As both RI and RII isoforms were expressed I used PKA isoform specific antagonist and agonists to alter the phosphorylation of catalytically inactive PDE4C2 (figures 4.10 & 4.11). These data suggests that an RI-PKA isoform was the predominant form responsible for the phosphorylation of catalytically inactive PDE4C2. If an AKAP tethers the PKA responsible for the phosphorylation of PDE4C2, one would expect to see an ablation of this phosphorylation following the disruption of the AKAP-PKA interaction. To study the possible involvement of an AKAP, the catalytically inactive PDE4C2 was co-expressed with Ht31, a commonly used PKA-AKAP disrupter (figure 4.10). Although the over-expression of Ht31 reduced the level of expression of PDE4C2, following normalisation of the densitometry data, it appears that the disruption of all PKA-AKAP interactions did indeed ablate the phosphorylation of catalytically inactive PDE4C2. Therefore this simple experiment may be an indication that the PDE4C2 isoform can associate with a PKA-AKAP complex. If time had allowed, I would have performed the same co-transfections with the other catalytically inactive species at basal cAMP levels and agonist induced cAMP levels.

Following the Ht31 experiments, I investigated the possibility of an actual interaction of the PDE4C2 isoform with a PKA-AKAP complex. Immunoprecipitations of PDE4C2 were sent to two separate AKAP laboratories (Klussmann, FMP, Berlin & Tasken, Oslo.) for overlay analysis. Both RI and RII overlay assays were performed, and showed an AKAP of about 250 kD co-immunoprecipitated with PDE4C2. I have not shown the overlay results in this chapter as the blots were unclear, however they provided initial promising evidence of a possible PDE4C2-PKA-AKAP complex. Also, I would have liked to have pursued the study of the identification of the specific isoform of PKA which phosphorylated PDE4C2. My initial data suggests that an RI isoform was responsible, and I planned to further investigate using an approach involving PKA isoform specific

interfering RNA (siRNA). As a complex of a PDE4, RI-PKA and an AKAP has yet to be reported, a PDE4C2/RI PKA-AKAP complex would be potentially exciting. If the AKAP could be identified it may provide a functional role for PDE4C2 within a cell.

Samples	**4A generic**	4A4	4A10	2EL	**4B generic**	4B1	4B2	4B3	**4C generic**	**4D generic**	4D1	4D1/2	4D3	4D4	4D5	**3A generic**	**3B generic**	**7A generic**	Transferrin	B-Actin
Control - brain	+	+	-	+	+	+	+	+	+	+	+	+	+	+	+	+	+	+	+	+
Control - water	-	-	-	-	-	-	-	-	-	-	-	-	-	-	-	-	-	-	-	-
COS-1 No.1	+	+	+	+	**w**	-	+	-	+	+	+	+	w	-	+	-	+	+	-	+
COS-1 No.2	+	+	+	+	**w**	-	+	-	**w**	+	+	+	-	-	+	-	+	+	-	+
COS-1 No.3	+	+	+	+	-	w	+	-	+	+	+	+	w	-	+	-	+	+	-	+
COS-1 No.4	+	+	+	-	**w**	-	w	-	**w**	+	+	+	-	-	+	-	+	+	-	+
Consensus	+	+	+	+	**w**	-	+	-	+	+	+	+	+	-	+	-	+	+	-	+

Figure 4.1 mRNA PDE4 expression profile of COS1 cells. The gel represents a typical PDE mRNA profile of COS1 cells. Total RNA was isolated from COS1 cells, synthesised to cDNA and subjected to PCR using primers designed to specific PDE isoforms (see appendix for primer details). The table shows a summary of 4 different PCR analyses; brain cDNA was used as a positive control, water as a negative control and 'w' indicates a weak band.

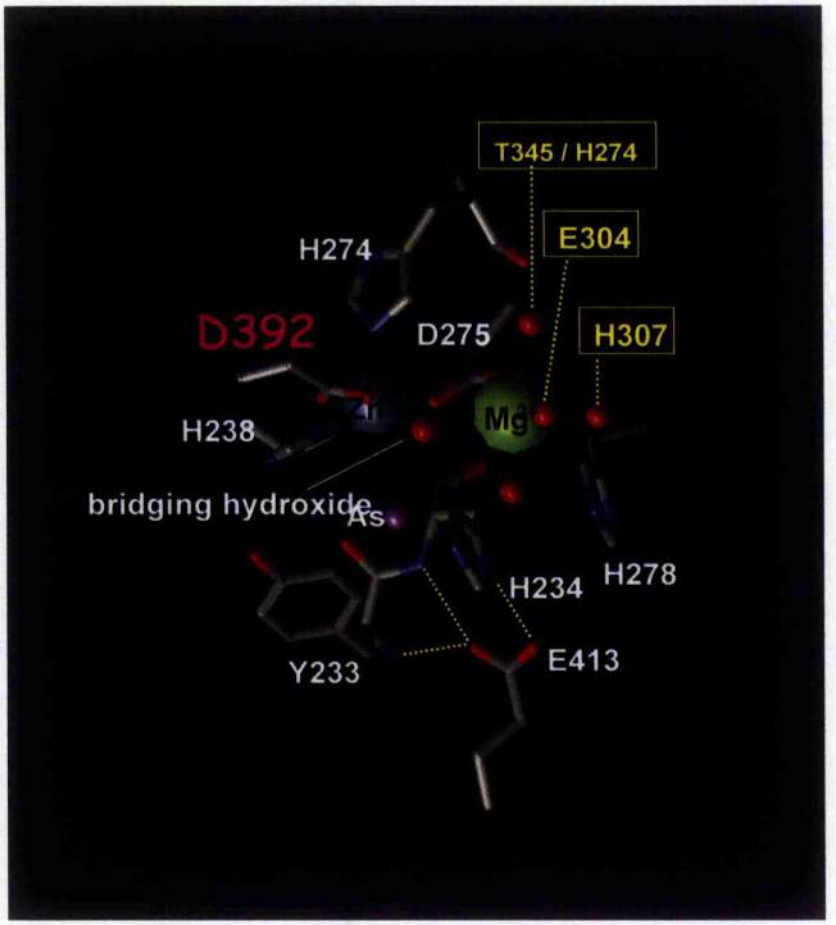

Figure 4.2 Schematic structure of the PDE4B2 core catalytic unit illustrating metal ion environment. The divalent cations (Zn^{2+} and Mg^{2+}) involved in the catalytic mechanism are represented as balls. A singal point mutation of amino acid D392 disrupts the binding of the metal ions and renders the PDE4 inactive. Diagram adapted from a Houslay review (Houslay and Adams, 2003)

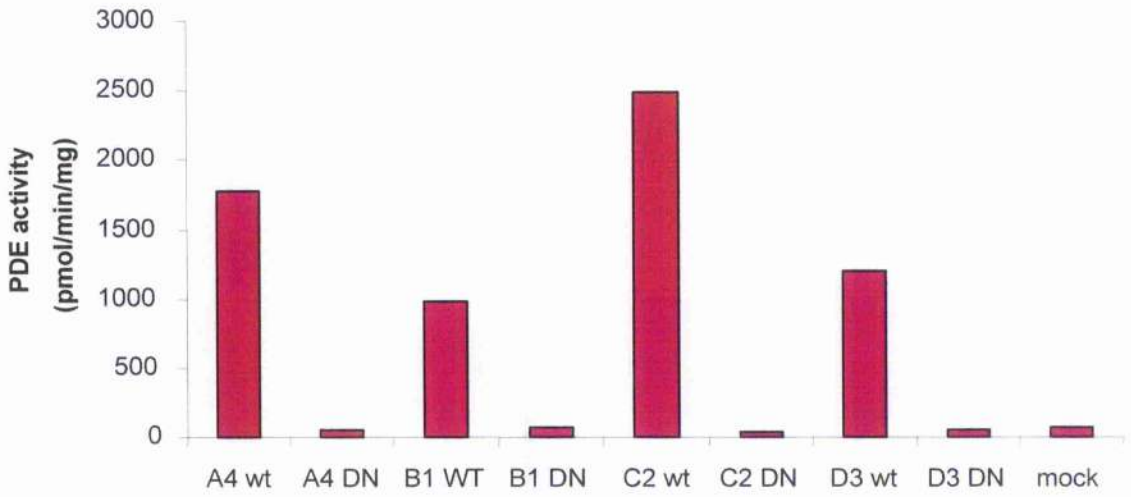

Figure 4.3. Comparison of PDE activities of wild type and dominant negative/catalytically inactive PDE4s. COS1 cells were transiently transfected with wild type (wt) and dominant negative (DN) PDE4 isoforms, and the PDE activity of lysates was analysed by PDE assay (Marchmont & Houslay, 1980). Mock indicates the transfection of empty vector (pcDNA3). Represents one PDE assay.

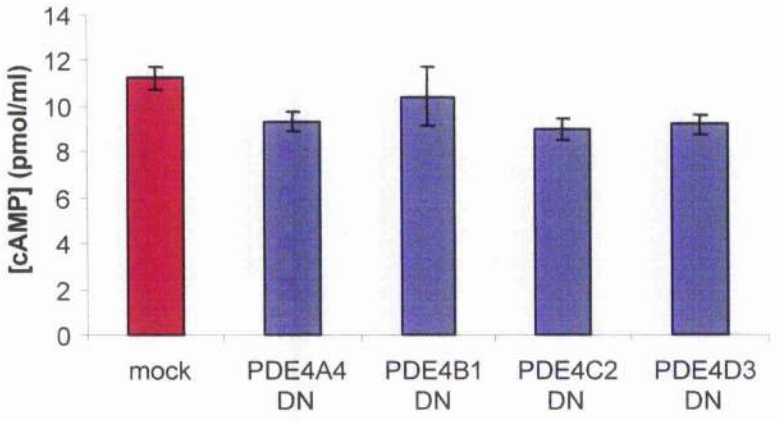

Figure 4.4 cAMP concentration per 10^6 cells following dominant negative over expression in COS1 cells. Mock indicates transfection of empty vector (pcDNA3). cAMP levels in COS1 cells transiently transfected with the indicated dominant negative. n=3 +/- S.E.

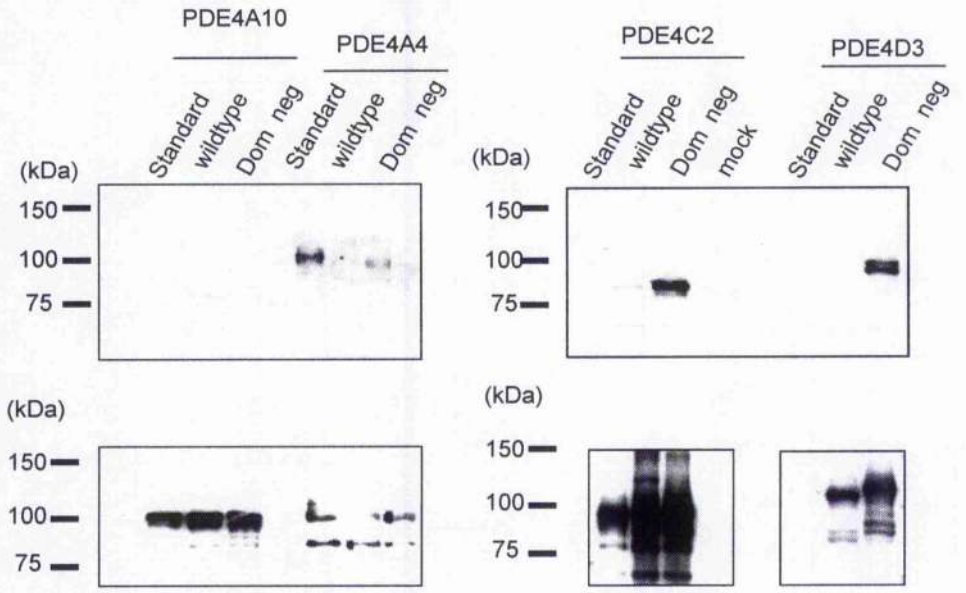

Figure 4.5a PKA phosphorylation of dominant negative/catalytically inactive PDE4 long form at basal cAMP levels. The indicated wild type and dominant negative PDE4 isoforms were overexpressed in COS1 cell. Lysates of HEK cells transfected with the relevant wt PDE4 isoforms are indicated as standards. Lysates were subjected to SDS-PAGE analysis and the PKA phosphorylation status was determined using PS54-UCR1 antiserum (upper panels). To check expression and loading, blots were stripped and re-probed with relevant pan PDE4 subfamily antibodies (lower panel).

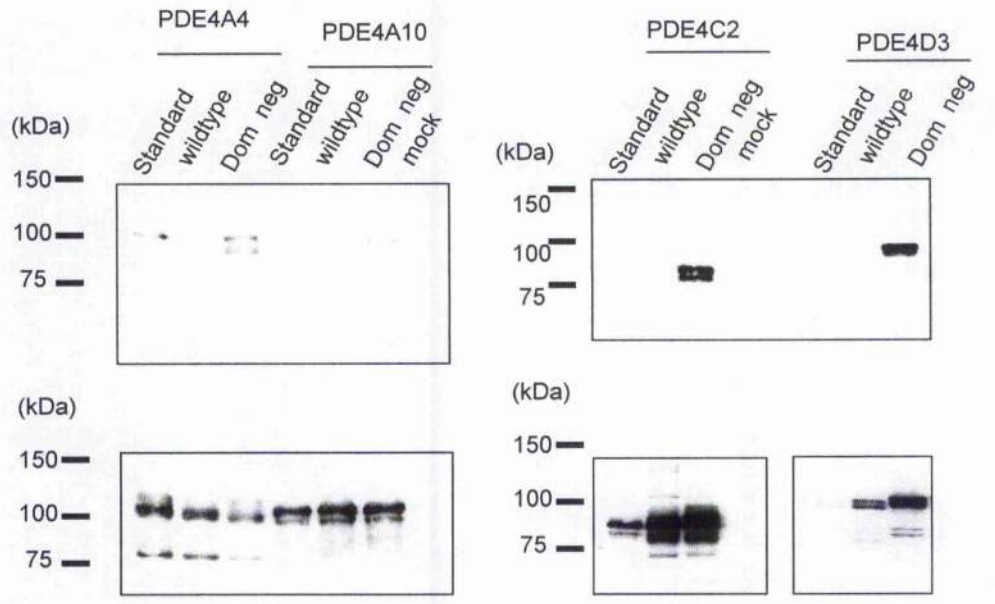

Figure 4.5b PKA phosphorylation of dominant negative/catalytically inactive PDE4 long form at elevated levels of cAMP induced by forskolin. Lysates of HEK cells transfected with the relevant wt PDE4 isoforms are indicated as standards The indicated wild type and dominant negative PDE4 isoforms were over expressed in COS1 cell. Two days post transfection, cells were treated with forskolin (100 μM) for 10 min, lysates were subjected to SDS-PAGE analysis and the PKA phosphorylation status was determined using PS54-UCR1 antiserum (upper panels). To check expression and loading, blots were stripped and re-probed with relevant pan PDE4 subfamily antibodies (lower panel).

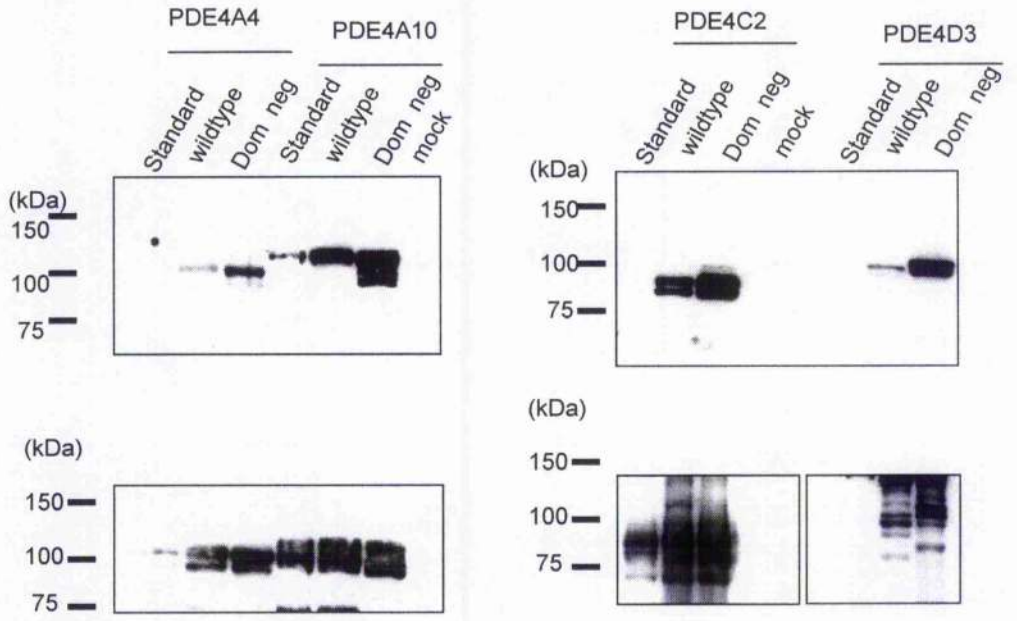

Figure 4.5c PKA phosphorylation of dominant negative/catalytically inactive PDE4 long form at near maximal cAMP levels. Lysates of HEK cells transfected with the relevant wt PDE4 isoforms are indicated as standards The indicated wild type and dominant negative PDE4 isoforms were over expressed in COS1 cell. Two days post transfection, cells were treated with the general PDE inhibitor IBMX (100 μM) and forskolin (100 μM) for 10 min. Lysates were subjected to SDS-Page analysis and the PKA phosphorylation status was determined using PS54-UCR1 antiserum (upper panels). To check expression and loading, blots were stripped and re-probed with relevant pan PDE4 subfamily antibodies (lower panel).

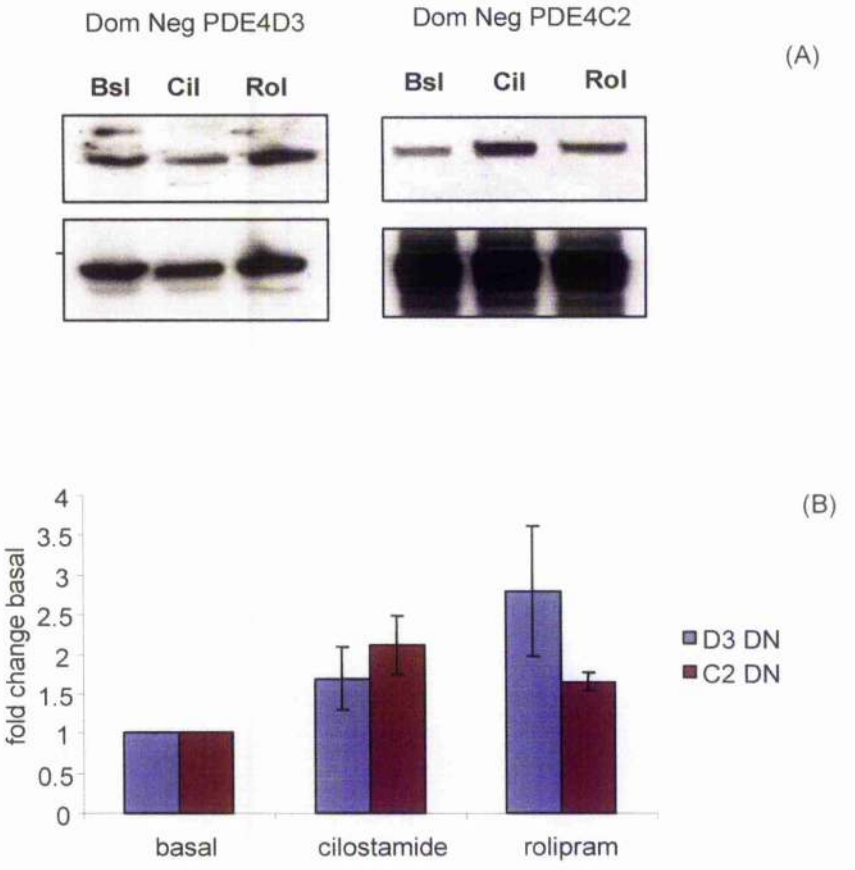

Figure 4.6 Differential PKA phosphorylation of dominant negative PDE4D3 and PDE4C2 following PDE4 or PDE3 inhibition. (A) COS1 cells were transiently transfected with dominant negative/catalytically inactive PDE4D3 and PDE4C2 long forms. The cells were treated with the selective PDE4 inhibitor Rolipram (Rol) (10 μM), and the selective PDE3 inhibitor Cilostamide (Cil) (10 μM) for 10 min. Bsl indicates resting cells. Lysates were subjected to western blot analysis; PS54-UCR1 (upper panel) and pan PDE4 subfamily (lower panel) antibodies. (B) Quantification of the PKA phosphorylation from the western blots (Quantity One software). Data was normalised for loading and represented as fold change basal. N=2 +/- S.E

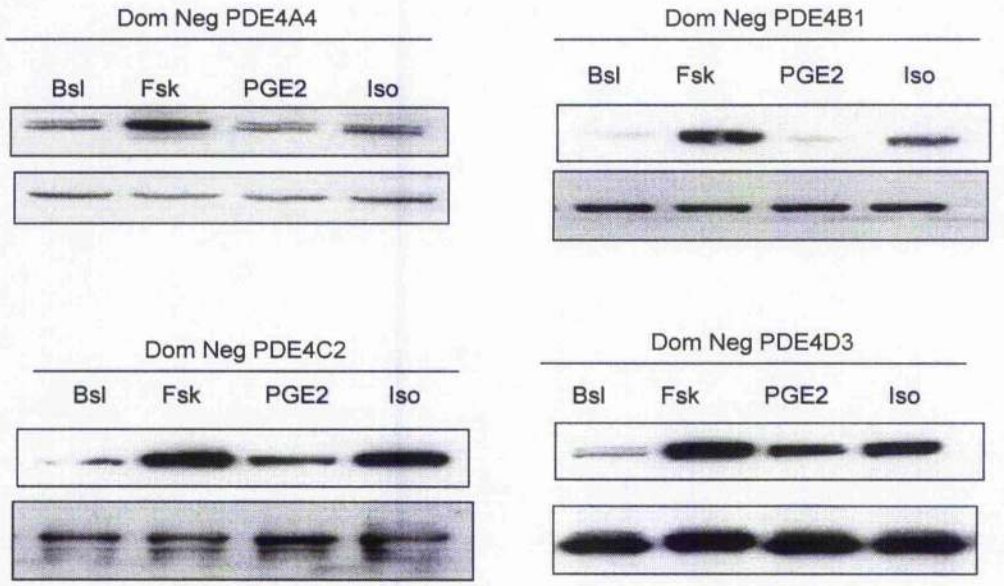

Figure 4.7a PKA phosphorylation of dominant negative PDE4s in response to different Gs-coupled agonists. COS1 cells were transiently transfected with the indicated dominant negative PDE4 isoforms. Cells were treated for 5 min PGE2 (1 μM), Isoproterenol (Iso) (1 μM) and forskolin (Fsk) (100 μM). Bsl indicates basal adenylyl cyclase activity. Lysates were subjected to western blot analysis; PS54-UCR1 antibody (upper panels), pan PDE4 sub family antibody (lower panels). Represents three separate transfections.

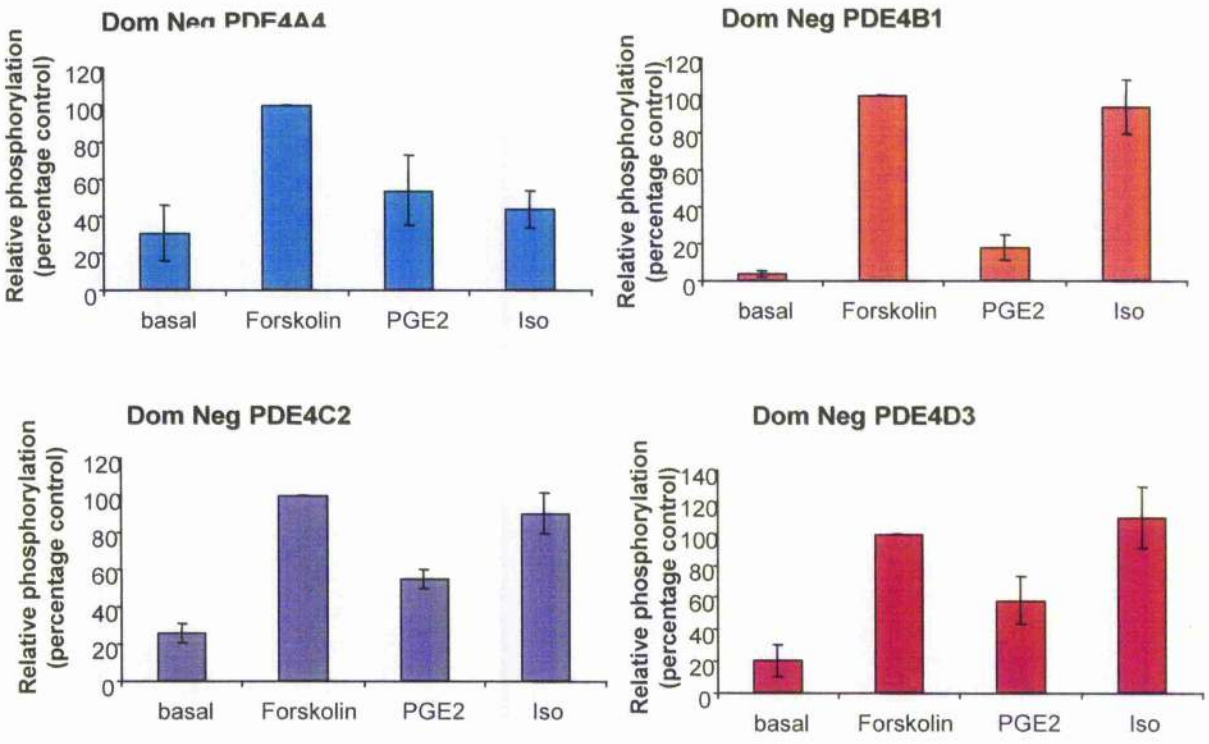

Figure 4.7b Quantification of level of PKA phosphorylation of catalytically inactive/ dominant negative PDE4s in response to different G-coupled agonists. The western blots from the previous experiment (figure 4.6a) were scanned and the phosphorylated bands were analysed by densitometry (Quantity One software analysis). All data corrected for loading and represented as percentage control (forskolin). N=3 +/- S.E.

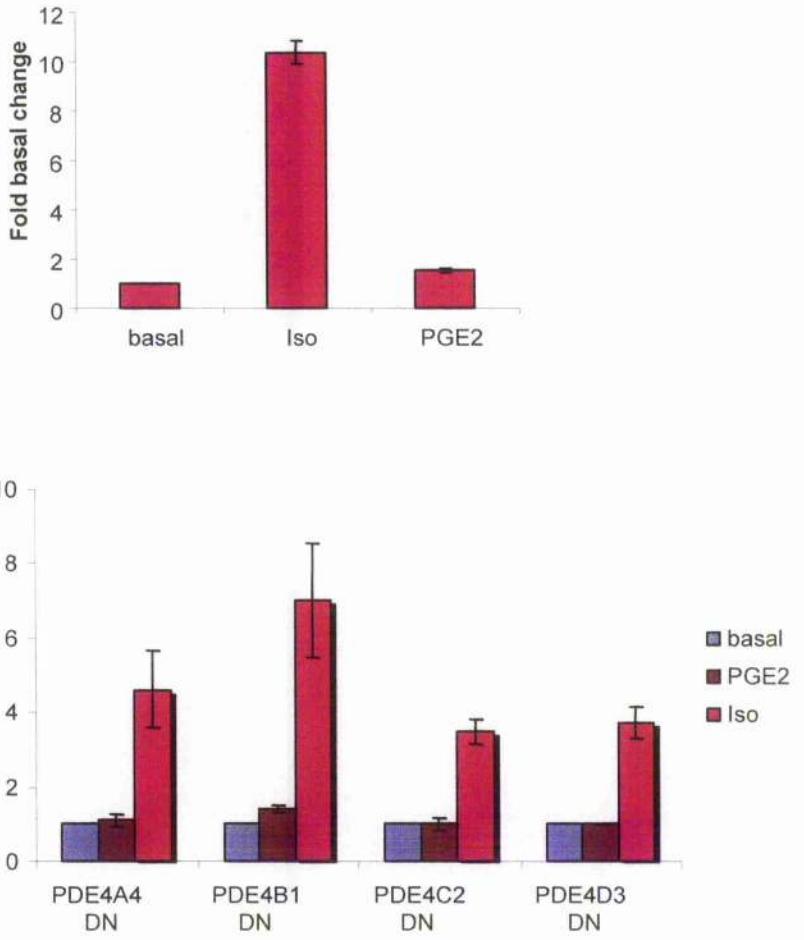

Figure 4.7c Comparison of cAMP levels following Gs-coupled receptor activation in COS1 cells overexpressing the indicated catalytically inactive/dominant negative PDE4s. Upper graph represents global increases in cAMP level in COS1 cells in response to Isoproterenol (10 μM) or PGE2 (1μM) stimulation. COS1 cells were transiently transfected with the indicated dominant negative PDE4s and subjected to 5 min stimulation with Isoproterenol (10 μM) or PGE2 (1 μM) (lower graph). Basal indicates resting cAMP levels. Results are shown as fold basal change. N=3 +/- S.E.

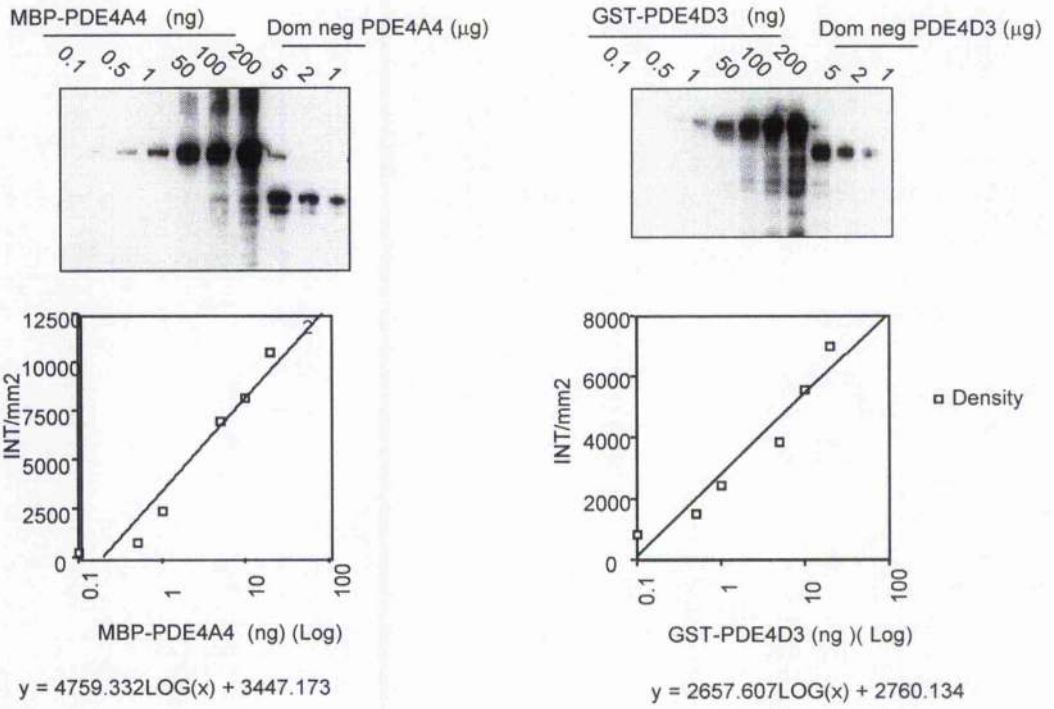

Figure 4.8a Quantification of expression levels of catalytically inactive/dominant negative PDE4D3 and PDE4A4 vectors transiently transfected into COS1 cells. A range of concentrations (μg) of lysates from a previous PKA phosphorylation experiment (figure 4.6) was subjected to SDS-PAGE analysis alongside a range of concentrations (ng) of purified recombinant *E. coli* expressed PDE4A4 (MBP tagged) and PDE4D3 (GST fusion protein). Western blots (top panels) were probed with the relevant pan PDE4 subfamily antibodies, and a standard curve was generated using densitometry software (Quantity One). This data represents one of two separate quantifications.

	Expression (pmol)
PDE4A4	0.026 +/- 0.002
PDE4D3	0.024 +/- 0.014

Figure 4.8b Quantification of expression levels of catalytically inactive/dominant negative PDE4D3 and PDE4A4 vectors transiently transfected into COS1 cells. Using the equation of the line calculated from the standard curves; (MBP-PDE4A4 y = 4759.332LOG(x) + 3447.173 and GST-PDE4D3 y = 2657.607LOG(x) + 2760.134), the number of pmol of overexpressed PDE4A4 and PDE4D3 present in 5 μg of COS1 lysate was calculated. Data represents two separate experiments.

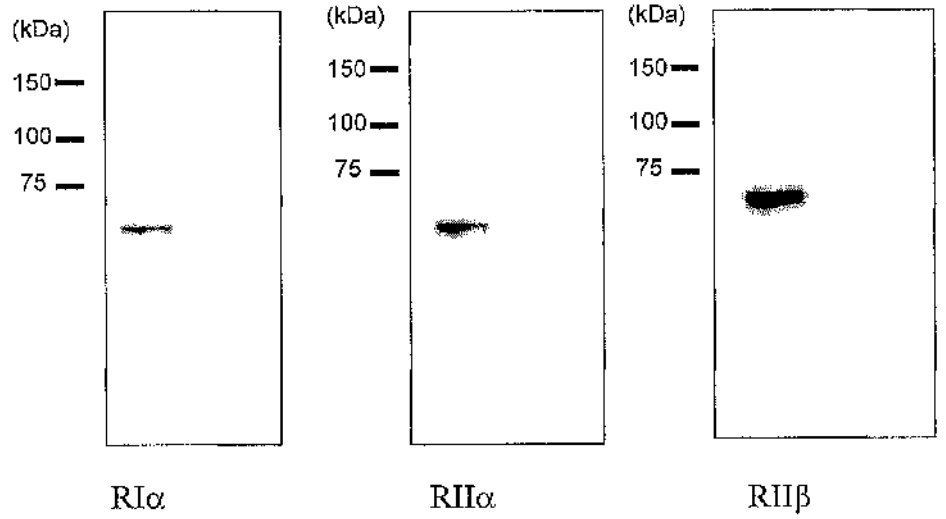

Figure 4.9 Endogenous expression of protein kinase A regulatory subunits in COS1 cells. COS1 lysates were separated by gel electrophoresis and subjected to western blotting with regulatory subunit specific antibodies.

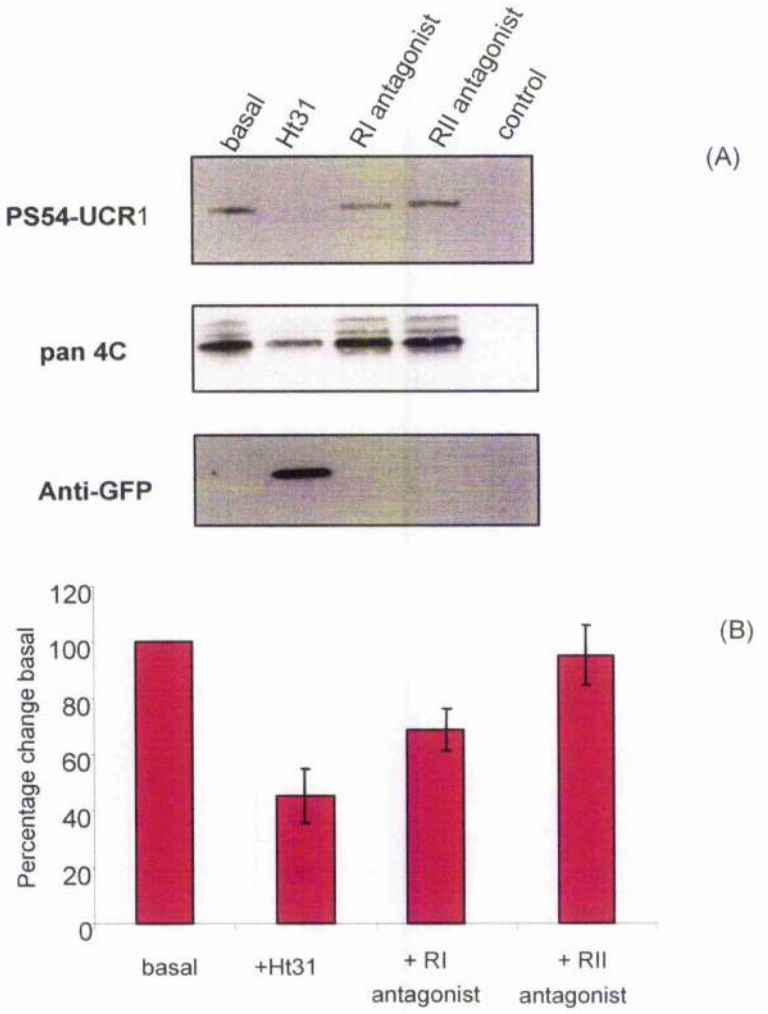

Figure 4.10 Assessment of AKAP involvement and Identification of the PKA subtype responsible for the phosphorylation catalytically/dominant negative PDE4C2 at basal cAMP levels. See next page for full figure legend.

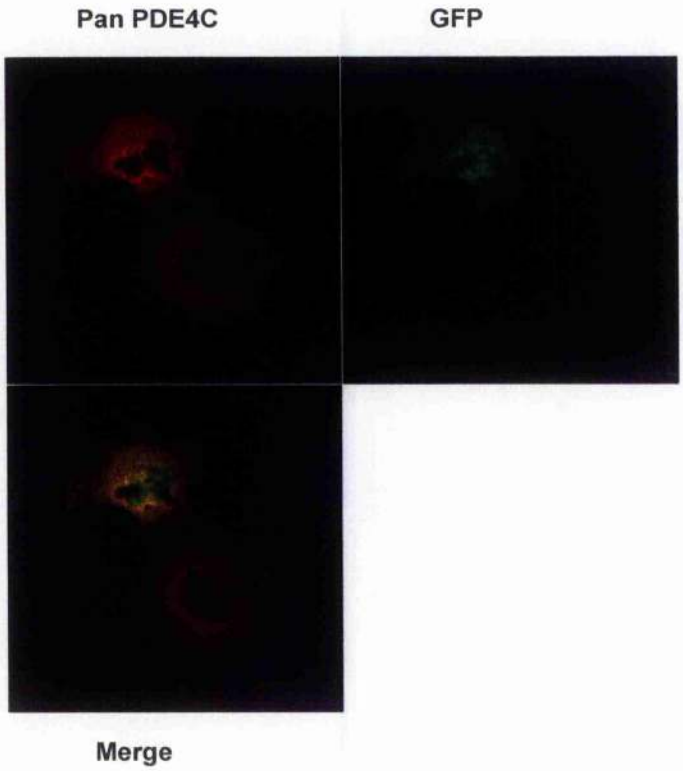

(C)

Figure 4.10 Assessment of AKAP involvement and Identification of the PKA subtype responsible for the phosphorylation catalytically/dominant negative PDE4C2 at basal cAMP levels. (A) COS1 cells were transiently transfected with dominant negative PDE4C2 and subjected to 24 h treatment with RI and RII specific antagonists. Lysates were subjected electrophoresis and analysed with PS54-UCR1 (upper panel) and pan PDE4C (middle panel) antibodies. To asses AKAP involvement, GFP-tagged Ht31 was co-transfected with dominant negative PDE4C2 and the phosphorylation was assessed at basal conditions. The middle and lower panels show co-transfection. Control indicates mock transfection. (B) The densitometry of the bands was analysed, corrected for loading/expression and represented as a percentage change basal (n+3 =/- S.E.). (C) A confocal image indicating the co-expression of GFP-Ht31 and dominant negative PDE4C2. Transfected cells were stained with pan PDE4C antibody and excited at 488 nm to show the expression of Ht31 (green fluorescence) and PDE4C2 (rhodamine staining). The yellow colour shown in the overlay indicates co-expression. Represents one of three experiments.

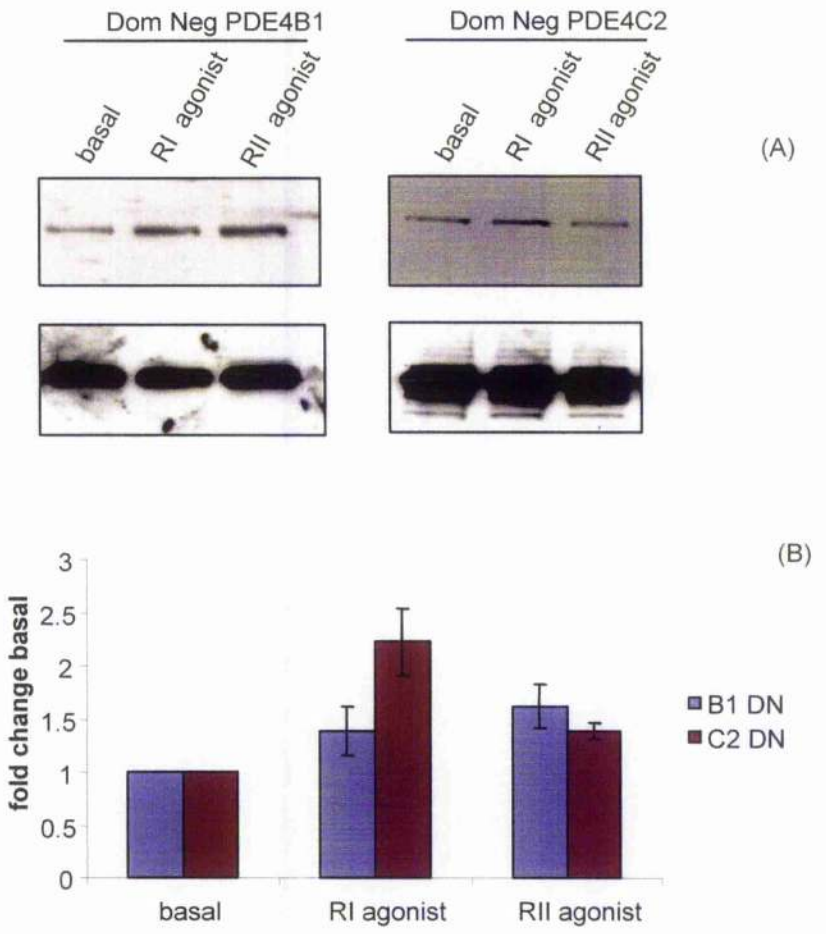

Figure 4.11 Pharmacological analysis and identification of the PKA subtype which is responsible for the phosphorylation of catalytically inactive/dominant negative PDE4C2 and PDE4B2 isoforms . COS1 cells were transiently transfected with dominant negative PDE4B1 or PDE4C2. On day two of transfection, cells were subjected to 10 min incubation with selective agonists of RI and RII forms of PKA. (A) Lysates were analysed by western blot; PS54-UCR1 (upper panels) and the relevant pan PDE4 subfamily antibodies (lower panels). (B) Densitometry analysis was performed on the phospho bands and data corrected for loading. N=2 +/- S.E.

Chapter 5

Analysis of gene expression following overexpression of catalytically inactive PDE4 isoforms

5.1 Introduction

Protein-protein interaction is a reversible process subject to the law of Mass Action, where the rapidity at which equilibria can be altered depends upon the concentration of constituents and their affinity for each other. Our group (Houslay review, 2003) and various others (Tasken *et al.*, 2001; Dodge *et al.*, 2001) have previously demonstrated that specific PDE4 isoforms can interact with various anchor or signal scaffold proteins in cells. This is thought to be responsible for controlling compartmentalised cAMP signalling. Indeed, recent studies (Mongillo *et al.*, 2004) using a genetically encoded cAMP sensor, show this to be the case at least for PDE4B and PDE4D in cardiac myocytes. My novel approach to evaluating this question has been using so-called 'dominant negative' constructs. This is where specific PDE4 isoforms have been subtly engineered, by a single point mutation in the catalytic site to be catalytically inactive and then overexpressed in cells. The philosophy of such an approach is that when the dominant negative PDE4s are chronically overexpressed in cells then, given reversible equilibrium occurring between endogenous examples of PDE4s and its particular anchor, the catalytically recombinant isoform should serve to displace and so replace endogenous active examples of that specific PDE4 isoform at its targeted anchor site. We hypothesise that such a catalytically inactive PDE4 would now ablate control of a distinct cAMP pool previously controlled by the displaced particular PDE4 isoform. This is different from a siRNA approach directed at a specific isoform where all of that isoform, be it anchored or not, would be ablated. With my dominant negative approach functional 'inactivation by displacement' would be restricted to the anchored fraction of that specific isoform only.

Here then I set out to study if catalytically inactive PDE4s might exert specific differential effects upon on the model HEK 293 cell line at the level of gene expression. The advent of DNA microarray technology allows a quantitative read-out of relative gene expression of tens of thousands of different genes. For the experiments discussed in this

chapter, U133A GeneChips© (Affymetrix, Inc, Santa Clara, CA) were used to analyse potential changes in gene expression following the overexpression of catalytically inactive PDE4s in HEK293 cells. The U133A oligonucleotide chip contained probes for a total of 22283 human genes.

5.1.1 DNA microarray overview

DNA microarray technology serves as an important tool to study regulation and function of genes, as it allows the generation of large amounts of data on thousands of genes in a single assay. Several methods have been described for producing microarrays (Harrington *et al,* 2000), with the most basic types including spotted microarrays and high-density oligonucleotide arrays. Generally, each array consists of thousands of different DNAs (PCR products or oligonucleotides) which are attached to a solid support (Schena *et al,* 1996; Harrington *et al,* 2000). The changes in gene expression are analysed by laser scanning, and thence the intensity of fluorescently labelled RNA or DNA (prepared from mRNA) hybridising to complementary DNA on the chip determined.

Spotted arrays allow the measurement of the relative gene transcript levels differing between control (reference) and experimental (test) RNAs. On spotted arrays, genes are represented by pre-synthesised single or double stranded DNA fragments of several hundred base pairs in length which are bound to glass slides (Harrington *et al,* 2000). Different fluorophores are incorporated into the cDNAs of control and test DNAs, and the labelled DNAs are mixed together prior to hybridisation to the array chip. By measuring the fluorophore signal intensities and calculating signal ratios, relative amounts of a gene transcript in the two samples can be calculated.

Commercially available oligonucleotide arrays consist of sets of oligomers synthesised *in situ* on glass wafers using a photolithographic manufacturing process (Harrington *et al,* 2000). Oligonucleotide arrays involve the labelling of the test mRNA via conversion to biotinylated cRNA and each sample is hybridised to a separate arrays. These transcript levels are calculated by reference to cRNA spikes of known concentration added to the hybridisation mixture. This method allows differences in mRNA levels between samples

(produced on separate arrays of the same type) to be calculated by comparing their respective hybridisation patterns. High-density oligonucleotide arrays allow great flexibility in sample comparisons and the oligo probes are uniquely designed to represent the cognate gene thus minimising cross-hybridisation between similar sequences.

Upon processing of the fluorescent array image, three basic steps are required for data analysis: data normalisation, data filtering, and pattern identification (Harrington *et al,* 2000). Following normalisation, data reduction can be achieved by filtering out uninformative genes. Patterns within the data are identified and interpreted by computer analysis via data mining programs.

Results

The U133A oligonucleotide GeneChip© (Affymetrix, Inc, Santa Clara, CA) allowed us to analyse the response of HEK293 cells to the chronic overexpression of different catalytically inactive PDE4s. Fold changes in gene expression were calculated by analysing the difference in gene expression between samples of mRNA isolated from HEK293 cells overexpressing a catalytically inactive PDE4 and mRNA isolated from HEK293 cells overexpressing empty vector (pcDNA) as the control sample.

I chose to study the individual effects of four different catalytically inactive PDE4s, namely PDE4A4, PDE4B2, PDE4D3 and PDE4D5 isoforms upon gene expression levels. These isoforms are all expressed endogenously in HEK293 cells which I set out to use here as a test case because the cells are easy to transfect and well characterised as far as PDE4s go. Furthermore, it has previously been shown that these specific PDE4 isoforms are expressed in human U937 monocytic cells where they provide distinct functional roles consistent with compartmentalisation of cAMP signalling (MacKenzie *et al,* 2000). If specific PDE4s control discrete functional 'pools' of cAMP, one could reason that overexpression of a catalytically inactive PDE4 would cause cAMP signalling through that specific 'pool' to increase. This local increase in cAMP could either, (i)

activate PKA, (ii) activate Epac, (iii) activate a cAMP gated ion channel or (iv) activate an unidentified cAMP signalling system. Therefore, I decided to investigate, by the use of catalytically inactive PDE4A4, PDE4B2, PDE4D3 and PDE4D5 constructs, the putative compartmentalisation of these PDE4 isoforms in a human derived cell line (HEK293 cells).

5.2 PDE4 mRNA expression profile of HEK293 cells

The expression of these chosen PDE4 isoforms in HEK293 cells has previously been shown by western blot in our laboratory (unpublished data, Houslay laboratory). I decided also to obtain evidence for transcripts of these specific PDE4 isoforms in this cell line. In order to do this, RNA was isolated from HEK293 cells and sent to Rachael Barber (Novartis, Horsham) for analysis by RT-PCR. PDE4 generic primers and primers designed to detect specific PDE4 isoforms (see Appendix for details) were used to build a PDE4 profile of this cell line. cDNA from brain tissue was used as a positive control and water as a negative control. Amplicons for generic PDE4A, PDE4B, PDE4C, PDE4D, PDE3B and PDE7A were observed. The isoform specific primers identified the following transcripts for PDE4 isoforms: PDE4A4, PDE4A10, 2EL, PDE4B1, PDE4B2, PDE4B3, PDE4D1, PDE4D1/D2, PDE4D3 and PDE4D5 (figure 5.1). PDE4 isoforms, namely PDE4A4, PDE4B2, PDE4D3 and PDE4D5 chosen for microarray analysis are expressed endogenously in HEK293 cells.

5.2.1 Overexpression of catalytically inactive PDE4s and microarray analysis of gene expression

HEK293 cells were transfected with the selected catalytically inactive PDE4 cloned into the pcDNA vector (Invitrogen), and, as a control, HEK293 cells were also transfected with empty pcDNA vector. The transfections were performed in triplicate, mRNA isolated and sent to Novartis (Genomics Dept, Basle, Switzerland). The microarray data was normalized, and statistical analysis performed also at Novartis (Genomics

Department Basle, Switzerland). The fold change in gene expression between cells overexpressing catalytically inactive and cells overexpressing the empty control vector (pcDNA) was calculated from the mean expression values. The p-values were calculated by performing a heteroscedastic student's t-test.

The tables of microarray data provided in this chapter list all fold-changes of gene expression of greater than 5-fold and of p-values less than 0.05 (tables 5.1- tables 5.4). Furthermore, I have provided a CD within the appendix listing all fold changes of gene expression of p-values less than 0.05, and of p-values less than 0.01. However, from all the microarray data presented in this chapter, I will only discuss the most striking changes in expression of mRNA levels, including changes in levels of mRNA of proteins involved cAMP signalling.

5.2.1.1 Changes in gene expression unique to the overexpression of catalytically inactive PDE4A4

The changes in gene expression following the overexpression of PDE4A4 are shown in a tabular format (table 5.1). The left-hand column shows the fold-change in gene expression compared to the vector only control, the middle column provides the p-values and the last column details the gene description as provided by the manufacturer of the U133A oligonucleotide GeneChip© (Affymetrix, Inc, Santa Clara, CA). Up-regulation of gene expression is shown by a positive fold-change and down-regulation of gene expression is shown by a negative fold-change.

It can be seen that the overxepression of catalytically inactive PDE4A4 caused a greater than 5-fold up-regulation in levels of mRNA from 19 different genes and a down-regulation of mRNA expression levels of 8 different genes. Most strikingly, a 24-fold up-regulation in expression in mRNA for an inositol 1, 4, 5-triphosphate receptor (type 3) was observed. A change in the expression of mRNA for this receptor was not observed following the overexpression of catalytically inactive PDE4B2, PDE4D3 or PDE4D5

(tables 5.2, 5.3 & 5.4). The inositol 1, 4, 5-triphosphate receptors (IP3 receptors) constitute as family of Ca^{2+} channels which facilitate the mobilisation of intracellular Ca^{2+} stores. Cross-talk between cAMP signalling and Ca^{2+} has been reported in cardiac myoctes (MacLennan & Kranias, 2003). IP3 receptors can be directly phosphorylated by PKA which alters, depending on the cell or tissue type, the flux of Ca^{2+} (Patel *et al,* 1999). The promoter region of the IP3 receptors does not contain a CRE site. Therefore, the overexpression of catalytically inactive PDE4A4 may, unlike the other catalytically inactive PDE4s, have increased the levels of cAMP in a distinct 'pool' resulting in the up-regulation of gene expression the IP3 receptor.

Both up-regulation and down-regulation of different G-protein coupled receptors was observed following the overexpression of catalytically inactive PDE4A4 and PDE4D3 (tables 5.1 & 5.3). A change in the expression levels of mRNA of lysophosphatidic acid G-protein-coupled receptor 4 (EDG4) was only observed following the overexpression of catalytically inactive PDE4A4. The mRNA expression levels of EDG4 increased by some 12-fold (table 5.2). This G-protein coupled receptor belongs to the lysophosphatidic acid (LPA) receptor family, and couples to the $G_{i/o}$, $G_{12/13}$ and G_q proteins (Contos *et al,* 2000). LPA stimulates cell proliferation through the activation of tyrosine kinase and MAP kinase (Moolenaar *et al,* 1997), it has also been shown to increase intracellular Ca^{2+} levels and inositol phosphates (Contos *et al,* 2000). The promoter region of EDG4 has not been shown to posses a CRE site. As only the overexpression of catalytically inactive PDE4A4 provides a change in the gene expression of EDG4, this suggests that only endogenous expressed PDE4A4 in HEK293 cells maybe controlling a distinct 'pool' of cAMP which, when manipulated with catalytically inactive PDE4A4, alters the transcriptional regulation of EDG4.

A striking down-regulation, of some 20-fold, was seen for the mRNA expression levels of PACE4C (kexin-like protease) only following the overexpression of inactive PDE4A4. PACE4C is a member of the subtilisin/Kex2p family (Nakayama, 1997). The subtilisin/Kex2p family are a family of endoproteases which are responsible for the conversions of precursors of peptide hormones, neuropeptides and many other proteins into their biologically active forms (Nakayama, 1997). PACE4 is responsible for the

activation of transforming growth factor-β (TGFβ)-related factors such as bone morphogenetic proteins (Tsuji *et al.*, 2003). The biological activity of TGFβ molecules can be regulated by PACE4 which anchors heparin sulphate proteoglycans to the extracellular matrix (ECM) (Tsuji *et al.*, 2003). It is postulated that the interaction of PACE4 and heparin sulphate proteoglycans might play an important role in the spatial and temporal regulation TGFβ-related factor's biological activity (Tsuji *et al.*, 2003).

5.2.1.2 Changes in gene expression unique to the overexpression of catalytically inactive PDE4B2

Overexpression of catalytically inactive PDE4B2 in HEK293 cells only resulted in the up-regulation of mRNA expression greater than 5-fold of one gene, and the down-regulation of mRNA expression greater than 5-fold of four different genes (table 5.2).

Interestingly, a 7-fold decrease in the expression of mRNA encoding RING finger protein 22 (RNF22) was only observed following the overexpression of catalytically inactive PDE4B2 (table 5.3). Over the last 5 years, RING finger proteins have been identified as key mediators in the ubiquitinylation of proteins (Joazeiro & Weissman, 2000). Ubiquitinylation plays an important in the regulation of the levels of plasma membrane proteins through proteasomal degradation and by facilitating endocytosis (Joazeiro & Weissman, 2000). Protein ubiquitinylation begins with the formation of a thiol-ester linkage between ubquitin (Ub) and the Ub activating enzyme (E1). Ub is then transferred, through a thiol-ester linkage, to an Ub conjugating enzyme (E2). Ubiquitin ligase (E3) interacts with E2 and the protein target allowing the transfer of Ub to the target protein, thus provide specificity to Ub conjugation (Joazeiro & Weissman, 2000). RING finger proteins now represent the largest class of E3s to date.

The overexpression of catalytically inactive PDE4B2 resulted in both the up-regulation and the down-regulation of a few genes. This suggests that the cAMP 'pool' controlled by endogenous PDE4B2 has little effect upon gene expression. However, the observation

that the mRNA levels of RING finger protein 22 (RNF22) are down-regulated, suggests that PDE4B2 may serve to influence the ubiquitinylation of an as yet unidentified protein.

5.2.1.3 Changes in gene expression unique to the overexpression of catalytically inactive PDE4D3

Following the overexpression of catalytically inactive PDE4D3, a greater than 5-fold up-regulation in levels of mRNA was observed from 8 different genes and a greater than 5-fold down-regulation of mRNA expression levels of 4 different genes was observed (table 5.3).

Interestingly, upon comparison of the microarray data generated following overexpression of each of the catalytically inactive PDE4s, a down-regulation in the gene expression of a GPCR was only observed following the overexpression of catalytically inactive PDE4D3 (table 5.3). A down-regulation of two different types of GPCR was observed, 5-fold down-regulation of G-protein coupled channel (hGIRK1) and a near 8-fold down-regulation of a GPCR (HG38)

G-protein coupled inwardly rectifying potassium channel (GIRK) are expressed in heart, the nervous systems and endocrine tissues where they control post-synaptic inhibitory signalling and hormone secretion by pertussis toxin sensitive GPCRs (Sadja *et al,* 2003). GIRK channels are modulated by a variety of different factors such as phosphatidylinositol-4, 5-biphosphate (PIP_2), Na^{+}, Mg^{2-}, oxidation-reduction, phosphorylation and acidification (Sadja *et al,* 2003).

HG38 is an orphan G-coupled receptor, which when its sequence is compared to those of other G-protein coupled receptor families, shares an overall identity of ~ 35% with the FSH, TSH and LH/hGC of the glycoprotein hormone receptor subfamily (McDonald *et al,* 1998). As with all glycoprotein receptors, HG38 is predicted to have a large extracellular domain with Leucine-rich repeats (LRR) which would potentially allow protein-protein interactions (McDonald *et al,* 1998). The *in vivo* function of HG38 has yet to elucidated, but as the three other members of the glycoprotein receptor subfamily

play pivotal roles in growth, development and reproduction, it is expected that HG38 will have a similar role.

With respect to the regulation of GPCR gene expression, only the overexpression of catalytically inactive PDE4D3 resulted in the down-regulation of hGIRK and HG38 (table 5.3). However, in contrast, the overexpression of a different catalytically inactive PDE4, namely PDE4A4, resulted in an up-regulation of a GPCR, specifically EDG4 (tables 5.1). These data suggests that PDE4A4 and PDE4D3 may act on distinct pools of cAMP and thus act on different signalling pathways resulting in differential gene regulation of specific GPCRs

5.2.1.4 Changes in gene expression unique to the overexpression of catalytically inactive PDE4D5

Overexpression of catalytically inactive PDE4D5 in HEK293 cells resulted in the up-regulation of mRNA expression greater than 5-fold of seven different genes and the down-regulation of mRNA expression greater than 5-fold of six different genes (table 5.4).

Although PDE4D3 and PDE4D5 are splice variants from the PDE4D subfamily, and are both long isoforms, they are known to interact with distinct signalling scaffold proteins. Interestingly, here we see that analysis of the microarray data produces some clear differences in the regulation of the levels of gene expression following the overexpression of the catalytically inactive species of each of these specific isoforms. Most interestingly, an 8-fold down-regulation of the gene expression of phospholipase D, and a 7-fold down-regulation of the gene expression of Glucose Transporter-like Protein (SLC2A9) were only evident following the overexpression of catalytically inactive PDE4D5.

Phospholipase D (PLD) enzymes constitute a family of phosphodiesterases that catalyse the hydrolysis of phosphatidylcholine (PtdCho) to generate choline and phosphatidic acid (PtdOH). Phospholipase D is involved a variety of physiological processes such as

endocytosis, exocytosis, vesicle coat recruitment, and budding from the Golgi apparatus (Liscovitch *et al,* 2000; Freyberg *et al,* 2003). Much of the research on has focused on the regulation of PLD activity by PKCα (Ca^{2+}-dependent form of PKC), PKCδ, rac- and Rho-GTPases, and small GTP-binding proteins such as ARF (Cockcroft *et al,* 1994; Hammond *et al,* 1997; Han *et al,* 2002; Freyberg *et al,* 2003; Liscovitch *et al,* 2000).

Facilitative glucose carriers such as members of the SLC2A family enable the transport of hexoses across the plasma membrane, and are important mediators in body sugar homeostasis. A novel member of the SLC2A family, SLC2A9 (GLUT9), was recently identified and characterised (Augustia *et al,* 2004). This study showed that SLC2A9 was expressed in human kidney proximal tubules, predominantly in the basal lateral membrane.

As an up-regulation of phospholipase D (PLD) mRNA and down-regulation of SLC2A9 mRNA was observed only following the overexpression of catalytically inactive PDE4D5, this suggests that the endogenous form of this PDE4 isoform, via control of cAMP levels, can influence the gene expression of signalling proteins of two different signalling pathways.

5.2.1.5 Common changes in levels of gene expression following overexpression of the catalytically inactive PDE4s.

Overexpression of catalytically inactive PDE4A4, PDE4D3 and PDE4D5 also provided identical changes in certain sets of genes that were either up-regulated or down-regulated. Common changes in gene expression are listed in table 5.5, along and I will discuss below a few examples of common changes of gene expression.

An 8-fold up-regulation in the expression of mRNA of secretogranin II (chromogranin C) was observed following the overexpression of catalytically inactive PDE4A4, PDE4D3 or PDE4E5 (table 5.5). Secretogranin II is a member of the secretogranin/chromogranin secretory protein family. Secretogranin/chromogranin secretory proteins are released from secretory vesicles together with hormones or neurotransmitters. Secretogranin II is

the precursor of the neuropeptide secretoneurin (Fischer-Colbrie *et al,* 1995). It has been reported that the regulation of synthesis of secretogranin II can be influenced by various different second messengers, including cAMP, Ca^{2+}, cGMP (Fischer-Colbrie *et al,* 1995). Interestingly, up-regulation of the mRNA expression of secretogranin II was achieved in bovine chromaffin cells by forskolin treatment (Fischer-Colbrie *et al,* 1990). This up-regulation was thought to be due to presence of CRE in the promoter of secretogranin II (Schimmel *et al,* 1992). My observation of an up-regulation of the mRNA expression of secretogranin II following the overexpression of either catalytically inactive PDE4A4, PDE4D3 or PDE4E5 is most probably result of an increase of cAMP and subsequent activation of CRE .

The up-regulation of the mRNA expression of cytosolic phospholipase A_2 gamma ($cPLA_{2\gamma}$) of 9-fold and 8-fold was evident following the overexpression of catalytically inactive PDE4A4 or PDE4D3 respectively (tables 5.1 & 5.4). Phospholipase A_2 (PLA_2) is a key mediator, via the liberation of arachidonic acid, in the synthesis of eicosanoids which include prostaglandins, thromboxanes and leukotrienes. So far three different isoforms of $cPLA_2$ have been identified, $cPLA_{2\alpha}$, $cPLA_{2\gamma}$ and $cPLA_{2\beta}$. Each isoform of $cPLA_2$ possesses a consensus MAPK phosphorylation site (PXSP motif) and it has been shown that MAPK phosphorylation of $cPLA_{2\alpha}$ increases its intrinsic enzymatic activity, augmenting Ca^{2+}-induced arachidonic acid release (Hirabayashi & Shimizu, 2000). A variety of cytokines, IL-1, TNFα, epidermal growth factor and interferon-γ have been shown to increase the synthesis of mRNA of $cPLA_{2\alpha}$ in several cell models (Hirabayashi & Shimizu, 2000).

5.3 Discussion

A spatially distinct elevation of cAMP and/or PKA activation, as achieved by replacement of an endogenous PDE4 by a catalytically inactive PDE4 species, could alter gene expression by a number of different ways. Proof of the dominant negative/catalytically inactive principle has already been shown, whereby overexpression of inactive PDE4D5 in cardiac myocytes, saturated the β–arrestin sites for PDE and

enhanced isoproterenol-stimulated membrane associated PKA activity (Perry *et al*, 2002, Baillie *et al*, 2003).

PKA can exert long term effects on cellular functioning by altering the functions of a variety of nuclear proteins including a large number of transcription factors, nuclear hormone receptors, transcriptional activators/repressors and chromatin-associated proteins (Shabb, 2001). PKA can also indirectly exert effects upon transcriptional regulation via activation of the MAP kinase cascade. Also, it is possible that PKA may indirectly exert its effects upon transcription via the phosphorylation of another, unidentified signalling protein. In a recent review of physiological substrates of PKA (Shabb, 2001), it was shown that since the discovery of PKA in the 70s, the list of identified PKA substrates has quadrupled in the last decade and it is highly likely that many more PKA targets are yet to be identified. Research using the recently discovered Epac specific activator, 8-pCPT-2'-*O*-Me-cAMP, proposes that not all PKA-independent effects of cAMP can be attributed to Epac. This paves the way for the future discovery of further cAMP targets with cAMP binding domains not similar to that of Epac and PKA (Bos, 2003). Thus, there is a wide variety of identified and yet to be identified mechanisms by which cAMP can alter regulation of gene transcription, via direct or indirect actions.

My study, utilising the catalytically inactive PDE4 species as a form of manipulating different pools of cAMP did indeed provide data showing differential gene expression. The use of microarray technology allowed me to identify the changes in gene expression in a HEK293 cell model following the overexpression of catalytically inactive PDE4s. I identified, upon comparing the microarray data between the different inactive PDE4 species, many differences in gene expression. As we believe that the different catalytically inactive PDE4s alter different pools of cAMP, one would expect the general PDE4 inhibitors, namely rolipram and ariflo, to 'knock' out all PDE4s and thus result in a more global increase in cAMP. Therefore, we would expect the inhibition of all PDE4s by rolipram and ariflo to encompass all changes in gene expression, with regards to those changes observed following overexpression of the catalytically inactive PDE4s. However

this was not the case, as shown in tables 5.6 and 5.7. Here, the actual gene changes observed following 48hr treatment of HEK cells with rolipram or with ariflo are listed in tables. It is quite clear from these data that ariflo or rolipram treatment resulted in quite different changes in gene expression compared to those observed with any of the catalytically inactive PDE4 isoforms. This suggests that not only do overexpression of catlytically inactive PDE4s subtly alter distinct cAMP pools, but that one cAMP pool may control another.

However, the non-physiological effects of the overexpression of the inactive species must be taken into account. It is possible that overexpressed PDE4 species bind aberrantly to other proteins allowing non-specific, non-physiological effects. If time had allowed, I would have confirmed the changes in gene observed by RT-PCR and northern blot analysis. Furthermore, I would have studied the effects of such gene expression at the level of protein expression by SDS-PAGE analysis. Finally, it would be interesting to further assess gene changes following the manipulation of cAMP pools by means of siRNA. Designing PDE4 isoform specific siRNA would provide a different approach to 'knocking out' the PDE4 isoforms and studying their effects on gene expression.

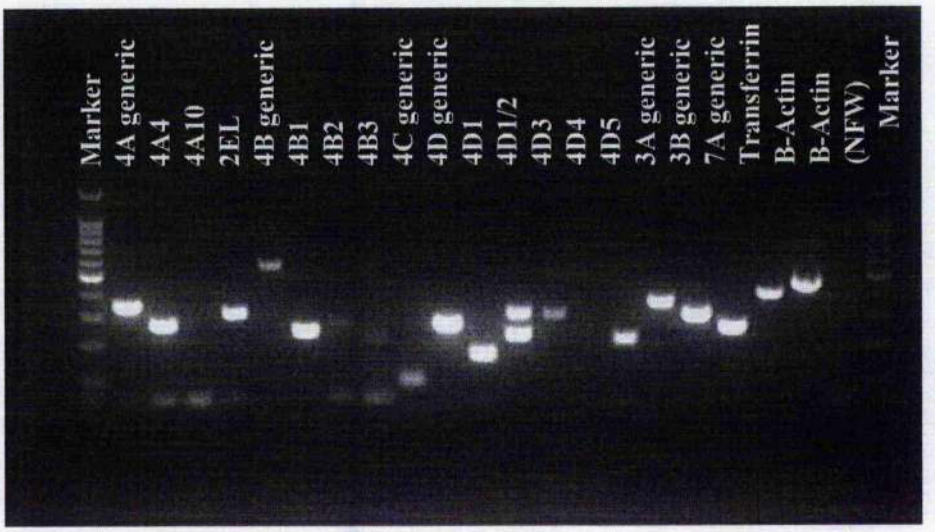

Figure 5. 1 The PDE mRNA expression profile of HEK293 cells. The gel represents a typical PDE mRNA profile of HEK293 cells. Total RNA was isolated from HEK293 cells, synthesised to cDNA and subjected to PCR using primers designed to specific PDE isoforms (see appendix for primer details).

Fold change	p-value	Description
24.815	*0.014907*	gb:D26351.1 /DEF=Human mRNA for type 3 inositol 1,4,5-trisphosphate receptor, complete cds.
21.037	*0.001538*	Consensus includes gb:AK000847.1 /DEF=Homo sapiens cDNA FLJ20840 fis, clone ADKA02336. zinc finger protein 236
11.395	*0.033203*	gb:NM_004720.3 /DEF=Homo sapiens endothelial differentiation, lysophosphatidic acid G-protein-coupled receptor, 4 (EDG4), mRNA.
9.510	*0.001942*	Consensus includes gb:NM_003530.1 /DEF=Homo sapiens H3 histone family, member B (H3FB), mRNA.
9.238	*0.000583*	gb:AF065214.1 /DEF=Homo sapiens cytosolic phospholipase A2 gamma (cPLA2 gamma) mRNA, complete cds
7.724	*0.000723*	gb:NM_003469.2 /DEF=Homo sapiens secretogranin II (chromogranin C) (SCG2), mRNA.
7.270	*0.022009*	gb:NM_005263.1 /DEF=Homo sapiens growth factor independent 1 (GFI1), mRNA.
7.262	*0.001139*	gb:AF133207.1 /DEF=Homo sapiens protein kinase (H11) mRNA, complete cds.
7.176	*9.79E-05*	gb:NM_030795.1 /DEF=Homo sapiens stathmin-like-protein RB3 (RB3), mRNA.
6.618	*0.000201*	Consensus includes gb:AA284829 /FEA=EST Weakly similar to Z139_HUMAN ZINC FINGER PROTEIN 13 H.sapiens
5.899	*0.00023*	gb:NM_005794.1 /DEF=Homo sapiens short-chain alcohol dehydrogenase family member (HEP27), mRNA.
5.653	*0.035828*	gb:NM_000783.1 /DEF=Homo sapiens cytochrome P450, subfamily XXVIA, polypeptide 1 (CYP26A1), mRNA
5.616	*0.007183*	gb:NM_005132.1 /DEF=Homo sapiens Rec8p, a meiotic recombination and sister chromatid cohesion phosphoprotein of the rad21p family (REC8), mRNA.
5.393	*5.16E-05*	gb:NM_016639.1 /DEF=Homo sapiens type I transmembrane protein Fn14 (FN14), mRNA
5.387	*0.004982*	gb:NM_001421.1 /DEF=Homo sapiens E74-like factor 4 (ets domain transcription factor) (ELF4), mRNA.

Fold change	p-value	Description
5.378	*0.004279*	gb:NM_003543.2 /DEF=Homo sapiens H4 histone family, member H (H4FH), mRNA.
5.329	*0.049943*	Consensus includes gb:AK024281.1 /DEF=Homo sapiens cDNA FLJ14219 fis, clone NT2RP3003800, highly similar to Rattus norvegicus tyrosine protein kinase pp60-c-src mRNA.
5.165	*0.015786*	gb:NM_016184.1 /DEF=Homo sapiens C-type (calcium dependent, carbohydrate-recognition domain) lectin, superfamily member 6 (CLECSF6), mRNA
5.132	*0.001163*	Moderately similar to ALU7_HUMAN ALU SUBFAMILY SQ SEQUENCE CONTAMINATION WARNING ENTRY H.sapiens
-5.403	*0.025632*	gb:NM_017417.1 /DEF=Homo sapiens UDP-N-acetyl-alpha-D -galactosamine:polypeptide N-acetylgalactosaminyltransferase 8 (GalNAc-T8) (GALNT8), mRNA.
-5.951	*0.021371*	CLONE=IMAGE:4478872 /UG=Hs.155530 interferon, gamma-inducible protein 16 /FL=gb:AF208043.1
-6.468	*0.0219*	Consensus includes gb:AL133015.1 /DEF=Homo sapiens mRNA; cDNA DKFZp434O2417 (from clone DKFZp434O2417
-7.418	*0.009077*	Consensus includes gb:AI815033 CLONE=IMAGE:2420736 /UG=Hs.55947 KIAA0805 protein
-9.581	*0.018937*	Consensus includes gb:D50604 /DEF=Human beta-cytoplasmic actin (ACTBP9) pseudogene /FEA=CDS /DB_XREF=gi:2094759
-12.693	*0.020161*	gb:NM_004571.1 /DEF=Homo sapiens PBXknotted 1 homeobox 1 (PKNOX1), mRNA.
-20.430	*0.005259*	gb:D28513.1 /DEF=Human mRNA for PACE4C (kexin-like protease), complete cds
-38.900	*0.04771*	Consensus includes gb:AF279774.1 /DEF=Homo sapiens clone N4 NTera2D1 teratocarcinoma mRNA.

Table 5.1 Changes in levels of mRNA levels following overexpression of catalytically inactive PDE4A4. The fold change was calculated from the mean expression values between the PDE4A4 sample and the empty vector control sample (pcDNA). P-values were calculated by the heteroscedastic students t-test .

Fold change	p-value	Description
5.367127496	0.0042	gb:NM_005132.1 /DEF=Homo sapiens Rec8p, a meiotic recombination and sister chromatid cohesion phosphoprotein of the rad21p family (REC8), mRNA.
-6.730308219	0.0060	gb:NM_030769.1 /DEF=Homo sapiens hypothetical protein similar to swine acylneuraminate lyase (C1ORF13), mRNA.
-6.877358491	0.0009	Consensus includes gb:AF271088.1 /DEF=Homo sapiens deleted in azoospermia (DAZ) mRNA, partial cds.
-7.163461538	0.0004	gb:NM_006458.1 /DEF=Homo sapiens ring finger protein 22 (RNF22), mRNA.
-8.509615385	0.0074	Consensus includes gb:AW445040 CLONE=IMAGE:2733928 /UG=Hs.300863 lethal (3) malignant brain tumor l(3)mbt protein Drosophila) homolog

Table 5.2 Changes in levels of mRNA levels following overexpression of catalytically inactive PDE4B2. The fold change was calculated from the mean expression values between the PDE4B2 sample and the empty vector control sample (pcDNA). P-values were calculated by the heteroscedastic students t-test .

Fold change	p-value	Description
8.3821	0.0007	gb:AF065214.1 /DEF=Homo sapiens cytosolic phospholipase A2 gamma (cPLA2 gamma) mRNA, complete cds.
8.2313	0.0011	Consensus includes gb:NM_003530.1 /DEF=Homo sapiens H3 histone family, member B (H3FB), mRNA.
8.0520	0.0008	gb:AF133207.1 /DEF=Homo sapiens protein kinase (H11) mRNA, complete cds
7.9606	0.0074	gb:NM_003469.2 /DEF=Homo sapiens secretogranin II (chromogranin C) (SCG2), mRNA
6.2408	0.0001	gb:NM_030795.1 /DEF=Homo sapiens stathmin-like-protein RB3 (RB3), mRNA.
5.9783	0.0005	Consensus includes gb:AA284829 Weakly similar to Z139_ HUMAN ZINC FINGER PROTEIN 13 H.sapiens
5.2637	0.0002	gb:NM_003543.2 /DEF=Homo sapiens H4 histone family, member H (H4FH), mRNA.
5.0220	0.0005	gb:NM_016639.1 /DEF=Homo sapiens type I transmembrane protein Fn14 (FN14), mRNA.
-5.4160	0.0015	gb:U39196.1 /DEF=Human clone hGIRK1 G-protein coupled inwardly rectifying potassium channel mRNA, complete cds.
-5.5022	0.0240	Consensus includes gb:AI986120 CLONE=IMAGE:2494024 /UG=Hs.241257 latent transforming growth factor beta binding protein 1 /FL=gb:M34057.1 gb:NM_000627.1
-7.5607	0.0141	gb:AF062006.1 /DEF=Homo sapiens orphan G protein-coupled receptor HG38 mRNA, complete cds.
-7.7203	0.0247	Consensus includes gb:BG256677 /CLONE=IMAGE:4478872 /UG=Hs.155530 interferon, gamma-inducible protein 16 /FL=gb:AF208043.1

Table 5.3 Changes in levels of mRNA levels following overexpression of catalytically inactive PDE4D3. The fold change was calculated from the mean expression values between the PDE4D3 sample and the empty vector control sample (pcDNA). P-values were calculated by the heteroscedastic students t-test .

Fold change	p-value	Description
11.1798	0.0045	gb:NM_018452.1 /DEF=Homo sapiens uncharacterized bone marrow protein BM033 (BM033), mRNA.
10.7529	0.0102	Consensus includes gb:AK000847.1 /DEF=Homo sapiens cDNA FLJ20840 DB_XREF=gi:7021168 /UG=Hs.283619 zinc finger protein 236
8.1575	0.0096	gb:NM_003469.2 /DEF=Homo sapiens secretogranin II (chromogranin C) (SCG2), mRNA.
7.2607	0.0014	gb:AF133207.1 /DEF=Homo sapiens protein kinase (H11) mRNA, complete cds.
7.1487	0.0127	gb:NM_005794.1 /DEF=Homo sapiens short-chain alcohol dehydrogenase family member (HEP27), mRNA.
5.4997	0.0033	gb:NM_001421.1 /DEF=Homo sapiens E74-like factor 4 (ets domain transcription factor) (ELF4), mRNA.
5.4270	0.0004	gb:NM_030795.1 /DEF=Homo sapiens stathmin-like-protein RB3 (RB3), mRNA.
-6.0505	0.0000	Consensus includes gb:U78581.1 /DEF=Human type I phosphatidylinositol-4-phosphate 5-kinase beta (STM7) mRNA, partial cds.
-6.5605	0.0199	Consensus includes gb:AI983428 /CLONE=IMAGE:2510766 /UG=Hs.146428 collagen, type V, alpha 1
-7.0000	0.0480	gb:NM_020041.1 /DEF=Homo sapiens solute carrier family 2 (facilitated glucose transporter), member 9 (SLC2A9), mRNA.
-7.8070	0.0012	Consensus includes gb:AU147830 Homo sapiens cDNA FLJ12295 fis, clone MAMMA1001818
-8.2156	0.0440	gb:L11702.1 /DEF=Human phospholipase D mRNA, complete cds.
-17.5996	0.0198	Consensus includes gb:BG256677 interferon, gamma-inducible protein 16 /FL=gb:AF208043.1

Table 5.4 Changes in levels of mRNA levels following overexpression of catalytically inactive PDE4D5 . The fold change was calculated from the mean expression values between the PDE4D5 sample and the empty vector control sample (pcDNA). P-values were calculated by the heteroscedastic students t-test .

Description	Fold change			
	4A4	4B2	4D3	4D5
secretogranin II (chromogranin C)	7.724	-	7.9606	8.1575
H3 histone family, member B (H3FB)	9.510	-	8.2313	-
cytosolic phospholipase A2 gamma (cPLA2 gamma)	9.238	-	8.3821	-
protein kinase (H11)	7.262	-	8.052	7.2607
stathmin-like-protein RB3 (RB3),	7.176	-	6.2408	5.4270
Human zinc finger protein13	6.618	-	5.9783	-
Human zinc finger protein 236	21.037	-	-	10.729
short-chain alcohol dehydrogenase family member (HEP27),	5.899	-	-	7.1487
Rec8p, a meiotic recombination and chromatid cohesion phosphoprotein	5.616	5.367	-	-
type I transmembrane protein Fn14	5.393	-	5.0220	-
E74-like factor 4 (ets domain transcription factor) (ELF4),	5.387	-	-	5.4997
H4 histone family, member H (H4FH)	5.387	-	5.2637	-
interferon, gamma-inducible protein 16	-5.951	-	-7.7203	-17.5996

Table 5.5 Common changes in mRNA levels following overexpression of catalytically inactive PDE4 isoforms .The fold change was calculated from the mean expression values between the PDE4 isoform sample and the empty vector control sample (pcDNA). The p-values are listed in the previous tables (tables 5.2-5.5).

Fold change	p-value	Description
6.9474	0.0003	gb:NM_021064.1 /DEF=Homo sapiens **H2A histone family, member P (H2AFP),** mRNA
5.2371	0.0035	gb:NM_014298.2 /DEF=Homo sapiens **quinolinate phosphoribosyltransferase (nicotinate-nucleotide pyrophosphorylase (carboxylating)) (QPRT),** mRNA.
5.2029	0.0071	gb:BC002439.1 /DEF=Homo sapiens, **Tat-interacting protein (30kD),** clone MGC:1318, mRNA,
-7.7763	0.0032	gb:NM_020193.1 /DEF=Homo sapiens **GL002 protein (GL002),** mRNA.
-8.3592	0.0059	Consensus includes gb:AK025352.1 /DEF=Homo sapiens cDNA: **FLJ21699 fis,** clone COL09829.
-19.1500	0.0081	gb:AY014283.1 /DEF=Homo sapiens **NYD-SP6** mRNA, complete cds.

Table 5.6 Changes in levels of mRNA levels following treatment of HEK293 cells with rolipram (10μM). The fold change was calculated from the mean expression values between the rolipram sample and the HEK293 sample (untreated cells). P-values were calculated by the heteroscedastic students t-test .

Fold change	P-value	Description
52.1667	0.0141	gb:NM_006410.1 /DEF=Homo sapiens Tat-interacting protein (30kD) (TIP30), mRNA.
6.3719	0.0287	gb:NM_021064.1 /DEF=Homo sapiens H2A histone family, member P (H2AFP), mRNA.
5.0319	0.0133	gb:BC002439.1 /DEF=Homo sapiens, Tat-interacting protein (30kD), clone MGC:1318, mRNA, complete cds.
-5.2119	0.0176	Consensus includes gb:BF508616 /FEA=ESTCLONE= IMAGE:3085646 UG=Hs.79347 KIAA0211gene product
-5.5766	0.0234	gb:NM_021094.1 /DEF=Homo sapiens solute carrier family 21 (organic anion transporter), member 3 (SLC21A3), mRNA
-5.9844	0.0071	gb:AY014283.1 /DEF=Homo sapiens NYD-SP6 mRNA, complete cds, hypothetical protein /FL=gb:AY014283.1
-6.4173	0.0321	Consensus includes gb:AA017721 /FEA=EST /DB_XREF=gi:1479910 DB_XREF=est:ze39f11.s1 /CLONE=IMAGE:361389
-6.4737	0.0054	Consensus includes gb:AK025352.1 /DEF=Homo sapiens cDNA: FLJ21699 fis, clone COL09829. /FEA=mRNA
-7.0661	0.0161	gb:NM_007345.1 /DEF=Homo sapiens zinc finger protein 236 (ZNF236), mRNA. /FEA=mRNA
-7.1133	0.0017	Consensus includes gb:BG281679/CLONE=IMAGE:4544871 , Highly similar to YXHUT thymidylate synthase H.sapiens
-7.8990	0.0437	Cluster Incl. AF007155:Homo sapiens clone 23763 unknown mRNA, partial cds /cds=(0,314) /gb=AF007155 /gi=2852635 /ug=Hs.168694 /len=1369
-9.2475	0.0026	Consensus includes gb:U80771.1 /DEF=Human EST clone 25267 mariner transposon Hsmar1 sequence.
-10.4778	0.0055	Consensus includes gb:AC004472 /DEF=Homo sapiens chromosome 9, P1 clone 11659 /FEA=CDS
-11.0465	0.0117	gb:BC004241.1 /DEF=Homo sapiens, Similar to laminin, alpha 4, clone MGC:10389, mRNA, complete cds.
-13.5385	0.0375	/CLONE=IMAGE:2421293 /UG=Hs.182982 golgin-67 /FL=gb:NM_015003.1 gb:AF204231.
-15.2347	0.0075	aryl hydrocarbon receptor nuclear translocator-like /FL=gb:AB000812.1 gb:AF044288.1
-32.1667	0.0071	Consensus includes gb:BE504895ATP-binding cassette, sub-family B (MDR/TAP), member 9

Table 5.7. Changes in levels of mRNA levels following treatment of HEK293 cell with ariflo (please see next page for full table legend).

Table 5.7 Changes in levels of mRNA levels following treatment of HEK293 cells with ariflo (10μM). The fold change was calculated from the mean expression values between the ariflo sample and the HEK293 sample (untreated cells).P-values were calculated by the heteroscedastic students t-test.

Chapter 6

Compartmentalisation of cAMP phosphodiesterases in rat neonatal cardiac myocytes

6.1 Introduction

Crosstalk between two second messenger pathways, Ca^{2+} and cAMP plays an important role in controlling cardiac function (MacLennan & Kranias; Nature reviews 2003) (General Introduction, figure 1.13). The majority of the mass of the myocardium is comprised of cardiac myocytes, and alterations in cytosolic Ca^{2+} concentrations allow cardiac myocytes to contract and relax in dynamic fashion. The rate of relaxation and force of contraction (chronotropic response and inotropic response) can be influenced by cAMP through the phosphorylation of specific target proteins by PKA. Several channels, pumps and receptors involved in the Ca^{2+} fluxes within the cardiac myocytes are controlled through their PKA phosphorylation status and thus are regulated by altered intracellular cAMP concentrations (Simmerman & Jones, 1998) (See main introduction). Additionally, the cyclic nucleotide cGMP has been shown to increase Ca^{2+} currents via L-type Ca^{2+} channels and thereby exert a chronotropic effect (Haynes *et al*, 1996; Musialek *et al*, 2000; Vandecasteele *et al*, 2001)

Various studies have shown that a range of different PDE variants are expressed within the cardiac myocytes. These include the PDE1, PDE2, PDE3, PDE4 and PDE5 families (Maurice *et al*, 2003). However, it is the PDE3 and PDE4 families that are believed to provide the major cAMP-hydrolysing phosphodiesterase activities present in heart (Takahashi *et al.*, 2002; Wechsler *et al.*, 2002; Mongillo *et al.*, 2004). In fact, it has been shown that enzymes of the PDE4 family provide over twice the cAMP-hydrolysing activity as the PDE3 family, with isoforms of the PDE4D sub-family providing over two thirds of the total PDE4 activity (Mongillo *et al.*, 2004). Recently published studies utilising a fluorescence-resonance-energy-transfer (FRET) approach (Zaccolo & Pozzan, 2002; Mongillo *et al.*, 2004) have elegantly shown the presence of distinct pools of cAMP within cardiac myocytes. Additionally, the spatial confinement of different PDEs to discrete compartments has been shown using immunofluorescence coupled to analysis by confocal imaging techniques. In order to gain insight into the functional compartmentalisation of particular PDEs within the cardiac myocytes, I chose to study the effect of the selective inhibition of specific cAMP-hydrolysing PDEs on two different

cAMP targets, ERK and phospholamban (PLB).These were chosen to probe distinct facets of cAMP signalling using spatially distinct target proteins as described below.

ERK can be both positively and negatively regulated by cAMP. This depends on the expression of various signalling networks including the presence of distinct isoforms of Raf. Thus, elevated cAMP levels can lead to ERK activation through the action of B-Raf. The mechanism through which this occurs is not unequivocally established, although current consensus is that it involves PKA action, possibly serving to phosphorylate Rap1, which then activates B-Raf (Dumaz *et al,* 2002; Dhillon *et al,* 2002; Bos, 2003). It had previously been suggested that activation of ERK can also occur in response to increased cellular cAMP level by a mechanism independent of PKA. This mechanism had been proposed to involve the activation of Rap-1 by cAMP-stimulated GTPase exchange proteins (Epac). Following the binding of Epac to Rap1, it was suggested that Rap-1 binds to and activates B-Raf, and also directly binds to and inactivates Raf-1 (Vossler *et al,* 1997; Schmitt & Stork, 2002). However, following the development of an Epac-specific cAMP analogue, these proposed mechanisms are doubted and remain controversial (Enserink *et al,* 2002; Bos, 2003). The use of this analogue supports the evidence that regulation Raf-1/B-Raf and ERK is mediated by PKA, in a manner independent of Rap-1. Also, the use of this analogue indicates that cAMP induced activation of Rap1 is indeed mediated by Epac, but doubts that this activation results in the activation of ERK (Bos, 2003). PKA can also exert an inhibitory effect on ERK and does this in cells where Raf-1 is present and coupled to ERK activation. In such a system then inhibition ensues via the direct phosphorylation of Raf-1 by PKA (De Rooij *et al.,* 1998; Kawasaki *et al.,* 1998).

The MAPK signalling cascade is thought to play a role in regulating gene expression during hypertrophy (Gillespie-Brown *et al.,* 1995). The cardiac myocyte is a terminally differentiated cell, however, in response to pathophysiological stress, it adapts hypertrophically as an initial compensatory mechanism. A number of characteristic modifications distinguish the hypertrophic cardiac myocyte from normal maturational growth (Chien *et al.,* 1991). Following hypertrophic stimulus, genes which are only normally expressed in the fetal ventricle are re-expressed such as atrial natriuretic factor

(ANF), skeletal muscle α–actin (SkM α–actin) and β–myosin heavy chain (β–MHC) (Chien *et al.,* 1991). Hypertrophic agonists, such as phenylephirine, activate ERKs and MEKs (Bogoyevitch *et al.,* 1995). It has been shown that the activation of MEK/ERK cascade can stimulate ANF, SkM α–actin, β–MHC and *c-fos,* promoter activity, and thus may play a role in the development of the hypertrophic phenotype in the cardiac myocytes (Gillespie-Brown *et al.,* 1995).

Phospholamban (PLB) is small transmembrane protein located on the sacroplasmic reticulum (SR) and is involved on the regulation of Ca^{2+} uptake into the SR. It is a 6.1 kDa protein that forms a homopentamer, where it binds to and inhibits the sarcoplasmic reticulum Ca^{2+}ATPase (SERCA2a). Upon phosphorylation of PLB by either PKA (Ser 16) or CaM kinase (Thr 17), the inhibitory effect of PLB on SERCA2a is relieved and Ca^{2+} can now be pumped back into the SR (General introduction; figure 1.13). On a physiological setting, the dysfunction of PLB has been implicated in diminished contractility and cardiomyopathy (Hagemann & Xiao, 2002). Such studies have indicated that either enhanced phosphorylation of PLB or disruption of the PLB and SERCA2a interaction may prevent the progression of chronic heart failure (Minamisawa *et al.,* 1999; Haghighi *et al,* 2001; Sato *et al.,* 2001; MacLennan & Kranias, 2003).

Both PLB and ERK1/2 have quite different functional effects within cardiac myocytes, and their activity can both be regulated by PKA action. Briefly, the direct phosphorylation of PLB by PKA allows the release of the inhibitory constraint upon SERCA2 and is an important factor in controlling cytosolic Ca^{2+} concentrations. In contrast to this, PKA can exert an indirect effect upon phosphorylation and activation of ERK1/2 by MEK and is believed to regulate hypertrophy through the control of cardiac gene expression (Clerk *et al,* 1998). As the tethering of PKA to distinct subcellular compartments by AKAPs has also previously been reported within cardiac myocytes (Ruher, 2004), one could propose that the phosphorylation status of ERK1/2 and PLB is influenced by different 'pools' of cAMP. Therefore, for my study, I set out to alter selectively both cAMP degradation, through inhibition of specific PDEs, and also to activate selectively different GPCRs in order to generate cAMP distinctly. In doing so, I

hoped to either generate or manipulate functionally distinct pools of cAMP. As an output for these experiments I examined the effects upon ERK1/2 and PLB phosphorylation.

Results

For each experiment within this chapter primary cultures of cardiac myocytes were isolated from 2-3 day old neonatal rat (Sprague Dawley) hearts.

6.1.1 cAMP phosphodiesterase activity in rat neonatal cardiac myocytes

The PDE activity of homogenates of rat neonatal cardiac myocytes was assayed (figure 6.1), and total PDE activity was found to be 102+/- 8 pmol min^{-1} mg protein (mean +/- SD; n=8) (Mongillo *et al.*, 2004). In order to obtain a PDE activity profile, the PDE2, PDE3 and PDE4 was determined by the use of selective PDE inhibitors, EHNA (20μM), cilostamide (10μM) and rolipram (10μM), respectively. The presence of PDE1 activity was determined by the addition of Ca^{2+}CaM or addition of EGTA to asses whether this would cause an increase in PDE activity.

This approach showed that around 90% of total PDE activity was due to PDE3 and PDE4 activity, with around two thirds of the total being provided by PDE4 alone (figure 6.1). Less than 10% of total PDE activity was provided by other PDE families of which PDE2 provides over half (data not shown), PDE1 activity was negligible.

Mongillo *et al* also show that PDE4 provided almost 60% of total PDE activity and this was dissected into PDE4 sub-family specific activity. This was done by immunopurification using sub-family specific antisera. It was found that isoforms of the PDE4A and PDE4B family contributed less than 10% of total PDE4 activity, whereas PDE4D contributed some 60% and PDEB to some 30% (Mongillo *et al.*, 2004)

6.1.1.1 Selective PDE inhibition and phosphorylation of phospholamban and ERK1/2

In the following experiments, the PKA phosphorylation status of phospholamban (PLB) was detected by a commercially available polyclonal antibody (Upstate Technology). This antibody is specific to PKA phosphorylated PLB and is generated to a synthetic peptide (RAS*TIEMPQQAR), where the phosphorylated Ser 16 is indicated by *. The phosphorylation status of Erk1 and Erk2 (ERK1/2) was detected by a commercially available antibody (New England Biolabs). This antibody detects the phosphorylation of Thr183 and Tyr185 of rat Erk2 by MAP kinase kinase (MEK) or the phosphorylation of Thr202 and Tyr204 of human Erk1. The use of such antibodies allowed me to study the direct effect of PKA upon the phosphorylation status of PLB, and the MEK mediated phosphorylation status of ERK1/2, thus the indirect possible effect of PKA upon ERK1/2.

Myocytes were incubated for 10 min with specific PDE inhibitors EHNA (20μM) for PDE2, cilostamide (10μM) for PDE3 and rolipram (10μM) for PDE4, or different combinations of these inhibitors (figure 6.2). The lysates were separated by electrophoresis and immunoblotted to detect phosphorylation of ERK1/2 by MEK and the phosphorylation of the monomeric form of PLB by PKA. So as to provide loading and normalization controls, blots were stripped and re-probed with antibodies specific ERK2 and antibodies specific to PLB. Densitometry analysis was performed with Quantity One software (BioRad) and normalized using the total ERK and total PLB control blots. With respect to PLB, a small increase in its phosphorylation was observed with PDE3 inhibition (cilostamide) or PDE4 inhibition (rolipram), whilst PDE2 inhibition (EHNA) had no effect. However, in contrast to this, a 3 to 5 fold increase in the PKA phosphorylation status of PLB was observed upon the addition of both PDE2 and PDE3 inhibitors together. Most strikingly, however, a 12 to 15 fold increase in the level of phosphorylation of PLB by PKA was seen upon PDE3 and PDE4 inhibition.

With respect to phosphorylation of ERK1/2 by MEK, selective inhibition of PDE2 (EHNA), PDE3 (cilostamide) or PDE4 (rolipram) alone had negligible effects (figure

6.2). However, a more pronounced effect was observed upon the inhibition of both PDE2 and PDE3, and upon inhibition of both PDE3 and PDE4. The inhibition of both PDE2 and PDE3 provided a 2-3 fold increase in ERK1/2 phosphorylation by MEK, and inhibition of both PDE3 and PDE4 also provided a 2-3 fold increase in the level of phosphorylation of ERK1/2 by MEK. In contrast, a small increase in ERK1/2 phosphorylation was observed following the inhibition of both PDE2 and PDE4.

6.1.2 Time-dependent changes in phosphorylation of ERK1/2 and phospholamban in response to selective β1 and β2 adrenergic receptor activation, adenosine receptor activation and EP receptor activation.

It has been reported by many laboratories that stimulatory β1 and β2 adrenergic receptors are coupled to different functional outputs in cells, although both receptors activate adenylyl cyclases. The β–adrenergic receptor (β–AR)-mediated cAMP signalling pathway is one of the best characterized signalling systems in cardiac myocytes. Catecholamines released by the sympathetic nervous system act through the β-ARs to influence the contractile state of the heart as a compensatory mechanism to preserve the function of the heart in response to stress. Both β1 AR receptors, and β2 AR receptors couple to Gs leading to the activation of adenylyl cyclase. However, it has been suggested that different signalling properties exist between the two receptors as only the pathway of β1–AR mediated activation of adenylyl cyclase can be inhibited by M_2 muscarinic cholinergic receptor activation (Aprigliano *et al,* 1997). Differences in distribution of β AR-receptors to the plasma membrane of cardiac myocytes have been shown (Rybin *et al,* 2000). All β2 AR receptors have been shown to be enriched in caveloae (flask-shaped invaginations of the plasma membrane), whereas only a fraction of the β1 AR receptors are found in caveloae (Rybin *et al,* 2000).

Prostaglandin PGE2, which is released from a variety cells, can act on cardiac function via EP1, EP2, EP3 or EP4 receptors. It has been shown that PGE2 can increase cAMP levels within cardiac myocytes and thereby induce hypertrophic cell growth (Mendez & LaPointe, 2001). In contrast to this, adenosine has been reported to exert a contractile

effect on the heart through simulation of the Gs-coupled adenosine A2a receptor, expressed in cardiac myocytes (Liang & Morley, 1996; Marla & Mustafa, 1998). However, the stimulation of the A2a receptor has been shown to exhibit a distinct inotropic response compared to that of the β AR receptor, suggesting that although the β AR and A2a receptors are both Gs-coupled they exert distinct cellular actions, which may reflect actions exerted through compartmentalised cAMP signalling (Liang & Morley, 1996).

As a prelude to studying the phosphorylation status of ERK1/2 and PLB, following the manipulation of cAMP levels using either selective GPCR activation or selective PDE inhibition, I started by studying the time-dependent phosphorylation status of both PLB and ERK1/2 following β1 and β2 adrenergic receptor activation, adenosine activation and EP receptor activation. I also determined the total PDE activity, PDE4 activity alone and PDE3 activity alone over the time period of such β1 and β2 adrenergic receptor activation.

Cardiac myocytes were treated over the same time period with the selective partial β1 AR agonist, xametrol hexifumarate (10μM) (Tocris, USA) or with the specific β2 AR agonist, procaterol hydrochloride (10μM) (Tocris, USA) in order to study the time-dependent phosphorylation status of both PLB and ERK1/2 (figure 6.3a). Lysates were collected at the indicated times and subjected to electrophoretic separation. The antibodies specific to phosphorylated ERK1/2 and phosphorylated PLB (described in section 6.1.2) were used to detect the MEK phosphorylation status of ERK1/2 and the PKA phosphorylation status of PLB. So as to provide loading controls, blots were stripped and reprobed with antibodies specific ERK2 and antibodies specific to PLB.

Phosphorylation of ERK1/2 was seen in untreated cells and in the case of challenge of myocytes with either the β1 AR agonist (xameterol) and the β2 AR agonist (procaterol) agonists, a similar small time-dependent increase in ERK1/2 phosphorylation was observed (figure 6.3a).

PKA phosphorylated PLB species was not detected in untreated cells (figure 6.3a). However, following the challenge of the cardiac myocytes either the β1 AR agonist (xameterol) or the β2 AR agonist (procaterol), PLB appeared to undergo phosphorylation to similar levels (figure 6.3a).

In order to assess the total PDE activity, specific PDE4 activity and the specific PDE3 activity over the time period of treatment with the selective β receptor agonists, lysates were collected at the indicated time points and PDE assays performed (figure 6.3b) (Marchmont and Houslay, 1980). Compared to treatment of cardiac myocytes with xameterol, treatment with procaterol provided a larger change in PDE3 and PDE4 activities over the same time period (figure 6.3b).

In order to study time-dependent phosphorylation status of both PLB and ERK1/2 following adenosine A2a receptor activation and EP receptor activation, cardiac myocytes were challenged over the same time period with PGE2 (1μM) (SIGMA) and CGS 21680 (10μM) (SIGMA) (figure 6.4a). Cell lysates were collected at the indicated time points, subjected to gel electrophoresis and immunoblotted with the antibodies specific to MEK phosphorylated ERK1/2 and PKA phosphorylated PLB (figure 6.4a). To provide loading controls, blots were stripped and reprobed with antibodies specific ERK2 and antibodies specific to PLB.

After 5 min of stimulation with A2a receptor agonist (CGS 21680), it is clear that ERK1/2 becomes phosphorylated with a maximum phosphorylation achieved after 10 min (figure 6.4a). However, after 20 min challenge with CGS 21680, the phosphorylation status of ERK1/2 was attenuated (figure 6.4a). In contrast to this, a maximum level of phosphorylation of ERK1/2 was observed at some 2 min after challenge of cardiac myocytes with PGE2 and this level was maintained throughout the time period (figure 6.4a).

PKA phosphorylation of PLB was observed in lysates from untreated cells (figure 6.4a). However, treatment of cardiac myocytes over the same time period with either

CGS21680 or PGE2 resulted in a similar increase in phosphorylation state of PLB. This level was maintained using challenge with either CGS 21680 or PGE2 (figure 6.4a).

The total PDE activity, specific PDE4 activity and the specific PDE3 activity was assessed over the time period of CGS 21680 and PGE2 treatment. The lysates were collected at the indicated time points and PDE assays performed (figure 6.4b) (Marchmont and Houslay, 1980). Treatment of cardiac myocytes over a time period with CGS 21680 provided a minimal change in PDE3 activity (figure 6.4b). However, an initial decrease in PDE4 activity, was observed upon CGS 21680 treatment, which rapidly increased some 10 min after initial exposure to CGS 21680 treatment. In contrast, treatment of cardiac myocytes over the same time period with PGE2 provided a noticeable increase in PDE3 activity, as well as an increase in PDE4 activity (figure 6.5b).

6.1.3 Global cAMP levels following selective GPCR activation

Cardiac myocytes were subjected to treatment for the same time period with one of either procaterol, xameterol, CGS 21680 or PGE2 in order to assess changes in global levels of cAMP following the selective activation of β1 and β2 adrenergic receptors, adenosine A2a receptor and EP receptors, respectively. Lysates were collected at the indicated time points and cAMP assays performed (figure 6.5) (Materials and methods). The results are represented here as fold change over basal levels (figure 6.5) with cAMP concentration measured in pmol per well of myocytes. For each agonist 1-3 fold changes were observed at 5 min stimulation, and generally the changes in cAMP levels for treatment of each agonist over the same time period were very similar.

6.1.4 Differential effects of selective PDE inhibition and Gs-coupled agonist stimulation upon ERK1/2 and phospholamban phosphorylation status

Figure 6.2 of this chapter, shows the effect of selective PDE inhibition on phosphorylation of ERK1/2 by MEK and phosphorylation of PLB by PKA at resting cAMP levels (unstimulated cells). In order to manipulate distinct pools of cAMP in cardiac myocytes and study this effect upon the phosphorylation status of ERK1/2 and PLB, I chose to alter cAMP degradation through selective PDE inhibition with activation of distinct GPCRs.

Cardiac myocytes were pretreated for 5 min with either the PDE2 inhibitor (EHNA) (20μM), PDE3 inhibitor (cilostamide) (10μM) or the PDE4 inhibitor rolipram (10μM) (figure 6.6a). Following selective PDE inhibition, cardiac myocytes were subjected to 10 min stimulation with either the adenosine receptor agonist CGS 21680 or with PGE2 (figure 6.6a), and 10 min stimulation with the β1 or β2 agonists (figure 6.6b). Lysates were harvested, subjected to gel electrophoresis and analysed by immunoblotting with the antibodies specific to MEK phosphorylated ERK1/2 and PKA phosphorylated PLB (figures 6.6a & 6.6b). In order to provide loading controls, blots were stripped and reprobed with antibodies specific ERK2 and antibodies specific to PLB.

Following PDE4 inhibition (rolipram) and CGS 21680 treatment, a prominent increase ERK1/2 phosphorylation was observed. However, in contrast, a very small increase in ERK1/2 phosphorylation was observed following PDE4 inhibition and PGE2 treatment (figure 6.6a). The most striking increase in ERK1/2 phosphorylation was observed following PDE2 inhibition (EHNA) and PGE2 treatment (figure 6.6a).

In the case of PLB, contrasting results were observed following the analysis of the PKA phosphorylation status. An increase in the PKA phosphorylation status of PLB was observed following PDE2, PDE3 or PDE4 inhibition, upon a subsequent treatment of the cardiac myocytes with CGS 21680 (figure 6.6a). The largest increase in the PKA phosphorylation status PLB was observed following PDE4 inhibition and treatment with CGS 21680 (figure 6.6a). However, pretreatment of cardiac myocytes with the PDE3,

PDE3 or PDE4 inhibitors and subsequent PGE2 treatment resulted in minimal increases in PLB phosphorylation (figure 6.6a). Interestingly, upon the direct comparison of the phosphorylation of PLB to the phosphorylation of ERK1/2, it appears that only PGE2 treatment and inhibition of PDEs indicate differential regulation of the phosphorylation of PLB and ERK1/2 (figure 6.6a). Most strikingly, EHNA and PGE2 treatment resulted in a large increase in ERK1/2 phosphorylation, yet had no effect on PLB phosphorylation (figure 6.6a).

Cardiac myocytes were pretreated with PDE2, PDE3 or PDE4 inhibitors and then subjected to selective β1 and β2 adrenergic stimulation (procaterol and xameterol respectively). Lysates were separated by gel electrophoresis and the MEK phosphorylation status of ERK1/2 and PKA phosphorylation status of PLB was analysed by immunoblot (figure 6.6b). Only small differences were observed comparing the phosphorylation status of ERK1/2 following procaterol or xameterol treatments. PDE4 inhibition (rolipram) and xameterol or procaterol treatment, however, resulted in an increase in the phosphorylation status of ERK1/2 through the action of these β adrenergic agonists (figure 6.6b). Intriguingly, pretreatment of myocytes with the PDE3 inhibitor and subsequent stimulation with either procaterol or xameterol resulted in an attenuation of ERK1/2 phosphorylation compared to agonist only treatment (figure 6.6b). PDE2 inhibition (EHNA) of cardiac myocytes and treatment with procaterol or xameterol did not provide any increase in the phosphorylation of ERK1/2 compared procaterol or xameterol treatment alone (figure 6.6b)

Analysis of PLB phosphorylation identified some differences between treatment with selective β1 and β2 adrenergic agonists, procaterol and xameterol, but only with prior PDE inhibition. High levels of phosphorylation of PLB were observed with treatment of myocytes with either procaterol or xameterol. However, only upon the pre-incubation of cardiac myocytes with rolipram (PDE4 inhibition) and subsequent treatment with procaterol (β2 receptor agonist) was there an increase in PLB phosphorylation compared to procaterol only (figure 6.6b).

Pretreatment with the PDE3 inhibitor and procaterol or xameterol treatment resulted in a decrease in PLB phosphorylation compared to agonist only (figure 6.6b).

6.2 Discussion

It is now widely accepted that cAMP signalling in cardiac myocytes is compartmentalised (Steinberg & Brunton, 2001; Kapiloff, 2003). These studies originated from functional ones comparing the action of non-selective β adrenergic receptor agonist isoproterenol with PGE2. More recently, studies using selective PDE inhibitors following Ca^{2+} signalling and direct visualization of cAMP have furthered the notion of compartmentalisation. In these studies, I have extended this notion to look and see whether compartmentalisation has relevance to important PLB and ERK1/2 signalling proteins. Furthermore, I have extended the range of GPCRs analysed to cover not only the adenosine A2a receptor and EP receptors, but also to discriminate between the β1 and β2 adrenergic receptors and undertaken an appraisal of regulation by the important PDE2/3/4 families.

Using this strategy I show that, depending on which PDE family is inhibited, or indeed depending on which PDE families are inhibited together, differential effects are observed upon phosphorylation of ERK1/2 by MEK and phosphorylation of PLB by PKA. I also show that the generation of distinct pools by selective PDE inhibition and subsequent activation of different G-protein coupled receptors provide differential effects upon ERK1/2 phosphorylation and PLB phosphorylation.

Cardiac myocytes account for approximately 60 percent of cell mass of the heart and the search for novel therapeutics to treat cardiac myopathies is of much current interest. The PDE profiles have been characterized for cardiac tissue from several different species. I chose to use the rat neonatal cardiac myocytes for my study as the well understood PDE1, PDE2, PDE3, and PDE4 isoforms have all been reported to be expressed there (Kostic *et al.*, 1997; Zhao *et al.*, 1997; Kakkar *et al.*, 1999; Sadhu *et al.*, 1999; Movesian, 2002; Wechsler *et al.*, 2002; Baillie *et al.*, 2001; Houslay & Adams, 2003; Maurice *et al.*,

2003; Mongillo et al., 2004) and for which there are selective inhibitors (Francis *et al.*, 2001).

Firstly, the total PDE activity was measured and by use of the selective inhibitors available for the PDE1, PDE2, PDE3 and PDE4 families, each family's percentage contribution to total PDE activity in myocytes was calculated. PDE4 was found to contribute to approximately 60% of total PDE activity, PDE3 contributed to approximately 30%, PDE1 and PDE2 combining to provide less than 10% of total PDE activity. These data indicate PDE4, which exclusively hydrolyses cAMP, to be the most abundant PDE in rat neonatal cardiac myocytes.

By use of selective PDE inhibitors, I also studied the influence of PDE2, PDE3 and PDE4 families upon the regulation of different pools of cAMP under basal adenylyl cyclase activity (figure 6.2). Treatment of cardiac myocytes with PDE2, PDE3 or PDE4 inhibitors resulted in minimal increases in phosphorylation of ERK1/2 by MEK. However, inhibition of both PDE3 and PDE4 enzymes together provided a clear increase in ERK1/2 phosphorylation. The inhibition of PDE2 and PDE3 together, also provided an increase in ERK1/2 phosphorylation. The selective inhibition of the PDE2, PDE3 or PDE4 families did not increase phosphorylation of ERK1/2 and suggests that at basal cAMP levels individual PDE enzyme families are not responsible for the regulation of the cAMP pool associated with the ERK MAP kinase cascade. However, the selected inhibition of combinations of the PDE families resulted in increases in ERK1/2 phosphorylation. PDE2 and PDE3, PDE3 and PDE4 inhibition provided increases in ERK1/2 phosphorylation but, interestingly, the inhibition of PDE2 and PDE4 had no effect on ERK1/2 phosphorylation. This suggests that the PDE3 enzymes act only in concert with enzymes of the PDE2 and/or PDE4 families to regulate ERK phosphorylation and activation.

Different effects of selective PDE inhibition on PLB phosphorylation by PKA were observed. The inhibition of the PDE3 enzymes only resulted in a small increase in PLB phosphorylation. PDE4 inhibition also provided an increase in phosphorylation but was less than that of PDE3 inhibition. Most strikingly, a 10-fold increase in phosphorylation

of PLB was evident following the inhibition of both PDE3 and PDE4 enzymes. Again, such an additive effect of PDE3 and PDE4 inhibition suggest that enzymes these two PDE families may act in concert to tailor the 'pool' of cAMP influencing the phosphorylation of PLB and may be involved in the regulation the uptake of Ca^{2+} into the SR.

The second messenger cAMP can influence, in the short term, the rate of excitation-contraction coupling of the heart. Several pharmacological effectors can activate Gs-coupled receptors on cells of the cardiovascular system and thus stimulate adenylyl cyclase (AC) to produce cAMP. In order to alter distinct 'pools' of cAMP, and thus to study the effect upon PLB phosphorylation by PKA and of ERK1/2 phosphorylation by MEK, I used selective PDE inhibitors and either the β1 or β2 receptor selective agonists (xametrol and procaterol), or the adenosine A2a receptor agonist (CGS 21680) or the EP receptor agonist (PGE2) to activate AC.

I show, through treatment of cardiac myocytes over the same time periods, that xameterol, procaterol, CGS 21680 and PGE2 agonists provided increases in the PKA phosphorylation of PLB and MEK phosphorylation of ERK1/2 (figures 6.2-6.5). Also, I show that treatment of cardiac myocytes with the same agonists over the same time periods resulted in similar increases (several fold) in global cAMP levels. Transient increases in the PDE3 and PDE4 activity are also observed following challenge of myocytes over the same time period with each of the agonists. These data indicate that selective activation of β1 and β2 adrenergic receptors, adenosine A2a receptor and EP receptors each stimulated the production of cAMP which results in the PKA phosphorylation of PLB and MEK phosphorylation of ERK1/2.

Distinct pools of cAMP in the cardiac myocytes were manipulated by selective PDE inhibition and activation of different GPCRs (figures 6.6a and figures 6.6b). The most striking differences in the phosphorylation of PLB and phosphorylation of ERK1/2 were observed following specific PDE inhibition and then subsequent treatment of cardiac

myocytes with either the A2a receptor agonist (CGS 21680) or the EP receptors agonist (PGE2).

Pretreatment with the PDE4 inhibitor (rolipram) and then treatment of cardiac myocytes with CGS 21680, provided a pronounced increase in phosphorylation of ERK1/2 by MEK and phosphorylation of PLB by PKA (figure 6.6a). Whereas, PDE2 or PDE4 inhibition and treatment with CG 21680 had a small effect on PLB phosphorylation but had no effect on ERK1/2 phosphorylation (figure 6.6a). However, in contrast, only pretreatment of cardiac myocytes with the PDE2 inhibitor and subsequent treatment with PGE2 resulted in an increase in ERK1/2 phosphorylation. Interestingly, PDE2 inhibition and PGE2 treatment did not provide an increase in PLB phosphorylation (figure 6.6b). Pretreatment with PDE3 or PDE4 inhibitors and subsequent PGE2 challenge did not provide an increase in ERK1/2 phosphorylation although small increases in PLB phosphorylation were observed (figure 6.6b).

To gain functional insight into the compartmentalisation of PDEs within cardiac myocytes, I manipulated levels of cAMP within distinct 'pools' by using selective PDE inhibitors to alter cAMP degradation and activated different GPCRs to stimulate adenylyl cyclase. I chose to study the PKA phosphorylation of PLB and MEK phosphorylation of ERK1/2 (indirectly activated by PKA) as outputs. The differences in phosphorylation of PLB and phosphorylation of ERK1/2 I observed following such manipulation of cAMP with PDE inhibitors alone, or with PDE inhibition and selected GPCR activation, provides further evidence of PDE compartmentalisation within cardiac myocytes.

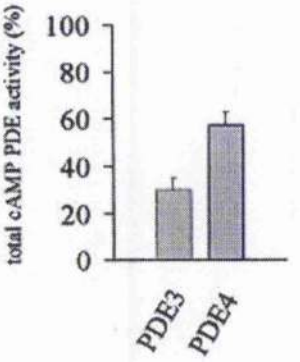

Figure 6.1 cAMP PDE activity in rat neonatal cardiac myocytes. Graph is taken from published data (Mongillo *et al.*, 2004). Data are means +/- SD of 6 separate experiments from different cardiac myocyte preparations. Lysates from neonatal myocytes (1-3 day old) were assayed for PDE activity. Lysates expressed a level of cAMP PDE activity of 102 +/- 8 pmol $min^{-1}mg\ protein^{-1}$. PDE3 activity was calculated from the fraction of total PDE activity inhibited by cilostamide (10μM) and PDE4 activity was calculated from the fraction inhibited by rolipram (10μM).

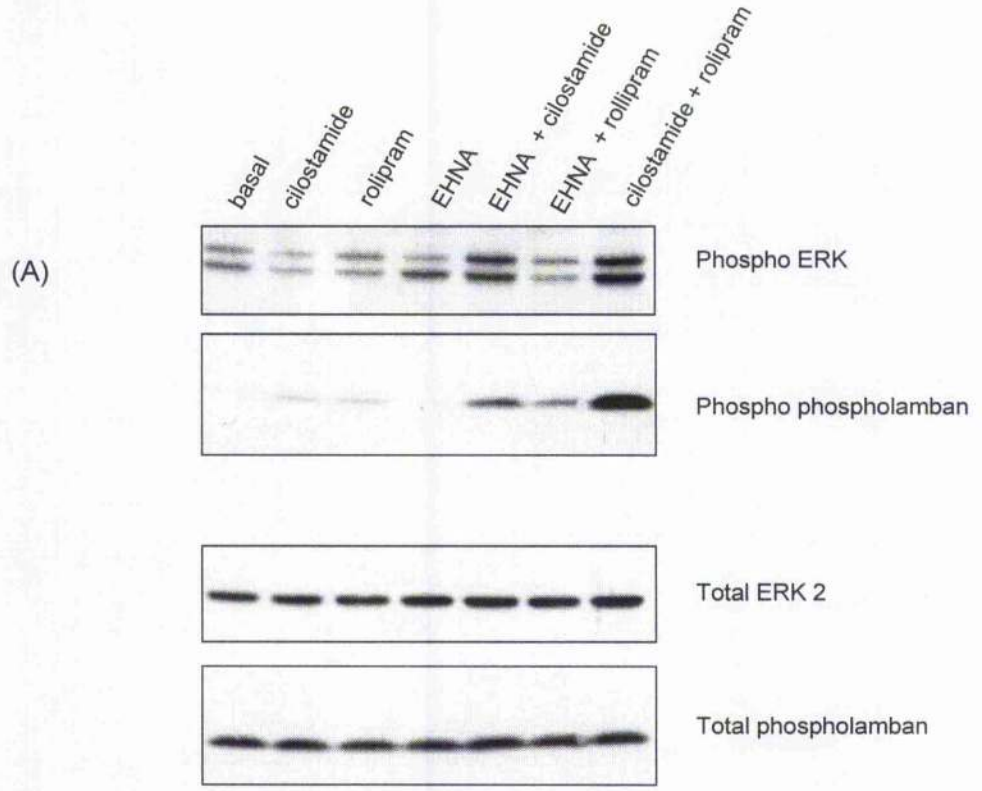

Figure 6.2 Effect of selective PDE inhibition on ERK and phospholamban phosphorylation. See next page for full figure legend.

(B)

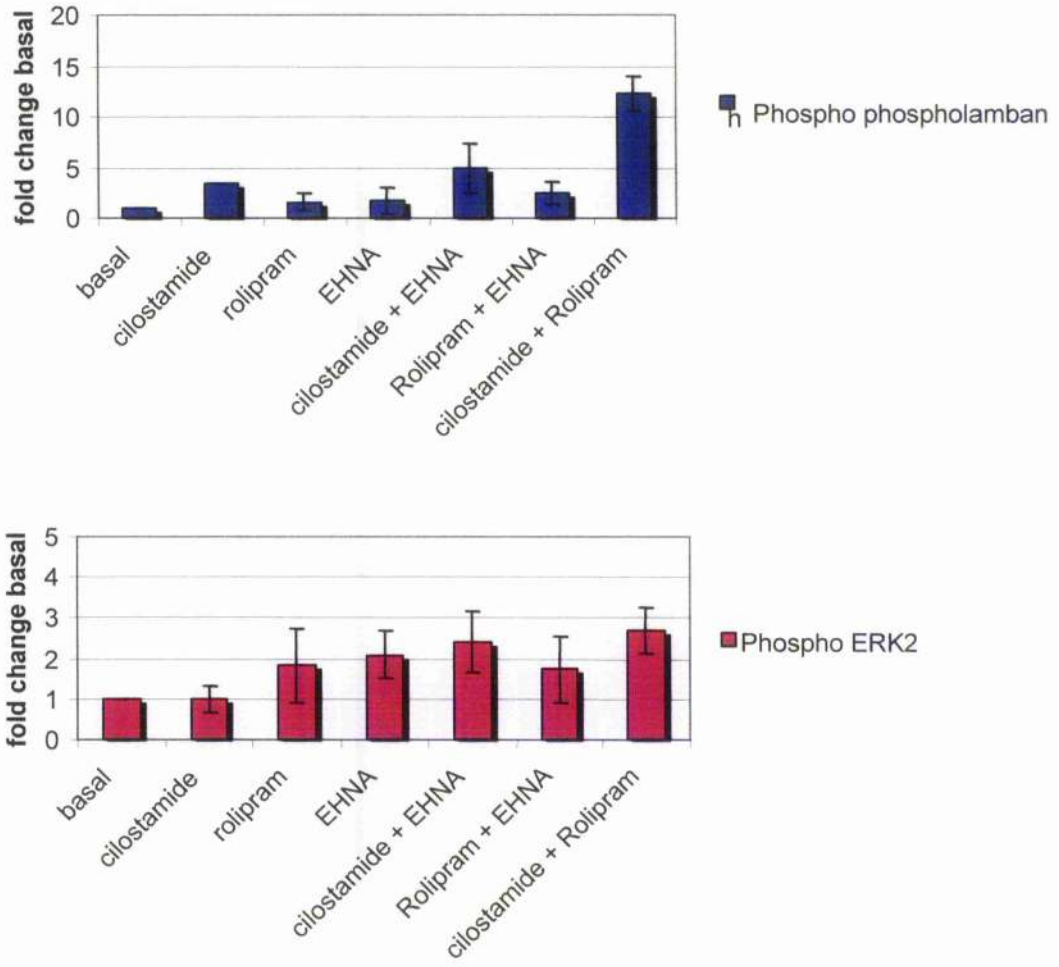

Figure 6.2 Effect of selective PDE inhibition on ERK and phospholamban phosphorylation. Neonatal cardiac myocytes were incubated for 10 min with the indicated PDE inhibitors; ciloastamide (1μM), rolipram (10μM), EHNA (30μM). Lysates were separated by electrophoresis. (A) The phosphorylation of ERK1/ERK2 and phospholamban was analysed by western blotting. (B) Densitometry analysis of western blots was performed with Quantity One software. Data was normalised by the 'total' ERK and 'total' phospholamban bands. The effect of the inhibitors are compared to basal (untreated cells). N=3 +/- S.E.

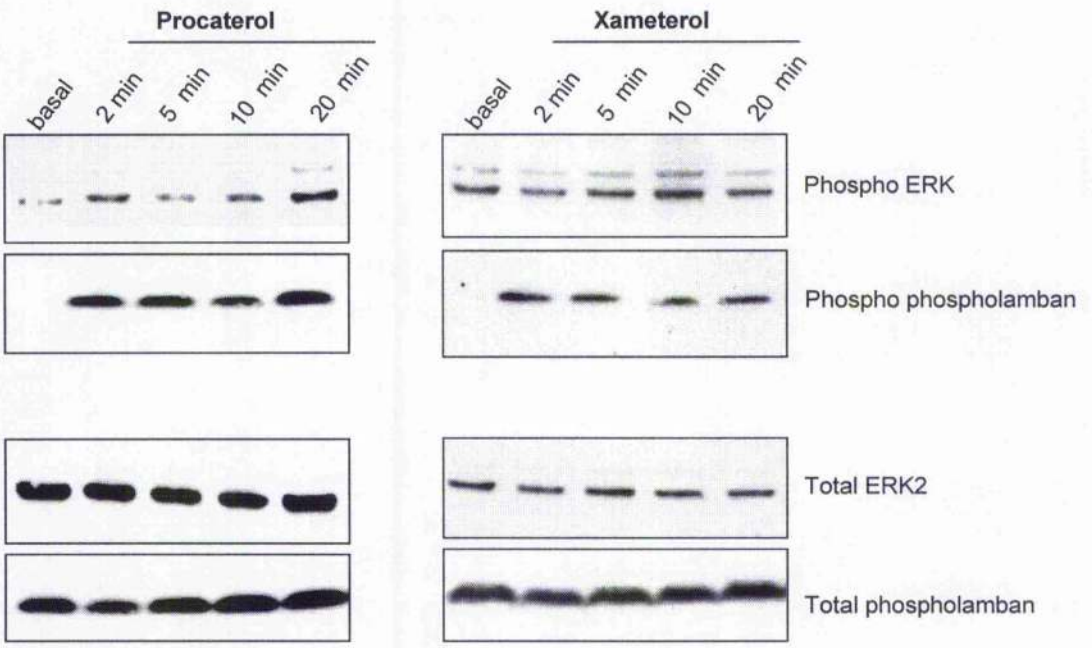

Figure 6.3a Determination of ERK and phospholamban phosphorylation following β_1 and β_2 agonist challenge. Neonatal myocytes were incubated with Xameterol hemifumarate (10μM) (a β_1 selective partial agonist) and Procaterol hydrochloride (10μM) (a specific β_2 agonist) for the indicated time points. Lysates were separated by electrophoresis. The phosphorylation of ERK1/ERK2 and phospholamban was analysed by western blotting. Blots represent typical time courses.

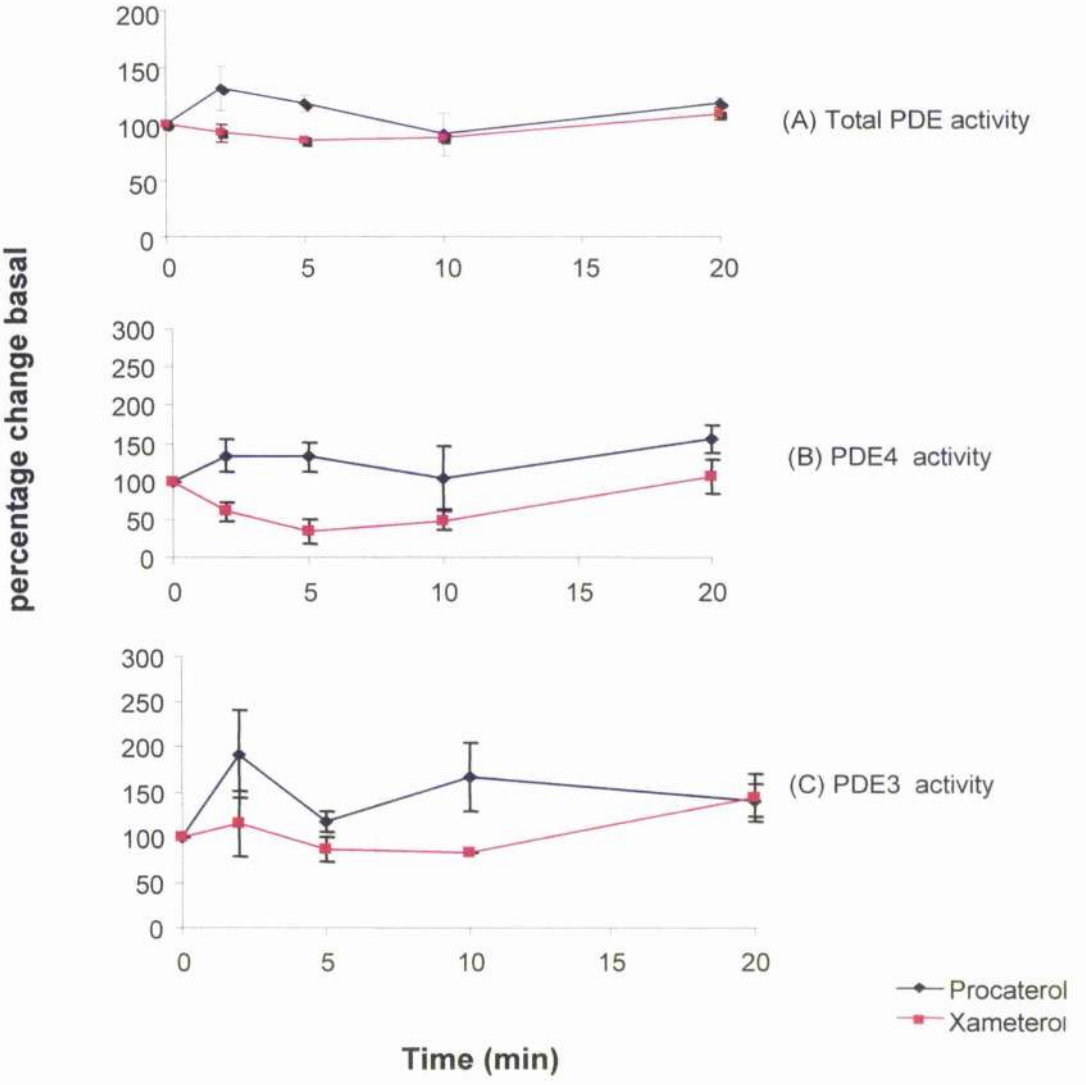

Figure 6.3b Determination of total PDE activity, PDE4 and PDE3 activity following β_1 and β_2 agonist challenge. Neonatal cardiac myocytes were harvested at the indicated time points and whole cell lysates were analysed for PDE activity. PDE3 activity was calculated from the fraction of total PDE activity inhibited by cilostamide (10μM) and PDE4 activity was calculated from the fraction inhibited by rolipram (10μM). N=3 +/- S.E

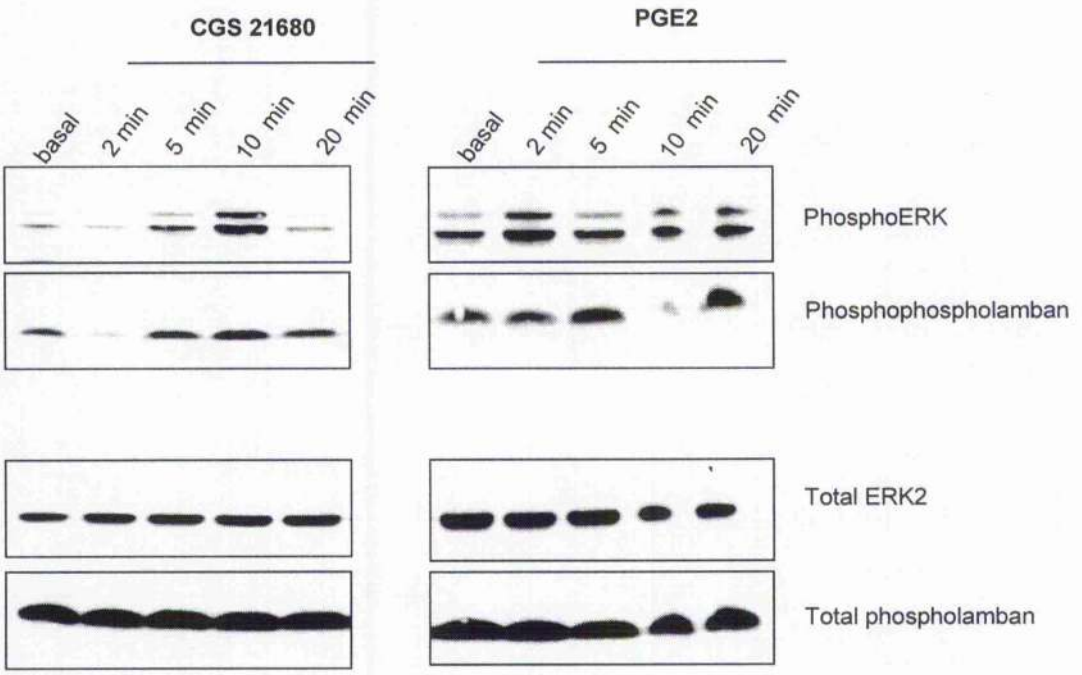

Figure 6.4a Determination of ERK and phospholamban phosphorylation following adenosine A2a receptor and EP receptor activation. Neonatal myocytes were incubated with CGS 21680 (10μM) (selective A2a receptor agonist) and PGE2 (1μM) (EP receptor agonist) for the indicated time points. Lysates were separated by electrophoresis. The phosphorylation of ERK1/ERK2 and phospholamban was analysed by western blotting. Blots represent a typical time course which were performed at least three times.

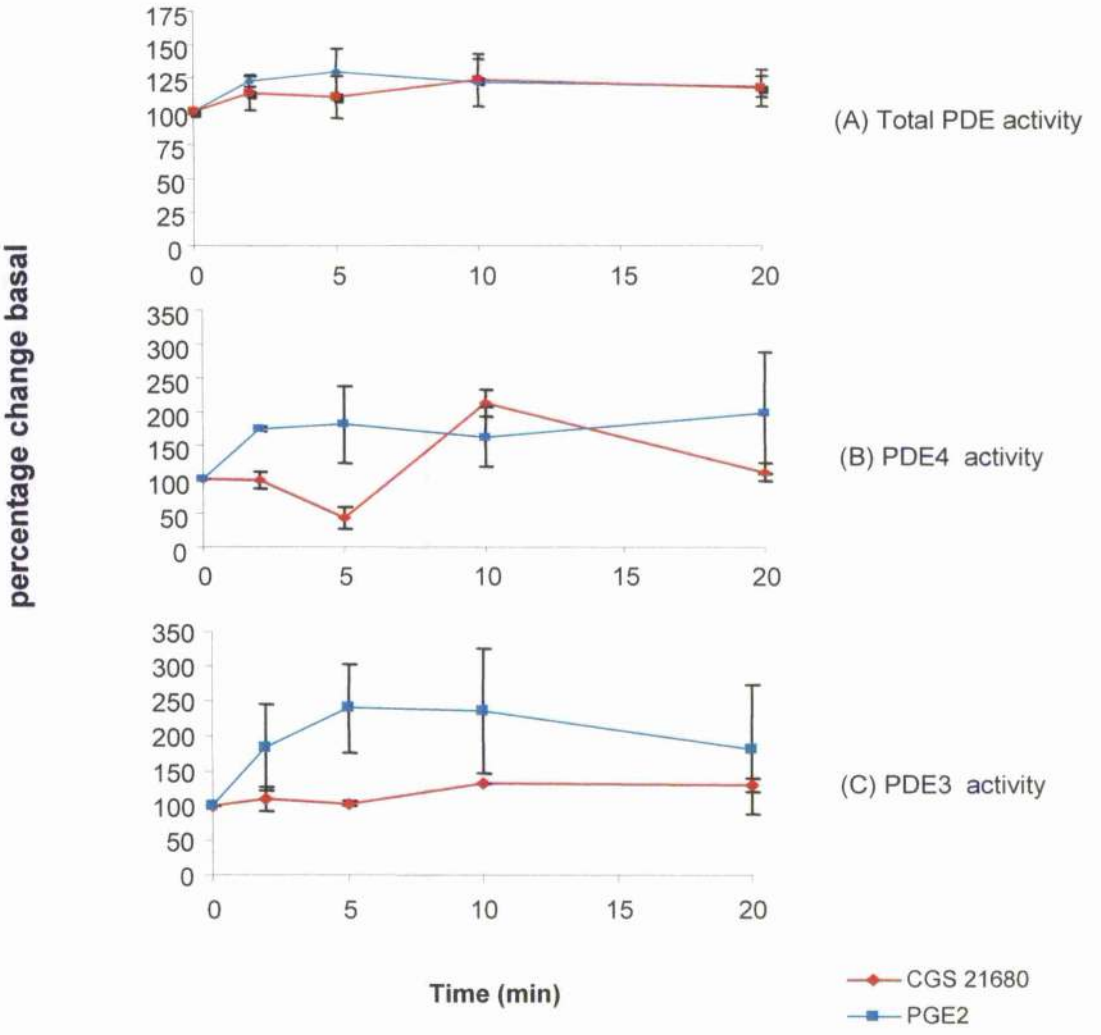

Figure 6.4b Determination of total PDE activity, PDE4 and PDE3 activity adenosine A2a receptor and EP receptor activation. Neonatal cardiac myocytes were harvested at the indicated time points and whole cell lysates were analysed for PDE activity. PDE3 activity was calculated from the fraction of total PDE activity inhibited by cilostamide (10μM) and PDE4 activity was calculated from the fraction inhibited by rolipram (10μM). The activity following agonist challenge is compared to basal (untreated cells) and is represented here as a percentage change. N=3 +/- S.E

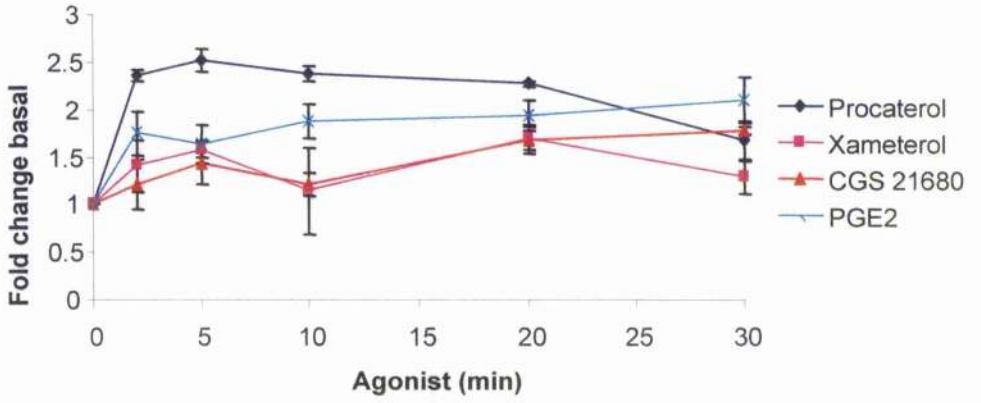

Figure 6.5 Analysis of cAMP levels following different Gs-coupled receptor activation. Neonatal cardiac myocytes were incubated with the following agonists: Procaterol (10μM), Xameterol (10μM), PGE2 (1μM) and CGS 21680 (10μM) for the indicated time points. cAMP levels per well (6 well plate) were measured and the data represented as fold change basal. N=3 +/-S.E.

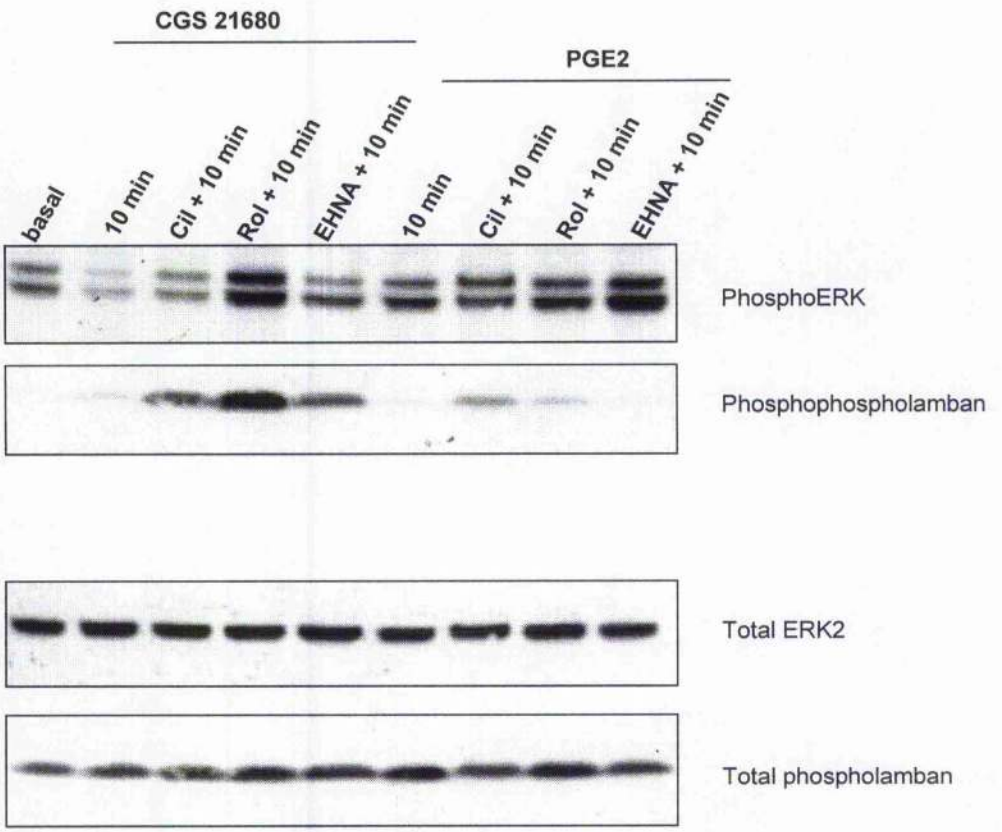

Figure 6.6a ERK and phospholamban phosphorylation following selective PDE inhibition and adenosine A2a receptor activation or EP receptor activation. Neonatal myocytes were pretreated with the specific PDE inhibitors and incubated with CGS 21680 (10μM) and PGE2 (1μM) for the indicated time points. Lysates were separated by electrophoresis. The phosphorylation of ERK1/ERK2 and phospholamban was analysed by western blotting. data n=2

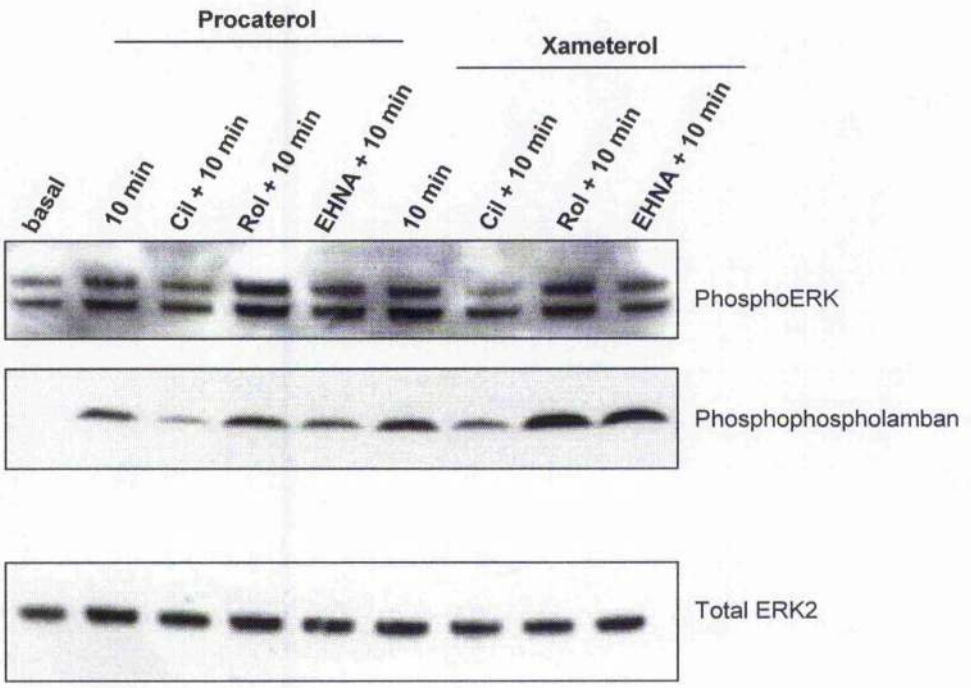

Figure 6.6b ERK and phospholamban phosphorylation following selective PDE inhibition and β_1 or β_2 adrenergic receptor activation. Neonatal myocytes were pretreated with the specific PDE inhibitors and incubated with procaterol (10μM) or xameterol (10μM) for the indicated time points. Lysates were separated by electrophoresis. The phosphorylation of ERK1/ERK2 and phospholamban was analysed by western blotting. Data n=2

Chapter 7

General discussion and future directions

Discussion

The phosphorylation of cellular proteins by protein kinases produces a conformational change which can affect the protein's function. Within the cAMP signalling system, cAMP is detected by protein kinase A (PKA) which serves to phosphorylate, and alter the function of a wide array of proteins.

It had been previously established the long isoform PDE4D3 is a target for phosphorylation and activation by PKA, and this rapid activation has been postulated to act as means of desensitization to the cellular cAMP response, (Sette *et* al., 1994; Alvarez *et* al., 1995; Sette and Conti, 1996; Hoffman *et al.*, 1998). Biochemical analysis of PDE4D3 has shown that the Ser 13 within the unique N-terminal and Ser 54 site within the UCR1 are phosphorylated by PKA (Sette and Conti, 1996; Hoffman *et al.*, 1998). However, mutational studies have also shown that only PKA phosphorylation of Ser 54 is required for activation (Sette and Conti, 1996), with the role of Ser 13 unknown. Also it has been reported that the PKA phosphorylation of PDE4D3 results in an altered electrophoretic mobility on SDS-PAGE (Sette and Conti, 1996; Hoffman *et al.*, 1998). The reason for this mobility 'shift', which has been suggested to indicate the activation of this enzyme, has yet to be explained (Sette and Conti, 1996; Oki *et al*, 1998). For the first time antiserum has been developed to the two specific PKA sites in PDE4D3, (namely Ser 54 and Ser 13), providing the means to study the PKA phosphorylation of PDE4D3 at these two sites in response to cell activation.

In chapter 3, I show, subsequent to activation of adenylyl cyclase, a time-dependent decrease in the mobility of PDE4D3. At 1 min of IBMX and forskolin challenge both a low mobility and high mobility species existed and for the remainder of the time points, the majority of PDE4D3 shifts to a low mobility species. Within the same time course, this 'band shift' was paralleled by a similar one detected using the antisera specific for PKA phosphorylated Ser 54 (PS54-UCR1) within UCR1. At the 1 min time point, PS54-UCR1 detected a 'band-shift' which is akin to both de-phosphorylated and

phosphorylated PDE4D3. However, the antiserum specific for PKA phosphorylated Ser 13 (PS13-4D3), within the unique N-terminal, only detected a single low mobility species at all time points. A time-dependent increase in phosphorylation was also observed with PS13-UCR1. This suggests that in COS1 cells the PKA phosphorylation of both sites are required for the mobility shift and that the phosphorylation of Ser 54 may even precede that of Ser 13. The notion that the phosphorylation of both sites is required for the 'band-shift' is further suggested by mutation of either of these sites to alanine preventing the PKA mediated change in mobility of long-form PD4D3 (MacKenzie *et al*, 2002). The mobility shift observed indicates a conformational change. This is extremely interesting as a recent paper (Michel *et al.*, 2004) suggests a function of this conformational change. This paper suggests that PKA phosphorylation of Ser 13 within the N-terminal of PDE4D3 facilitates the interaction of PDE4D3 with mAKAP. They propose a model where under resting conditions PDE4D3 binds to mAKAP and following hormonal stimulation of the cell, mAKAP-bound PKA is activated. The catalytic subunits of PKA phosphorylate local substrates including the mAKAP bound PDE4D3. The phosphorylation of Ser 13 increases the affinity of PDE4D3 for mAKAP and phosphorylation or Ser 54 causes a 2-fold increase in the activity of PDE4D3, resulting in hydrolysis of cAMP. The signalling system is reset with the return to basal cAMP levels. As my data indicates that Ser 54 is phosphorylated before Ser 13, it could be possible that PDE4D3 is phosphorylated and activated in the cytosol and is then recruited to mAKAP to lower local cAMP levels. Thus, I would like to have studied the recruitment of PDE4D3 to mAKAP in whole cells.

Three other PDE4 gene families (A, B and C) generate a range of long-form PDE4s and all long-forms contain a PKA consensus sequence Arg-Arg-Glu-Ser-Phe. I show that PKA can phosphorylate the cognate target serine within the UCR1 of long-form PDE4s from each sub-family. In COS1 cells the PS54-UCR1 antibody detected the PKA phosphorylation of transiently transfected PDE4A8, PDE4B1, PDE4C2 and PDE4D5 following the activation of adenylyl cyclase. For each long-form, this phosphorylation was ablated using the PKA inhibitor H89 and by mutating the putative target serine to alanine. This analysis may serve as a model of the phosphorylation and activation of

endogenous PDE4s where PKA is activated in response to localised increases in cAMP. As it is now known that PKA can phosphorylate and activate long forms from each of the four subfamilies, and different PDE4 isoforms can be targeted to specific subcellular regions, one could suggest that this PKA-mediated activation could serve to control distinct pools of cAMP. In cardiac myocytes, the recruitment of PDE4D3 and PDE4D5 by β-arrestin (Perry *et al.*, 2002, Baillie *et al.*, 2003) to the β_2-adrenergic receptor upon isoproterenol stimulation provides a source of cAMP degradation directly to the site of cAMP generation. The interaction of PDE4D3 with mAKAP (Kapiloff *et al.*, 1999; Dodge *et al.*, 2001; Michel *et al.*, 2004) allows a negative feedback loop whereby local increases in cAMP result in activation of PKA, phosphorylation of the local PKA substrates, including phosphorylation and activation of PDE4D3, which in turn degrades cAMP and allows a return to resting cAMP levels. It is also possible that other long PDE isoforms also serve to function as a means of desensitisation to local increases in cAMP. As AKAPs play a pivotal role in the compartmentalisation of signalling modules, and PDE4D3 has already been reported to interact with several AKAPs, one could assume that other PDE4s interact with such signalling complexes to provide control of local cAMP pools.

Over the decades, researchers in the field of cellular signalling have been posed with the question of 'how do diffusible second messengers such as cAMP achieve specificity of their action?' (Brunton, 2003).Growing evidence of compartmentalisation seems to address this question. An early series of experiments performed cardiac myocytes led the hypothesis that (i) not all cAMP gains access to all PKA, (ii) not all PKA has access to all possible substrates and (iii) not all cAMP has access to all cellular PDEs (Steinberg & Brunton, 2001; Brunton, 2003). These experiments involved stimulating different GPCRs on cardiac myocytes with two different agonists, PGE1 and isoproterenol. Both agonists resulted in an activation of adenylyl cyclase (AC) and subsequent production of cAMP. However the down-stream effects of PKA activation was quite different for each agonist. Isoproterenol treatment resulted in phosphorylation of troponin I and proteins involved in glycogen metabolism, whereas PGE1 treatment resulted in cAMP accumulation and PKA activation, but phosphorylation of troponin I or glycogen metabolism proteins was not

observed (Brunton *et al.*, 1981). The addition of PDE inhibitors and PGE1 allowed the PKA-dependent phosphorylation of such proteins. These basic observations paved the way for the postulate of compartmentalisation of cAMP signalling molecules. The structural basis for sub-cellular compartmentalisation underpinning cAMP signalling in cells is only, now, beginning to be understood.

Recently, it has been shown that GPCRs, G-proteins and AC may be localized to specific membrane compartments by the enrichment in or exclusion from caveolae (invaginations of the plasma membranes classed as a subset of lipid rafts) (Dodge *et al.*, 2001; Ostrom *et al*, 2004). PKA can be confined to distinct subcellular compartments, along with phosphatases, different substrates of PKA, and other proteins, by association with A-kinase anchoring proteins (AKAPs) (Scott Review, 2003). The spatially distinct localisation of PDEs, in particular PDE4s, has been show to be achieved through their interaction with a variety of subcellular structures. For example, PDE4 isoforms can interact with phosphatidic acid, the immunophillin XAP2, receptor associated with C kinase 1 (RACK1), β-arrestin, AKAPs, myomegalin and also SRC family tyrosine kinases through their SH3 domains (Perry *et al*, 2002; Baillie *et al*, 2003; Houslay Review, 2003; Bolger *et al*, 2003).

The steady state levels of cAMP that is reached in resting cells will depend not only on AC activity but also on PDE activity. As AC is localised with its active site at the cytosol surface of the plasma membrane, in some cases to different compartments of the plasma membrane, PDEs will have the key role in generating and tailoring intracellular cAMP gradients from the point source(s) of cAMP produced by AC. These gradients can then be expected to control selectively anchored Epac and PKA activity within the cell. We hypothesized that in resting cells, PDE4s anchored indirectly or directly to AKAPs will be poised to control cAMP levels and thus exert effects on AKAP-anchored PKA. In order to investigate this possibility, I needed a read out specific for PDE4 isoform action and for PKA activation. What better target to choose that long PDE4 isoforms, whose UCR1 can be phosphorylated by PKA and whose activity one would surmise could regulate cAMP gradients. In order to specifically gauge phosphorylation at this site by

PKA I took advantage of the PS54-UCR1 antibody which detects PKA phosphorylation of all long PDE4 isoforms, hence providing an immediate readout for the action of PKA on a specific PDE.

Secondly, we developed an approach to render PDE4s catalytically inactive by a single point mutation, which allowed us to develop a dominant negative strategy. We surmised that such a discrete mutation should have little or no effect on the gross structure of the PDE4. Thus the chronic overexpression of the inactive PDE4s can be expected to displace and thereby replace, the cognate, active endogenous PDE4s. In doing this, there now would be no active anchored PDE4 to constrain PKA activity and the recombinant inactive PDE4 would itself provide a readout of this by offering a localised specific substrate to be phosphorylated by the appropriately active PKA. This approach allowed me to identify particular PDE4 isoforms as being specifically involved in constraining the activity of a distinct pool of PKA. Cells have been suggested as being either 'low' or 'high' cycling conditions for cAMP signalling (Houslay & Milligan, 1997). This reflects cells that vary in their basal levels for adenylyl cyclase activity. Thus, low cycling cells have low basal AC activity, whereupon challenge with PDE inhibitors has little effect on global cAMP levels, whilst these are elevated upon GPCR stimulation of AC. In contrast to this, high cycling cells have active cAMP generation, with levels kept low by active PDE activity. In these cells even at basal conditions PDE inhibitors cause a profound increase in cAMP levels. In both instances, however, little is known about what regulates basal cAMP levels compared to GPCR-stimulated cAMP levels. This is despite the fact that in most cells there is a measurable PKA activity that, perhaps, reflects compartmentalised activation. Here then I set out to evaluate the ability of PKA to phosphorylate catalytically inactive/dominant negative PDE4 isoforms under basal and stimulated conditions to obtain an insight into the possible importance of various PDE4 isoforms to these distinct scenarios and thus identify selective actions.

My study, utilising a range of catalytically inactive PDE4 isoforms, shows that in the model COS1 cell line then the dominant negative PDE4C2 and PDE4D3 are able to be phosphorylated by PKA by basal adenylyl cyclase activity. This suggests that out of the

four different PDE4 isoforms evaluated here, namely PDE4A4, PDE4A10, PDE4C2 and PDE4D3, only PDE4C2 and PDE4D3 are held in close proximity to and regulate discrete sub-populations of PKA under basal levels of cAMP generation. Interestingly, it has been suggested that at least in some cells the actions of PDE3 and PDE4 may synergise with each other (Dousa, 1999). In order to explore this I decide to evaluate whether the PDE3 selective inhibitor, cilostamide could alter the phosphorylation of these two isoforms under basal conditions. In doing this I found out that the selective PDE3 inhibitor cilostamide increased the PKA phosphorylation of inactive PDE4C2 but not of inactive PDE4D3. This suggests that under conditions of basal cAMP production the actions of PDE4C2 and PDE3 may act synergistically on the same cAMP pool, but this is different from the pool regulated by PDE4D3. Interestingly, whilst addition of the selective PDE4 inhibitor had potentiating effect on the phosphorylation status of PDE4C2, it selectively increased the phosphorylation status of PDE4D3. This suggests that PDE4D3 controls a pool of cAMP that is also regulated by an endogenous PDE4 species in COS1 cells that is not PDE4C2. Thus, both PDE4C2 and PDE4D3 appear to be anchored close to PKA that is able to access cAMP in resting cells. Thereby, the activity of these PDE4 species must be crucial in controlling the associated PKA activity. It would seem that these two isoforms control distinct pools, one of which is shared with PDE3 and another shared with a different PDE4 isoform in these cells.

Next, I set out to investigate whether the activation of different Gs-coupled receptors could selectively perturb the phosphorylation status of individual catalytically inactive PDE4 isoforms. The two different Gs coupled agonists were used here, namely isoproterenol and PGE2 were selected, as it had previously reported that these agonists can activate AC and PKA but generate different cellular responses at least in cardiac myocytes (Steinberg & Brunton, 2001; Brunton, 2003). Interestingly, I found that the PKA phosphorylation status of inactive PDE4A4 and PDE4B1 was quite different depending agonist stimulation. In doing this I found that PGE2 and isoproterenol had a similar effect on PDE4A4 phosphorylation status, on isoproterenol stimulation, there resulted an increased phosphorylation of PDE4B1 that was not seen with PGE2. This data

indicates that these PDE4s are able to sample different pools of cAMP controlled by PGE2 and isoproterenol stimulation

As discussed previously, the PDE4D3 isoform has been shown to be capable of interacting with the AKAP, mAKAP in cardiac myocytes where it can regulate the activity of PKA (Dodge *et al*, 2001, Tasken *et al*, 2001). As I observed PKA phosphorylation of both inactive PDE4D3 and inactive PDE4C2 at basal cAMP levels, I hypothesised that this may be due to the close proximity of PKA. Thus, I decided to investigate the possibility of an AKAP involvement in the PKA phosphorylation and control of PDE4C2 activity. To do this I utilised Ht31, an established tool that has been used to disrupt PKA-AKAP anchoring specifically. Thus, using this I set out to try and disrupt the PKA phosphorylation of inactive PDE4C2. Using this, I found that the co-expression of Ht31 and inactive PDE4C2 did indeed reduce the ability of PKA to phosphorylate inactive PDE4C2 species at basal cAMP levels. This suggests that PDE4C2 is either anchored to an AKAP complex, or is in close proximity to a PKA-AKAP complex able to regulate this PKA isoform or is able to reversibly and specifically interact with an active AKAP bound PKA fraction. I also show that, by utilising a selective RI-PKA agonist and a selective RII-PKA agonist, that the RI-PKA form is the predominant form responsible for the PKA phosphorylation of PDE4C2.

Following the Ht31 experiments, I investigated the possibility of an actual interaction of the PDE4C2 isoform with a PKA-AKAP complex. Immunoprecipitates of PDE4C2 were sent to two separate AKAP laboratories (Klussmann, FMP, Berlin. & Tasken, Oslo) for overlay analysis. Both RI and RII overlay assays were performed, and these tentatively identified a putative AKAP of about 250 kD co-immunoprecipitated with PDE4C2. I have not shown the overlay results in this chapter as these are preliminary data done by others and the results are not clear. Nevertheless, they provide initial promising evidence of a possible PDE4C2-PKA-AKAP complex. To date, the only PDE4 isoform to be shown to interact with an AKAP is long form PDE4D3. The PDE4C2 isoform is also a long form which has shown to be phosphorylated and activated by PKA (MacKenzie *et al.*, 2001), thereby an interaction with an AKAP would allow another means of specific

targeting and degradation of local cAMP. In order to clarify such a complex, immunoprecipitations of PDE4C2 should be repeated and the presence of any AKAPs should be clarified by overlay assay. If an AKAP of a defined size is present, one could first see if this AKAP is a known AKAP by western blotting with commercially available antibodies. The co-immunoprecipitation of an AKAP with PDE4C2 could be further clarified by SDS PAGE and analysis of any bands present in the gel by mass spectrometry,

If I was able to pursue this project then I would have liked to identify the specific type of PKA isoform which serves to phosphorylate PDE4C2 in these cells. My initial data suggests that an RI isoform was responsible, and I would plan to further investigate this further using an approach involving small interfering RNA (siRNA) to knock down specifically and selectively each PKA isoform. As very few RI binding AKAPs have been characterized, the identification of a PDE4C2/RI-PKA-AKAP cellular complex would potentially be very exciting. The identification of such a complex would show for the first time an AKAP-PDE4 interaction involving a PDE4 isoform other than PDE4D3, it also would show for the first time a RI-PKA-AKAP to bind a PDE4.

As a means to study the compartmentalisation of cAMP signalling and regulation of gene expression, I overexpressed selected catalytically inactive PDE4 isoforms in HEK293 cells, and subsequent microarray analysis to determine changes in levels of the transcripts of a wide range of genes. I hypothesised that, according to the dominant negative strategy discussed earlier, if I overexpressed an inactive PDE4 it would replace its endogenous counterpart. This displacement of an anchored pool of active endogenous PDE4 by the cognate inactive recombinant PDE4 might, in certain situations, result in increases in levels of distinct pools of cAMP and thus subsequent activation of specific sub-populations of PKA. In phosphorylating sets of anchored target proteins this might lead to changes in the expression of distinct subsets of genes.

A spatially distinct elevation of cAMP and/or PKA activation might be expected to alter gene expression in a number of different ways. PKA can exert long term effects on cellular functioning by altering the functions of a variety of nuclear proteins including

various transcription factors, nuclear hormone receptors, transcriptional activators/repressors and chromatin-associated proteins (Shabb, 2001). The most common promoter element to exert transcriptional effects via cAMP is the cAMP-responsive element CRE. Nevertheless, this would be expected to give a single output irrespective of the source of PKA acting to phosphorylate CREB, unless the compartmentalised signal exerted effects on other signalling factors that impinged on CRE-bearing promoters such as to alter their functioning. NF-κB is another transcriptional factor regulated by PKA phosphorylation (Shabb, 2001). In its inactive state, NF-κB is tethered to the inhibitor protein I-κB in the cytosol. I-κB also binds to the C subunit of PKA. Activation of NF-κB is triggered when I-κB is targeted for degradation by in a phosphorylation-dependent manner by the ubiquitin-26S proteosome pathway. NF-κB is then free to translocate to the nucleus and its transcriptional activity is stimulated by PKA phosphorylation by the PKA released from I-κB. PKA can also indirectly exert effects upon transcriptional regulation via activation of the MAP kinase cascade. PKA-dependent activation of ERK1/2 can occur via B-Raf. Once ERK is activated it phosphorylates RSK and both translocate to the nucleus where they activate CREB (Wang *et al.*, 2003). Also, it is possible that PKA may indirectly exert effects upon transcription via the phosphorylation of other, as yet, unidentified signalling protein(s). In a recent review of physiological substrates of PKA (Shabb, 2001), it was shown that since the discovery of PKA in the 70's, the list of identified PKA substrates has quadrupled over the last decade. It is highly likely that many more PKA targets are yet to be identified. Recently, Epacs have been discovered as new routes through which cAMP can exert effects on cells. However, the precise way in which Epacs signal into cells is not clear and, its effects on gene expression have yet to be elucidated. Furthermore, since the discovery of the Epac specific activator, 8-pCPT-2'-*O*-Me-cAMP, it has now been postulated that not all PKA-independent effects of cAMP can be attributed to Epac but may involve as yet unknown additional cAMP signalling entities. In the future, this might lead to the discovery of further cAMP targets with cAMP binding domains not similar to that of Epac and PKA (Bos, 2003). Thus, there are a number of distinct way through which cAMP may be able to alter gene expression in cells via both direct and indirect actions.

My study utilising the catalytically inactive PDE4 species as a form of manipulating different pools of cAMP does indeed provide data indicating differential gene expression. This suggests that different pools of cAMP controlled by specific PDE4 isoforms may exert differential effects upon transcriptional regulation. However, it must be taken to account that the overexpression of the inactive PDE4 species may bind aberrantly to other proteins, allowing non-physiological effects. Additionally, as the half-lives of mRNA differ, the efficacy and efficiency of translation and other post-translational events affecting mRNA also differs, one cannot simply assume that the mRNA levels correlates directly to protein levels. Thus, the next step of my study would have been to investigate whether the implied changes in mRNA expressions levels observed here caused changes at the level of protein expression. I would also like to confirm the indicated changes in transcript levels using Northern blotting and RT-PCR.

As mentioned at the start of this discussion, a set of simple experiments involving treatment of cardiac myocytes with different Gs-coupled agonists and the subsequent read-out of PKA action, led to the postulate that compartmentalisation of signalling molecules exists within a physiologically relevant cell model. Recently data published by Zaccolo *et al,* has elegantly shown the spatial confinement of PDEs and the presence of distinct pools of cAMP within cardiac myocytes (Zaccolo & Pozzan, 2002; Mongillo et al., 2004). Therefore a growing body of convincing evidence is accruing to show that cardiac myocytes, which comprise the majority of the mass of the myocardium, are highly compartmentalised cells as regards to cAMP signalling.

To gain functional insight into the compartmentalisation of PDEs within cardiac myocytes, I decide to perform a set of experiments where I manipulated levels of distinct 'pools' of cAMP. I did this by using selective PDE inhibitors to alter cAMP degradation and then activated different GPCRs to stimulate adenylyl cyclase. In order to probe distinct facets of cAMP signalling, I chose to study the PKA phosphorylation of PLB and the MEK phosphorylation of ERK1/2 (indirectly activated by PKA) as outputs. In short, I observed differences in phosphorylation of PLB and phosphorylation of ERK1/2 following such manipulation of cAMP with PDE inhibitors alone, or with PDE inhibition

and selected GPCR activation. My data provides further evidence of PDE compartmentalisation within cardiac myocytes. If time had prevailed, I would have liked to have used catalytically inactive PDE4 species, or siRNA to observe the functional effects of specific PDE4 isoforms upon the regulation of PKA phosphorylation of phospholamban. The PKA phosphorylation of phospholamban (PLB) is an important mediator of Ca^{2+} uptake into the sarcoplasmic reticulum (SR), and it is involved in the regulation of relaxation and contraction (MacLenna & Kranias, 2003). This small protein binds to and inhibits the sarcoplasmic reticulum Ca^{2+} ATPase (SERCA2A). Following hormonal stimulation of the β–adrenergic receptors, PLB has been shown to be phosphorylated by PKA. A conformational change then ensues, and the inhibition of SERCA2A is relieved, allowing an increase of conductance of Ca^{2+} into the SR and it is the removal of Ca^{2+} from the cytosol which triggers relaxation. With respect to contraction and relaxation, signalling events in cardiac myocytes in response to hormonal stimulation must occur on a millisecond timescale. Several channels and pumps involved in the regulation of the cytosolic Ca^{2+} transients can be phosphorylated by PKA, also contractile proteins such as Troponin I have been shown to be substrates of PKA. Therefore, with such a short timescale, one could propose that pre-programmed signalling modules may serve to allow a distinct and rapid response to the elevation of cAMP. A specifically anchored PDE, in the case of PDE-AKAP interaction, may provide a means of cAMP degradation direct to the site of PKA action. As PLB plays such an important role in the regulation of relaxation, it would be very exciting to show that PDE(s) are involved in the regulation of the phosphorylation status of PLB.

Initially, I studied the PKA phosphorylation of the two PKA sites found with PDE4D3 and found that the phosphorylation of the Ser 54 (responsible for activation) precedes that of Ser 13. Then, I show by using the using the antisera specific for PKA phosphorylated UCR1 (PS54-UCR1) that long form PDE4s from each subfamily are phosphorylated by PKA in vivo. Overall, I hoped to show by a novel approach, the compartmentalisation of cAMP phosphodiesterases within a cellular system. I hypothesised that different catalytically inactive long form PDE4s would alter distinct cAMP 'pools' by displacing their endogenous active counterparts. By detecting the PKA phosphorylation of the

inactive PDE4 through use of the novel PS54-UCR1 antibody, I employed the catalytically inactive PDE4 itself as a readout of PKA activity. In doing so, I found that different PDE4s are capable of sampling different pools of cAMP generated by different Gs-coupled agonists. Also, my data indicates that PDE4D3 and PDE4C2 may be held in close proximity to, and play a role in the regulation of discrete sub-populations of PKA under basal levels of cAMP. Furthermore, I studied the effect of altering the concentration of discrete compartments of cAMP on gene expression by overexpressing catalytically inactive PDE4s in HEK293 cells and performing microarray analysis. This study demonstrated the influence of specific PDE4 isoforms on gene regulation controlled by compartmentalised cAMP signalling. Finally, on a more physiological scale, I chose to study the function of compartmentalised PDEs within cardiac myocytes. In doing so, I selected two different PKA targets as outputs (PLB and ERK1/2) and show that manipulation of cAMP levels with PDE inhibitors alone, or with PDE inhibitors and selected GPCR activation, that the PKA status of PLB and ERK1/2 are differentially controlled by specific PDE families.

Appendix

PDE VARIANT	PRIMER NAME	PRIMER SEQUENCES (5' - 3')	FRAGMENT LENGTH (bp)
4A	4A(3)F	ATA TCA ATG GCC CAG ATA CCG T	338
	4A(2&3)R	GCA TGC TCT GAA ACA GAC AGG	
4A4B	4A4B(4&5)F	CGG AAA GGA GCC TGT CTC TG	257
	4A4B(5)R	AGT GCC ATG GAA GGA CGA GG	
4A10	4A10(5&6)F	AGA TCT GTC AGC TTC GAG GCA G	281
	4A10(5)R	AGT GAG AAG TTG CTA CGG ACG C	
2EL	2EL(3)F	GTC CAA GCA CAT GAC CCT CCT	301
	2EL(3)R	CCG AGC CTG TAC CTG AGA CTT	
4B	4B(4)F	TCT GAA GGA CCT GAG AAG GAG	546
	4B(2&4)R	ACA CAG GTT GGC AGA CAA AGG	
4B1	4B1(4)F	AAA GCA GGA GTG TGA TGA CGG	236
	4B1(3&4)R	CGT TGT CAA AGG CAG TGT GGT	
4B2	4B2(2)F	CCT TGA GAT GGC AAA GCA CTC	264
	4B2(2)R	AAT CAC AGT GGT GCT CTG CCT	
4B3	4B3(3)F	AAA AGC ATT CGG CAG CGT C	214
	4B3(3)R	TCG ACA TCG CCT TTG GTG A	
4C	4CF	ATG GAT GGT AAA GCC CTT TGG CTC TTG G	95
	4CR	GTC TCC CTA AAT GGG TGG GAA AGT GAA G	
4D	4DF	CCC TTG ACT GTT ATC ATG CAC ACC	262
	4DR	GAT CTA CAT CAT GTA TTG CAC TGG C	
4D1	4D1(3)F	CTT TCC CTG TCT CTT CGC AGA	163
	4D1(2&3)R	GTG AGC TCC CGA TTA AGC ATC	
4D1/2	4D1/2(2)F	ATA TGA AGG AGC AGC CCT CAT G	221 & 307
	4D1/2(2&3)R	CCA GAC CGA CTC ACT TCA GAG A	
4D3	4D3(5)F	GCG AAC ATG ATG CAC GTG AA	292
	4D3(5)R	TGG CCA AGA CCT GAG CAA AT	
4D4	4D4(6)F	AGA AAT CCA GGA TGT CCT GGC	347
	4D4(5&6)R	TGC TAG GTG CTC GAT CTT GCA	
4D5	4D5(6)F	TGC CAG CTG CAC AAA GTT GAC C	212
	4D5(6)R	TTC TCG GAG AGA TCA CTG GAG A	
3A	3A(2)F	GCA GGC ATA GAA AAT CAA TCC C	353
	3A(2)R	CTG GTG TTG CAA TGT GAA AGC T	
3B	3B(2)F	TAC AAA TGC CCC TCA GGC AGT	305
	3B(2)R	CTG CCA GTT TGA TGC ACA CCT	
7A	7A(2)F	AGA CAAT GCT TGG ACA CGT GG	254
	7A(2)R	GCT GGC ATC ACT CAC TTG GAA	
TF	TF.F	TTA CAG TGG CTG TAT TCT GCT CG	401
	TF.R	TGC TGT TCT CAT GGA AGC TAT GG	
BA	BAF	CAT CGT CAC CAA CTG GGA CGA C	466
	BAR	CGT GGC CAT CTC TTG CTC GAA G	

Primer sequences used for mRNA expression profiles of HEK293 cells and COS1 cells

Alvarez R, Sette C, Yang D, Eglen R M, Wilhelm R, Shelton E R and Conti M (1995) Activation and Selective Inhibition of a Cyclic AMP-Specific Phosphodiesterase, PDE-4D3. *Molecular Pharmacology* **48**: pp 616-622.

Antoni FA (2000) Molecular Diversity of Cyclic AMP Signalling. *Frontiers in Neuroendocrinolgy* **21**: pp 103-132.

Aprigliano O, Rybin V O, Pak E, Robinson R B and Steinberg S F (1997) Beta(1)- and Beta(2)-Adrenergic Receptors Exhibit Differing Susceptibility to Muscarinic Accentuated Antagonism. *American Journal of Physiology-Heart and Circulatory Physiology* **41**: pp H2726-H2735.

Augustin R, Carayannopoulos M O, Dowd L O, Phay J E, Moley J F and Moley K H (2004) Identification and Characterization of Human Glucose Transporter-Like Protein-9 (GLUT9): Alternative Splicing Alters Trafficking. *Journal of Biological Chemistry* **279**: pp 16229-16236.

Baillie GS, MacKenzie S J, McPhee I and Houslay M D (2000) Sub-Family Selective Actions in the Ability of Erk2 MAP Kinase to Phosphorylate and Regulate the Activity of PDE4 Cyclic AMP-Specific Phosphodiesterases. *British Journal of Pharmacology* **131**: pp 811-819.

Baillie GS, Sood A, McPhee I, Gall I, Perry S J, Lefkowitz R J and Houslay M D (2003) Beta-Arrestin-Mediated PDE4 cAMP Phosphodiesterase Recruitment Regulates Beta-Adrenoceptor Switching From G(s) to G(i). *Proceedings of the National Academy of Sciences of the United States of America* **100**: pp 940-945.

Ballard SA, Gingell C J, Tang K, Turner L A, Price M E and Naylor A M (1998) Effects of Sildenafil on the Relaxation of Human Corpus Cavernosum Tissue in Vitro and on the Activities of Cyclic Nucleotide Phosphodiesterase Isozymes. *Journal of Urology* **159**: pp 2164-2171.

Bartsch O, Bartlick B and Ivell R (2004) Phosphodiesterase 4 Inhibition Synergizes With Relaxin Signaling to Promote Decidualization of Human Endometrial Stromal Cells. *Journal of Clinical Endocrinology and Metabolism* **89**: pp 324-334.

Beard MB, Huston E, Campbell L, Gall I, McPhee I, Yarwood S, Scotland G and Houslay M D (2002) In Addition to the SH3 Binding Region, Multiple Regions Within the N-Terminal Noncatalytic Portion of the cAMP-Specific Phosphodiesterase, PDE4A5, Contribute to Its Intracellular Targeting. *Cellular Signalling* **14**: pp 453-465.

Beard MB, Olsen A E, Jones R E, Erdogan S, Houslay M D and Bolger G B (2000) UCR1 and UCR2 Domains Unique to the cAMP-Specific Phosphodiesterase Family Form a Discrete Module Via Electrostatic Interactions. *Journal of Biological Chemistry* **275**: pp 10349-10358.

Beavo JA (1995) Cyclic-Nucleotide Phosphodiesterases - Functional Implications of Multiple Isoforms. *Physiological Reviews* **75**: pp 725-748.

Bers DM (2002) Cardiac Excitation-Contraction Coupling. *Nature* **415**: pp 198-205.

Bloom TJ and Beavo J A (1996) Identification and Tissue-Specific Expression of PDE7 Phosphodiesterase Splice Variants. *Proceedings of the National Academy of Sciences of the United States of America* **93**: pp 14188-14192.

Bogoyevitch MA, Andersson M B, Gillespie-Brown J, Clerk A, Glennon P E, Fuller S J and Sugden P H (1996) Adrenergic Receptor Stimulation of the Mitogen-Activated Protein Kinase Cascade and Cardiac Hypertrophy. *Biochemical Journal* **314 (Pt 1)**: pp 115-121.

Bolger GB, McCahill A, Huston E, Cheung Y F, McSorley T, Baillie G S and Houslay M D (2003a) The Unique Amino-Terminal Region of the PDE4D5 cAMP Phosphodiesterase Isoform Confers Preferential Interaction With Beta-Arrestins. *Journal of Biological Chemistry* **278**: pp 49230-49238.

Bolger GB, McCahill A, Yarwood S J, Steele M S, Warwicker J and Houslay M D (2002) Delineation of RAID1, the RACK1 Interaction Domain Located Within the Unique N-Terminal Region of the cAMP-Specific Phosphodiesterase, PDE4D5. *BMC Biochemistry* **3**: pp 24.

Bolger GB, Peden A H, Steele M R, MacKenzie C, McEwan D G, Wallace D A, Huston E, Baillie G S and Houslay M D (2003b) Attenuation of the Activity of the cAMP-Specific Phosphodiesterase PDE4A5 by Interaction With the Immunophilin XAP2. *Journal of Biological Chemistry* **278**: pp 33351-33363.

Bos JL (2003) Epac: a New CAMP Target and New Avenues in cAMP Research. *Nature Reviews Molecular Cell Biology* **4**: pp 733-738.

Bourne HR (1997) How Receptors Talk to Trimeric G Proteins. *Current Opinion in Cell Biology* **9**: pp 134-142.

Brown RL, Ord T, Moss S B and Williams C J (2002) A-Kinase Anchor Proteins As Potential Regulators of Protein Kinase a Function in Oocytes. *Biology of Reproduction* **67**: pp 981-987.

Brunton LL, Hayes J S and Mayer S E (1981) Functional Compartmentation of Cyclic-Amp and Protein-Kinase in Heart. *Advances in Cyclic Nucleotide Research* **14**: pp 391-397.

Burton KA, Johnson B D, Hausken Z E, Westenbroek R E, Idzerda R L, Scheuer T, Scott J D, Catterall W A and Mcknight G S (1997) Type II Regulatory Subunits Are Not Required for the Anchoring-Dependent Modulation of Ca2+ Channel Activity by cAMP-Dependent Protein Kinase. *Proceedings of the National Academy of Sciences of the United States of America* **94**: pp 11067-11072.

Cali JJ, Zwaagstra J C, Mons N, Cooper D M F and Krupinski J (1994) Type-Viii Adenylyl-Cyclase - A Ca2+/Calmodulin-Stimulated Enzyme Expressed in Discrete Regions of Rat-Brain. *Journal of Biological Chemistry* **269**: pp 12190-12195.

Carr DW, Cutler R E, Cottom J E, Salvador L M, Fraser I D C, Scott J D and Hunzicker-Dunn M (1999) Identification of CAMP-Dependent Protein Kinase Holoenzymes in Preantral- and Preovulatory-Follicle-Enriched Ovaries, and Their Association With A-Kinase-Anchoring Proteins. *Biochemical Journal* **344**: pp 613-623.

Carver LA and Bradfield C A (1997) Ligand-Dependent Interaction of the Aryl Hydrocarbon Receptor With a Novel Immunophilin Homolog in Vivo. *Journal of Biological Chemistry* **272**: pp 11452-11456.

Chang YH, Conti M, Lee Y C, Lai H L, Ching Y H and Chern Y J (1997) Activation of Phosphodiesterase IV During Desensitization of the A(2A) Adenosine Receptor-Mediated Cyclic AMP Response in Rat Pheochromocytoma (PC12) Cells. *Journal of Neurochemistry* **69**: pp 1300-1309.

Chien KR, Knowlton K U, Zhu H and Chien S (1991) Regulation of Cardiac Gene Expression During Myocardial Growth and Hypertrophy: Molecular Studies of an Adaptive Physiologic Response. *FASEB J* **5**: pp 3037-3046.

Chrivia JC, Uhler M D and Mcknight G S (1988) Characterization of Genomic Clones Coding for the C-Alpha and C-Beta Subunits of Mouse cAMP-Dependent Protein-Kinase. *Journal of Biological Chemistry* **263**: pp 5739-5744.

Clerk A, Michael A and Sugden P H (1998) Stimulation of the P38 Mitogen-Activated Protein Kinase Pathway in Neonatal Rat Ventricular Myocytes by the G Protein-Coupled Receptor Agonists, Endothelin-1 and Phenylephrine: a Role in Cardiac Myocyte Hypertrophy? *Journal of Cell Biology* **142**: pp 523-535.

Cockcroft S, Thomas G M, Fensome A, Geny B, Cunningham E, Gout I, Hiles I, Totty N F, Truong O and Hsuan J J (1994) Phospholipase D: a Downstream Effector of ARF in Granulocytes. *Science* **263**: pp 523-526.

Colledge M and Scott J D (1999) AKAPs: From Structure to Function. *Trends in Cell Biology* **9**: pp 216-221.

Conti M, Richter W, Mehats C, Livera G, Park J Y and Jin C (2003) Cyclic AMP-Specific PDE4 Phosphodiesterases As Critical Components of Cyclic AMP Signaling. *Journal of Biological Chemistry* **278**: pp 5493-5496.

Contos JJ, Ishii I and Chun J (2000) Lysophosphatidic Acid Receptors. *Molecular Pharmacology* **58**: pp 1188-1196.

Cooper DM (2003) Regulation and Organization of Adenylyl Cyclases and cAMP. *Biochemical Journal* **375**: pp 517-529.

Cooper DM, Mons N and Karpen J W (1995) Adenylyl Cyclases and the Interaction Between Calcium and cAMP Signalling. *Nature* **374**: pp 421-424.

Corbin JD and Francis S H (1999) Cyclic GMP Phosphodiesterase-5: Target of Sildenafil. *Journal of Biological Chemistry* **274**: pp 13729-13732.

De Arcangelis V, Coletti D, Conti M, Lagarde M, Molinaro M, Adamo S, Nemoz G and Naro F (2003) IGF-I-Induced Differentiation of L6 Myogenic Cells Requires the Activity of cAMP-Phosphodiesterase. *Molecular Biology of the Cell* **14**: pp 1392-1404.

de Rooij J, Rehmann H, van Triest M, Cool R H, Wittinghofer A and Bos J L (2000) Mechanism of Regulation of the Epac Family of cAMP-Dependent RapGEFs. *Journal of Biological Chemistry* **275**: pp 20829-20836.

de Rooij J, Zwartkruis F J T, Verheijen M H G, Cool R H, Nijman S M B, Wittinghofer A and Bos J L (1998) Epac Is a Rap1 Guanine-Nucleotide-Exchange Factor Directly Activated by Cyclic AMP. *Nature* **396**: pp 474-477.

de Tejada IS, Angulo J, Cuevas P, Ferndandez A, Moncada I, Allona A, Lledo E, Korschen H G, Niewohner U, Haning H, Pages E and Bischoff E (2001) The Phosphodiesterase Inhibitory Selectivity and the in vitro and in vivo Potency of the New PDE5 Inhibitor Vardenafil. *International Journal of Impotence Research* **13**: pp 282-290.

Dhillon AS and Kolch W (2002) Untying the Regulation of the Raf-1 Kinase. *Archives of Biochemistry and Biophysics* **404**: pp 3-9.

Dhillon AS, Meikle S, Yazici Z, Eulitz M and Kolch W (2002a) Regulation of Raf-1 Activation and Signalling by Dephosphorylation. *EMBO Journal* **21**: pp 64-71.

Dhillon AS, Pollock C, Steen H, Shaw P E, Mischak H and Kolch W (2002b) Cyclic AMP-Dependent Kinase Regulates Raf-1 Kinase Mainly by Phosphorylation of Serine 259. *Molecular and Cellular Biology* **22**: pp 3237-3246.

DiSanto ME, Glaser K B and Heaslip R J (1995) Phospholipid Regulation of a Cyclic AMP-Specific Phosphodiesterase (PDE4) From U937 Cells. *Cell Signal* **7**: pp 827-835.

Dodge K and Scott J D (2000) AKAP79 and the Evolution of the AKAP Model. *FEBS Letters* **476**: pp 58-61.

Dodge KL, Khouangsathiene S, Kapiloff M S, Mouton R, Hill E V, Houslay M D, Langeberg L K and Scott J D (2001) MAKAP Assembles a Protein Kinase A/PDE4 Phosphodiesterase cAMP Signaling Module. *EMBO Journal* **20**: pp 1921-1930.

Dousa TP (1999) Cyclic-3 ',5 '-Nucleotide Phosphodiesterase Isozymes in Cell Biology and Pathophysiology of the Kidney. *Kidney International* **55**: pp 29-62.

Dumaz N, Light Y and Marais R (2002) Cyclic AMP Blocks Cell Growth Through Raf-1-Dependent and Raf-1-Independent Mechanisms. *Molecular and Cellular Biology* **22**: pp 3717-3728.

Eardley I and Cartledge J (2002) Tadalafil (CIALIS (TM)) for Men With Erectile Dysfunction. *International Journal of Clinical Practice* **56**: pp 300-304.

EcklyMichel A, Martin V and Lugnier C (1997) Involvement of Cyclic Nucleotide-Dependent Protein Kinases in Cyclic AMP-Mediated Vasorelaxation. *British Journal of Pharmacology* **122**: pp 158-164.

Enserink JM, Christensen A E, de Rooij J, van Triest M, Schwede F, Genieser H G, Doskeland S O, Blank J L and Bos J L (2002) A Novel Epac-Specific cAMP Analogue Demonstrates Independent Regulation of Rap1 and ERK. *Nature Cell Biology* **4**: pp 901-906.

Erdogan S and Houslay M D (1997) Challenge of Human Jurkat T-Cells With the Adenylate Cyclase Activator Forskolin Elicits Major Changes in cAMP Phosphodiesterase (PDE) Expression by Up-Regulating PDE3 and Inducing PDE4D1 and PDE4D2 Splice Variants As Well As Down-Regulating a Novel PDE4A Splice Variant. *Biochemical Journal* **321**: pp 165-175.

Essayan DM, KageySobotka A, Lichtenstein L M and Huang S K (1997) Regulation of Interleukin-13 by Type 4 Cyclic Nucleotide Phosphodiesterase (PDE) Inhibitors in Allergen-Specific Human T Lymphocyte Clones. *Biochemical Pharmacology* **53**: pp 1055-1060.

Fawcett L, Baxendale R, Stacey P, McGrouther C, Harrow I, Soderling S, Hetman J, Beavo J A and Phillips S C (2000) Molecular Cloning and Characterization of a Distinct Human Phosphodiesterase Gene Family: PDE11A. *Proceedings of the National Acadamey of Sciences of the United States of America* **97**: pp 3702-3707.

Fisch JD, Behr B and Conti M (1998) Enhancement of Motility and Acrosome Reaction in Human Spermatozoa: Differential Activation by Type-Specific Phosphodiesterase Inhibitors. *Human Reproduction* **13**: pp 1248-1254.

Fisher DA, Smith J F, Pillar J S, St Denis S H and Cheng J B (1998) Isolation and Characterization of PDE8A, a Novel Human cAMP-Specific Phosphodiesterase. *Biochemical and Biophysical Research Communications* **246**: pp 570-577.

Freyberg Z, Siddhanta A and Shields D (2003) "Slip, Sliding Away": Phospholipase D and the Golgi Apparatus. *Trends in Cell Biology* **13**: pp 540-546.

Gao TY, Yatani A, DellAcqua M L, Sako H, Green S A, Dascal N, Scott J D and Hosey M M (1997) cAMP-Dependent Regulation of Cardiac L-Type Ca2+ Channels Requires Membrane Targeting of PKA and Phosphorylation of Channel Subunits. *Neuron* **19**: pp 185-196.

Georget M, Mateo P, Vandecasteele G, Lipskaia L, Defer N, Hanoune J, Hoerter J, Lugnier C and Fischmeister R (2003) Cyclic AMP Compartmentation Due to Increased cAMP-Phosphodiesterase Activity in Transgenic Mice With a Cardiac-Directed Expression of the Human Adenylyl Cyclase Type 8 (AC8). *FASEB Journal* **17**: pp 1380-1391.

Gillespie-Brown J, Fuller S J, Bogoyevitch M A, Cowley S and Sugden P H (1995) The Mitogen-Activated Protein Kinase Kinase MEK1 Stimulates a Pattern of Gene Expression Typical of the Hypertrophic Phenotype in Rat Ventricular Cardiomyocytes. *Journal of Biological Chemistry* **270**: pp 28092-28096.

Grange M, Sette C, Cuomo M, Conti M, Lagarde M, Prigent A F and Nemoz G (2000) The CAMP-Specific Phosphodiesterase PDE4D3 Is Regulated by Phosphatidic Acid Binding - Consequences for cAMP Signaling Pathway and Characterization of a Phosphatidic Acid Binding Site. *Journal of Biological Chemistry* **275**: pp 33379-33387.

Guipponi M, Scott H S, Kudoh J, Kawasaki K, Shibuya K, Shintani A, Asakawa S, Chen H, Lalioti M D, Rossier C, Minoshima S, Shimizu N and Antonarakis S E (1998) Identification and Characterization of a Novel Cyclic Nucleotide Phosphodiesterase Gene (PDE9A) That Maps to 21q22.3: Alternative Splicing of mRNA Transcripts, Genomic Structure and Sequence. *Human Genetics* **103**: pp 386-392.

Hagemann D, Kuschel M, Kuramochi T, Zhu W Z, Cheng H P and Xiao R P (2000) Frequency-Encoding Thr(17) Phospholamban Phosphorylation Is Independent of Ser(16) Phosphorylation in Cardiac Myocytes. *Journal of Biological Chemistry* **275**: pp 22532-22536.

Hagemann D and Xiao R P (2002) Dual Site Phospholamban Phosphorylation and Its Physiological Relevance in the Heart. *Trends in Cardiovascular Medicine* **12**: pp 51-56.

Haghighi K, Schmidt A G, Hoit B D, Brittsan A G, Yatani A, Lester J W, Zhai J, Kimura Y, Dorn G W, MacLennan D H and Kranias E G (2001) Superinhibition of Sarcoplasmic Reticulum Function by Phospholamban Induces Cardiac Contractile Failure. *Journal of Biological Chemistry* **276**: pp 24145-24152.

Hamilton SE and Hurley J B (1990) A Phosphodiesterase Inhibitor Specific to A Subset of Bovine Retinal Cones. *Journal of Biological Chemistry* **265**: pp 11259-11264.

Hammond SM, Jenco J M, Nakashima S, Cadwallader K, Gu Q, Cook S, Nozawa Y, Prestwich G D, Frohman M A and Morris A J (1997) Characterization of Two Alternately Spliced Forms of Phospholipase D1. Activation of the Purified Enzymes by Phosphatidylinositol 4,5-Bisphosphate, ADP-Ribosylation Factor, and Rho Family Monomeric GTP-Binding Proteins and Protein Kinase C-Alpha. *Journal of Biological Chemistry* **272**: pp 3860-3868.

Han JM, Kim Y, Lee J S, Lee C S, Lee B D, Ohba M, Kuroki T, Suh P G and Ryu S H (2002) Localization of Phospholipase D1 to Caveolin-Enriched Membrane Via Palmitoylation: Implications for Epidermal Growth Factor Signaling. *Molecular Biology Cell* **13**: pp 3976-3988.

Han P, Werber J, Surana M, Fleischer N and Michaeli T (1999) The Calcium/Calmodulin-Dependent Phosphodiesterase PDE1C Down-Regulates Glucose-Induced Insulin Secretion. *Journal of Biological Chemistry* **274**: pp 22337-22344.

Harndahl L, Jing X J, Ivarsson R, Degerman E, Ahren B, Manganiello V C, Renstrom E and Holst L S (2002) Important Role of Phosphodiesterase 3B for the Stimulatory Action of cAMP on Pancreatic Beta-Cell Exocytosis and Release of Insulin. *Journal of Biological Chemistry* **277**: pp 37446-37455.

Harrington CA, Rosenow C and Retief J (2000) Monitoring Gene Expression Using DNA Microarrays. *Current Opinion in Microbiology* **3**: pp 285-291.

Hayes JS and Brunton L L (1982) Functional Compartments in Cyclic-Nucleotide Action. *Journal of Cyclic Nucleotide Research* **8**: pp 1-16.

Hayes JS, Brunton L L and Mayer S E (1980) Selective Activation of Particulate cAMP-Dependent Protein-Kinase by Isoproterenol and Prostaglandin-E1. *Journal of Biological Chemistry* **255**: pp 5113-5119.

Hoffmann R, Baillie G S, MacKenzie S J, Yarwood S J and Houslay M D (1999) The MAP Kinase ERK2 Inhibits the Cyclic AMP-Specific Phosphodiesterase HSPDE4D3 by Phosphorylating It at Ser579. *EMBO Journal* **18**: pp 893-903.

Hoffmann R, Wilkinson I R, McCallum J F, Engels P and Houslay M D (1998) cAMP-Specific Phosphodiesterase HSPDE4D3 Mutants Which Mimic Activation and Changes in Rolipram Inhibition Triggered by Protein Kinase A Phosphorylation of Ser-54: Generation of a Molecular Model. *Biochemical Journal* **333**: pp 139-149.

Hosoi R, Ishikawa M, Kobayashi K, Gee A, Yamaguchi M and Inoue O (2003) Effect of Rolipram on Muscarinic Acetylcholine Receptor Binding in the Intact Mouse Brain. *Journal of Neural Transmission* **110**: pp 363-372.

Houslay MD (2001) PDE4 cAMP-Specific Phosphodiesterases. *Progress in Nucleic Acid Research and Molecular Biology, Vol 69* **69**: pp 249-315.

Houslay MD and Adams D R (2003) PDE4 cAMP Phosphodiesterases: Modular Enzymes That Orchestrate Signalling Cross-Talk, Desensitization and Compartmentalization. *Biochemical Journal* **370**: pp 1-18.

Houslay MD and Baillie G S (2003) The Role of ERK2 Docking and Phosphorylation of PDE4 cAMP Phosphodiesterase Isoforms in Mediating Cross-Talk Between the cAMP and ERK Signalling Pathways. *Biochemical Society Transactions* **31**: pp 1186-1190.

Houslay MD and Milligan G (1997) Tailoring cAMP-Signalling Responses Through Isoform Multiplicity. *Trends Biochemical Science* **22**: pp 217-224.

Huai Q, Colicelli J and Ke H M (2003) The Crystal Structure of AMP-Bound PDE4 Suggests a Mechanism for Phosphodiesterase Catalysis. *Biochemistry* **42**: pp 13220-13226.

Huston E, Beard M, McCallum F, Pyne N J, Vandenabeele P, Scotland G and Houslay M D (2000) The cAMP-Specific Phosphodiesterase PDE4A5 Is Cleaved Downstream of Its SH3 Interaction Domain by Caspase-3 - Consequences for Altered Intracellular Distribution. *Journal of Biological Chemistry* **275**: pp 28063-28074.

Imai A, Nashida T and Shimomura H (1996) Expression of mRNA Encoding AMP-Specific Phosphodiesterase Isoforms in Rat Parotid Glands. *Biochemistry and Molecular Biology International* **40**: pp 1175-1181.

Ishibashi K, Fujioka T and Ui M (1999) Decreases in CAMP Phosphodiesterase Activity in Hepatocytes Cultured With Herbimycin A Due to Cellular Microtubule Polymerization Related to Inhibition of Tyrosine Phosphorylation of Alpha-Tubulin. *European Journal of Biochemistry* **260**: pp 398-408.

Iwami G, Kawabe J, Ebina T, Cannon P J, Homey C J and Ishikawa Y (1995) Regulation of Adenylyl Cyclase by Protein Kinase A. *Journal of Biological Chemistry* **270**: pp 12481-12484.

Jackman AL, Melin C J, Kimbell R, Brunton L, Aherne G W, Theti D S and Walton M (2002) A Rationale for the Clinical Development of the Thymidylate Synthase Inhibitor ZD9331 in Ovarian and Other Solid Tumours. *Biochimica et Biophysica Acta-Molecular Basis of Disease* **1587**: pp 215-223.

Jahnsen T, Hedin L, Kidd V J, Beattie W G, Lohmann S M, Walter U, Durica J, Schulz T Z., Schiltz E, Browner M, Lawrence C B, Goldman D, Ratoosh S L and Richards J S (1986) Molecular-Cloning, cDNA Structure, and Regulation of the Regulatory Subunit of Type-II cAMP-Dependent Protein-Kinase From Rat Ovarian Granulosa-Cells. *Journal of Biological Chemistry* **261**: pp 2352-2361.

Jaski BE, Fifer M A, Wright R F, Braunwald E and Colucci W S (1985) Positive Inotropic and Vasodilator Actions of Milrinone in Patients With Severe Congestive Heart-Failure - Dose-Response Relationships and Comparison to Nitroprusside. *Journal of Clinical Investigation* **75**: pp 643-649.

Jin SLC, Richard F J, Kuo W P, D'Ercole A J and Conti M (1999) Impaired Growth and Fertility of cAMP-Specific Phosphodiesterase PDE4D-Deficient Mice. *Proceedings of the National Academy of Sciences of the United States of America* **96**: pp 11998-12003.

Joazeiro CA and Weissman A M (2000) RING Finger Proteins: Mediators of Ubiquitin Ligase Activity. *Cell* **102**: pp 549-552.

Johnson DA, Akamine P, Radzio-Andzelm E, Madhusudan M and Taylor S S (2001) Dynamics of CAMP-Dependent Protein Kinase. *Chem Reviews* **101**: pp 2243-2270.

Jurevicius J and Fischmeister R (1996) CAMP Compartmentation Is Responsible for a Local Activation of Cardiac Ca^{2+} Channels by Beta-Adrenergic Agonists. *Proceedings of the National Academy of Sciences of the United States of America* **93**: pp 295-299.

Jurevicius J, Skeberdis V A and Fischmeister R (2003) Role of Cyclic Nucleotide Phosphodiesterase Isoforms in cAMP Compartmentation Following Beta(2)-Adrenergic Stimulation of I-Ca,I-L in Frog Ventricular Myocytes. *Journal of Physiology-London* **551**: pp 239-252.

Kao A, Manzi S, Cunningham A, Krishnaswami S, Edmundowicz D, Brunton L and Wasko M C M (2002) Atherosclerosis in RA Women: Inflammatory Risk Factors for Vascular Calcification. *Arthritis and Rheumatism* **46**: pp S512.

Kapiloff MS, Jackson N and Airhart N (2001) mAKAP and the Ryanodine Receptor Are Part of a Multicomponent Signaling Complex on the Cardiomyocyte Nuclear Envelope. *Journal of Cell Science* **114**: pp 3167-3176.

Kapiloff MS, Schillace R V, Westphal A M and Scott J D (1999) mAKAP: an A-Kinase Anchoring Protein Targeted to the Nuclear Membrane of Differentiated Myocytes. *Journal of Cell Science* **112**: pp 2725-2736.

Kawasaki H, Springett G M, Mochizuki N, Toki S, Nakaya M, Matsuda M, Housman D E and Graybiel A M (1998) A Family of cAMP-Binding Proteins That Directly Activate Rap1. *Science* **282**: pp 2275-2279.

Kennelly PJ and Krebs E G (1991) Consensus Sequences As Substrate Specificity Determinants for Protein Kinases and Protein Phosphatases. *Journal of Biological Chemistry* **266**: pp 15555-15558.

Kitamura T, Kitamura Y, Kuroda S, Hino Y, Ando M, Kotani K, Konishi H, Matsuzaki H, Kikkawa U, Ogawa W and Kasuga M (1999) Insulin-Induced Phosphorylation and Activation of Cyclic Nucleotide Phosphodiesterase 3B by the Serine-Threonine Kinase Akt. *Molecular and Cellular Biology* **19**: pp 6286-6296.

Krebs EG and Beavo J A (1979) Phosphorylation-Dephosphorylation of Enzymes. *Annual Reviews Biochemistry* **48**: pp 923-959.

Lai HW, Minami M, Satoh M and Wong Y H (1995) Gz Coupling to the Rat Kappa-Opioid Receptor. *FEBS Letters* **360**: pp 97-99.

Laliberte F, Han Y X, Govindarajan A, Giroux A, Liu S, Bobechko B, Lario P, Bartlett A, Gorseth E, Gresser M and Huang Z (2000) Conformational Difference Between PDE4 Apoenzyme and Holoenzyme. *Biochemistry* **39**: pp 6449-6458.

Laliberte F, Liu S, Gorseth E, Bobechko B, Bartlett A, Lario P, Gresser M J and Huang Z (2002) In Vitro PKA Phosphorylation-Mediated Human PDE4A4 Activation. *FEBS Letters* **512**: pp 205-208.

Lario PL, Bobechko B, Bateman K, Kelly J, Vrielink A and Huang Z (2001) Purification and Characterization, of the Human PDE4A Catalytic Domain (PDE4A(330-723)) Expressed in Sf9 Cells. *Archives of Biochemistry and Biophysics* **394**: pp 54-60.

Lasley RD and Smart E J (2001) Cardiac Myocyte Adenosine Receptors and Caveolae. *Trends in Cardiovascular Medicine* **11**: pp 259-263.

Lee ME, Markowitz J, Lee J O and Lee H (2002) Crystal Structure of Phosphodiesterase 4D and Inhibitor Complex. *FEBS Letters* **530**: pp 53-58.

Lefievre L, de Lamirande E and Gagnon C (2002) Presence of Cyclic Nucleotide Phosphodiesterases PDE1, Existing As a Stable Complex With Calmodulin, and PDE3A in Human Spermatozoa. *Biology of Reproduction* **67**: pp 423-430.

Liang W, Curran P K, Hoang Q, Moreland R T and Fishman P H (2004) Differences in Endosomal Targeting of Human Beta(1)- and Beta(2)-Adrenergic Receptors Following Clathrin-Mediated Endocytosis. *Journal of Cell Science* **117**: pp 723-734.

Lim J, Pahlke G and Conti M (1999a) Activation of the cAMP-Specific Phosphodiesterase PDE4D3 by Phosphorylation - Identification and Function of an Inhibitory Domain. *Journal of Biological Chemistry* **274**: pp 19677-19685.

Liscovitch M, Czarny M, Fiucci G and Tang X (2000) Phospholipase D: Molecular and Cell Biology of a Novel Gene Family. *Biochemal Journal* **345 Pt 3**: pp 401-415.

Liu H and Maurice D H (1997) Regulation of cAMP Phosphodiesterase 4 (PDE4) in Rat Aortic Smooth Muscle Cells: The Role of cAMP. *Molecular Biology of the Cell* **8**: pp 83.

Liu S, Laliberte F, Bobechko B, Bartlett A, Lario P, Gorseth E, Van Hamme J, Gresser M J and Huang Z (2001) Dissecting the Cofactor-Dependent and Independent Bindings of PDE4 Inhibitors. *Biochemistry* **40**: pp 10179-10186.

Loughney K, Snyder P B, Uher L, Rosman G J, Ferguson K and Florio V A (1999) Isolation and Characterization of PDE10A, a Novel Human 3 ', 5 '-Cyclic Nucleotide Phosphodiesterase. *Gene* **234**: pp 109-117.

Lugnier C, Keravis T, Le Bec A, Pauvert O, Proteau S and Rousseau E (1999) Characterization of Cyclic Nucleotide Phosphodiesterase Isoforms Associated to Isolated Cardiac Nuclei. *Biochimica et Biophysica Acta-General Subjects* **1472**: pp 431-446.

Luttrell LM, Roudabush F L, Choy E W, Miller W E, Field M E, Pierce K L and Lefkowitz R J (2001) Activation and Targeting of Extracellular Signal-Regulated Kinases by Beta-Arrestin Scaffolds. *Proceedings of the National Academy of Sciences of the United States of America* **98**: pp 2449-2454.

MacKenzie SJ, Baillie G S, McPhee I, Bolger G B and Houslay M D (2000) ERK2 Mitogen-Activated Protein Kinase Binding, Phosphorylation, and Regulation of the PDE4D cAMP-Specific Phosphodiesterases - The Involvement of COOH-Terminal Docking Sites and NH2-Terminal UCR Regions. *Journal of Biological Chemistry* **275**: pp 16609-16617.

MacKenzie SJ, Baillie G S, McPhee I, MacKenzie C, Seamons R, McSorley T, Millen J, Beard M B, van Heeke G and Houslay M D (2002) Long PDE4 cAMP Specific Phosphodiesterases Are Activated by Protein Kinase A-Mediated Phosphorylation of a Single Serine Residue in Upstream Conserved Region 1 (UCR1). *British Journal of Pharmacology* **136**: pp 421-433.

MacKenzie SJ and Houslay M D (2000) Action of Rolipram on Specific PDE4 cAMP Phosphodiesterase Isoforms and on the Phosphorylation of cAMP-Response-Element-Binding Protein (CREB) and P38 Mitogen-Activated Protein (MAP) Kinase in U937 Monocytic Cells. *Biochemical Journal* **347**: pp 571-578.

MacLennan DH and Kranias E G (2003) Phospholamban: A Crucial Regulator of Cardiac Contractility. *Nature Reviews Molecular Cell Biology* **4**: pp 566-577.

Manganiello VC, Taira M, Degerman E and Belfrage P (1995) Type-Iii cGMP-Inhibited Cyclic-Nucleotide Phosphodiesterases (PDE-3 Gene Family). *Cellular Signalling* **7**: pp 445-455.

Marala RB and Mustafa S J (1998) Immunological Characterization of Adenosine A(2A) Receptors in Human and Porcine Cardiovascular Tissues. *Journal of Pharmacology and Experimental Therapeutics* **286**: pp 1051-1057.

Marchmont RJ and Houslay M D (1980) Insulin Activates a Rat Liver Peripheral Plasma-Membrane Cyclic AMP Phosphodiesterase by a Phosphorylation Mechanism. *Biochemal Society Transactions* **8**: pp 537-538.

Marks AR (2001) Ryanodine Receptors/Calcium Release Channels in Heart Failure and Sudden Cardiac Death. *Journal of Molecular and Cellular Cardiology* **33**: pp 615-624.

Martinez SE, Wu A Y, Glavas N A, Tang X B, Turley S, Hol W G J and Beavo J A (2002) The Two GAF Domains in Phosphodiesterase 2A Have Distinct Roles in Dimerization and in cGMP Binding. *Proceedings of the National Academy of Sciences of the United States of America* **99**: pp 13260-13265.

Masumoto K, Fujioka A, Nakahama K, Inouye S I T and Shigeyoshi Y (2003) Effect of Phosphodiesterase Type 4 on Circadian Clock Gene Per1 Transcription. *Biochemical and Biophysical Research Communications* **306**: pp 781-785.

Matousovic K, Tsuboi Y, Walker H, Grande J P and Dousa T P (1997) Inhibitors of Cyclic Nucleotide Phosphodiesterase Isozymes Block Renal Tubular Cell Proliferation Induced by Folic Acid. *Journal of Laboratory and Clinical Medicine* **130**: pp 487-495.

Maurice DH, Palmer D, Tilley D G, Dunkerley H A, Netherton S J, Raymond D R, Elbatarny H S and Jimmo S L (2003) Cyclic Nucleotide Phosphodiesterase Activity, Expression, and Targeting in Cells of the Cardiovascular System. *Molecular Pharmacology* **64**: pp 533-546.

McCahill A, Warwicker J, Bolger G B, Houslay M D and Yarwood S J (2002) The RACK1 Scaffold Protein: a Dynamic Cog in Cell Response Mechanisms. *Molecular Pharmacology* **62**: pp 1261-1273.

Mccartney S, Little B M and Scott J D (1995) Analysis of A Novel A-Kinase Anchoring Protein-100, (Akap 100). *Biochemical Society Transactions* **23**: pp S268.

McDonald T, Wang R, Bailey W, Xie G, Chen F, Caskey C T and Liu Q (1998) Identification and Cloning of an Orphan G Protein-Coupled Receptor of the Glycoprotein Hormone Receptor Subfamily. *Biochemical and Biophysical Research Communications* **247**: pp 266-270.

McPhee I, Cochran S and Houslay M D (2001) The Novel Long PDE4A10 Cyclic AMP Phosphodiesterase Shows a Pattern of Expression Within Brain That Is Distinct From the Long PDE4A5 and Short PDE4A1 Isoforms. *Cellular Signalling* **13**: pp 911-918.

McPhee I, Yarwood S J, Scotland G, Huston E, Beard M B, Ross A H, Houslay E S and Houslay M D (1999) Association With the SRC Family Tyrosyl Kinase LYN Triggers a Conformational Change in the Catalytic Region of Human cAMP-Specific Phosphodiesterase HSPDE4A4B - Consequences for Rolipram Inhibition. *Journal of Biological Chemistry* **274**: pp 11796-11810.

Meliton AY, Munoz N M, Liu J, Lambertino A T, Boetticher E, Myo S, Myou S, Zhu X D, Johnson M and Leff A R (2003) Blockade of LTC4 Synthesis Caused by Additive Inhibition of GIV-PLA(2) Phosphorylation: Effect of Salmeterol and PDE4 Inhibition in Human Eosinophils. *Journal of Allergy and Clinical Immunology* **112**: pp 404-410.

Mery PF, Pavoine C, Pecker F and Fischmeister R (1995) Erythro-9-(2-Hydroxy-3-Nonyl)Adenine Inhibits Cyclic GMP-Stimulated Phosphodiesterase in Isolated Cardiac Myocytes. *Molecular Pharmacology* **48**: pp 121-130.

Michaeli T, Bloom T J, Martins T, Loughney K, Ferguson K, Riggs M, Rodgers L, Beavo J A and Wigler M (1993) Isolation and Characterization of A Previously Undetected Human cAMP-Phosphodiesterase by Complementation of cAMP Phosphodiesterase-Deficient Saccharomyces-Cerevisiae. *Journal of Biological Chemistry* **268**: pp 12925-12932.

Michel JJC, Dodge K L, Wong W, Mayer N C, Langeberg L K and Scott J D (2004) PKA-Phosphorylation of PDE4D3 Facilitates Recruitment of the mAKAP Signalling Complex. *Biochemical Journal* **381**: pp 587-592.

Michel JJC and Scott J D (2002) AKAP Mediated Signal Transduction. *Annual Review of Pharmacology and Toxicology* **42**: pp 235-257.

Minamisawa S, Hoshijima M, Chu G, Ward C A, Frank K, Gu Y, Martone M E, Wang Y, Ross J, Jr., Kranias E G, Giles W R and Chien K R (1999) Chronic Phospholamban-Sarcoplasmic Reticulum Calcium ATPase Interaction Is the Critical Calcium Cycling Defect in Dilated Cardiomyopathy. *Cell* **99**: pp 313-322.

Mongillo M, McSorley T, Evellin S, Sood A, Lissandron V, Terrin A, Huston E, Hannawacker A, Lohse M J, Pozzan T, Houslay M D and Zaccolo M (2004) Fluorescence Resonance Energy Transfer-Based Analysis of cAMP Dynamics in Live Neonatal Rat Cardiac Myocytes Reveals Distinct Functions of Compartmentalized Phosphodiesterases. *Circulation Research* **95**: pp 67-75.

Moolenaar WH, Kranenburg O, Postma F R and Zondag G C (1997) Lysophosphatidic Acid: G-Protein Signalling and Cellular Responses. *Current Opinion in Cell Biology* **9**: pp 168-173.

Moon EY and Lerner A (2003) PDE4 Inhibitors Activate a Mitochondrial Apoptotic Pathway in Chronic Lymphocytic Leukemia Cells That Is Regulated by Protein Phosphatase 2A. *Blood* **101**: pp 4122-4130.

Morley JF and Liang B T (1996) A Novel Gs-Mediated Cyclic AMP-Independent Stimulatory Mechanism Via the Adenosine A2a Receptor in Intact Cardiac Cell. *Circulation* **94**: pp 266.

Movsesian MA (2000) Therapeutic Potential of Cyclic Nucleotide Phosphodiesterase Inhibitors in Heart Failure. *Expert Opinion on Investigational Drugs* **9**: pp 963-973.

Movsesian MA and Alharethi R (2002) Inhibitors of Cyclic Nucleotide Phosphodiesterase PDE3 As Adjunct Therapy for Dilated Cardiomyopathy. *Expert Opinion on Investigational Drugs* **11**: pp 1529-1536.

Movsesian MA, Komas N, Krall J and Manganiello V C (1996) Expression and Activity of Low K-m CGMP-Inhibited CAMP Phosphodiesterase in Cardiac and Skeletal Muscle. *Biochemical and Biophysical Research Communications* **225**: pp 1058-1062.

Murray F, MacLean M R and Pyne N J (2002) Increased Expression of the cGMP-Inhibited cAMP-Specific (PDE3) and cGMP Binding cGMP-Specific (PDE5) Phosphodiesterases in Models of Pulmonary Hypertension. *British Journal of Pharmacology* **137**: pp 1187-1194.

Murthy KS, Zhou H P and Makhlouf G M (2002) PKA-Dependent Activation of PDE3A and PDE4 and Inhibition of Adenylyl Cyclase V/VI in Smooth Muscle. *American Journal of Physiology-Cell Physiology* **282**: pp C508-C517.

Musialek P, Rigg L, Terrar D A, Paterson D J and Casadei B (2000) Role of cGMP-Inhibited Phosphodiesterase and Sarcoplasmic Calcium in Mediating the Increase in Basal Heart Rate With Nitric Oxide Donors. *Journal of Molecular and Cellular Cardiology* **32**: pp 1831-1840.

Nakata A, Ogawa K, Sasaki T, Koyama N, Wada K, Kotera J, Kikkawa H, Omori K and Kaminuma O (2002) Potential Role of Phosphodiesterase 7 in Human T Cell Function: Comparative Effects of Two Phosphodiesterase Inhibitors. *Clinical and Experimental Immunology* **128**: pp 460-466.

Nakayama K (1997) Furin: a Mammalian Subtilisin/Kex2p-Like Endoprotease Involved in Processing of a Wide Variety of Precursor Proteins. *Biochemal Journal* **327 (Pt 3)**: pp 625-635.

Nemoz G, Sette C and Conti M (1997a) Selective Activation of Rolipram-Sensitive, cAMP-Specific Phosphodiesterase Isoforms by Phosphatidic Acid. *Molecular Pharmacology* **51**: pp 242-249.

Nemoz G, Sette C and Conti M (1997b) Selective Activation of Rolipram-Sensitive, cAMP-Specific Phosphodiesterase Isoforms by Phosphatidic Acid. *Molecular Pharmacology* **51**: pp 242-249.

Nichols MR and Morimoto B H (1999) Tyrosine Kinase-Independent Inhibition of Cyclic-AMP Phosphodiesterase by Genistein and Tyrphostin 51. *Archives of Biochemistry and Biophysics* **366**: pp 224-230.

Nikolaev VO, Bunemann M, Hein L, Hannawacker A and Lohse M J (2004) Novel Single Chain cAMP Sensors for Receptor-Induced Signal Propagation. *Journal of Biological Chemistry* **279**: pp 37215-37218.

Oki N, Takahashi S I, Hidaka H and Conti M (2000b) Short Term Feedback Regulation of cAMP in FRTL-5 Thyroid Cells. Role of PDE4D3 Phosphodiesterase Activation. *Journal of Biological Chemistry* **275**: pp 10831-10837.

Osinski MT and Schror K (2000) Inhibition of Platelet-Derived Growth Factor-Induced Mitogenesis by Phosphodiesterase 3 Inhibitors - Role of Protein Kinase A in Vascular Smooth Muscle Cell Mitogenesis. *Biochemical Pharmacology* **60**: pp 381-387.

Ostrom RS, Gregorian C, Drenan R M, Xiang Y, Regan J W and Insel P A (2001) Receptor Number and Caveolar Co-Localization Determine Receptor Coupling Efficiency to Adenylyl Cyclase. *Journal of Biological Chemistry* **276**: pp 42063-42069.

Ostrom RS, Violin J D, Coleman S and Insel P A (2000) Selective Enhancement of Beta-Adrenergic Receptor Signaling by Overexpression of Adenylyl Cyclase Type 6: Colocalization of Receptor and Adenylyl Cyclase in Caveolae of Cardiac Myocytes. *Molecular Pharmacology* **57**: pp 1075-1079.

Ozaki N, Shibasaki T, Kashima Y, Miki T, Takahashi K, Ueno H, Sunaga Y, Yano H, Matsuura Y, Iwanaga T, Takai Y and Seino S (2000) cAMP-GEFII Is a Direct Target of cAMP in Regulated Exocytosis. *Nature Cell Biology* **2**: pp 805-811.

Patel S, Joseph S K and Thomas A P (1999) Molecular Properties of Inositol 1,4,5-Trisphosphate Receptors. *Cell Calcium* **25**: pp 247-264.

Pawson T (1994) SH2 and SH3 Domains in Signal-Transduction. *Advances in Cancer Research, Vol 64* **64**: pp 87-110.

Perry SJ, Baillie G S, Kohout T A, McPhee I, Magiera M M, Ang K L, Miller W E, McLean A J, Conti M, Houslay M D and Lefkowitz R J (2002) Targeting of Cyclic AMP Degradation to Beta 2-Adrenergic Receptors by Beta-Arrestins. *Science* **298**: pp 834-836.

Pyne NJ and Furman B L (2003) Cyclic Nucleotide Phosphodiesterases in Pancreatic Islets. *Diabetologia* **46**: pp 1179-1189.

Reinhardt RR, Chin E, Zhou J, Taira M, Murata T, Manganiello V C and Bondy C A (1995) Distinctive Anatomical Patterns of Gene-Expression for cGMP-Inhibited Cyclic-Nucleotide Phosphodiesterases. *Journal of Clinical Investigation* **95**: pp 1528-1538.

Rhee SG and Bae Y S (1997) Regulation of Phosphoinositide-Specific Phospholipase C Isozymes. *Journal of Biological Chemistry* **272**: pp 15045-15048.

Richter W and Conti M (2002) Dimerization of the Type 4 cAMP-Specific Phosphodiesterases Is Mediated by the Upstream Conserved Regions (UCRs). *Journal of Biological Chemistry* **277**: pp 40212-40221.

Richter W, Unciuleac L, Hermsdorf T, Kronbach T and Dettmer D (2001) Identification of Substrate Specificity Determinants in Human cAMP-Specific Phosphodiesterase 4A by Single-Point Mutagenesis. *Cellular Signalling* **13**: pp 159-167.

Rickards KJ, Page C P, Lees P, Gettinby G and Cunningham F M (2003) In Vitro and Ex Vivo Effects of the Phosphodiesterase 4 Inhibitor, Rolipram, on Thromboxane Production in Equine Blood. *Journal of Veterinary Pharmacology and Therapeutics* **26**: pp 123-130.

Ron D, Chen C H, Caldwell J, Jamieson L, Orr E and Mochly-Rosen D (1994) Cloning of an Intracellular Receptor for Protein Kinase C: a Homolog of the Beta Subunit of G Proteins. *Proceedings of the National Academy of Sciences of the United States of America* **91**: pp 839-843.

Rose RJ, Liu H, Palmer D and Maurice D H (1997) Cyclic AMP-Mediated Regulation of Vascular Smooth Muscle Cell Cyclic AMP Phosphodiesterase Activity. *British Journal of Pharmacology* **122**: pp 233-240.

Rosman GJ, Martins T J, Sonnenburg W K, Beavo J A, Ferguson K and Loughney K (1997) Isolation and Characterization of Human cDNAs Encoding a cGMP-Stimulated 3',5'-Cyclic Nucleotide Phosphodiesterase. *Gene* **191**: pp 89-95.

Ruehr ML, Russell M A and Bond M (2004) A-Kinase Anchoring Protein Targeting of Protein Kinase A in the Heart. *Journal of Molecular Cell Cardiology* **37**: pp 653-665.

Ruehr ML, Russell M A, Ferguson D G, Bhat M, Ma J, Damron D S, Scott J D and Bond M (2003a) Targeting of Protein Kinase A by Muscle A Kinase-Anchoring Protein (mAKAP) Regulates Phosphorylation and Function of the Skeletal Muscle Ryanodine Receptor. *Journal of Biological Chemistry* **278**: pp 24831-24836.

Rybalkin SD, Bornfeldt K E, Sonnenburg W K, Rybalkina I G, Kwak K S, Hanson K, Krebs E G and Beavo J A (1997) Calmodulin-Stimulated Cyclic Nucleotide Phosphodiesterase (PDE1C) Is Induced in Human Arterial Smooth Muscle Cells of the Synthetic, Proliferative Phenotype. *Journal of Clinical Investigation* **100**: pp 2611-2621.

Rybin VO, Xu X, Lisanti M P and Steinberg S F (2000) Differential Targeting of Beta -Adrenergic Receptor Subtypes and Adenylyl Cyclase to Cardiomyocyte Caveolae. A Mechanism to Functionally Regulate the cAMP Signaling Pathway. *Journal of Biological Chemistry* **275**: pp 41447-41457.

Sadhu K, Hensley K, Florio V A and Wolda S L (1999) Differential Expression of the Cyclic GMP-Stimulated Phosphodiesterase PDE2A in Human Venous and Capillary Endothelial Cells. *Journal of Histochemistry & Cytochemistry* **47**: pp 895-905.

Sadja R, Alagem N and Reuveny E (2003) Gating of GIRK Channels: Details of an Intricate, Membrane-Delimited Signaling Complex. *Neuron* **39**: pp 9-12.

Saldou N, Obernolte R, Huber A, Baecker P A, Wilhelm R, Alvarez R, Li B, Xia L, Callan O, Su C, Jamagin K and Shelton E R (1998) Comparison of Recombinant Human PDE4 Isoforms: Interaction With Substrate and Inhibitors. *Cellular Signalling* **10**: pp 427-440.

Salvador LM, Flynn M P, Avila J, Reierstad S, Maizels E T, Alam H, Park Y K, Scott J D, Carr D W and Hunzicker-Dunn M (2004) Neuronal Microtubule-Associated Protein 2D Is a Dual A-Kinase Anchoring Protein Expressed in Rat Ovarian Granulosa Cells. *Journal of Biological Chemistry* **279**: pp 27621-27632.

Satoh N, Sato T, Shimada M, Yamada K and Kitada Y (2001) Lusitropic Effect of MCC-135 Is Associated With Improvement of Sarcoplasmic Reticulum Function in Ventricular Muscles of Rats With Diabetic Cardiomyopathy. *Journal of Pharmacology and Experimental Therapeutics* **298**: pp 1161-1166.

Savany A, Abriat C, Nemoz G, Lagarde M and Prigent A F (1996) Activation of a Cyclic Nucleotide Phosphodiesterase 4 (PDE4) From Rat Thymocytes by Phosphatidic Acid. *Cellular Signalling* **8**: pp 511-516.

Schena M, Shalon D, Heller R, Chai A, Brown P O and Davis R W (1996) Parallel Human Genome Analysis: Microarray-Based Expression Monitoring of 1000 Genes. *Proceedings of the National Academy of Sciences of the United States of America* **93**: pp 10614-10619.

Schmitt JM and Stork P J S (2002a) G Alpha and G Beta Gamma Require Distinct Src-Dependent Pathways to Activate Rap1 and Ras. *Journal of Biological Chemistry* **277**: pp 43024-43032.

Schmitt JM and Stork P J S (2002b) PKA Phosphorylation of Src Mediates cAMP's Inhibition of Cell Growth Via Rap1. *Molecular Cell* **9**: pp 85-94.

Scotland G, Beard M, Erdogan S, Huston E, McCallum F, MacKenzie S J, Peden A H, Pooley L, Rena N G, Ross A H, Yarwood S J and Houslay M D (1998) Intracellular Compartmentalization of PDE4 Cyclic AMP-Specific Phosphodiesterases. *Methods* **14**: pp 65-79.

Scott JD (2003) A-Kinase-Anchoring Proteins and Cytoskeletal Signalling Events. *Biochemical Society Transactions* **31**: pp 87-89.

Scott JD, Glaccum M B, Zoller M J, Uhler M D, Helfman D M, Mcknight G S and Krebs E G (1987) The Molecular-Cloning of A Type-II Regulatory Subunit of the cAMP-Dependent Protein-Kinase From Rat Skeletal-Muscle and Mouse-Brain. *Proceedings of the National Academy of Sciences of the United States of America* **84**: pp 5192-5196.

Sette C and Conti M (1996) Phosphorylation and Activation of a cAMP-Specific Phosphodiesterase by the cAMP-Dependent Protein Kinase. Involvement of Serine 54 in the Enzyme Activation. *Journal of Biological Chemistry* **271**: pp 16526-16534.

Sette C, Iona S and Conti M (1994a) The Short-Term Activation of A Rolipram-Sensitive, cAMP-Specific Phosphodiesterase by Thyroid-Stimulating Hormone in Thyroid Frtl-5 Cells Is Mediated by A cAMP-Dependent Phosphorylation. *Journal of Biological Chemistry* **269**: pp 9245-9252.

Sette C, Iona S and Conti M (1994b) The Short-Term Activation of a Rolipram-Sensitive, cAMP-Specific Phosphodiesterase by Thyroid-Stimulating Hormone in Thyroid FRTL-5 Cells Is Mediated by a cAMP-Dependent Phosphorylation. *Journal of Biological Chemistry* **269**: pp 9245-9252.

Sette C, Vicini E and Conti M (1994c) The Ratpde3/Ivd Phosphodiesterase Gene Codes for Multiple Proteins Differentially Activated by cAMP-Dependent Protein-Kinase. *Journal of Biological Chemistry* **269**: pp 18271-18274.

Shabb JB (2001) Physiological Substrates of cAMP-Dependent Protein Kinase. *Chem Reviews* **101**: pp 2381-2411.

Shakur Y, Holst L S, Landstrom T R, Movsesian M, Degerman E and Manganiello V (2001) Regulation and Function of the Cyclic Nucleotide Phosphodiesterase (PDE3) Gene Family. *Progress in Nucleic Acid Research and Molecular Biology, Vol 66* **66**: pp 241-277.

Shepherd M, McSorley T, Olsen A E, Johnston L A, Thomson N C, Baillie G S, Houslay M D and Bolger G B (2003b) Molecular Cloning and Subcellular Distribution of the Novel PDE4B4 cAMP-Specific Phosphodiesterase Isoform. *Biochemical Journal* **370**: pp 429-438.

Shepherd M, McSorley T, Olsen A E, Johnston L A, Thomson N C, Baillie G S, Houslay M D and Bolger G B (2003a) Molecular Cloning and Subcellular Distribution of the Novel PDE4B4 cAMP-Specific Phosphodiesterase Isoform. *Biochemal Journal* **370**: pp 429-438.

Shepherd MC, Baillie G S, Stirling D I and Houslay M D (2004) Remodelling of the PDE4 cAMP Phosphodiesterase Isoform Profile Upon Monocyte-Macrophage Differentiation of Human U937 Cells. *British Journal of Pharmacology* **142**: pp 339-351.

Sheth SB, Chaganti K, Bastepe M, Ajuria J, Brennan K, Biradavolu R and Colman R W (1997) Cyclic AMP Phosphodiesterases in Human Lymphocytes. *British Journal of Haematology* **99**: pp 784-789.

Simmerman HKB and Jones L R (1998) Phospholamban: Protein Structure, Mechanism of Action, and Role in Cardiac Function. *Physiological Reviews* **78**: pp 921-947.

Soderling SH, Bayuga S J and Beavo J A (1998) Identification and Characterization of a Novel Family of Cyclic Nucleotide Phosphodiesterases. *Journal of Biological Chemistry* **273**: pp 15553-15558.

Soderling SH, Bayuga S J and Beavo J A (1999) Isolation and Characterization of a Dual-Substrate Phosphodiesterase Gene Family: PDE10A. *Proceedings of the National Academy of Sciences of the United States of America* **96**: pp 7071-7076.

Soderling SH and Beavo J A (2000) Regulation of cAMP and cGMP Signaling: New Phosphodiesterases and New Functions. *Current Opinion in Cell Biology* **12**: pp 174-179.

Steinberg SE (2004) Beta(2-)Adrenergic Receptor Signaling Complexes in Cardiomyocyte Caveolae/Lipid Rafts. *Journal of Molecular and Cellular Cardiology* **37**: pp 407-415.

Steinberg SF and Brunton L L (2001) Compartmentation of G Protein-Coupled Signaling Pathways in Cardiac Myocytes. *Annual Review of Pharmacology and Toxicology* **41**: pp 751-773.

Sullivan M, Rena G, Begg F, Gordon L, Olsen A S and Houslay M D (1998) Identification and Characterization of the Human Homologue of the Short PDE4A cAMP-Specific Phosphodiesterase RD1 (PDE4A1) by Analysis of the Human HSPDE4A Gene Locus Located at Chromosome 19p13.2. *Biochemical Journal* **333**: pp 693-703.

Sunahara RK, Dessauer C W and Gilman A G (1996) Complexity and Diversity of Mammalian Adenylyl Cyclases. *Annual Review of Pharmacology and Toxicology* **36**: pp 461-480.

Takahashi K, Osanai T, Nakano T, Wakui M and Okumura K (2002) Enhanced Activities and Gene Expression of Phosphodiesterase Types 3 and 4 in Pressure-Induced Congestive Heart Failure. *Heart and Vessels* **16**: pp 249-256.

Tasken K and Aandahl E M (2004) Localized Effects of cAMP Mediated by Distinct Routes of Protein Kinase A. *Physiological Reviews* **84**: pp 137-167.

Tasken KA, Collas P, Kemmners W A, Witczak O, Conti M and Tasken K (2001) Phosphodiesterase 4D and Protein Kinase A Type II Constitute a Signaling Unit in the Centrosomal Area. *Journal of Biological Chemistry* **276**: pp 21999-22002.

Taylor SS, Buechler J A and Yonemoto W (1990) cAMP-Dependent Protein-Kinase - Framework for A Diverse Family of Regulatory Enzymes. *Annual Review of Biochemistry* **59**: pp 971-1005.

Thomas MK, Francis S H and Corbin J D (1990) Substrate-Directed and Kinase-Directed Regulation of Phosphorylation of A cGMP-Binding Phosphodiesterase by cGMP. *Journal of Biological Chemistry* **265**: pp 14971-14978.

Tilley DG and Maurice D H (2002) Vascular Smooth Muscle Cell Phosphodiesterase (PDE) 3 and PDE4 Activities and Levels Are Regulated by Cyclic AMP in Vivo. *Molecular Pharmacology* **62**: pp 497-506.

Tiwari S, Felekkis K, Moon E Y, Flies A, Sherr D H and Lerner A (2004) Among Circulating Hematopoietic Cells, B-CLL Uniquely Expresses Functional EPAC1, but EPAC1-Mediated Rap1 Activation Does Not Account for PDE4 Inhibitor-Induced Apoptosis. *Blood* **103**: pp 2661-2667.

Tsuji A, Sakurai K, Kiyokage E, Yamazaki T, Koide S, Toida K, Ishimura K and Matsuda Y (2003) Secretory Proprotein Convertases PACE4 and PC6A Are Heparin-Binding Proteins Which Are Localized in the Extracellular Matrix. Potential Role of PACE4 in the Activation of Proproteins in the Extracellular Matrix. *Biochimca and Biophysica Acta* **1645**: pp 95-104.

Turko IV, Ballard S A, Francis S H and Corbin J D (1999) Inhibition of Cyclic GMP-Binding Cyclic GMP-Specific Phosphodiesterase (Type 5) by Sildenafil and Related Compounds. *Molecular Pharmacology* **56**: pp 124-130.

Vandecasteele G, Verde I, Rucker-Martin C, Donzeau-Gouge P and Fischmeister R (2001) Cyclic GMP Regulation of the L-Type Ca^{2+} Channel Current in Human Atrial Myocytes. *Journal of Physiology-London* **533**: pp 329-340.

Verde I, Pahlke G, Salanova M, Zhang G, Wang S, Coletti D, Onuffer J, Jin S L C and Conti M (2001) Myomegalin Is a Novel Protein of the Golgi/Centrosome That Interacts With a Cyclic Nucleotide Phosphodiesterase. *Journal of Biological Chemistry* **276**: pp 11189-11198.

Verde I, Vandecasteele G, Lezoualc'h F and Fischmeister R (1999) Characterization of the Cyclic Nucleotide Phosphodiesterase Subtypes Involved in the Regulation of the L-Type Ca^{2+} Current in Rat Ventricular Myocytes. *British Journal of Pharmacology* **127**: pp 65-74.

Vossler MR, Yao H, York R D, Pan M G, Rim C S and Stork P J S (1997) cAMP Activates MAP Kinase and Elk-1 Through a B-Raf- and Rap1-Dependent Pathway. *Cell* **89**: pp 73-82.

Wagner B, Jakobs S, Habermeyer M, Hippe F, Cho-Chung Y S, Eisenbrand G and Marko D (2002) 7-Benzylamino-6-Chloro-2-Piperazino-4-Pyrrolidino-Pteridine, a Potent Inhibitor of cAMP-Specific Phosphodiesterase, Enhancing Nuclear Protein Binding to the CRE Consensus Sequence in Human Tumour Cells. *Biochemical Pharmacology* **63**: pp 659-668.

Walsh DA, Perkins J P and Krebs E G (1968) An Adenosine 3',5'-Monophosphate-Dependant Protein Kinase From Rabbit Skeletal Muscle *Journal of Biological Chemistry* **243**: pp 3763-3765.

Walsh KB and Long K J (1994) Properties of A Protein-Kinase C-Activated Chloride Current in Guinea-Pig Ventricular Myocytes. *Circulation Research* **74**: pp 121-129.

Wang DG, Deng C J, Bugaj-Gaweda B, Kwan M, Gunwaldsen C, Leonard C, Xin X N, Hu Y H, Unterbeck A and De Vivo M (2003) Cloning and Characterization of Novel PDE4D Isoforms PDE4D6 and PDE4D7. *Cellular Signalling* **15**: pp 883-891.

Wang P, Wu P, Egan R W and Billah M M (2000) Cloning, Characterization, and Tissue Distribution of Mouse Phosphodiesterase 7A1. *Biochemical and Biophysical Research Communications* **276**: pp 1271-1277.

Wechsler J, Choi Y H, Krall J, Ahmad F, Manganiello V C and Movsesian M A (2002) Isoforms of Cyclic Nucleotide Phosphodiesterase PDE3A in Cardiac Myocytes. *Journal of Biological Chemistry* **277**: pp 38072-38078.

Wei S, Kasuya Y, Yanagisawa M, Kimura S, Masaki T and Goto K (1997) Studies on Endothelium-Dependent Vasorelaxation by Hydralazine in Porcine Coronary Artery. *European Journal of Pharmacology* **321**: pp 307-314.

Wilkie TM, Gilbert D J, Olsen A S, Chen X N, Amatruda T T, Korenberg J R, Trask B J, Dejong P, Reed R R, Simon M I, Jenkins N A and Copeland N G (1992) Evolution of the Mammalian G-Protein Alpha-Subunit Multigene Family. *Nature Genetics* **1**: pp 85-91.

Xu RX, Hassell A M, Vanderwall D, Lambert M H, Holmes W D, Luther M A, Rocque W J, Milburn M V, Zhao Y, Ke H and Nolte R T (2000) Atomic Structure of PDE4: Insights into Phosphodiesterase Mechanism and Specificity. *Science* **288**: pp 1822-1825.

Xu RX, Rocque W J, Lambert M H, Vanderwall D E, Luther M A and Nolte R T (2004) Crystal Structures of the Catalytic Domain of Phosphodiesterase 4B Complexed With AMP, 8-Br-AMP, and Rolipram. *Journal of Molecular Biology* **337**: pp 355-365.

Yang JC, Drazba J A, Ferguson D G and Bond M (1998) A-Kinase Anchoring Protein 100 (AKAP100) Is Localized in Multiple Subcellular Compartments in the Adult Rat Heart. *Journal of Cell Biology* **142**: pp 511-522.

Yang Q, Paskind M, Bolger G, Thompson W J, Repaske D R, Cutler L S and Epstein P M (1994) A Novel Cyclic-Gmp Stimulated Phosphodiesterase From Rat-Brain. *Biochemical and Biophysical Research Communications* **205**: pp 1850-1858.

Yarfitz S and Hurley J B (1994) Transduction Mechanisms of Vertebrate and Invertebrate Photoreceptors. *Journal of Biological Chemistry* **269**: pp 14329-14332.

Yarwood SJ, Steele M R, Scotland G, Houslay M D and Bolger G B (1999) The RACK1 Signaling Scaffold Protein Selectively Interacts With the cAMP-Specific Phosphodiesterase PDE4D5 Isoform. *Journal of Biological Chemistry* **274**: pp 14909-14917.

Yuasa K, Kotera J, Fujishige K, Michibata H, Sasaki T and Omori K (2000) Isolation and Characterization of Two Novel Phosphodiesterase PDE11A Variants Showing Unique Structure and Tissue-Specific Expression. *Journal of Biological Chemistry* **275**: pp 31469-31479.

Zaccolo M and Pozzan T (2002) Discrete Microdomains With High Concentration of cAMP in Stimulated Rat Neonatal Cardiac Myocytes. *Science* **295**: pp 1711-1715.

Zhao Y, Zhang H T and O'Donnell J M (2003) Inhibitor Binding to Type 4 Phosphodiesterase (PDE4) Assessed Using [H^3]Piclamilast and [H^3]Rolipram. *Journal of Pharmacology and Experimental Therapeutics* **305**: pp 565-572.

Zhu B, Kelly J, Lowry D, Underwood T and Thompson W J (1999) Activation and Phosphorylation of PDE4 in Rat Microvascular Endothelial Cells (RPMVEC). *FASEB Journal* **13**: pp A792.